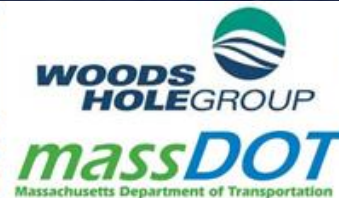


MassDOT-FHWA Pilot Project Report: *Climate Change and Extreme Weather Vulnerability Assessments and Adaptation Options for the Central Artery*

Project Team:

*Kirk Bosma, P.E., Woods Hole Group, Inc.
Ellen Douglas, P.E., Ph.D., UMass Boston
Paul Kirshen, Ph.D., University of New Hampshire
Katherin McArthur, MassDOT
Steven Miller, MassDOT
Chris Watson, M.Sc., UMass Boston*



**MassDOT-FHWA
Pilot Project Report:
Climate Change and Extreme
Weather Vulnerability Assessments
And Adaptation Options for the Central Artery**

June 2015

Project Team:

Kirk Bosma, P.E., Woods Hole Group, Inc.
Ellen Douglas, P.E., Ph.D., UMass Boston
Paul Kirshen, Ph.D., University of New Hampshire
Katherin McArthur, MassDOT
Steven Miller, MassDOT
Chris Watson, M.Sc., UMass Boston

Acknowledgements

The authors wish to thank many people for their assistance in this project. They include, but are not limited to, Lt. Dave Albanese, Jeff Amero, John Anthony, Kathleen Baskin, Natalie Beauvais, David Belanger, Carolyn Bennett, John Bolduc, Dennis Carlberg, Bruce Carlisle, Joe Choiniere, Michael Chong, Lisa Dickson, Nate Dill, David Dinocco, Jeff Dusenbery, Kerry Emanuel, Rob Evans, Joe Famely, M. Leslie Fields, John Gendall, William A. Gode-von Aesch, Marybeth Groff, Robert Hamilton, Robyn Hannigan, Elizabeth Hanson, Arden Herrin, Eric Holmes, Nick Hugon, Mike Hutcheon, Bob Hutchen, Christian Jacqz, Charlie Jewell, Ron Killian, Leland Kirshen, Julia Knisel, Brian Knowles, Stephanie Kruel, Wes LaParl, Elise Leduc, Donna Lee, Vivien Li, Kevin Lopes, Rebecca Lupes, Kristen Mathieu, Rick McCullough, Lisa Grogan-McCulloch, Connor McKay, John McVann, Ellen Mecray, Stephen Morash, Dan Mullaly, Cynthia Nurmi, Paul Nutting, Daniel Nvule, Robbin Peach, William Pisano, Owen O'Riordan, Geoffrey Rainoff, Vandana Rao, Lawanda Riggs, Leo Scanlon, Stephen Estes-Smargiassi, Carl Spector, John Sullivan, Nadine Sweeney, Rob Thieler, Kevin Walsh, Peter Walworth, Sarah White, Norman Willard, John Winkelman, Steve Woelfel, Julie Wormser, Florence Wortzel, Arben Zhuri, Rich Zingarelli.

Table of Contents

Executive Summary	<i>i</i>
Introduction	<i>1</i>
1.1 The Big Dig	<i>1</i>
1.2 Motivation for this Project	<i>1</i>
1.3 Project Objectives and Approach.....	<i>2</i>
1.4 Overall Process	<i>4</i>
1.5 A Comparison of this Study with Others.....	<i>6</i>
Geographical Scope and Data Gathering	<i>9</i>
2.1 Preliminary Data Acquisition	<i>9</i>
2.2 Tunnel Tour.....	<i>9</i>
2.3 Initial Review of Assets.....	<i>10</i>
2.4 Mini-Pilot Asset Inventory	<i>11</i>
2.5 Preliminary Institutional Knowledge (IK) Meeting – July 26, 2013	<i>12</i>
2.6 Maximo.....	<i>13</i>
2.7 MMIS.....	<i>14</i>
2.8 First Institutional Knowledge (IK) Meeting – September 16, 2013.....	<i>14</i>
2.9 Second Institutional Knowledge Meeting – October 22, 2013	<i>14</i>
2.10 Geographical Scope of the Potentially Critical Areas of the CA/T	<i>16</i>
2.11 Technical Advisory Committee Meetings	<i>16</i>
2.12 MBTA Tunnel Tours	<i>17</i>
2.13 Stakeholder Engagement.....	<i>19</i>
2.14 Other Informational and Coordination Meetings.....	<i>20</i>
Asset Inventory and Elevation Surveys	<i>21</i>
3.1 Detailed Asset Inventory (Field Visits).....	<i>21</i>
3.2 Elevation Surveys.....	<i>21</i>
3.3 Assets and Facilities	<i>22</i>
3.4 CA/T Database.....	<i>22</i>
3.5 Structures and Structural Systems.....	<i>23</i>
3.6 Geodatabase Development	<i>26</i>
Hydrodynamic Analysis.....	<i>28</i>
4.1 Model Selection.....	<i>29</i>

4.2	<i>Description of ADCIRC.....</i>	33
4.3	<i>Description of SWAN.....</i>	34
4.4	<i>Coupling Waves and Currents.....</i>	35
4.5	<i>Model Development.....</i>	36
4.6	<i>Model Calibration and Validation.....</i>	49
4.7	<i>Sea Level Rise and Storm Climatology</i>	57
4.8	<i>Developing the Composite Probability Distribution of Storm-Related Flooding ..</i>	75
4.9	<i>BH-FRM Results</i>	77
	<i>Vulnerability Assessment</i>	95
5.1	<i>Development of the Vulnerability Assessment Process</i>	95
5.2	<i>Results of Vulnerability Assessment of Individual Structures</i>	99
	<i>Adaptation.....</i>	104
6.1	<i>Local Adaptation Plan</i>	104
6.2	<i>Regional Adaptations.....</i>	105
	<i>Conclusions and Lessons Learned.....</i>	112
7.1	<i>Conclusions.....</i>	112
7.2	<i>Additional Notable Project Findings.....</i>	113
7.3	<i>Lessons Learned.....</i>	113
7.4	<i>Continuing Work</i>	116
	<i>References</i>	117

List of Figures

<i>Figure ES-1. Schematic of the Central Artery/Tunnel (CA/T) system.</i>	<i>i</i>
<i>Figure 1-1. Schematic of the Central Artery/Tunnel (CA/T) system.</i>	<i>3</i>
<i>Figure 1-2. Potential flooding in Boston due to an extreme storm surge (5 ft) on top of spring tide. Source: www.tbha.org.</i>	<i>4</i>
<i>Figure 1-3. FHWA framework for assessing the vulnerability of transportation systems to climate change and extreme weather (source: Fig 1 from FHWA, 2012, pg 2). ...</i>	<i>5</i>
<i>Figure 2-1. On left, the assumed number of assets to be evaluated in this pilot project (~40) compared to, on right, a representation of the number of assets that actually existed within the system (on the order of thousands).</i>	<i>11</i>
<i>Figure 2-2. Screen shot of photo gallery archiving system developed for this project.</i>	<i>12</i>
<i>Figure 2-3. Example map provided by MassDOT District 6 staff at preliminary IK meetings.</i>	<i>13</i>
<i>Figure 2-4. Map created for first IK meeting.</i>	<i>15</i>
<i>Figure 2-5. Magnified sections of maps used in IK meetings, showing annotations.</i>	<i>16</i>
<i>Figure 4-1. Bathtub model results for Boston Harbor area showing a maximum water surface elevation of 12 feet NAVD88.</i>	<i>29</i>
<i>Figure 4-2. Dynamic numerical model results for Boston Harbor area showing a maximum water surface elevation of 12 feet NAVD88.</i>	<i>29</i>
<i>Figure 4-3. Comparison typical ADCIRC grid resolution (dots) and SLOSH grid resolution (lines) (Sparks, 2011).</i>	<i>33</i>
<i>Figure 4-4. Schematic showing the coupling of the ADCIRC and SWAN models.</i>	<i>36</i>
<i>Figure 4-5. Comprehensive domain of the ADCIRC mesh showing coarse nodal spacing in the deep waters on the Eastern boundary, and increased nodal resolution in the littoral areas of the model domain.</i>	<i>38</i>
<i>Figure 4-6. The finite element ec95d ADCIRC mesh used to provide initial coarse mesh (ADCIRC.org, 2013)</i>	<i>39</i>
<i>Figure 4-7. Finite element mesh for the intermediate (NOAA NE VDatum) mesh used to resolve the coastal waters in greater resolution (Yang, et al., 2013).</i>	<i>39</i>
<i>Figure 4-8. MassDOT focus area for the fine mesh (main image), inland extent of the high resolution domain (top inset), and complete model domain (bottom inset) for perspective. The blue outline in the main figure shows the upland extent of the model domain.</i>	<i>41</i>
<i>Figure 4-9. High resolution mesh grid in the vicinity of downtown Boston.</i>	<i>41</i>
<i>Figure 4-10. New Charles River Dam (NCRD).</i>	<i>46</i>
<i>Figure 4-11. Amelia Earhart Dam (AED).</i>	<i>47</i>
<i>Figure 4-12. Location of tide stations in the vicinity of Boston Harbor. These stations were used for calibration of the BH-FRM model.</i>	<i>53</i>
<i>Figure 4-13. Model calibration results for the Blizzard of 1978. Comparison of modeled time series of water surface elevation with observed high water mark in Swampscott, Massachusetts.</i>	<i>55</i>
<i>Figure 4-14. Model calibration results for the Blizzard of 1978. Comparison of modeled time series of water surface elevation with observed high water mark in Winthrop, Massachusetts.</i>	<i>55</i>

<i>Figure 4-15. Model calibration results for the Blizzard of 1978. Comparison of modeled time series of water surface elevation with observed high water mark in Cohasset, Massachusetts.....</i>	<i>56</i>
<i>Figure 4-16. Model calibration results for the Blizzard of 1978. Comparison of observed high water marks to peak model results at the same locations within Boston Harbor.</i>	<i>57</i>
<i>Figure 4-17. Model validation results for the Perfect Storm of 1991. Comparison of modeled time series of water surface elevation with observed high water mark in Narragansett Bay, Rhode Island.</i>	<i>58</i>
<i>Figure 4-18. Selection of sea level rise rates that span multiple time frame (modified from Figure ES1 in Global Sea Level Rise Scenarios for the United States National Climate Assessment, NOAA Technical Report OAR CPO-1, December 12, 2012).</i>	<i>61</i>
<i>Figure 4-19. Example of the tropical storm track lines associated with one of the global climate model storm sets from WindRiskTech, Inc.</i>	<i>62</i>
<i>Figure 4-20. Cumulative distribution function of historical extra-tropical storms affecting Boston Harbor area.</i>	<i>64</i>
<i>Figure 4-21. Annual number of tropical cyclones (vertical axis) including hurricanes and tropical storms in the North Atlantic, beginning in 1870 (acknowledgement to Dr. Kerry A. Emanuel, Massachusetts Institute of Technology).....</i>	<i>67</i>
<i>Figure 4-22. Annual number of tropical cyclones (green) compared to average ocean surface temperature (blue) during August to October (acknowledgement to Dr. Kerry A. Emanuel, Massachusetts Institute of Technology).....</i>	<i>67</i>
<i>Figure 4-23. Post-1970 PDI (green), compared to ocean surface temperature in the Atlantic (blue) (acknowledgement to Dr. Kerry A. Emanuel, Massachusetts Institute of Technology).....</i>	<i>68</i>
<i>Figure 4-24. Hurricane Surge Index (HSI) at landfall compared to annual exceedance probability. The red line represents the distribution of the 20th century storms used in this study, while the blue line represents the distribution of the 21st century storms used in this study.....</i>	<i>68</i>
<i>Figure 4-25. Extra-tropical storm surge CDF based on residual high water levels at Boston.</i>	<i>70</i>
<i>Figure 4-26. Time series of model sea level (feet, NAVD88) versus hours over the two day maximum sustained winds. Each model run uses the same meteorological forcing, but gives the tides an added phase (in hours), as indicated in the legend. Notice the location of maximum high water changes with increasing delay, but since the storm duration is so long, this is not a temporal linear process.</i>	<i>73</i>
<i>Figure 4-27. Time series of model sea level (feet, NAVD88) versus hours for a representative hurricane event. Each model run uses the same meteorological forcing, but gives the tides an added phase (in hours), as indicated in the legend.....</i>	<i>73</i>
<i>Figure 4-28. Maximum predicted water level as a function of tidal delay in the tropical storm model simulations (blue line) in Boston Harbor. There is a strong sinusoidal fit (red line) to the results that was utilized to produce an equation utilized as a transfer function.</i>	<i>74</i>
<i>Figure 4-29. Maximum predicted water level (normalized by the spring high tide level) in the tropical storm model simulations (blue line) in Boston Harbor. Values above 1 indicate an increased expected maximum water level relative to the expected high</i>	

	<i>tidal value. Red shaded regions are the runs where the maximum meteorological forcing occurs during the rising tide.....</i>	<i>75</i>
<i>Figure 4-30.</i>	<i>Example AMS flood probabilities for a Nor'easter (blue diamonds) and hurricane (red square) and the combined flood probability distribution (open diamonds).</i>	<i>77</i>
<i>Figure 4-31.</i>	<i>Snapshot of a typical hurricane (tropical) storm simulation within BH-FRM for a storm event that impacted the Boston area.</i>	<i>78</i>
<i>Figure 4-32.</i>	<i>BH-FRM results showing probability of flooding in 2013.....</i>	<i>81</i>
<i>Figure 4-33a.</i>	<i>BH-FRM results showing probability of flooding in 2030. An additional 0.74 in (1.9 cm) due to subsidence was added to the 0.62 feet SLR.....</i>	<i>82</i>
<i>Figure 4-33b.</i>	<i>BH-FRM results showing probability of flooding in 2070. An additional 2.5 in (6.3 cm) due to subsidence was added to the 3.2 feet SLR..</i>	<i>83</i>
<i>Figure 4-34.</i>	<i>BH-FRM results showing flooding depth for a 1% probability of flooding in 2013.....</i>	<i>85</i>
<i>Figure 4-35a.</i>	<i>BH-FRM results showing flooding depth for a 1% probability of flooding in 2030. An additional 0.74 in (1.9 cm) due to land subsidence was added to the 0.62 feet SLR.</i>	<i>86</i>
<i>Figure 4-35b.</i>	<i>BH-FRM results showing flooding depth for a 1% probability of flooding in 2070. An additional 2.5 in (6.3 cm) due to land subsidence was added to the 3.2 feet SLR.</i>	<i>87</i>
<i>Figure 4-36.</i>	<i>Example exceedance probability curve for 93 Granite Ave. in Milton, Massachusetts (MassDOT Fuel Depot Complex).....</i>	<i>88</i>
<i>Figure 4-37.</i>	<i>BH-FRM wave results for a typical extra-tropical (Nor'easter) event.....</i>	<i>90</i>
<i>Figure 4-38.</i>	<i>BH-FRM results showing probability of flooding in 2013 for the 93 Granite Ave. location.</i>	<i>91</i>
<i>Figure 4-39.</i>	<i>BH-FRM results showing flooding depth for a 1% flooding probability in 2013 at the 93 Granite Ave. location.</i>	<i>91</i>
<i>Figure 4-40.</i>	<i>BH-FRM results showing flooding depth for a 1% flooding probability in 2013 at the 93 Granite Ave. location, as well as residence time and local flood pathways.</i>	<i>93</i>
<i>Figure 4-41.</i>	<i>BH-FRM results showing probability of flooding in 2030 for the 93 Granite Ave. location. An additional 0.74 in (1.9 cm) due to land subsidence was added to the 0.62 feet SLR.</i>	<i>93</i>
<i>Figure 4-42.</i>	<i>BH-FRM results showing flooding depth for a 1% flooding probability in 2030 at the 93 Granite Ave. location. An additional 0.74 in (1.9 cm) due to land subsidence was added to the 0.62 feet SLR.</i>	<i>94</i>
<i>Figure 4-43.</i>	<i>BH-FRM results showing flooding depth for a 1% flooding probability in 2030 at the 93 Granite Ave. location, as well as residence time and local flood pathways. An additional 0.74 in (1.9 cm) due to land subsidence was added to the 0.62 feet SLR.</i>	<i>94</i>
<i>Figure 5-1.</i>	<i>Location of mini-pilot Facilities and Structures listed in Table 5-1.</i>	<i>97</i>
<i>Figure 5-2.</i>	<i>Example of 1% interpolated flood-depth map overlain with nodal information (data points) for a typical CA/T Structure – specifically Vent Building 6 (VB6) in South Boston.</i>	<i>99</i>
<i>Figure 5-3.</i>	<i>Street View of Combined Bins 7UG, 7MD, and 7GC (from Google Earth).</i>	<i>103</i>

<i>Figure 6-1. Flood entry point locations that are viable sites for regional adaptations under the 2013 scenario (Milton site not shown).</i>	107
<i>Figure 6-2. Flood entry point locations that are viable sites for regional adaptations under the 2030 scenario.</i>	107
<i>Figure 6-3. Flood entry point locations that are viable sites for regional adaptations under the 2070 scenario.</i>	108

List of Tables

<i>Table 2-1. Expertise and input from the first TAC meeting.</i>	18
<i>Table 4-1. Summary of data inputs and sources.</i>	37
<i>Table 4-2. Tidal constituents used to develop tidal boundary condition for BH-FRM.</i>	43
<i>Table 4-3. Present day (2013) and projected future return period rainfall event total precipitation amounts (inches).</i>	43
<i>Table 4-4. Present day (2013) and projected future return period peak discharge flows (cubic feet per second) for the Charles River.</i>	44
<i>Table 4-5. Present day (2013) and projected future return period peak discharge flows (cubic feet per second) for the Mystic River.</i>	44
<i>Table 4-6. Manning’s n values applied in BH-FRM based on land cover types.</i>	45
<i>Table 4-7. Pump summary for BH-FRM dams (all pumps have maximum capacity of 1400 cfs).</i>	48
<i>Table 4-8. Calibration water surface elevation error measures for average tidal conditions. Relative error based on the average tidal range at each station.</i>	53
<i>Table 4-9. Calibration water surface elevation error measures for the Blizzard of 1978.</i>	54
<i>Table 4-10. Validation water surface elevation error measures for the Perfect Storm of 1991.</i>	58
<i>Table 5-1. List of facilities and structure for mini-pilot analysis.</i>	96
<i>Table 5-2. The vulnerability results of non-Boat Section Structures for flooding scenarios: “2013” indicates present vulnerability, “2013 to 2030” indicates vulnerability over the period from the just past the present to 2030, “2030 to 2070 or to 2100” indicates vulnerability over the period just past 2030 to 2070 under a higher SLR scenario, or over the period just past 2030 to 2100 under a lower SLR scenario. Underlined Structures are Complexes; Italicized Structures are located within each Complex.</i>	101
<i>Table 5-3. Flood depths of the at-grade land around Boat Sections with Portals: “2013” indicates present vulnerability, “2013 to 2030” indicates vulnerability over the period from the just past the present to 2030, “2030 to 2070 or to 2100” indicates vulnerability over the period just past 2030 to 2070 under a higher SLR scenario, or over the period just past 2030 to 2100 under a lower SLR scenario.</i>	102
<i>Table 6-1. Dimensions, and estimated material and installation costs, for Complexes and Structures listed in Table 5 -2 requiring walls or other specific solutions: except where noted, installation of all walls or other solutions recommended in the period either just after 2030 to 2070 under a higher SLR scenario, or just after 2030 to 2100 under a lower SLR scenario</i>	109

Table 6-2. Number of lanes and dimensions, and material and installation costs, for the Portals requiring gates in listed Table 5 -3: “2013” indicates installation recommended now, “<2030” indicates installation recommended during the period from the just past the present to 2030, “<2070 or <2100” indicates installation recommended over the period just past 2030 to 2070 under a higher SLR scenario, or over the period just past 2030 to 2100 under a lower SLR scenario..... 110

Table 6-3. A summary of the locations identified for regional adaptations. 111

EXECUTIVE SUMMARY

What is the Central Artery/Tunnel system?

Interstate 93 (I-93) is a nearly 200-mile long North-South major transportation corridor for northern New England. Built in the mid-to late 1950's, I-93 was an elevated six-lane highway as it traversed the heart of downtown Boston. Urban fragmentation, infrastructure deterioration and traffic congestion due to heavy usage prompted the replacement of the so-called "Central Artery" of Boston with an "eight-to-ten lane state-of-the-art underground highway, two new bridges over the Charles River, [an extension of] I-90 to Boston's Logan International Airport and Route 1A." The Central Artery/Tunnel Project (CA/T) is comprised of more than 160 lane-miles, more than half of them in tunnels, six interchanges and 200 bridges. As one of the most valuable components of Massachusetts' transportation infrastructure, its maintenance, protection and enhancement are a priority for the Commonwealth. Over the more than twenty years that have passed since the genesis of the CA/T project, climate conditions have changed, and they are expected to continue to change over the course of the 21st century and beyond. In order to keep Massachusetts Department of Transportation's (MassDOT) commitment to the people of the Commonwealth to preserve and protect their public assets, it is vital to consider the implications of these new conditions and plan for their potential impacts.



Figure ES-1. Schematic of the Central Artery/Tunnel (CA/T) system.

On January 23, 2013, the project team submitted a proposal to the Federal Highway Administration's (FHWA) request for Pilot Projects: Climate Change and Extreme Weather Vulnerability Assessments and Adaptation Options Analysis. Funding was awarded by FHWA in February 2013 and Notice to Proceed was issued by MassDOT on April 16, 2013. The two main objectives of this pilot project were to 1) assess the vulnerability of CA/T to sea level rise (SLR) and extreme storm events, and 2) investigate and present adaptation options to reduce identified vulnerabilities. The results of these two project objectives support a third objective, still on-going, to establish an emergency response plan for tunnel protection and/or shut down in the event of a major storm.

What is a vulnerability assessment?

The fourth assessment report (AR4) of the Intergovernmental Panel on Climate Change (IPCC, 2007) defines vulnerability as "the degree to which a system is susceptible to and unable to cope with, adverse effects of climate change, including climate variability and extremes". Vulnerability is assessed by evaluating the system's *exposure, sensitivity and adaptive capacity*. *Exposure* identifies the degree to which the system will be impacted by climate change and extreme weather events. For example, is a roadway exposed to potential flooding, and if so, by how much? For this project, our analysis of exposure was focused on potential flooding due to coastal storm surge and wave action resulting from extreme coastal storms (hurricanes and Nor'easters) combined with SLR. Some consideration was given to river flooding. *Sensitivity* refers to how the system responds to the identified impacts. For instance, if the roadway is flooded, how does this affect system performance; is the roadway completely impassable or will closure of one lane suffice? *Adaptive capacity* refers to the ability of the system to accommodate impacts and/or recover from the impacts. For instance, if a roadway is flooded, does the roadway drainage system have the capacity to transmit the flooding away from the road quickly so that traffic flow is minimally impacted or are there alternative routes? Once the current and future system vulnerability was assessed and quantified, the next step was to develop conceptual adaptation strategies that would be used by MassDOT to develop a strategic plan for reducing vulnerability and improving system recovery under current and future extreme conditions.

How did we approach such a complex project and who, besides the project team, was involved?

An initial assessment of CA/T Assets within the project domain found that the number of potential Assets that would need to be cataloged and investigated was considerably larger than had been envisioned in the original proposed scope and timeline of this pilot project. Based on this information, we revised our approach in the following ways: 1) We developed a "mini-pilot" approach, where we selected Assets within the CA/T domain to use in methodology development and testing (described in Sec. 2.4) before expanding to the entire system; and 2) We pursued what became known as "Institutional Knowledge (IK)" meetings (described in Sec. 2.5), which brought in the key MassDOT personnel whose expertise helped us identify the appropriate Assets and to prioritize the appropriate risk and vulnerability approach. A Technical Advisory Committee (TAC), made up of experts in coastal processes, modeling, and vulnerability assessments, reviewed the methodology and technical approach of the project. A key priority for this project was to develop products that, to the degree possible, are useful to other Boston agencies and stakeholders who are also doing adaptation work. We provided a project summary fact sheet (see Appendix III) to those interested in knowing more about the project. We convened two stakeholder meetings during the project with other organizations carrying out vulnerability assessments in metro Boston, one near the beginning to outline our approach and our anticipated deliverables and the other towards the end of the project, to obtain feedback about preliminary findings and maps. There were numerous other meetings with interested agencies as described in Section 2.13 and further listed in Appendix

IV. Coordinating with interested stakeholders turned out to be a much larger effort than originally anticipated, but resulted in better communication of project goals and deliverables and even greater interest in and relevancy of project outcomes.

How did we create the Central Artery Database?

As the CA/T database was developed, there was a need to develop an expanded information hierarchy based on increased understanding of the CA/T system. Although the original project focus was on “Assets,” a more specific primary definition of Assets as individual items that collectively comprise the CA/T system was developed. Facilities were then defined as functional collection of Assets. As an example, a pump station is a Facility, and the pumps and electrical controls that comprise a pump station are the Assets. For the purpose of identifying and locating the numerous Facilities associated with the CA/T, we developed a relational database (CATDB) to interface with a GIS and with Maximo (the primary MassDOT database). As the CATDB development proceeded, we further developed the expanded information hierarchy (described in Section 3.5) to include two additional primary definitions: Structures and Structural Systems. Structures are defined as buildings or other types of structures that, either partially or completely, have potential at-grade exposures to water infiltration during flood events. Each Structure contains one or more Facilities. For example, Storm Water Pump Station 15 (D6-SW15-FAC) Facility is located within the Ventilation Building (VB) 4 (D6-VB4-FAC) Facility, and VB4 is located partially above the ground surface. Structural Systems are defined as a collection of vertically or horizontally adjacent Structures. The implications of a

Structural System is that during a coastal flooding event, the vulnerability identified at any one Structure significantly increases the vulnerability of all adjacent Structures within the Structural System. Other structural definitions include the following: a Portal, which is the specific area of transition into or out of a Tunnel; a Boat Section, defined as a Tunnel Section that is open at the top – a paved roadway “floor” with two sidewalls and without a “roof;” and a Boat Section with Portal, defined as a Boat Section that either enters into, or exits out of a Tunnel at a Portal.

How did we model the effects of coastal storms and climate change?

SLR by itself and SLR combined with storm events have most commonly been evaluated by simply increasing the water surface elevation and comparing the new water elevation with the topographic elevations of the land. While this rudimentary “bathtub” approach may be viable to provide a first order identification of potentially vulnerable areas, it does not accurately represent the dynamic nature of coastal storm events needed for a comprehensive analysis such as this one. The hydrodynamic modeling utilized for this study is based on mathematical representations of the processes that affect coastal water levels such as riverine flows, tides, waves, winds, storm surge, sea level rise, and wave set-up, at a fine enough resolution to identify site-specific locations that may require adaptation alternatives. An initial evaluation of over 10 circulation models was completed by the MassDOT project team. The ADvanced CIRculation model (ADCIRC) was selected because of its ability to accommodate complex geometries and bathymetries and heterogeneous parameter values. ADCIRC has the ability to include a wide variety of meteorological forcings, and is a model commonly used to predict coastal

inundation caused by storm surge. A full description of ADCIRC is given in Section 4.2. Storm-induced waves were simulated in concert with the hydrodynamics by coupling the Simulating WAves Nearshore (SWAN) Model with ADCIRC. A full description of SWAN is included in Section 4.3 and the coupling of ADCIRC and SWAN is described in Section 4.4.

The first step in building the ADCIRC-SWAN model was construction of the modeling mesh, which is the digital representation of the domain geometry that provides the spatial discretization on which the model equations are solved. The mesh was developed at three resolutions: 1) a regional-scale mesh (ec95d ADCIRC mesh, described in Section 4.5.1.1), which is a previously validated model mesh used in numerous Federal Emergency Management Agency (FEMA) studies, National Oceanic and Atmospheric Administration (NOAA) operational models, and most recently the United States Army Corps of Engineers North Atlantic Coast Comprehensive Study (NACCS); 2) a local-scale mesh (described in Section 4.5.1.2) providing an intermediate level of mesh resolution to transition from the ec95d mesh to the highly resolved mesh needed along the Massachusetts coastline; and 3) a site-specific mesh (described in Section 4.5.1.3) of sufficient resolution to ensure that all critical topographic and bathymetric features that influence flow dynamics within the CA/T system were captured. The site-specific mesh includes areas of open water, along with a substantial portion of the upland subject to present and future flooding.

A unique feature of this Boston Harbor Flood Risk Model (BH-FRM) was the ability to simulate flow conditions (a combination of pumping and sluicing) at the New Charles River and Amelia Earhart dams within the CA/T domain. River

discharge hydrographs for present and future climate conditions were dynamically included in the model, thus allowing for the assessment of pumping operations in managing upstream water levels. A summary of dam operations and a full description of the dam and pump boundary conditions, as well as model assumptions, are included in Section 4.5.3. The BH-FRM model was calibrated using both normal tidal conditions and a representative storm, the Blizzard of 1978, and then validated with the Perfect Storm of 1991. These storms represented the highest water levels observed at the Boston tide gage and their impacts were well documented. Model calibration and validation demonstrated that ADCIRC-SWAN was very good at simulating important coastal storm processes and impacts. Model calibration and validation details are included in Sections 4.6.2 and 4.6.3, respectively.

SLR scenarios were selected for four distinct time periods (2013, 2030, 2070, and 2100) to bracket the potential future sea level rise outcomes for the Boston Harbor area. Our selected SLR estimates were taken from Figure ES1 of Global Sea Level Rise Scenarios for the United States National Climate Assessment (NOAA Technical Report OAR CPO-1, December 12, 2012). The 2030 and 2070 scenarios assume a high (Hi) emissions trajectory while the 2100 scenario assumes an intermediate high (IH) trajectory; hence the 2070 and 2100 scenarios are represented by the same model simulations. The final sea level heights were adjusted for local subsidence following Kirshen et al. (2008). Both tropical (i.e., hurricanes) and extra-tropical (i.e., Nor'easters) storm conditions were evaluated in the model. A Monte Carlo statistical approach was utilized to estimate the probability of flooding throughout the Boston Harbor region. While hurricanes are intense, fast moving storms that have a

significant impact on coastal communities, they are not as common in the northeast as Nor'easters (at least in the contemporary and historical time frames). Historical water level records and historical meteorological records were used to identify a set of Nor'easters to be simulated in the model. In addition to storm intensity and direction, the timing of a storm relative to the tidal cycle is an important consideration. We found that the timing of the peak hurricane surge is very important while the timing of the peak Nor'easter surge has little effect on maximum water levels. This is because hurricanes tend to be fast moving systems, hence the likelihood of peak surge occurring at the same time as peak high tide is relatively low when compared to Nor'easters, which typically last for 24 hours or more. The probability of flooding due to both hurricanes and Nor'easters was estimated by developing composite probability distributions for flooding as outlined in Section 4.8. Under current (circa 2013) and near-term future (2030) climate conditions, the probability of flooding due to Nor'easters dominates because the annual average frequency of nor'easters (~2.3) is much higher than that of hurricanes (~0.34). However, later in the century (2070 to 2100), hurricanes play a larger role than they do currently and have the same order of magnitude of importance as Nor'easters.

How can the results of the BH-FRM be used?

The results of BH-FRM simulations (as outlined above) for 2013, 2030 and 2070 (Hi)/2100 (IH) were used to generate maps of potential flooding and associated water depths throughout the area of interest. These maps are presented in Section 4.9 and Appendix VI and can be used to identify locations, Structures, Assets, etc. that lie within different flood risk levels. For example, a building that lies within the 2%

flood exceedance probability zone would have a 2% chance of flooding in any year (under the assumed climate scenario). Stakeholders can then determine if that level of risk is acceptable, or if some action may be required to improve resiliency, engineer an adaptation, consider relocation, or implement an operational plan.

Under current (2013) conditions, flooding is present in downtown Boston (from the North End through the Financial District, intersecting the Rose Kennedy Greenway, entrances to I93 and other CA/T structures), South Boston (from the east side of Fort Point Channel through the Innovation District to the Massport terminals), East Boston (near the entrance to the Sumner and Callahan tunnels through the East Boston Greenway along Rt. 1A) and along waterfront areas of East Boston, Charlestown and Dorchester. However, the exceedance probabilities of this flooding is generally quite low; hence, the vulnerability concerns under current climate conditions are mostly focused on Boat Sections with Portals as described in more detail below and in Chapter 5. Under near-term future (2030) conditions, flooding increases in both spatial extent and probability. For example, the area of flooding in the vicinity landward of the New England Aquarium and Long Wharf area has expanded and the probability of flooding has increased. By 2030, neither dam is overtopped or flanked for any reasonable risk level (i.e., less than 0.1%). There is some flooding that occurs upstream of the dams; however this is caused by precipitation effects due to poor drainage and higher river discharge, not coastal storm surge. Late in the century (2070 Hi or 2100 IH), the situation become much different, with both the extent and probability of flooding becoming much greater across metro Boston and the surrounding communities. Flood probabilities in downtown Boston, East Boston and South

Boston exceed 10 percent in many locations. Flooding in South Boston and East Boston is extensive with flood probabilities exceeding 50%. The CRD and AE dams are flanked or overtopped, resulting in more extensive inland flooding in Cambridge, Somerville and Charlestown.

BH-FRM generated maps can also be used to assess flood entry points and pathways and thereby identify potential regional adaptations. In many cases, large upland areas are flooded by a relatively small and distinct entry point (e.g., a low elevation area along the coastline). BH-FRM also produces information on the depth of flooding at every node in the model domain that can be expected at various flood exceedances.

What were the results of the vulnerability assessment (VA)?

The MassDOT IK Team stated that “any water at grade is a problem” because of possible leaky foundations, doorways, etc. at grade and that there is essentially no adaptive capacity in the system. Hence, rather than being able to prioritize structures based on differing sensitivities, we determined that all structures have an equal priority for adaptation. We recommended, however, that all structures be inspected for possible flood pathways at grade, that all outfalls discharging in the Boston Harbors be equipped with tide gates, and all doorways exposed to possible flooding should be water tight. For Boat-Sections, we did not have an adequate assessment of whether or not the surrounding walls can withstand flood waters or whether or not they are water tight. We therefore assumed that the ground level elevations surrounding each Boat Section were the critical threshold elevations regardless of the higher elevations of any surrounding walls. The vulnerability of the structures was assessed

under their original design conditions of 0.1 % flood exceedance for portals and 1 % exceedance for all other structures. The results of the VA and a list of the individual facilities and structures that were identified are detailed in Section 5.2. The same 12 Portals are flooded under present (2013) and 2030 conditions (see Table 5.2). Six non-boat section Structures experience flooding under current conditions and nineteen additional non-boat section Structures become flooded by 2030. By the end of the century (2070 to 2100), depending upon the actual rate of SLR, an additional twenty-six Structures may become vulnerable and the number of vulnerable Boat Sections with Portals increases dramatically (see Table 5-3).

What adaptation strategies were recommended?

Adaptation is generally defined as the process of adjusting to the vulnerability of climate change. It consists of a series of actions taken over time and space (Kirshen et al., 2014). We evaluated local adaptation options for protecting the individual non-Boat Section Structures and Boat Sections with Portals over time as flooding increases (Chapter 6). Focusing first on local actions means that MassDOT is less reliant on other organizations and agencies to manage the CA/T adaptation as it will own the land necessary for any changes and will only have to manage its own efforts. The adaptation plan for the non-Boat Section Structures was based upon requirement that no flooding be allowed near the foundations of the Structures. If flood depths were less than 2 feet, then relatively inexpensive temporary flood barriers would be used. Once flood depths exceeded 2 feet around any portion of the structure perimeter, a wall would be constructed around the flooded perimeter area. As the extent and depth of the flooding increases over time, the wall

height would be increased; hence, any wall constructed as a local adaptation will be designed to be adjustable above its initial height for protection beyond 2030. None of the flood depths around the non-Boat Section Structures in 2013 or in the period from now through 2030 exceeded 2 feet, suggesting that no major adaptation actions are need in the near term.

Since walls at the boat sections were not assessed for either structural or water tight integrities, we recommended that MassDOT perform these assessments while considering adaptation options. Flood water flowing into the Boat Sections with Portals from the sides needs to be kept from entering the tunnels by watertight gates – covering the full height of the portal. A gate would be installed when the flood depth exceeded 0.5 feet at most of the land surrounding Boat Section walls. At depths less than this, relatively inexpensive methods are assumed to be used such as local blocking of the lower part of the Portals with sand bags, or inflatable dams. Details of adaptation structures and cost estimates are included in Section 6.1. The total materials and installation costs for protecting non-Boat Section Structures through 2100 was estimated to be nearly \$47 million (see Table 6-1). The materials and installation costs for watertight gates at Portals to protect the Tunnels was estimated to be approximately \$27 million under current (2013) conditions, with an additional \$19 million needed for protection through 2030. Additional costs to protect the Tunnels through late 21st century (2070 or 2100, depending on the rate of SLR) was estimated to be nearly \$150 million (see Table 6-2).

Regional adaptation solutions were also explored (Section 6.2). Whereas local adaptation options focus on protecting individual structures, regional adaptation

focuses on flood pathways, where a larger upland area is flooded by water arriving from a vulnerable section of the coastline. Regional solutions can be more cost effective than local adaptation solutions but often require coordination between and investment by multiple stakeholders. Three flood pathways that could be addressed by regional solutions were identified under current (2013) climate conditions: near the Schrafft's building in Charlestown, the East Boston Greenway and the MassDOT property on Granite Ave., in Milton. An additional flood pathway (near Liberty Plaza in East Boston) was identified under near term future conditions (by 2030). In addition to those already mentioned, a number of additional flood pathways were identified under late 21st century conditions (by 2070 or 2100), including Wood Island and Jefferies Point in East Boston, the western side of Fort Point Channel and the Charles River dam and adjacent land. Conceptual engineering strategies and cost estimates were presented (Table 6-2).

What were the major findings of this project?

This pilot project has illustrated the value of combining a state-of-the-art hydrodynamic flood model with agency-driven knowledge and priorities to assess vulnerabilities and develop adaptation strategies for a complex, interconnected system such as the CA/T. From an infrastructure maintenance and planning perspective, this vulnerability assessment offers both good news and bad. The good news is that the extent of flooding under current climatic conditions is fairly limited with low exceedance probabilities. This allows MassDOT to focus their efforts on reducing the vulnerability of individual Structures and on local adaptation strategies. The bad news is that 1) vulnerable Structures requiring major adaptation under current conditions include some Tunnel

Portals and 2) the vulnerability and number of such Portals affected more than triples by 2070. By late 21st century (2070 or 2100, depending on actual rate of SLR), there is considerable flooding at non-boat structures. Additional notable findings include:

- The interconnected and complex nature of urban environments requires interaction with multiple stakeholders at various steps in the assessment.
- The lack of redundancy and the critical nature of each structure make the CA/T system potentially extremely vulnerable.
- Results of the modeling and vulnerability assessment yielded

almost immediate project and engineering design implications that may not have been realized without the high-resolution modeling and analysis.

- In complex systems like the CA/T, the number and spatial extent of vulnerable Structures increase over time as SLR rises and the intensity of some storms increase, suggesting that local adaptation options may be most applicable in the near-term and regionally based adaptations (safeguarding multiple Structures for multiple stakeholders) will become more cost-effective and necessary solutions in the long-term.

INTRODUCTION

1.1 The Big Dig

Interstate 93 (I-93) is a nearly 200-mile long North-South major transportation corridor for northern New England, beginning at the intersection with Interstate 95 in Canton, Massachusetts and ending at the intersection with Interstate 91 near St. Johnsbury, Vermont. Built in the mid-to-late 1950's, I-93 was an elevated six-lane highway as it traversed the heart of downtown Boston. Urban fragmentation, infrastructure deterioration and traffic congestion due to heavy usage prompted the replacement of the so-called "Central Artery" of Boston with an "eight-to-ten lane state-of-the-art underground highway, two new bridges over the Charles River, [an extension of] I-90 to Boston's Logan International Airport and Route 1A, [which also] created more than 300 acres of open land and reconnected downtown Boston to the waterfront."¹

The Central Artery/Tunnel Project (CA/T), affectionately known as "The Big Dig" is comprised of more than 160 lane-miles, more than half of them in tunnels, six interchanges and 200 bridges. "...the Big Dig is modern America's most ambitious urban-infrastructure project, spanning six presidents and seven governors, costing \$14.8 billion, and featuring many never-before-done engineering and construction marvels."² Figure 1-1 shows a schematic of the CA/T system available on the MassDOT website¹.

1.2 Motivation for this Project

The CA/T system is a critical link in the regional transportation network and a vitally important asset to not only the City of

"Hurricane Sandy made us acutely aware of our vulnerability to coastal storms and the potential for future, more devastating events due to changing sea levels and climate change...Absent improvements to our current planning and development patterns that account for future conditions, the next devastating storm will result in similar or worse impacts." US Army Corps North Atlantic Coast Comprehensive Study (2015, p1).

Boston, but to the surrounding communities for which Boston is an economic focus. In the event of a disaster, the CA/T is an irreplaceable critical link for evacuation, and for emergency response and recovery services. It also serves as an essential link to Logan International airport which is the major airport in the region. For all these reasons the CA/T must be considered to have a very low tolerance for risk of failure and hence, should require the highest level of preparedness. The CA/T was designed to withstand the 0.1% flood elevation (plus wave action) for tunnel entrances and the 1% flood elevation (plus wave action) for all other facilities and assets. However, to the best of our knowledge, sea level rise was not considered during CA/T design. Hence, the CA/T and associated structures are currently vulnerable to flooding from an extreme coastal storm. This vulnerability will increase in the future due to projected sea level rise (SLR) and increases in hurricane intensities due to climate change. In order to keep Massachusetts Department of Transportation's (MassDOT) commitment to the people of the Commonwealth to

¹ <http://www.massdot.state.ma.us/highway/thebigdig.aspx>

² http://city-journal.org/html/17_4_big_dig.html

preserve and protect their public assets, it is vital to consider the implications of these new conditions and plan for their potential impacts.

The CA/T is a critical link in the regional transportation network and a vitally important asset for the Boston metropolitan area. As one of the most valuable components of Massachusetts' transportation infrastructure, its maintenance, protection and enhancement are a priority for the Commonwealth.

As was made clear by Hurricane Sandy's impacts on New York City's tunnel system, any infrastructure located near the ocean, such as the CA/T in Boston, is vulnerable to storm-driven flooding. An initial analysis (Fig 1-2) sponsored by The Boston Harbor Association (TBHA) has shown that the present 100-year coastal storm event could easily render the Central Artery tunnel system impassible or, even worse, could flood the tunnel system completely. It is now virtually certain that climate change will result in continued SLR over the course of this century. The impact on major storm events, such as hurricanes and Nor'easters, is less certain, but there is a strong possibility that hurricane intensity will increase. Both impacts will cause the risk of flooding to substantially increase over time (Kirshen et al., 2008). This pilot project represents a proactive step by the Massachusetts Department of Transportation (MassDOT) to expand on the initial work done by TBHA by assessing the Central Artery's specific vulnerabilities and prepare plans to mitigate or prevent damage from future storm events. This required a parcel-level geographical and asset analysis, a dynamic hydrodynamic modeling and engineering analysis, and extensive

cooperation and coordination among the newly-integrated divisions within MassDOT and between MassDOT and other Federal, state, and local government agencies. It also required consideration of potential physical linkages between CA/T and the Massachusetts Bay Transit Authority's (MBTA) infrastructure, particularly the MBTA Blue Line.

1.3 Project Objectives and Approach

On January 23, 2013, the project team submitted a proposal to the Federal Highway Administration's (FHWA) request for Pilot Projects: Climate Change and Extreme Weather Vulnerability Assessments and Adaptation Analysis Options program. Funding was awarded by FHWA in February 2013 and Notice to Proceed was issued by MassDOT on April 16, 2013. The objectives of this pilot project were to 1) assess the vulnerability of CA/T to SLR and extreme storm events, and 2) investigate and present adaptation options to reduce identified vulnerabilities. The results of these two project objectives support a third objective, still on-going, to establish an emergency response plan for tunnel protection and/or shut down in the event of a major storm. The project was implemented in phases (listed below), some of which occurred simultaneously (i.e., Phases 1-4) and others which were based upon previous phases (i.e., Phases 5-7):

- PHASE 1: Define Geographical Scope
- PHASE 2: Inventory of Assets
- PHASE 3: Surveys of Critical Areas of Central Artery
- PHASE 4: Hydrodynamic Analysis
- PHASE 5: Vulnerability Assessment
- PHASE 6: Adaptation Strategies
- PHASE 7: Project report and presentations

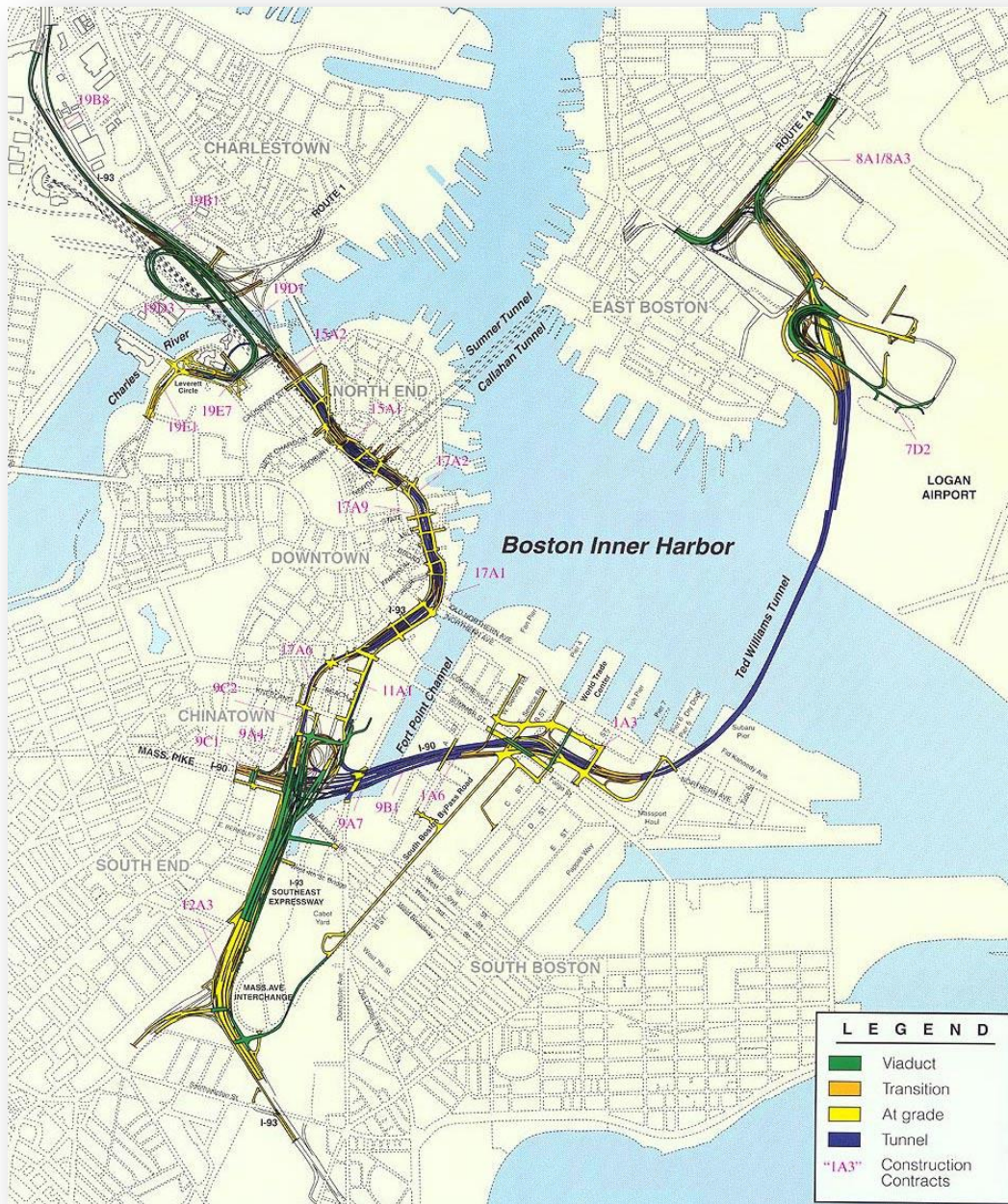


Figure 1-1. Schematic of the Central Artery/Tunnel (CA/T) system.



Figure 1-2. Potential flooding in Boston due to an extreme storm surge (5 ft) on top of spring tide. Source: www.tbha.org.

The timeline anticipated in the proposal was 18 months, but the immensity of the asset list discovered in Phase 2 (in the proposal we anticipated ~40 assets, but the actual number was over 8,000) and the much higher than expected computational requirements of Phase 4 resulted in an extension of the timeline by nearly seven months. Progress during the project was guided by input from a technical advisory committee made up of various subject experts and from MassDOT personnel. Comments from interested non-MassDOT agency stakeholders were elicited along the way through stakeholder meetings.

1.4 Overall Process

While not explicitly designed to follow the most recent FHWA procedures for climate change vulnerability and adaptation assessments, this project does follow the procedures described in some detail in FHWA (2012), specifically the three step process of defining the scope and objectives, assessing the vulnerability of the CA/T system and ultimately, incorporating this information into decision making. This approach is summarized in Figure 1-3. The fourth assessment report (AR4) of the Intergovernmental Panel on Climate Change (IPCC, 2007) defines vulnerability as "the

Vulnerability is assessed by evaluating the system's exposure, sensitivity and adaptive capacity.

degree to which a system is susceptible to, and unable to cope with, adverse effects of climate change, including climate variability and extremes". Vulnerability is assessed by evaluating the system's *exposure, sensitivity and adaptive capacity*. *Exposure* identifies the degree to which the system will be impacted by climate change and extreme weather events. For example, is a roadway exposed to potential flooding, and if so, how severely? For this project, our analysis of exposure was limited to potential flooding due to coastal storm surge and wave action

resulting from extreme coastal storms (hurricanes and Nor'easters) combined with sea level rise. Some consideration was given to river flooding. *Sensitivity* refers to how the system responds to the identified impacts. For instance, if the roadway is flooded, how does this effect system performance; is the roadway completely impassable or will closure of one lane suffice? *Adaptive capacity* refers to the ability of the system to accommodate impacts and/or recover from the impacts. For instance, if a roadway is flooded, does the roadway drainage system have the capacity to transmit the flooding away from the road quickly so that traffic flow is minimally impacted or are there alternative routes?

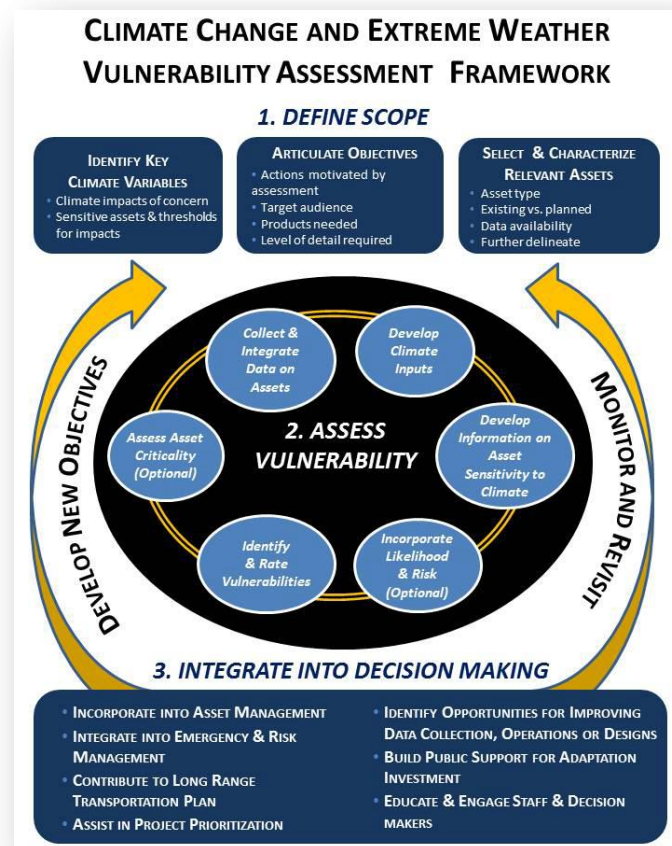


Figure 1-3. FHWA framework for assessing the vulnerability of transportation systems to climate change and extreme weather (source: Fig 1 from FHWA, 2012, pg 2).

A brief summary of our approach is as follows:

Step 1: Assess current vulnerabilities: Compile available information about current system stressors and how climate change may exacerbate those stressors or create new stressors to the system in the region and sector of interest. Analyze system exposure, sensitivity and adaptive capacity to current extreme events.

Step 2: Estimate future conditions: Select target timeframes and project climate change impacts. Given inherent uncertainties, quantify how these impacts will affect current system stressors. Our selected timeframes are 2013, 2030, 2070, and 2100.

Step 3: Assess future vulnerabilities: Analyze system exposure, sensitivity, and adaptive capacity to identified future impacts.

Once the current and future system vulnerability was assessed and quantified, the next step was to develop conceptual adaptation strategies that would be used by MassDOT to develop a strategic plan for reducing vulnerability and improving system recovery under current and future extreme conditions.

1.5 A Comparison of this Study with Others

Previous vulnerability studies in Boston, and even those concurrent to this one, have relied on either a “bathtub model” approach (i.e., the TBHA study results shown in Fig 1-2) or on simplified empirical or statistical models for assessing the impacts of sea level rise and storm surge on populations and property. Our study is unique for Boston in that we have developed a high resolution (grid cells on the order of 5 meters), physically-based, coupled hydrodynamic-wave numerical model that considers

spatially-varying bathymetric, topographic and frictional characteristics to quantify the magnitude and extent of flooding along the highly urbanized Boston coastline. Our approach is also unique in that rather than relying on one or several storm scenarios (i.e., a Category 3 hurricane) to assess vulnerability, we invoked a Monte Carlo storm simulation approach that allowed us to quantify the exceedance probabilities associated with flood depths at any location in the model. Furthermore, other studies (including FEMA Flood Insurance Studies) have performed only rudimentary or historically-based analysis of extratropical storms (known in New England as “Nor’easters”) which are known to be generally more damaging in New England than hurricanes because of their longer duration (typically 24-36 hours), their higher frequency (2 to 3 per year, on average) and their tracks (generally from the northeast, aligning with the opening of Massachusetts Bay). Because more than 70 percent of the annual maximum storm surge heights measured at the Boston tide gage resulted from “Nor’easters”, we included a large dataset (more than 200) of historical extratropical storms in the Monte Carlo storm simulation approach and estimated the probabilities of flooding from tropical and extratropical storms in quantifying flood exceedance probabilities.

Concurrently with this pilot project, the US Army Corps of Engineers (USACE) has been performing the North Atlantic Coast Comprehensive Study (NACCS; USACE, 2015). The motivation and approach of the NACCS are roughly similar to our pilot project, but the scope and project outputs are much broader in spatial extent. Initiated in response to the widespread devastation of Superstorm Sandy, the geographic scope of the NACCS is the US Atlantic coast from Virginia to Maine. The goals of the NACCS were to: “provide a risk management

Our study is unique for Boston in that we have developed a high resolution, physically-based, coupled hydrodynamic-wave numerical model to quantify the magnitude and extent of flooding along the highly urbanized Boston coastline.

framework consistent with the NOAA/USACE Infrastructure Systems Rebuilding Principles and support resilient coastal communities and robust, sustainable coastal landscape systems, considering future sea level and climate change scenarios, to manage risk to vulnerable populations, property, ecosystems, and infrastructure” (USACE, 2015). Similarities and differences between the NACCS and this pilot project are summarized below:

- Both studies followed a similar progression, beginning with delineation of geographic scope and identification of stakeholders and technical reviewers, utilizing numerical modeling and inundation mapping to assess risk, performing vulnerability analysis on affected communities and properties and identifying potential adaptation strategies to mitigate the vulnerabilities.
- Both studies used coupled hydrodynamic-wave numerical modeling and simulated a large number of synthetic tropical storms and historical extratropical storms to support a probabilistic flood vulnerability analysis. While the spatial extent of our hydrodynamic model grid was essentially identical to the NACCS, the resolution of our model grid in Boston Harbor and the surrounding communities was much higher (~5 m vs ~50 m per Winkelman, USACE, personal communication, Jan 30, 2015) as would

be expected for a pilot study focused on the CA/T system.

- NACCS simulated ~1,000 synthetic hurricanes, while our pilot project utilized a subset (~400) of over 20,000 synthetic tropical storms based on their direct impact on Boston and a larger number of historical extratropical storms (>200 vs 100 in NACCS) to develop exceedance probability distributions at each model node.
- Both studies selected scenarios of future sea level rise from peer-reviewed sources. However, in our pilot project modeling study, we accounted for a changing climatology after 2050 in the hydrodynamic model, whereas the NACCS used the same climatology for all simulations (Winkelman, 2015).
- A major difference between our pilot project and the NACCS lies in the way in which land-based inundation was evaluated. The NACCS model grid did not extend significantly onto land, whereas our model grid extended inland to the 30 ft (10 m) NAVD88 elevation contour. The extent of coastal flood hazard in NACCS was determined using flood maps created by FEMA and NOAA. The implications of this major difference in approach include: 1. Our model was able to account for the effects of the built environment on hydrodynamics and flood depths (using friction factors); 2. The computational requirements for our model runs increased exponentially with each climate change scenario (i.e., 2030, 2070/2100) because of a dramatic increase in inundated model nodes with each scenario; and 3. whereas the NACCS utilized FEMA and NOAA flood maps to determine the extent of vulnerability to coastal flooding, our model simulated flood depths at CA/T structures directly.

Hence, vulnerability was assessed directly from model output in our pilot project whereas it could only be interpolated from off-shore model output in the NACCS. While uncertainties exist in both approaches, we believe that direct land-based flood modeling resulted in less uncertainty in our infrastructure vulnerability analysis. However, this is not meant as a criticism of the NACCS study but rather as an expected outcome given the focus of our study.

- Infrastructure exposure and vulnerability were the primary focus of our pilot study while infrastructure was only one of several vulnerability indicators quantified in the NACCS. However, the model output from our pilot study can be used in future studies to quantify similar socio-economic and ecological indicators to those in the NACCS. In fact, in a follow-on project funded by MassDOT, we are refining the pilot project model grid along the entire Massachusetts coastline in order to develop indicators of socio-economic, ecological and infrastructure based vulnerability for coastal Massachusetts.

GEOGRAPHICAL SCOPE AND DATA GATHERING

The goals of this initial information gathering task were to determine the exact boundaries of the potentially critical areas of the CA/T for the purposes of this study, and to develop GIS datasets that represent MassDOT Assets³ associated with the CA/T system. Activities associated with this task included acquisition and review of data provided by MassDOT, field visits to various CA/T Assets and meetings with knowledgeable MassDOT staff. The final result of these activities was to define the geographic scope of this study as the entire CA/T system. The following discussion summarizes the progression of events that led to this decision. In general, MassDOT and the Project Team determined that the CA/T system comprises numerous interdependent systems, and that the “potentially critical areas of the CA/T” encompass the entire CA/T system.

2.1 Preliminary Data Acquisition

An introductory meeting was held with MassDOT GIS staff to acquire GIS data relevant to this project. On May 20, 2013, Chris Watson and Katherin McArthur met with Kevin Lopes and David Dinocco of MassDOT Highway Planning to discuss the scope of the project and coordinate delivery of GIS data to UMass Boston. Subsequent to this meeting, MassDOT provided to UMass Boston an ESRI-format geodatabase (BostonData.mdb) for use by the Project Team. This geodatabase primarily contained point, line and polygon feature classes (GIS datasets) representing MassDOT Assets associated with the CA/T,

³ Assets, as well as a few other specific terms such as Facilities, are treated as proper nouns for the purpose of this report and as such are defined in Chapter 3 below. Prior to the completion of Phase 1, we did not have working definitions of Assets and Facilities, which were developed as part of Phase 2.

The geographic scope of this study encompasses the entire CA/T system. Because it contains numerous interdependent systems, the entire CA/T system was determined to potentially be at risk.

and several feature classes that were derived from other public sources (e.g., MassGIS and Boston Redevelopment Agency). A listing of these feature classes is provided in Appendix I. Metadata for these feature classes was not provided by MassDOT. These datasets were reviewed by UMass Boston and were the basis for the preliminary evaluation of CA/T Assets, as discussed in more detail below. Additionally, MassDOT staff also provided several CAD record drawings in both CAD and PDF format as additional data sources. These record drawings were reviewed and relevant information was either converted from CAD to GIS, manually digitized into GIS from the PDFs, or recorded on an as-needed basis for later review. A summary of data provided by MassDOT is provided as Appendix I.

2.2 Tunnel Tour

On June 5, 2013, from approximately midnight until 3AM, the entire Project Team, including UMass Boston interns Connor McKay and Joe Choiniere, were escorted by MassDOT staff on a tour of representative CA/T Assets. Tour Guides were David Belanger, Dan Mulally, and Bob Hutchen of MassDOT. Rebecca Lupes of FHWA also joined us. The tour began in the parking lot for the District 6 Headquarters Building (185 Kneeland Street) and progressed to the following CA/T Assets:

- Storm Water Pump Station 9 (D6-SW09-FAC⁴) – a standalone building located behind 185 Kneeland Street
- Vent Building 3 (D6-VB03-FAC) – a facility located both inside and below the InterContinental Hotel on Atlantic Avenue
- Low Point Pump Station 7 (D6-LP07-FAC) and Tunnel Egress 405 (TE405) – facilities located within Vent Building 3
- Air Intake Structure (D6-AIS-FAC) - a facility (outside observation only) and a street-grade air vent grate associated with Low Point Pump Station 4 (D6-LP04-FAC) located at the intersection of Atlantic Avenue and Congress Street
- Vent Building 4 (D6-VB4-FAC) – a facility located on John F. Fitzgerald Surface Road
- Low Point Pump Station 8 (D6-LP08-FAC) – a facility located within Vent Building 4
- Ramp SA-CS (BIN7EK) and Ramp SA-CT (BIN7F6) – entrance ramps to I-93 Southbound and Callahan Tunnel generally located adjacent to Vent Building 4 – also observed stormwater curtain drains on these ramps
- District 6 Highway Operation Center (D6-HOC-FAC) – a facility located on Massport Haul Road
- Ventilation Buildings with multiple air intakes, fans, motors, controls, people and equipment entrances
- Pumps and Water Intakes and Outlets
- Conduits for Electrical and Other Utilities
- The Highway Operations Center

2.3 Initial Review of Assets

We performed an initial assessment of CA/T assets within the project domain using GIS and CAD data provided by MassDOT and found that the number of potential Assets that would need to be cataloged and investigated was considerably larger than had been envisioned in the original proposed scope and timeline of this pilot project (see Figure 2-1). Based on this information, we revised our approach in the following ways:

1. We developed a “mini-pilot” approach, where we selected Assets within the CA/T domain to use in methodology development and testing (described in Sec. 2.4) before expanding to the entire system; and
2. We pursued what became known as “Institutional Knowledge (IK)” meetings (described in Sec. 2.5), which brought in the key MassDOT personnel whose expertise helped us focus on the appropriate Assets and to prioritize the appropriate risk and vulnerability approach.

Based upon the June 5 tunnel tour, a tentative list of vulnerable roads, facilities, and equipment were identified:

- Tunnel Entrances and Exits
- Tunnel Egresses

⁴ See Section 2.6 below for discussion of the Maximo asset management system. Although Maximo was not in use by MassDOT District 6 in June 2013, Maximo codes are included here for reference.

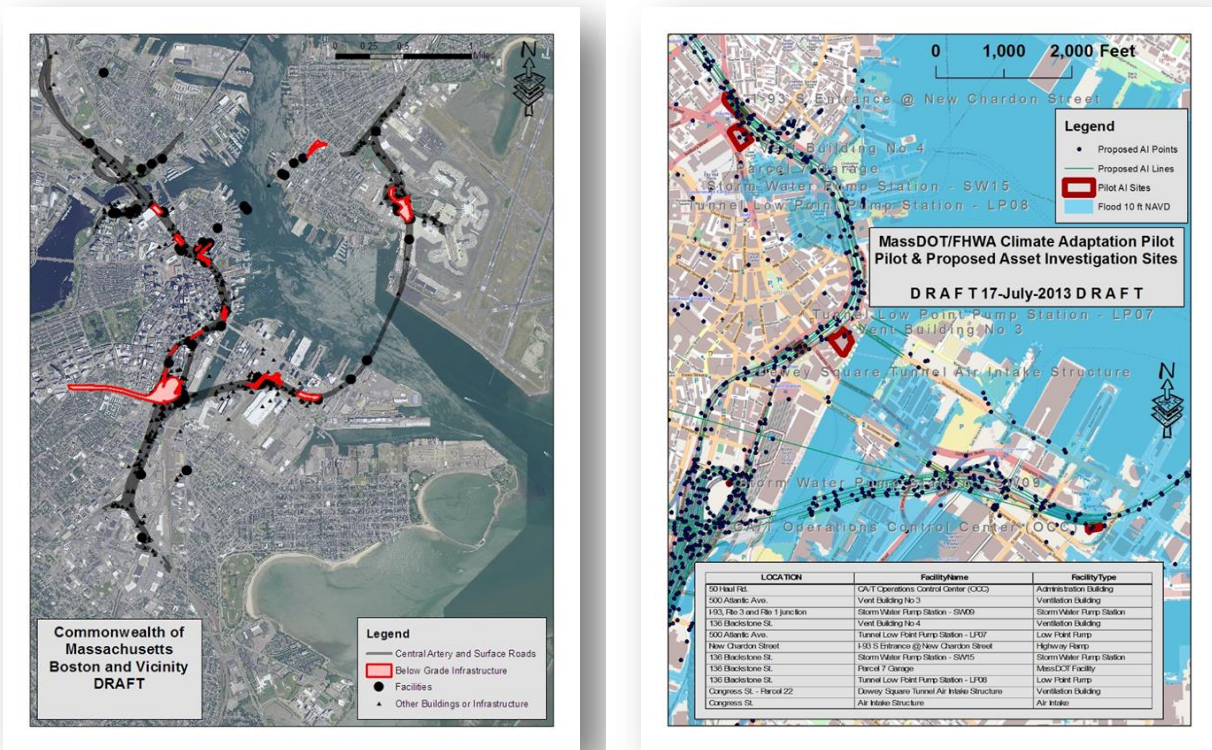


Figure 2-1. On left, the assumed number of assets to be evaluated in this pilot project (~40) compared to, on right, a representation of the number of assets that actually existed within the system (on the order of thousands).

2.4 Mini-Pilot Asset Inventory

The purpose of the mini-pilot approach was to develop and assess the inventory and vulnerability assessment methodology using a subset of CA/T Assets. The results of this task, combined with the “Institutional Knowledge” methodology, would also help to better define an approach for the Phase 2 full-scale Asset Inventory and allow us to identify a common language and set of Asset identifiers across datasets and personnel. For the mini-pilot Asset Inventory, we selected the representative Assets that we visited during the June 5, 2013 tunnel tour (see Section 2.2 above for a list of these Assets). The next step in the mini-pilot task was to visit each site in the field to collect photographs and other

relevant data. Field visits proceeded during the months of July and August, 2013, and an on-line gallery⁵ of photographs was developed for reference by the Project Team. During the field visits, potentially vulnerable features were identified, photographed and measured for height above ground surface using a survey rod. A sample of the photo gallery is provided in Figure 2-2.

⁵ This on-line gallery is no longer available and the photographs have been archived at Mass DOT Highway D6.

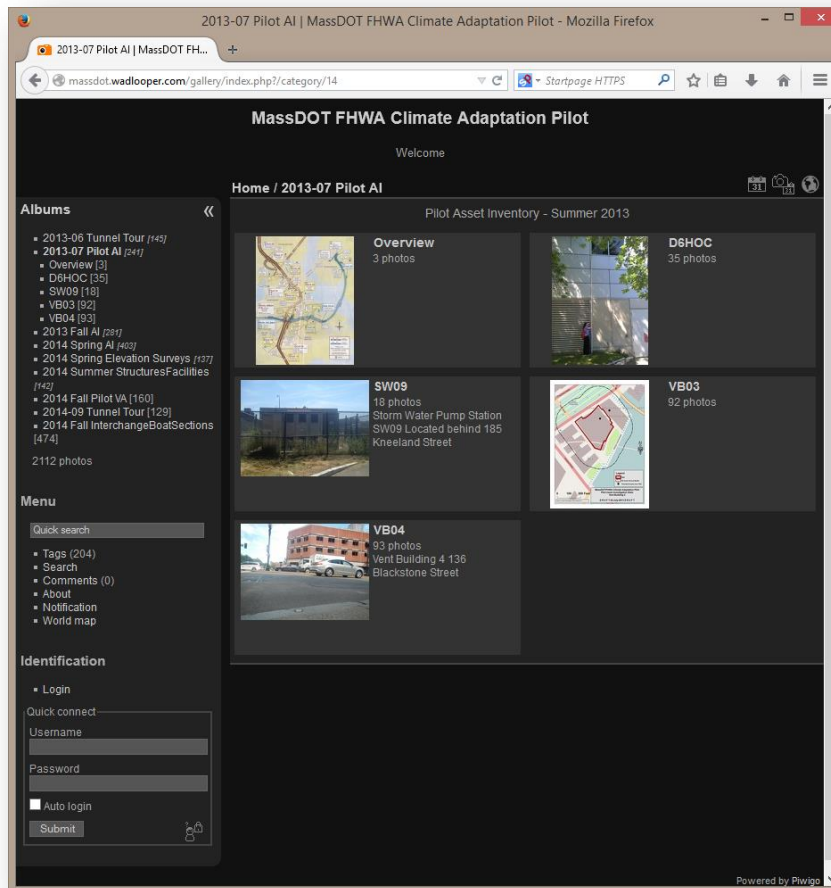


Figure 2-2. Screen shot of photo gallery archiving system developed for this project.

2.5 Preliminary Institutional Knowledge (IK) Meeting – July 26, 2013

A preliminary meeting was convened at MassDOT headquarters on July 26, 2013 to develop an approach for incorporating the institutional knowledge of key MassDOT personnel to prioritize Assets that needed to be investigated for the Asset inventory and vulnerability assessment. Project Team members met with Dan Mullaly to discuss how best to implement the proposed institutional knowledge (IK) approach. Mr. Mullaly is a Senior Electrical Engineer at MassDOT Highway Division 6 (D6). Additionally, prior to his employment at MassDOT, Mr. Mullaly was involved with

the construction of the CA/T system. Mr. Mullaly is particularly knowledgeable about the entire CA/T system and was, and continues to be, a significant resource for this project.

The primary focus of this initial meeting was to begin the detailed identification of CA/T Assets and to identify key MassDOT staff that could assist with this effort. Additionally, we discussed the need to obtain elevation and location data for the CA/T Assets. Mr. Mullaly provided the names of several key personnel, each of whom had specialized knowledge related to various types of CA/T Assets. Additionally, Mr. Mullaly provided a CA/T reference map

(see Figure 2-3) and information related to the IBM Maximo Asset and Maintenance Management System (Maximo), a centralized asset-management database system which was, in June 2013, in the process of being implemented for Highway Division 6 (D6). Additional information related to Maximo is discussed in Section 2.6.

The overall result of this meeting was a plan to coordinate meetings with appropriate D6 personnel to review and discuss the relevant GIS data presented on large-format plotted maps. Additionally, based on information obtained at this preliminary IK meeting, the Project Team revised and refined the Mini-Pilot Asset Inventory Screening Analysis as follows:

- The 10-foot NAVD88 flooding elevation data available from the 2012 TBHA report would be used to focus the IK process on the Assets most likely to be flooded during the present-day 100-year coastal flooding event.
- Elevation surveys would proceed without the assistance of a licensed surveyor (LS), using elevations obtained during the review of record drawings and from measurements (height above ground surface) obtained during the field visits. Elevations could then be confirmed by an LS at a later date.

2.6 *Maximo*

Maximo is a centralized asset-management database system currently being implemented for the Highway Division. As recommended by Mr. Mullaly, we contacted the Maximo project manager, Donna Lee. Ms. Lee explained that Maximo had been implemented across a majority of MassDOT Highway districts and was now focused on D6. Assets in the Maximo database would have a unique identifier and meetings to

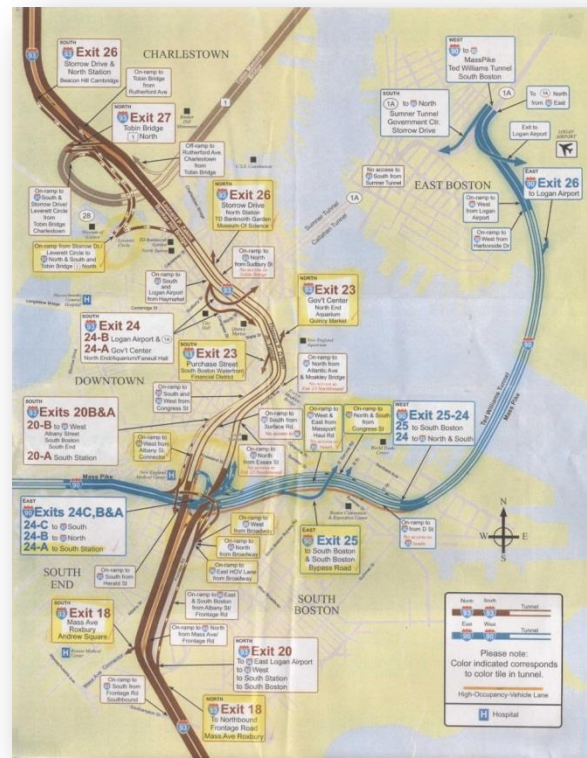


Figure 2-3. Example map provided by MassDOT District 6 staff at preliminary IK meetings.

discuss the hierarchy of D6 assets were ongoing. Ms. Lee also recommended and facilitated our access to the MassDOT D6 SharePoint site for the Maximo project. From this SharePoint site we obtained additional general information about Maximo and some record drawings related to the CA/T system that turned out to be particularly valuable to this project.

The overall purpose of Maximo is to replace the paper-based work order management system currently in use at the Division's Districts. The initial deployment of Maximo focused on signs, drainage components, drainage maintenance, mowing, sweeping, and road repair. Future asset classes and deployments may include lighting, facilities, ITS components, pavement markings, guardrails, signalized intersections, fence lines, and other assets. Maximo will also integrate with the Highway Department's

existing technologies, specifically GIS and the Massachusetts Management Accounting and Reporting System (MMARS, an internal accounting system). Additionally, for D6, the Maintenance Management Information System (MMIS) will be converted to Maximo and Maximo will be configured to track work performed on District 6 tunnels and bridges (MassDOT, 2013). However, because Maximo implementation was ongoing, and thus data were not yet available, Ms. Lee recommended contacting Mr. Geoffrey Rainoff, MassDOT D6 Highway System Civil Engineer, to obtain a copy of MMIS. She explained that the D6 Maximo database would incorporate the MMIS data, and that MMIS was likely available now for our use.

2.7 MMIS

We then contacted Mr. Rainoff to obtain a copy of available MMIS data. Mr. Rainoff explained that MMIS is a legacy work order program used primarily by the MEC (mechanical/electrical/communications) group at the D6 and includes an inventory of the D6 facility and roadway assets. Other modules (not reviewed as part of this project) include work orders, preventive maintenance scheduling templates and a preventive maintenance task library, along with miscellaneous support tables. The program has been in use since approximately 1998. The MMIS database contains facilities pertaining to the Central Artery and Massachusetts Turnpike operations. MMIS defines a facility as a ventilation building, pump station, electrical substation, toll plaza, maintenance facility, emergency response station, or administration building, etc. Mr. Rainoff provided us with three exports from MMIS:

- Vent Building Equipment List
- Pump Station Equipment List
- Other Structure Equipment List

We then imported these into a relational database and began the process of reviewing these data and correlating these equipment lists with the Assets known to date. We then correlated the data from MMIS, with the GIS Facility point features provided earlier. Additionally we were able to confirm that the entire collection of GIS and MMIS Assets were indeed too numerous to evaluate during this project. At this point we began to focus only on Facilities as defined in MMIS (ventilation building, pump station, etc.) and deemed critical by IK experts.

2.8 First Institutional Knowledge (IK) Meeting – September 16, 2013

Using the GIS and MMIS data, we developed a tentative map of CA/T Facilities flooded at a water level of 10 feet NAVD (based on TBHA data) for review at the first formal IK meeting with Dan Mullaly and Rick McCullough (Figure 2-4). This map divided the tentative project area into grids for detailed review by the IK team. A section of one of the detailed grid maps, including corrections and revisions collected at the meeting is shown in the left column of Figure 2-5. The primary result of this first IK meeting was a more complete understanding of the extent of the CA/T system and a collection of corrections and revisions to the GIS data. Additionally, Mr. McCullough provided several other maps and data sources for our use.

2.9 Second Institutional Knowledge Meeting – October 22, 2013

Using the corrections and revisions obtained at the first IK meeting, we developed a second CA/T map based on all information known to date (similar to the schematic map shown in Figure 1-1). This map again divided the tentative project area into grids for detailed review by the IK team. An example of corrections and revisions

collected at the second meeting is shown in the right column of Figure 2-5. The primary result of this second meeting was a final working definition of the extent of the CA/T system, as described below:

- West: Prudential Tunnel stormwater flows into SW07 which discharges into Fort Point Channel
- South: SW11 flows into SW12 which discharges into Fort Point Channel
- East: SW06 (Massport Facility) - failure of which has the potential to impact the

Ted Williams Tunnel via stormwater surface flow

- North: CANA (Central Artery North Area) tunnels

Other results of this meeting were additional insights on outfalls, Combined Sewer Outfalls (CSOs) and sanitary sewers and their interdependence/ interconnections with other systems (BWSC, Massport, etc.). The IK team also reaffirmed the previously identified need to coordinate with MBTA, particularly the Blue Line at the Aquarium Station.

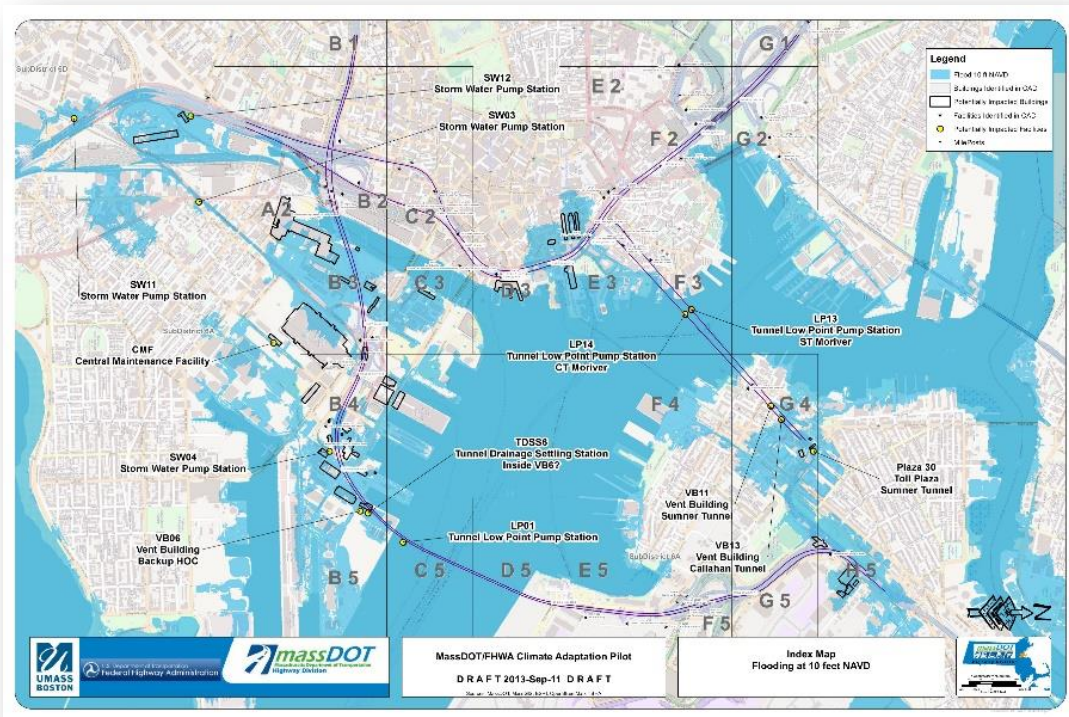


Figure 2-4. Map created for first IK meeting.



Figure 2-5. Magnified sections of maps used in IK meetings, showing annotations.

2.10 Geographical Scope of the Potentially Critical Areas of the CA/T

A significant result of the second IK meeting was that MassDOT and the Project Team determined that the CA/T system comprises numerous interdependent systems, and that the “potentially critical areas of the CA/T” encompass the entire CA/T system. This decision, in combination with the working definition of the extent of the CA/T system, completed this phase of the project. However, we also realized that the development of GIS datasets that represent MassDOT Assets associated with the CA/T system was far from complete, and this portion of the task would require additional efforts, as described in Chapter 3.

2.11 Technical Advisory Committee Meetings

The Technical Advisory Committee (TAC) was made up of the following people with expertise in modeling, the impacts of flooding or related policy:

- Norman Willard, US Environmental Protection Agency, (USEPA; replaced by

Lisa Grogan-McCulloch when Mr. Willard retired), Region 1

- John Winkelman, US Army Corps of Engineers (USACE)
- Rob Thieler, US Geological Survey (USGS), Regional Climate Services
- Rob Evans, Woods Hole Oceanographic Institution (WHOI)
- Ellen Mecray, National Oceanographic and Atmospheric Administration (NOAA)

The purpose of the TAC was a sounding board for methodology and to review the technical approach as appropriate. The first TAC meeting was held in Woods Hole, Massachusetts on July 9, 2013 from 10:00am to 12:00pm. The entire project team (Steve Miller and Katherin McArthur of MassDOT, Ellen Douglas and Chris Watson of UMass Boston, Kirk Bosma of Woods Hole Group, Inc. and Paul Kirshen of UNH) attended. The meeting began with a presentation of the project objectives and approach. Then the TAC members summarized their areas of expertise that could be helpful to the project and relevant datasets that they had access to. The

outcome of this meeting was a list of relevant datasets and other suggestions for the project. All agreed that a one-week lead time would be sufficient to review technical memos and other communications from the project team. Table 2-1 summarizes TAC expertise and suggestions made during the TAC meeting.

The TAC reviewed and commented on technical memos created during the course of the project (i.e., the sea level rise memo and the storm climatology memo included in Appendix II). A second TAC meeting was convened on January 30, 2015 to review the modeling approach and results. All members of the original TAC were present with the exception of Norman Willard of the EPA, who had retired and was replaced by Lisa Grogan-McCulloch, also of the EPA. An hour-long presentation of our modeling methodology and preliminary results was given. There were a few comments/suggestions made during this meeting:

- A comparison between our model and the NACCS study model should be made.
- The methodology and results of the extratropical dataset will need to be peer-reviewed. Suggestions were made about who would have the expertise to do such a review.
- It would be an interesting exercise to select a structure and quantify the various uncertainties (model, terrain, interpolation, etc.) and perform a sensitivity analysis on reliability.
- For public release, we should consider using risk categories similar to those used in IPCC AR5.

2.12 MBTA Tunnel Tours

Field visits to several Massachusetts Bay Transportation Authority (MBTA) subway tunnels were coordinated with MBTA staff to

facilitate our understanding of potentially vulnerable interconnections with the CA/T tunnels. Peter Walworth of the MBTA escorted us on two tours: the Silver Line below South Station and the Blue Line below Aquarium Station.

2.12.1 Silver Line at South Station

The tour started at the inbound Silver Line tunnel below South Station. This area is the westbound terminus for Airport and Seaport buses and no passengers are allowed past this point. A vent tunnel leading upwards to an area adjacent to the sidewalk entrance stairs for the South Station bus terminal was observed. In a utility room at tunnel level, a sump was observed that is allegedly connected into the CA/T (to date this connection has not been confirmed). The CA/T Tunnel Egress 201 adjacent to South Station that had not been previously located during the inventory of CA/T Facilities was also discovered.

2.12.2 Blue Line at Aquarium Station

The tour began in the Aquarium Station fare-access level for the Blue Line where a slurry wall existed; likely associated with the CA/T inside a maintenance closet. From this same closet on the fare-access level, a stairway was accessed that led up to the surface level and down to a dark flooded hallway. Mr. Walworth, previously aware of the flooding and lack of operating light fixtures, had brought a set of wading boots and an industrial-strength flashlight allowing access past the flooded area to a door that opened onto CA/T Ramp CN-SA. The tour ended at street level and identified Tunnel Egress TE-434, which had also not been previously located during the inventory of CA/T Facilities.

Table 2-1. Expertise and input from the first TAC meeting.

TAC Member	Related Expertise	Suggestions Made
Norman Willard, EPA, Region 1	EPA has a statutory responsibility to wetlands, water quality with a transportation focus. The agency and regional office also have initiatives related to smart growth, sustainability, and climate change impacts and adaptation.	<ul style="list-style-type: none"> to the extent possible, show how results can apply to other parts of the country. to the extent possible, make the information accessible to individuals and lay people. be prepared to answer why we chose 2030, 2070 and 2100.
John Winkelman, USACE (Corps)	Corps is doing a comprehensive, \$5M study along the eastern seaboard from the Carolinas to the Canadian Maritimes. Output will be water level at every km. Resolution will be about 50 m for the entire coastline. Using a joint probability approach for storm generation.	
Rob Thieler, USGS	<ul style="list-style-type: none"> Beach and dune erosion model. Hurricanes, Nor'easters will be included. Integrating LiDAR collection in the sandy zone (broadly defined), target date is Fall 2013. May include our study area. Timeframe for flyover is fall leaf off and then delivery in May 2014. Working with Northeast Climate Science Center, Kevin McGonagall. Identify areas that will experience inundation from SLR from VA to Canada. First results will be Fall 2013. Will highlight potential areas of change. 	<ul style="list-style-type: none"> interested in how to make this information accessible. will harvest information from our memos about urban area responses. What is the state of our knowledge about how these dynamically responding coasts are affected by SLR? would be best to cast everything in a probabilistic framework, related to IPCC probability scale, (i.e. Highly likely, likely).
Rob Evans, WHOI	Working with a coupled, nested, basin scale storm surge model, they are well aware of the pitfalls of storm surge modeling. Working with Kerry Emanuel of MIT, who has a synthetic model that generates a large suite of storms that can generate the statistics that elucidate storm frequencies. Can provide insight into what it represents.	
Ellen Mecray, NOAA	NOAA is building partnerships with infrastructure people, university networks, and NYC stakeholders. NOAA can offer storm frequency and river inflow information. Currently working on a blending of storm surge and wave modeling.	

2.13 Stakeholder Engagement

A key priority for this project has been to develop products that, to the degree possible, are useful to other Boston agencies and stakeholders who are doing adaptation work. We provided a project summary fact sheet (see Appendix III) to anyone interested in knowing more about the project. We convened two stakeholder meetings during the project, one near the beginning to outline our approach and our anticipated deliverables and the other towards the end, to obtain feedback about preliminary findings and maps. Stakeholders who showed interest in attending this meeting included:

- Carl Spector and Stephanie Krueel, City of Boston
- Vivien Li and Julie Wormser, The Boston Harbor Association (TBHA)
- Steve Woelfel, MassDOT planning
- Rich Zingarelli, Massachusetts Department of Conservation and Recreation (MassDCR) hazard mitigation
- Elizabeth Hanson, Formerly of Massachusetts Executive Office of Environmental and Energy Affairs (EOEEA)
- Daniel Nvule and Stephen Estes-Smargiassi, Massachusetts Water Resources Authority (MWRA)
- Sarah White and Julia Knisel, Massachusetts Coastal Zone Management (MassCZM)
- John Bolduc and Owen O’Riordan, City of Cambridge
- William Pisano, MWH Global (consultant to City of Cambridge)

- Natalie Beauvais and Lisa Dickson, Kleinfelder (consultant to Cambridge and Massport)
- Marybeth Groff, Massachusetts Emergency Management Agency (MEMA)
- Kathleen Baskin and Vandana Rao, EOEEA
- Charlie Jewell and John Sullivan, Boston Water and Sewer Commission (BWSC)
- Robbin Peach, Massport
- William A. Gode-von Aesch, MassDCR

The first stakeholder meeting was held on August 15, 2013 from 3:00 to 4:30pm at MassDOT headquarters. The meeting started with a presentation of the project objectives, approach and anticipated deliverables. The meeting generated a great deal of positive and informative discussion, which yielded the following suggestions (mostly related to datasets that may be useful): the updated version of the coastal structures inventory offers higher resolution for sea walls and barriers; the new FEMA transects would have up to date coastal information; Army Corps hurricane inundation maps may be useful; and final model output should be in a format suitable for incorporation into MassGIS. There was also discussion on how to “roll out” the results to the public because the public is starting to engage in this issue and it is important to refine the message before public release.

During the development of the project, a key priority became the development of products that would be useful to other Boston agencies and stakeholders.

A second stakeholder coordination meeting was held on September 24, 2013 as a result of the intense interest in the outcomes of this project, as well as the concern for a coordinated message from BWSC, City of Cambridge and MassDOT about the potential for future flooding in Boston. To ensure that common questions about model output would be addressed by the project team in a consistent manner, an FAQ sheet about the hydrodynamic modeling was created. This Frequently Asked Question (FAQ) document is included in Appendix III.

The final stakeholder meeting was held on November 24, 2014 from 1:00 to 3:00 pm at Boston Water and Sewer Commission headquarters. The first hour was devoted to presenting the methodology of the hydrodynamic modeling as background for understanding the details of the preliminary outputs in the form of probability and depth of flooding maps, which were presented. The purpose of this meeting was not to release maps but to get feedback from stakeholders with respect to map colors, legend, presentation, and usefulness of model output. The overwhelming consensus from the meeting was the maps and other model output would be extremely relevant and useful to all stakeholders. There was a great deal of discussion regarding the public release of maps and other products that would be useful to stakeholders. Some of the suggested additional products included maps of years until action is necessary, a user's guide for maps and other model output, a mapping webtool, a comparison of output from the various modeling efforts in Boston (i.e., TBHA, Massport, BWSC), and

a tool for teaching the public about risk. Most of these suggestions were outside of the scope of this current project, but could be considered in the future with additional time and funding.

2.14 Other Informational and Coordination Meetings

As this pilot project progressed, other groups and organizations, both within and outside of MassDOT, became interested in the anticipated outcomes. As noted in Sections 2.8 and 2.9, MassDOT employees were engaged through various IK meetings to explain data needs and in return were provided valuable information regarding internal data sources and the effects of flood water on the CA/T system. Details on the technical approach and expected products were provided to regional stakeholders such that the results of the FHWA pilot study could be integrated into their climate change related projects. For instance, through this project MassDOT became a key agency in the development of the Massachusetts Environmental Policy Act considerations for Climate Change and Sea Level Rise. This type of stakeholder engagement was also valuable in potential design projects. For example, designers working on the Rose Kennedy Greenway Parcel Cover Project engaged MassDOT for information on flood risks in the areas of Parcels 6, 12, and 18. Appendix IV lists additional meetings that occurred as a result of this project and represents the depth of interest generated by this type of engagement.

ASSET INVENTORY AND ELEVATION SURVEYS

During project scope development, we anticipated that the completion of Phase 1 would provide us with a complete understanding of the CA/T system as well as an accompanying GIS database such that all potential vulnerabilities to the system could be understood. As described in the proceeding chapter, due to both the complexity of the system and the lack of data available for use on this project, these objectives proved elusive. Therefore, the project plan was revised to address these issues, and having both a working definition of the CA/T and a clear definition of the extent of the project area, allowed us to begin (1) systematically identifying CA/T Assets and Facilities and (2) develop a GIS needed to support the Vulnerability Assessment (VA). Effectively, the revised plan was self-supporting: refinement to the GIS proceeded in parallel with the Detailed Asset Inventory (Field Visits) and Elevation Surveys, with each activity informing the others. Overall, this process was successful and sufficient information was gathered and processed to support the Vulnerability Assessment, as discussed in this Chapter. However, as also discussed in Section 3.4, significant datagaps still exist at the completion of this pilot project. Recommendations related to these datagaps are discussed in Section 3.4 (as well as in other sections of this report as applicable).

3.1 Detailed Asset Inventory (Field Visits)

Numerous field visits to known CA/T Facilities were performed following the methodologies developed for the “mini-pilot” described in Section 2.4 above. As new Facilities were discovered during the GIS development, these Facilities were added to the list of field visits to be performed. As new Facilities were

identified during the field visits, these Facilities were added into the GIS. This asset inventory work for the CA/T pilot project was designed to interact immediately with Maximo. MassDOT is planning to include climate change resilience into the new risk based asset management plan requirements.

3.2 Elevation Surveys

In order to ground truth existing elevation information (e.g., LiDAR) available for model development, target elevation surveys were conducted at critical flood pathway locations. A preliminary identification of potential areas of the most critical flood pathways and flooded areas was performed using a combination of GIS, field visits, and early model results. However, after completion of this preliminary but extensive list of areas, the development of the dynamic model (BH-FRM) grid had proceeded to the extent that many of these areas could be eliminated because the model did not require additional elevation information in these areas. Therefore, a short list was developed and reviewed in more detail, again using a combination of GIS and field visits.

This short list was eventually reduced to four areas where elevation information was incomplete:

- Beverly Street area (south of the Charles River Dam)
- Schrafft’s Building area (Mystic River at the Route 28 bridge)
- MBTA Aquarium Station area (Atlantic Avenue)
- Fort Point Channel area (Amtrak/MBTA property abutting the intersection of I-90 and I-93)

For the first three of these four areas, elevation surveys were performed by MassDOT survey crews and the results were incorporated into the model grid. We attempted to gain access to the fourth site for several months but ultimately were unsuccessful because of restrictions by Amtrak and MBTA. Hence, the elevation survey of the Fort Point Channel did not occur prior to completion of this report, and is therefore identified as a data gap. To accommodate this missing information, we reviewed existing field data and photographs and adjusted the model grid accordingly. These adjustments were sufficient to allow model runs to proceed, but the missing information could potentially impact the post-processing in these areas⁶. As discussed in sections that follow, review of the BH-FRM model results for this area for the 2013 and 2030 scenarios indicated that these particular areas are likely not impacted by flooding through 2030. However, as discussed in Section 6.2, a flood pathway becomes prevalent in the 2070/2100 time frames at the railroad crossing on the western side of Fort Point Channel. This represents a narrow entry point that produces flooding over a large urban area, including flooding of major roadways and significant MassDOT Structures. As of the date of publication of this report, survey activities in this area are proceeding in coordination with Amtrak and the MBTA.

3.3 Assets and Facilities

As discussed generally in Chapter 2, the data extracted from MMIS became the basis for a list of known CA/T Facilities. During development of this list of Facilities, we determined that MMIS was primarily a collection of Assets, which then allowed us to develop a preliminary working definition

⁶ See section 4.9 for discussion of “post-processing” and other processes associated with the BH-FRM

of Features and Assets. Assets are defined as individual items that collectively comprise the CA/T system. Facilities are defined as a functional collection of Assets. As an example, a pump station is a Facility, and the pumps and electrical controls that comprise a pump station are the Assets. Expanding on these definitions, and using the formal terminology associated with relational databases, this is known as a “one to many” relationship. For each Facility, there are one or more Assets associated with that Facility, and a Facility can be an Asset, but an Asset is not necessarily a Facility. Using these working definitions, we were able to proceed with the development of a relational database that would be used to interface with the GIS and support the needs of the VA. Additionally, these definitions allowed us to make a formal recommendation to MassDOT: to succeed efficiently, this project will focus on Facilities. With MassDOT’s concurrence, we agreed that assessing the vulnerability of individual CA/T Assets was beyond the scope of this project.

Assets are defined as individual items that collectively comprise the CA/T system. Facilities are defined as a functional collection of Assets.

3.4 CA/T Database

For the purpose of identifying and locating the numerous Facilities associated with the Central Artery/Tunnel system (CA/T), we developed a relational database (CATDB). The CATDB was designed to interface with a GIS and with Maximo. To facilitate communication between with Maximo databases, to the extent practicable, the primary identifier in CATDB is the Maximo “Location” code. As previously discussed,

in Spring 2013 Maximo had not yet been established at D6. Therefore, numerous MassDOT data sources, such as MMIS, were used to initially develop the CATDB. In October 2014, a copy of the Maximo database was provided to UMass Boston and Maximo Location codes were incorporated into the CATDB. However, while updating the CATDB to communicate with Maximo, we discovered numerous Facilities that were not include in Maximo. Therefore, Maximo Location codes were added to the CATDB for all Facilities available in Maximo. For all other Facilities identified during this project, the primary identifiers are codes extracted from MMIS or new codes developed on an as-needed basis. We recommend that these additional Facilities be included in future updates to Maximo.

3.5 Structures and Structural Systems

As the CATDB development proceeded, we determined that the definition of Facilities did not sufficiently encompass the information that we were collecting in the field and extracting from MMIS. Therefore, we developed an expanded information hierarchy to facilitate the database development, and eventually to support the VA. This expanded hierarchy included two new primary definitions: Structures and Structural Systems.

3.5.1 Structures

Structures in the CATDB are defined as buildings or other types of structures located, partially or completely, on or above the ground surface and therefore have at-grade exposures to water infiltration during flood events. Each Structure contains one or more Facilities. For example, Storm Water Pump Station 15 (D6-SW15-FAC) Facility is located within the Ventilation Building 4

(D6-VB4-FAC) Facility, and VB4⁷ is located partially above the ground surface. An example of a Structure that contains only one Facility would be the Storm Water Pump Station 9 (D6-SW09-FAC) Facility, where SW09 is a single building located partially above the ground surface.

3.5.2 Structural Systems

Structural Systems in the CATDB are defined as a collection of vertically or horizontally adjacent Structures. We assume that during a coastal flooding event, the vulnerability identified at any one Structure significantly increases the vulnerability of all adjacent Structures. To the extent practicable, Structural Systems in CATDB have secondary identification keys that relate each Structural System to the Maximo “Location” codes for all the Facilities located within the Structural System.

3.5.3 CATDB Hierarchy

Again, using relational database terminology, there is a “one to many” relationship between Structures and Facilities and a “one to many” relationship between Structural Systems and Structures. To the extent practicable, Structures in CATDB have secondary identification keys that relate each Structure to the Maximo “Location” codes for the Facilities associated with the Structure. Using these definitions of Structures and Structural Systems allowed us to begin to understand and document the functional relationships amongst the numerous interdependent and interconnected CA/T Facilities. However, during the IK meetings we learned that the hierarchies within Maximo were developed after significant effort by MassDOT staff, and as such the IK Team requested that we

⁷ After initial reference to the Maximo code, will generally drop the “D6-“ and “-FAC” from the acronyms used in this report

not impose an additional hierarchy onto the CA/T. After discussing this request, the Project Team decided that the CATDB hierarchies were critical to our understanding of the CA/T, specifically with respect to flooding vulnerabilities. Therefore, we maintained this hierarchy within the CATDB (Structural Systems<-Structures<-Facilities<-Assets) for the purposes of this project. However, we are not recommending that the CATDB hierarchy replace or expand the Maximo hierarchy, but rather that the CATDB hierarchy be used to facilitate discussions related to the vulnerability of the CA/T to coastal flooding.

3.5.4 Additional Definitions, Special Cases and Categories

As we proceeded to develop the CATDB and the associated GIS, we discovered that the definitions above did not encompass all configurations of the CA/T. Additionally, upon acquisition of Maximo data, we gained a more thorough understanding of the Maximo hierarchical system and incorporated this into the CATDB. Although it's possible that a more detailed database hierarchy could have been developed, we found that the CATDB hierarchy generally met the needs of this project. Therefore, to maintain the CATDB hierarchy we developed some additional definitions and categories of Facilities, summarized below. To the extent practicable, these Facilities in CATDB have primary or secondary identification keys that relate each Facility to the associated Maximo "Location."

- Tunnel Egresses and Stormwater Outfalls are defined in CATDB as Facilities. These Facilities are not identified in Maximo and are identified in CATDB using codes found in various other sources, such as MMIS. Because these Facilities are vulnerable to coastal

flooding, we recommend that they be added to Maximo as Facilities. Additionally, many Tunnel Egresses were observed and identified as Structures, such as TE425 located on the John F. Fitzgerald Surface Road

- Stand-alone Structural Systems are considered a special case in CATDB, and are defined as Structures that are not adjacent to other Structures. An example of a Stand-alone Structural System is the Depot-Main Complex Satellite Maintenance Rutherford Street Charlestown (D6A-DC03), which is effectively isolated geographically from the CA/T.
- Complexes are defined in Maximo and have been defined in CATDB as one or more Structures located on a common parcel of land. Complexes are also considered a special case of a Structural System as the individual Structures located on a Complex may not be adjacent. Vulnerability to flooding at a Complex may only impact some and not all operations occurring at the Complex and may not directly impact any or all of the Structures located on the Complex. Another example of a Complex is the Depot-Main Complex located at 93 Granite Ave (D6D-DC01) in Milton.
- The 93 Granite Ave (D6D-DC01) Complex is a special case because by definition it is not part of the CA/T. This Complex was included in the CATDB at the special request of MassDOT D6 staff and was evaluated for potential impacts to coastal flooding as part of this project as it is located within the geographic domain of the BH-FRM.
- To facilitate our understanding of the CA/T, Structures were categorized within CATDB into a collection of Structure Types generally following the Facility

Types identified in Maximo. These Structure Types, include, but are not limited to, the following:

- Administrative
- Air Intake Structure
- Boat Section
- Complex
- Electrical Substation
- Emergency Platform
- Emergency Response Station
- Fan Chamber
- Fuel Depot
- Groundwater Equilibration System
- Low Point Pump Station
- Maintenance Facility
- MBTA Station
- Operations
- Roadway
- Storm Water Pump Station
- Stormwater Outfall
- Toll Plaza
- Tunnel Egress
- Tunnel Portal
- Tunnel Section
- Ventilation Building
- Unknown / Miscellaneous

3.5.5 Tunnels, Ramp Areas and Roadway Areas

During review of the CAD drawings, we discovered the use of the terminology “Sections” as defined by others during the construction of the CA/T system. Sections generally represent types of paved roadways within the CA/T system. Several types of Sections, discussed in detail below have been incorporated into the CATDB. Individual Sections are identified in the CATDB by unique Bridge Identification Number (BIN) codes as available from the CAD drawings, or if not available, were assigned unique BIN codes within the CATDB. While the definition of a Bridge Section is obvious, we discovered that a Ramp Section is not a Ramp Area (as defined in Maximo, see below). For the

purposes of this report, a Ramp Section is a sloped earthen or concrete Structure that serves to connect a Bridge Section either up from, or down to, a surface-elevation paved roadway. Bridge Sections and Ramp Sections are not included in the CATDB (secondary impacts such as scour were not evaluated in this study). Similarly, other types or surface-grade paved roadways are not included in the CATDB.

We also submit that the definition of a Tunnel Section is obvious. Individual Tunnel Sections are only included in the CATDB as Structures if their identification significantly facilitated the VA, for example if a Tunnel Egress is located in the wall of a specific Tunnel Section. Tunnel Sections were, however, specifically incorporated into the GIS to facilitate system visualization.

A Portal is a special type of Tunnel Section, and is defined as the specific area of transition into or out of a Tunnel, specifically as defined above (a contiguous collection of Tunnel Sections). Portals are Structural Systems. An example of a Portal is the southbound entrance to the Sumner Tunnel in East Boston, specifically at the point at which Boat Section BINA07 enters into the Sumner Tunnel.

A Tunnel is defined as a contiguous collection of Tunnel Sections. Tunnels are Structural Systems and we discovered two interconnected types of Tunnels: Tunnels that are Roadways (as defined in Maximo, see below), and Tunnels that are Ramp Areas. An example of a Tunnel is the Ted Williams Tunnel (D6-TUN-TWT; I-90 Eastbound and Westbound below Boston Harbor).

A Roadway Area is defined as a contiguous collection of Sections of any type, including other surface-grade paved roadways, which in CATDB comprise an interstate or state highway. Roadway Areas are Structural

Systems. Generally, Roadway Areas comprise one direction of a divided highway, such as the I-93 Northbound Roadway Area (D6-93NB-ROA). An example of a Roadway Area Tunnel is I-93 Northbound within the Tip O'Neill Tunnel (D6-TUN-TON).

A Ramp Area is similarly defined as a contiguous collection of Sections of any type, including other surface-grade paved roadways, which comprise an entrance ramp to, or exit ramp from, one or more Roadway Areas. Ramp Areas are Structural Systems. An example of a Ramp Area Tunnel is Ramp D (D6 D RAA; Congress Street to I-93 from Ramp Area F).

3.5.6 Boat Sections

A Boat Section can be generally defined as a Tunnel Section that is open at the top -- a paved roadway "floor" with two sidewalls and without a "roof." Boat Sections are defined in CATDB as Structures, as they are located partially on and above the ground surface. Boat Sections have a secondary identification key that relates each Boat Section to a Ramp or Roadway Area using the Maximo "Location" code associated with the appropriate Ramp or Roadway Area. Typically, Boat Sections are configured with a sloped paved roadway on one end that leads either down to, or up from, a walled area below the ground surface where the paved roadway is located. Some Boat Sections lead into Portals, some do not lead into Portals, some have a sloped paved roadway on both ends, and some do not have sloped paved roadways on either end. To support the VA, we define two primary types of Boat Sections: Boat Sections with Portals and all other Boat Sections, defined as Open Boat Sections.

A Boat Section with Portal is defined as a Boat Section that either enters into, or exits out of a Tunnel at a Portal. A Boat Section

with Portal has a sloped paved roadway at one end which lead down into and/or up from a walled area where the roadway is located below the ground surface, or does not have sloped paved roadway and so leads into or out of any another type of Section. An example of a Boat Section with Portal is BINA07, the southbound entrance to the Sumner Tunnel in East Boston.

An Open Boat Section is defined as any Boat Section not associated with a Portal. Open Boat Sections have sloped paved roadways at one end, both ends, or neither end, which lead down into and/or up from a walled area where the road is located below the ground surface, or lead into or out of any another type of Section.

- An example of an Open Boat Section with sloped roadways on both ends is BIN1aN, located on Route 1A Southbound located north of Logan Airport.
- An example of an Open Boat Section with a sloped roadway on only one end is BIN7BM, a portion of Ramp L (I-93 Northbound to I-90 Eastbound), where this specific northbound Boat Section terminates at a single Tunnel Section and this Tunnel Section entrance is not a Portal. The Tunnel Section in this example exits into another Boat Section and this exit is again not a Portal. In CATDB we refer to this configuration as an "Overpass."
- An example of an Open Boat Section that leads only into or out of another Boat Sections is BIN7TL, which is one of several contiguous Open Boat Sections that comprise Ramp KK (I-93 North To I-90 West)

3.6 Geodatabase Development

With these CATDB definitions in place, we began formal development of the CA/T GIS

geodatabase (CATGDB) to provide spatial context for the CATDB data. The initial feature class (FC) imported into the CATGDB was the Facilities point FC obtained from the MassDOT geodatabase. Based on the feedback obtained at the IK meetings, we revised these Facilities point features and added new Facilities.

Using these Facility locations, information gained from field visits, and review of Google Earth, Google Street View, and Apple Maps, we began to formally identify Structures associated with each of the Facilities provided by MassDOT. For the most part, after identifying the appropriate Structure, the Structures polygon FC was developed by extracting polygons from the MassGIS Building Structures data (2-D, from 2011-2013 Ortho Imagery⁸). Polygon features representing Complexes were extracted from the City of Boston 2014 Parcel data (Parcels 14⁹). Polygon features representing Boat Sections, Tunnel Sections, Ramp Areas and Roadway Areas were extracted from CAD data provided by MassDOT.

Overall, the development of the CATGDB proceeded as discussed in Section 2; field visits informed the GIS database development, and the GIS database generated the need for more field visits. A timeline over which this occurred is provided in Appendix V. As of the writing of this report (May 29, 2015), the CATGDB was completed to the extent possible, given the available information. However, as mentioned previously, data gaps still exist.

⁸ <http://www.mass.gov/anf/research-and-tech/it-serv-and-support/application-serv/office-of-geographic-information-massgis/datalayers/structures.html>

⁹ <http://bostonopendata.boston.opendata.arcgis.com/datasets>

HYDRODYNAMIC ANALYSIS

Sea level rise, and sea level rise combined with storm events, has most commonly been evaluated by simply increasing the water surface elevation values and comparing the new water elevation with the topographic elevations of the land. While this rudimentary “bathtub” approach may be viable to provide a first order identification of potential areas that may be vulnerable to sea level rise, it does not accurately represent what may actually happen due to sea level rise, and is certainly unable to represent the dynamic nature of storm events. For example, the “bathtub” approach does not directly account for potential flooding pathways (does water have a pathway to actually migrate from the ocean/bay to low lying landward regions), it does not determine the volumetric flux of water that may be able to access these low-lying areas, and is unable to identify how long the flooding may last. Additionally, the “bathtub” approach does not account for critical physical processes that occur during a storm event, including waves and winds. Therefore, in many cases, this rudimentary “bathtub” approach results in predicting inundation in areas where flooding will not occur, while also misidentifying some areas as remaining dry that would be inundated.

Therefore, accurate sea level rise and storm surge modeling requires an improved representation of the physical processes, as well as accurate and higher resolution predictions of inundation due to the combination of sea level rise and storm surge for site-specific locations. The hydrodynamic modeling utilized for this study is geared towards a physics based approach to the water level increases and flooding. This type of coastal hydrodynamic modeling to determine water levels includes:

- An extensive understanding of the physical system as a whole
- Inclusion of the significant physical processes affecting water levels (e.g., riverine flows, tides, waves, winds, storm surge, sea level rise, wave set-up, etc.)
- Full consideration of the interaction between physical processes
- Characterization of forcing functions that correspond with real world observations
- Resolution that will be able to resolve physical and energetic processes, while also be able to identify site-specific locations that may require adaptation alternatives

Accurate sea level rise and storm surge modeling requires an improved representation of the physical processes, as well as accurate and higher resolution predictions of inundation due to the combination of sea level rise and storm surge for site-specific locations. This requires a physics based dynamic model.

Figure 4-1 shows the results of a representative “bathtub” model approach for the Boston Harbor Area with a combined sea level rise and storm surge maximum water surface elevation of approximately 12 feet NAVD88. This represents a flat water surface elevation that spreads across the entire landscape. Flooding is shown in areas landward of flood control structure (e.g., dams) and there is no temporal limitation to the flooding (the storm lasts an infinite amount of time) such that water can penetrate anywhere on the landscape with elevations less than 12 feet NAVD88.

Comparatively, Figure 4-2 shows the results from a dynamic modeling simulation (incorporating the relevant physical processes such as waves, surge, winds, etc.). There is a stark difference between the two results. Generally, the results indicate there is more flooding to the south as water is driven in that direction by the predominant wind and wave forcing. Similarly, there is less flooding to the north than the bathtub case, and the functioning of the dams and other urban features show reduced flooding in protected inland areas. While bathtub modeling represents a reasonable first order approach to assessing potential vulnerabilities, in areas with critical infrastructure and/or complex landscapes, dynamic modeling of climate change and storm events is crucial.

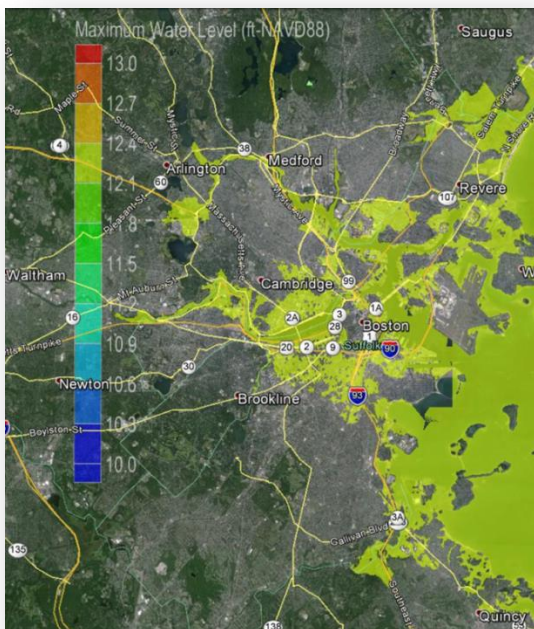


Figure 4-1. Bathtub model results for Boston Harbor area showing a maximum water surface elevation of 12 feet NAVD88.

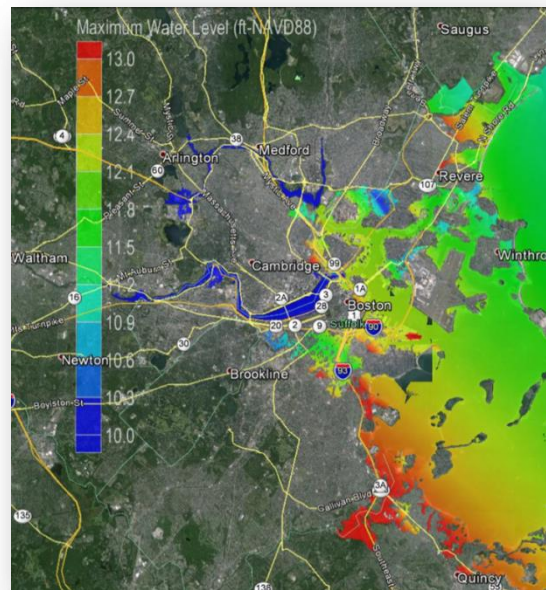


Figure 4-2. Dynamic numerical model results for Boston Harbor area showing a maximum water surface elevation of 12 feet NAVD88.

4.1 Model Selection

While there have been numerous model applications and studies that simulate storms and storm surge based impacts on coastal areas, there are far fewer numerical model applications that have included climate change impacts in the overall modeling effort. Additionally, while simulation of historical tropical storm events and tropical storm forecasting has been a regular occurrence, numerical simulations considering extra-tropical storm events have been far less common. As such, a number of potential storm surge models were evaluated to determine the most appropriate model for the Boston Harbor region and evaluation of the Central Artery system. A successful climate change model aids in vulnerability assessment and adaptation planning by providing information needed to make critical planning decisions. For a critical and important system such as the Central Artery, where the tolerance for risk to the system is low, a model was required

that incorporated the physics necessary to solve for water surface elevation, current velocities, waves, winds, river discharge, wave set-up and other important processes that may influence flooding risk. It was also required that the model be flexible enough to potentially link with other modeling tools (e.g., watershed models, ecological models) for a more comprehensive climate change assessment. Additionally, the Boston area has a number of site-specific features that required specialized model abilities, including:

- Handling the complex shape of Boston Harbor, including the islands, shoreline geometry, multiple rivers and channels, etc.
 - Ability to effectively deal with an urbanized and unique topography that will be flooded and drained during a storm surge event. To effectively model this situation, the selected model must be able to efficiently handle wetting and drying of an urban environment, while having sufficient detail to resolve any type of flow pathway network.
 - Variable vegetation and land cover types throughout the system that cause variable bottom friction. The successful model needs to be able to handle this by allowing for specification of variable bottom friction coefficients.
 - The selected model must be able to simulate flow control structures (dams, weirs, etc.), and their associated components (e.g., pumps) that were designed to have a flood control purpose. The model must not only be able to simulate these features, but must also do so with consideration of the proper hydraulics involved.
 - Ability to simulate the key physical processes (tides, winds, waves, surge, river discharge) and their influence on
- each other in a coupled numerical approach. For example, currents (tidal, storm driven) influence wave propagation, which in turn influences currents. Likewise, the increased water levels caused by storm surges influence the discharge of the rivers. These and other types of interactions needed to be handled by the selected model.
- Requirements to simulate a large area to capture the dynamics of tropical and extra-tropical storm events, which also requires an unstructured grid to allow for variable resolution.

A number of potential storm surge models were evaluated to determine the most appropriate model for the Boston Harbor region and evaluation of the Central Artery system.

An initial evaluation of over 10 circulation models was completed by the MassDOT project team, with a shortlist of possible selections narrowed to three (3) proven storm surge simulation models: (1) the ADvanced CIRCulation model (ADCIRC), (2) the Finite Volume Community Ocean Model (FVCOM), and (3) Sea, Lake, and Overland Surges from Hurricanes (SLOSH).

SLOSH, is a computerized numerical model developed by the National Weather Service (NWS) to estimate storm surge heights resulting from historical, hypothetical, or predicted hurricanes. The model takes into account the atmospheric pressure, size, forward speed, and trackline data. These parameters are used to create a model of the wind field which drives the storm surge. The SLOSH model consists of a set of physics equations which are applied to a specific locale's shoreline, incorporating the unique bay and river configurations, water

depths, bridges, roads, levees and other physical features.

However, SLOSH was removed from consideration for use in assessing sea level rise and storm surge risk for Central Artery for a number of reasons. Some of the primary reasons included:

- SLOSH is not capable of the high resolution modeling mesh that is required to simulate the urban Boston landscape. SLOSH model domains and resolutions are limited (resolution of 0.5 to 7 km), while significantly higher resolution of the domain is required to assess risks for the Central Artery system. In general, SLOSH is more of a regional model (better at predicting regional storm surge), but is not adequate for representing details in overland areas, especially for urban environments where vulnerabilities of individual structures and systems are important. Figure 4-3 provides a comparison between a typical SLOSH grid resolution and an ADCIRC grid resolution. The inability of the SLOSH model to capture the features of the land (e.g., variation in elevation) is evident.
 - It is difficult to simulate complicated shorelines in SLOSH due to its resolution and inflexible mesh. A model with an unstructured grid (such as ADCIRC or FVCOM) is preferred since the topography, shoreline, etc. can be accurately modeled.
 - SLOSH does not include dynamic tides. This is especially critical in the northeast, where tidal variations have a large impact on the potential flooding dynamics.
 - SLOSH does not model wave processes (e.g., surface waves, wave transformations, wave setup etc.).
- It is difficult (or almost impossible) to include important infrastructure and features that block or accelerate storm surge in SLOSH (e.g., highways, canals, dikes, dams, etc.).
 - SLOSH has been shown to over predict flood elevations, in some cases on the order of 20-25% (Sparks, 2011).
 - SLOSH cannot include the influence of freshwater discharge (e.g., Charles River, Mystic River, etc.), an important aspect of potential flooding in the Boston region.

FVCOM is a finite volume coastal ocean circulation model developed jointly by UMass Dartmouth and Woods Hole Oceanographic Institution. FVCOM implements an unstructured triangular cell grid and is solved numerically by a second-order accurate discrete flux calculation. Therefore, FVCOM allows the grid flexibility of finite element model with the numerical efficiency of a finite difference model. More details on the FVCOM model can be found in Chen et al. (2011). The model was originally developed for the determining flooding/drying process in the estuarine and coastal environment. However, the FVCOM model is only permitted for use in non-commercial academic research and education. As such, it was not evaluated further for use in the Climate Change and Extreme Weather Vulnerability Assessments and Adaptation Options of the Central Artery project.

The ADvanced CIRCulation model (ADCIRC), originally developed by Joannes Westerink, a civil engineer at the University of Notre Dame, and Richard Luettich, a marine scientist at the University of North Carolina, is a two-dimensional, depth-integrated, barotropic time-dependent long wave, hydrodynamic circulation model. ADCIRC models can be applied to

computational domains encompassing the deep-ocean, continental shelves, coastal seas, and small-scale estuarine systems. Typical ADCIRC applications include

modeling tides and wind driven circulation, analysis of hurricane storm surge and flooding, dredging feasibility and material disposal studies, larval transport studies, near shore marine operations. As described in more detail in Section 4.2, ADCIRC solves the shallow water equations for water surface elevation and velocity using a modified form of the continuity equation called the Generalized Wave Continuity Equation (GWCE).

ADCIRC employs the finite element method using grid linear triangles and is explicit in time. The code can be run in either a 2-D depth integrated mode or 3-D mode. When run in the 3-D mode, an equation of state is simultaneously solved including salinity and temperature. ADCIRC's wetting and drying is accomplished by elemental elimination in which an element is considered dry and removed from computations when the depth of water at one of its nodes is less than 5 cm (2 inches). ADCIRC is a code with an efficient matrix solver and an available multiple processor parallel version allowing for efficient simulations even with very large grids. Finite element models can maximize computational demands accordingly. Therefore, an ADCIRC model with a large number of nodes and higher resolution may be able to explicitly resolve the micro-topographic features.

Thus ADCIRC is an excellent model for coastal regions where complex geometries and bathymetries demand variable resolution. ADCIRC has the ability to include a wide variety of meteorological forcing, and there is active development for data assimilation and feedback to meteorological models. ADCIRC is

commonly used to predict coastal inundation caused by storm surge and is capable of accounting for various different ecological and structural surface roughness levels. ADCIRC also includes forcing from surface waves through mode coupling with the wave model SWAN.

Consequently, ADCIRC is a widely-used model available for commercial use. The

ADCIRC is an excellent model for coastal regions where complex geometries and bathymetries demand variable resolution and higher resolution can explicitly resolve the micro-topographic features.

model is used by the United States Army Corps of Engineers (USACE), National Oceanic and Atmospheric Administration (NOAA), and Federal Emergency Management Agency (FEMA) and has a very active user community providing excellent user support and continuous numerical improvements. The model has been widely used in storm surge modeling projects and is generally accepted as the leading model for simulation of storm surge. For example, FEMA currently uses ADCIRC to perform their storm surge inundation mapping for the National Flood Insurance Program (NFIP) Flood Insurance Rate Maps (FIRM). NOAA's National Weather Service Ocean Prediction Center currently uses ADCIRC to forecast storm events and project storm surge projections. Recently, the International Data Corporation (IDC) announced recipients of the High Performance Computing (HPC) Innovation Excellence Award at the ISC'13 supercomputer industry conference in Leipzig, Germany. ADCIRC was one of eleven international winners.

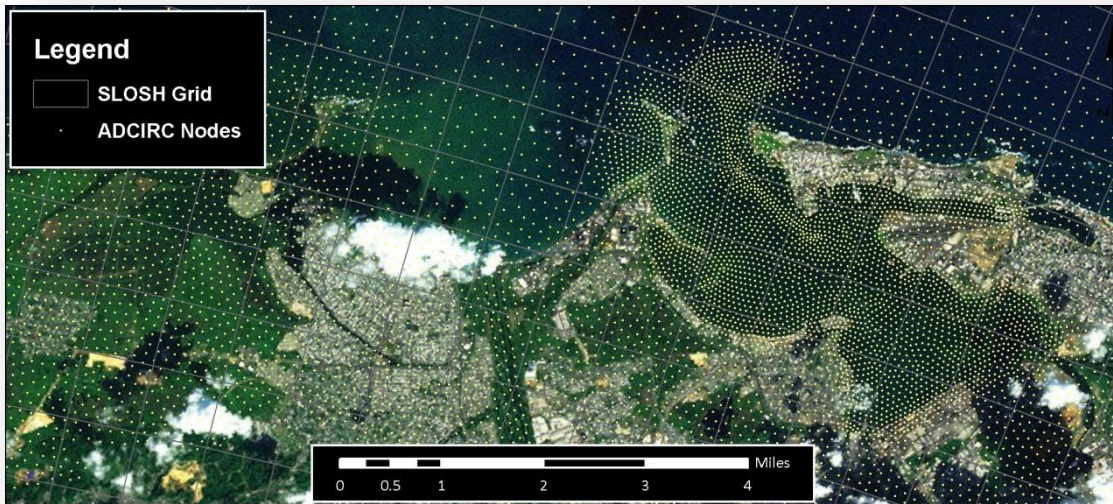


Figure 4-3. Comparison typical ADCIRC grid resolution (dots) and SLOSH grid resolution (lines) (Sparks, 2011).

Ultimately, ADCIRC was deemed sufficient to meet all the demanding and specific requirements for sea level rise and storm surge modeling for the Central Artery (as listed above), and therefore was selected as the hydrodynamic modeling tool to develop the Boston Harbor Flood Risk Model (BH-FRM). ADCIRC was applied to provide a complete and accurate representation of water surface elevations and tidal circulation throughout the Boston Harbor area and surrounding upland caused by combined sea level rise and storm surge processes.

4.2 Description of ADCIRC

The ADCIRC model is a finite-element hydrodynamic model that uses the generalized wave-continuity equation formulation based on the well-known, shallow-water equations (Le Mehaute, 1976; Kinnmark, 1984). ADCIRC solves the equations of motion for a moving fluid on a rotating earth. The water surface elevation is obtained from the solution of the depth-integrated continuity equation in Generalized Wave-Continuity Equation (GWCE) form, while the velocity is calculated from the momentum equations.

All nonlinear terms have been retained in these governing equations. These equations have been formulated using the traditional hydrostatic pressure and Boussinesq approximations and have been discretized in space using the finite element method and in time using the finite difference method. For a Cartesian coordinate system, the conservative form of the shallow-water equations are written: where t represents time, x , y are the Cartesian coordinate directions, ζ is the free surface elevation relative to the geoid, U , V are the depth-averaged horizontal velocities, $H = \zeta + h$ is the total water column depth, h is the bathymetric depth relative to the geoid, f is the Coriolis parameter, p_s is the atmospheric pressure at the free surface, g is the acceleration due to gravity, α is the Earth elasticity factor, η is the Newtonian equilibrium tide potential, ρ_0 is the reference density of water, M_x , M_y represents the depth-integrated horizontal momentum diffusion, D_x , D_y are the depth-integrated horizontal momentum dispersion terms, B_x , B_y are the depth-integrated baroclinic forcings, and τ_{sx} , τ_{sy} are the applied free surface stresses:

$$\frac{\partial \zeta}{\partial t} + \frac{\partial UH}{\partial x} + \frac{\partial VH}{\partial y} = 0 \quad (4.1)$$

$$\frac{\partial UH}{\partial t} + \frac{\partial UUH}{\partial x} + \frac{\partial UVH}{\partial y} - fVH = -H \frac{\partial}{\partial x} \left[\frac{p_s}{\rho_o} + g(\zeta - \alpha\eta) \right] + M_x + D_x + B_x + \frac{\tau_{sx}}{\rho_o} - \frac{\tau_{bx}}{\rho_o} \quad (4.2)$$

$$\frac{\partial VH}{\partial t} + \frac{\partial VUH}{\partial x} + \frac{\partial VVH}{\partial y} - fUH = -H \frac{\partial}{\partial y} \left[\frac{p_s}{\rho_o} + g(\zeta - \alpha\eta) \right] + M_y + D_y + B_y + \frac{\tau_{sy}}{\rho_o} - \frac{\tau_{by}}{\rho_o} \quad (4.3)$$

Further justification regarding the appropriateness of these equations in modeling tidal and atmospheric forces flows is provided by Blumberg and Mellor (1987), Westerink et al. (1989), and Luettich et al. (1992). These equations are modified and converted to spherical coordinates to handle large-scale global circulation problems. These governing equations form the basis for the ADCIRC model, and further details on the formulation of the model and the numerical solution can be found in Luettich and Westerink (2012).

4.3 Description of SWAN

In addition to capturing the circulation and flooding within the system, storm-induced waves also need to be simulated in concert with the hydrodynamics. For wave generation, propagation, and transformation, the project team has selected the SWAN Model developed at Delft University of Technology. SWAN (Simulating Waves Nearshore) accounts for the following wave related physics:

- Wave propagation in time and space, shoaling, refraction due to current and depth, frequency shifting due to currents and non-stationary depth
- Wave generation by wind
- Three- and four-wave interactions
- Whitecapping, bottom friction and depth-induced breaking
- Dissipation due to aquatic vegetation, turbulent flow and viscous fluid mud

- Wave-induced set-up
- Propagation from laboratory up to global scales
- Transmission through and reflection (specular and diffuse) against obstacles
- Diffraction

SWAN is a third generation spectral wind-wave model based on the wave action balance equation:

The left hand side of the equation describes kinematic processes, where the action density (N) is defined by the second equation where E is the energy density, and σ represents the radian frequencies in a frame of reference moving with current velocity (U). The first term on the left hand side is the change in energy density with respect to time, while the second is the propagation of energy in space with c_g being the wave group velocity. The third term on the left hand side defines the frequency shifts due to variations in depth and currents, while the fourth term represents depth induced and current induced refraction. The right hand side is a grouping of the source and sink terms as shown in equation 4.6. The first term on the right hand side S_{in} , represents wind generation/growth, the next two terms, S_{nl3} and S_{nl4} , represent nonlinear wave interactions. The final two terms of equation three represent energy dissipation due to bottom friction and wave breaking, respectively.

$$\frac{\delta N}{\delta t} + \nabla_{\vec{x}} \cdot [(\vec{c}_g + \vec{U})N] + \frac{\partial c_{\sigma} N}{\partial \sigma} + \frac{\partial c_{\theta} N}{\partial \theta} = \frac{S_{tot}}{\sigma} \quad (4.4)$$

$$N = \frac{E}{\sigma} \quad (4.5)$$

$$S_{tot} = S_{in} + S_{nl3} + S_{nl4} + S_{ds,w} + S_{ds,b} + S_{ds,br} \quad (4.6)$$

Both the SWAN wave model and the ADCIRC circulation model can be implemented on the same unstructured computational grid framework. Where SWAN is based on the action balance equation, which uses water levels, bottom roughness coefficients, wind stresses, and bathymetry as input variables, ADCIRC solves the shallow water equations and vertically averaged momentum equations where radiation stress gradients also play a key role in computations. Because both models can utilize the same grid, when the two models are coupled, there is no need for any interpolation or extrapolation to apply the outputs from one model into the other model as input conditions.

4.4 Coupling Waves and Currents

There are three ways in which simulation results can be passed between the models: one-way ADCIRC to SWAN, one-way SWAN to ADCIRC and two-way ADCIRC/SWAN. One-way ADCIRC to SWAN is used when currents impact waves, but waves only weakly impact currents. Such a case would be at an inlet with strong tidal currents with a deflated ebb shoal such that wave breaking and wave-induced currents are not significant. One-way SWAN to ADCIRC is used when the wave breaking induced radiation stress impacts circulation, but the circulation does not impact the waves. Such a case would be with waves breaking along the open coast. Two-way ADCIRC/SWAN is used when currents impact waves and waves impact currents.

This two-way formulation is applied in the BH-FRM model. The steering module facilitates the coupling of the current and wave model. Many repetitive tasks, such as updating input files with new radiation stresses or current vector fields and the interpolation of data between a finite-element mesh and a rectangular grid are handled by the steering module. The user specifies a total run time for which the combined models are executed, ADCIRC time intervals, and the time interval between SWAN executions. Since SWAN is a steady-state model, the user defines the spectra at each of the time intervals. ADCIRC requires a ramp period to allow for all forcings to be applied gradually over the entire system instead of shocking the system at once. Since SWAN's calculated radiation stress is one of the applied ADCIRC stresses, the spectra should bracket the time interval of interest and transition from low-energy conditions to peak wave conditions to allow for wave-induced current ramping. Figure 4-4 provides a schematic of how the model results are passed between the two models. This process is repeated until the total run time is reached.

ADCIRC requires a relatively small time step for model stability, while due to the nature of the SWAN model's schematization, the wave model can utilize a much larger time step. As such, the ADCIRC model uses a smaller time step, while the SWAN model used a larger time step. The coupling time, therefore, is set to the SWAN time step. Every ADCIRC time step solves the Generalized Wave Continuity Equation (GCWE) to determine

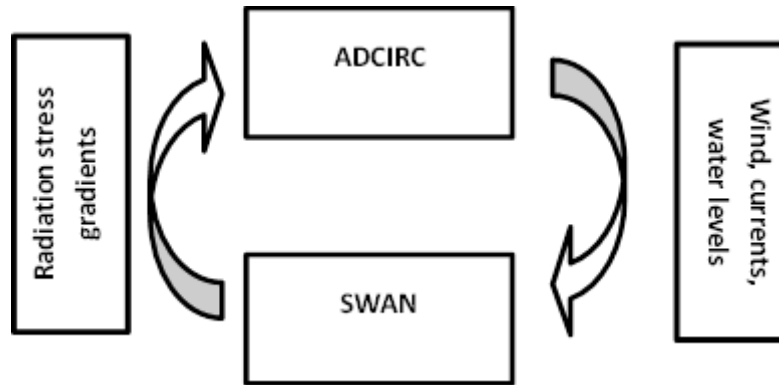


Figure 4-4. Schematic showing the coupling of the ADCIRC and SWAN models.

water levels and currents. Every SWAN time step of simulation time, the wind fields, currents, water levels, etc. are passed through to the SWAN model which in turn calculates waves, radiation stresses, etc. to be passed back into ADCIRC for the next simulation time calculation.

4.5 Model Development

This section describes the development of the BH-FRM model. The development of the model required configuration so that this particular application would best approximate the form and function of the real system (i.e., Boston Harbor). Model configuration involves compiling observed data from the actual system into the format required for the execution of ADCIRC and SWAN. This model development and configuration section presents details on the setup of the model, including the steps followed to generate the grid, input boundary conditions, and determination of other parameters needed for the model. Following model setup, the governing equations (as presented in section 4.2) are solved at each grid point through an iterative method. The model is then able to calculate the water surface elevation, velocity, waves, winds, etc. at each time step. Once a certain level of accuracy is attained, the model

advances to the next time step in the simulation and repeats the calculations. This methodology is continued until the model has simulated the entire time period of interest.

In developing, implementing, and analyzing results from the BH-FRM, data were obtained from State and federal agencies, independent contractors, and subject matter experts. Table 4-1 lists the data input type, the data provider(s), and the report section in which the data are discussed.

4.5.1 Mesh Generation

The first step in building the ADCIRC/SWAN model was construction of the modeling grid. The grid is a digital representation of the prototype's geometry that provides the spatial discretization on which the model equations are solved. Different numerical methods require different types of grids, each having unique geometrical requirements. The mesh building process involves using geo-referenced digital maps or aerial photos to define the model domain, then the mesh is generated within this domain providing the desired degree of spatial resolution, and topographic data are incorporated by

Table 4-1. Summary of data inputs and sources.

Data Input	Source	Report Section
Lidar and topography	MassGIS, MassDOT, USGS, NOAA CSC, site specific surveys	4.5.1
Bathymetry	NOAA/NGDC, USGS, site specific surveys	4.5.1
Land cover	MassGIS, USGS	4.5.2.3
River flow and hydrographs	BWSC, USGS, City of Cambridge, VHB	4.5.2.2
High water marks	USGS, Gadoury (1979)	4.6
Tides	NOAA Tides and Currents	4.5.2.1
Sea level rise scenarios	Parris et al. (2012)	4.7.1
Flood control structures	Massachusetts DCR, USACE, MCZM	4.5.3
Tropical storm climatology	Emanuel et al. (2006), Global climate models	4.7.2
Extra-tropical storm climatology	Vickery et al. (2013), ECMWF (2014), Myers and Malkin (1961)	4.7.3

interpolation of elevation values to mesh nodes or cells within the domain. For ADCIRC the computational mesh defines the spatial domain on which ADCIRC performs its calculations. ADCIRC uses an unstructured mesh allowing for flexibility in the number, location, and spacing of individual nodes defining the mesh. In regions where bathymetric and or topographic features are relatively uniform, such as in deep ocean waters offshore of the coastline, computational node spacing can be fairly coarse (on the order of kilometers). Conversely, in specific areas of interest with variations in depth bottom/land cover characteristics (e.g., friction) and where fine resolution output is required for analysis, the computational mesh spacing can be reduced (on the order of meters) to ensure that key features, either natural or anthropogenic, can be properly resolved in the model domain. Model runtime and demand on computing resources is directly related to the number of

nodes. By keeping the mesh coarse outside of the area of study, but increasing the nodal density in key areas, the computational time and intensity required for each simulation can be optimized. Figure 4.5 illustrates the variation in nodal density, with coarse model resolution along the eastern boundary and in the deeper waters offshore of the continental shelf, while the coastal waters in the nearshore have finer resolution to account for the more rapid change in bathymetric features in the littoral zone. The MassDOT mesh was developed in three levels of nodal density designated as coarse, intermediate, and fine mesh. For each layer of mesh density, the unstructured mesh scheme allows for mesh nodes from the coarse mesh to transition to the intermediate mesh, and subsequently from the intermediate mesh to the fine mesh. This allows for a smooth transition in the vicinity of the confluence of meshes.

4.5.1.1 Regional Mesh

The overall mesh development involved the adaptation of a regional mesh, which encompassed a majority of the western Atlantic Ocean, the entire Gulf of Mexico, and the entire Caribbean Sea. The regional mesh was the ec95d ADCIRC mesh, which is a previously validated model mesh used in numerous Federal Emergency Management Agency (FEMA) studies, National Oceanic and Atmospheric Administration (NOAA) operational models, FHWA Gulf Coast Phase 2 study, and most recently the United States Army Corps of Engineers North Atlantic Coast Comprehensive Study (NACCS). As such, the ec95d mesh has been widely used as the basis for more refined models. The ec95d mesh consists of 31,435 nodes, and includes associated bathymetric elevation data (Figure 4-6). This mesh was originally developed in 1995, and was verified with tidal elevation data from 65 stations throughout the model

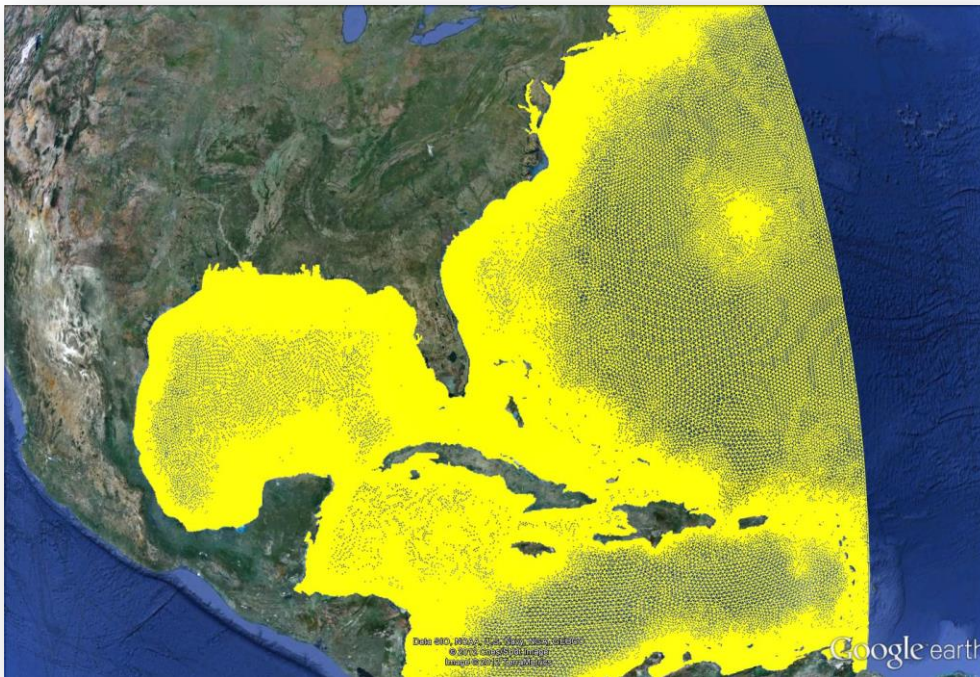


Figure 4-5. Comprehensive domain of the ADCIRC mesh showing coarse nodal spacing in the deep waters on the Eastern boundary, and increased nodal resolution in the littoral areas of the model domain.

domain (ADCIRC.org, 2013). Although there are more recent meshes developed for the Eastern United States on a nearshore scale, this is used to resolve the deep water bathymetry, and areas within the model domain required for far-field storm simulations and wind field evolution (i.e., the coast of the southeastern United States during tropical events).

4.5.1.2 Local Mesh

From ec95d, regions of nodal domain transition to the BH-FRM intermediate (local) mesh. This mesh provided higher resolution of the Northeast Atlantic, an intermediate level of mesh resolution was used to transition from the ec95d mesh to the highly resolved mesh needed along the Massachusetts coastline. In 2013, NOAA developed an ADCIRC mesh (Figure 4-7) to

develop tidal datums for the Gulf of Maine incorporating nodes from as far south as Long Island Sound (LIS) through Rhode Island, Massachusetts, New Hampshire, Maine, and as far north as the Bay of Fundy in Canada. This mesh, hereafter referred to as NOAA NE VDatum (Yang, et al., 2013), consists of 167,923 nodes and provided increased resolution in the offshore regions of New England than the ec95d mesh. This intermediate (local) mesh was utilized and adapted to provide a transition between the regional mesh and the site-specific BH-FRM mesh, which was developed for this study and spans the Massachusetts coastal waters (Buzzard's Bay, Cape Cod Bay, Boston Harbor, etc.). Careful integration of the regional and local meshes were required in order to ensure adequate interlacing.

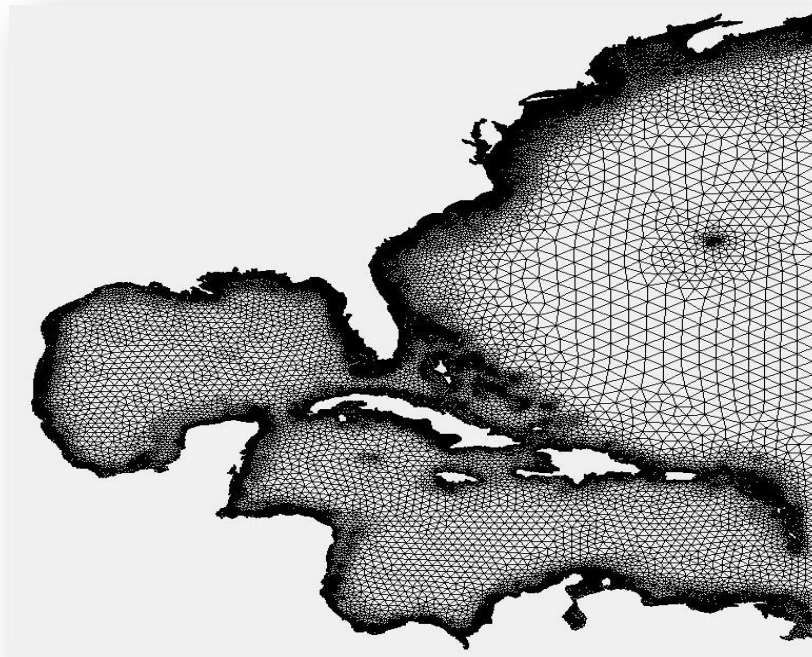


Figure 4-6. The finite element ec95d ADCIRC mesh used to provide initial coarse mesh (ADCIRC.org, 2013)

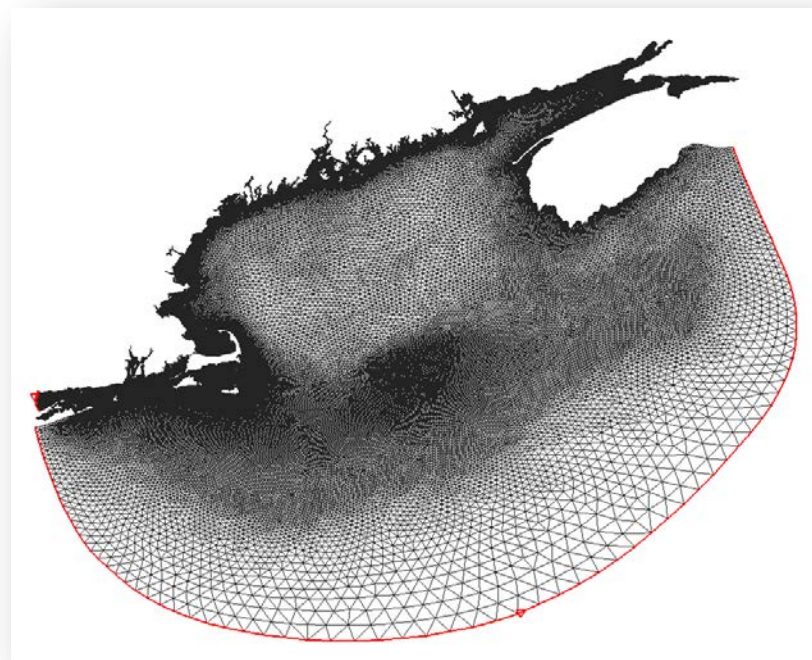


Figure 4-7. Finite element mesh for the intermediate (NOAA NE VDatum) mesh used to resolve the coastal waters in greater resolution (Yang, et al., 2013).

4.5.1.3 Site-specific Mesh Generation

While both the regional (ec95d) and local (NE VDatum) meshes have sufficient nodal density and large enough domains to adequately simulate storm evolution and bathymetric influenced ocean and shelf dynamics, additional mesh generation was required to simulate storm responses unique to the Massachusetts coastline and specifically to the Boston Harbor area. This also required model representation of upland areas constituting the urban Boston landscape. Figure 4-8 provides a summary of the site-specific mesh, indicating the Boston Harbor and City focus area (main

The site-specific mesh ensured that all critical topographic and bathymetric features that influence flow dynamics within the system were captured in the mesh.

image), along with the larger, regional model domain for perspective (bottom inset). The site-specific mesh includes areas of open water, along with a substantial portion of the upland subject to present and future flooding. The solid blue line on Figure 4-8 represents the inland extent of the site-specific mesh, which is necessary to simulate upland flooding from storm and sea level rise scenarios. The site-specific mesh was developed using feature arcs to delineate the centerlines and banks of waterways within the model domain and then a painstaking, manual method of assigning and developing individual nodes and elements to define features within the system was utilized. This manual development of the site-specific mesh ensured that all critical topographic and bathymetric features that influence flow dynamics within the system were captured in the mesh. A similar method was utilized

for the entire coast from Rhode Island to New Hampshire in the process of developing the site-specific mesh to ensure that all appropriate intertidal water bodies were captured in the model domain. Figure 4-9 illustrates a sample of the high-resolution, site-specific mesh in the vicinity of downtown Boston where node spacing is on the order of 5-10 meters (16-33 feet). In some areas, the resolution of the model was approximately 3 meters (10 feet).

4.5.1.4 Bathymetric and Topographic Data Sources

Bathymetric and topographic data were acquired from a number of sources to construct the elevation values within the model mesh. Bathymetric data sources primarily included:

- National Ocean Service (NOS) soundings
- NOAA Electronic Navigational Charts (ENCs) bathymetry
- Bathymetry archived by Bedford Institute of Oceanography (BIO), Dartmouth, Nova Scotia, Canada
- National Geospatial-Intelligence Agency (NGA) Digital Nautical Charts (DNCs)
- ETOPO2v2 archived by the NOAA National Geophysical Data Center (NGDC).
- Bathymetric data encompassed in existing ADCIRC meshes (e.g., ec95d mesh)
- Bathymetric data for the Charles River (MWH Global, 2014)
- Bathymetric data for the Mystic River (VHB, 2014)
- Site-specific survey data for Fort Point Channel (Woods Hole Group, 2012)
- NOAA survey data within Boston Harbor

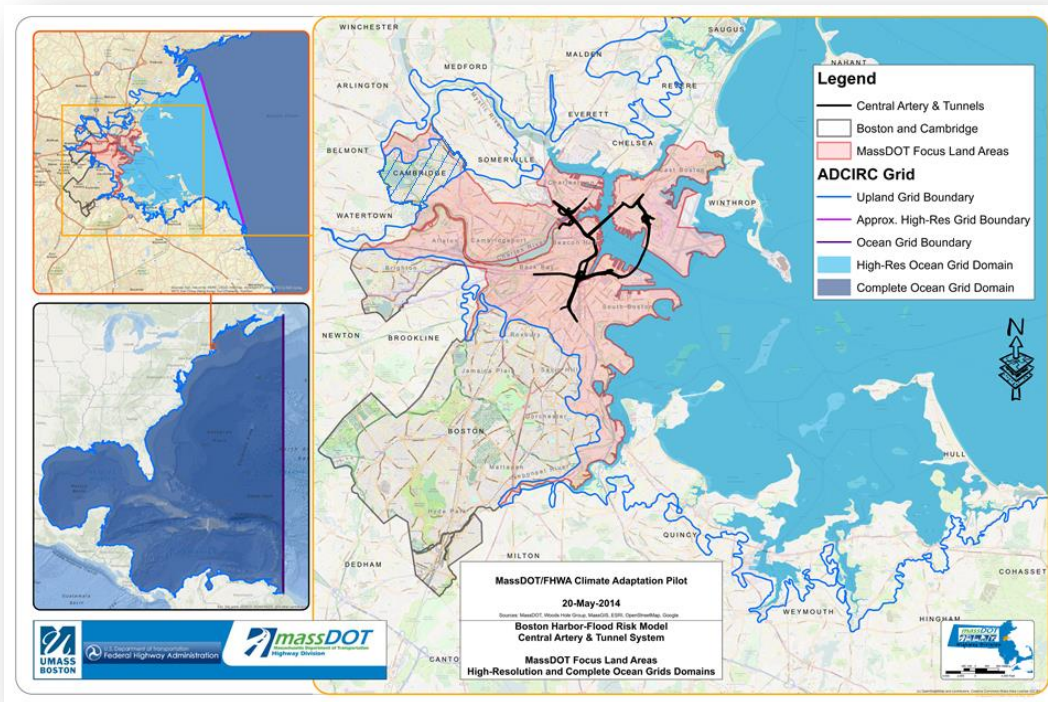


Figure 4-8. MassDOT focus area for the fine mesh (main image), inland extent of the high resolution domain (top inset), and complete model domain (bottom inset) for perspective. The blue outline in the main figure shows the upland extent of the model domain.



Figure 4-9. High resolution mesh grid in the vicinity of downtown Boston.

Topographic elevation data were primarily obtained from recent LiDAR data sets, including:

- 2011 U.S. Geological Survey Topographic LiDAR: LiDAR for the North East
- 2010 Federal Emergency Management Agency (FEMA) Topographic Lidar: Coastal Massachusetts and Rhode Island
- 2009 National Renewable Energy Laboratory/Boston Redevelopment Authority Topographic LiDAR: Boston, Massachusetts

In addition, site-specific surveys were conducted at key flooding locations (see Section 3.2) in order to ground truth the LiDAR data and provide more accurate, higher resolution topography in key areas within the city. All topographic and bathymetric data were checked for consistency, and when necessary converted to the NAVD88 vertical datum, then merged into a single data set. The merged elevation data set was linearly interpolated to the model grid and the grid was carefully checked to ensure accurate elevation information.

Since this region (Boston Harbor) is heavily urbanized, the elevations in the grid were not changed as a function of time. The coastline is generally hardened (e.g., seawalls, revetments, bulkheads, piers, etc.) such that morphologic changes are expected to be minor.

4.5.2 Boundary Conditions

In order for the BH-FRM model to compute storm surge, waves, flooding, winds, and other physical processes via the hydrodynamic computations, it is necessary to specify the model variables on the domain boundaries. Most of the model's boundary is considered to be the upland boundary, which for the BH-FRM model was specified

at an elevation of 30 feet NAVD88. This elevation provides the upper limit of expected water surface elevation during extreme storm events combined with sea level rise over the time period of evaluation (through 2100). At these upland boundaries, water is constrained to flow only parallel to the boundary; however, water never reaches this elevation under any storm simulation considered.

Other boundary conditions include astronomical and meteorological forcing conditions. For example, tidal forcing was applied at the open ocean boundary (section 4.5.2.1), river inflows were applied at the river boundaries (4.5.2.2), meteorological forcing (winds and pressures) were applied over the oceanic basin (section 4.7), sea level rise conditions were input (section 4.7), and the influence of dam operations and their associated pumps were developed as a new boundary condition in ADCIRC (section 4.5.3). Nodal attributes were also assigned to the model nodes throughout the domain to represent bottom friction (used to assist in model calibration), lateral eddy viscosity, surface directional wind reduction factors, and primitive weighting in the model's continuity equation. In addition, wave forcing was applied to the model through coupling with SWAN.

4.5.2.1 Tidal Forcing

Tidal forcing was applied using eight tidal harmonic constituents along the open ocean boundary. Each tidal constituent consisted of a frequency, amplitude, phase nodal factor and equilibrium argument. The constituents used were those from M2, S2, K2, N2, K1, O1, P1 and Q1 tides (Table 4-2). These tidal constituents were extracted from the FES95.2 global database and interpolated to the ADCIRC open boundary nodes. These eight main constituents comprise the majority of the expected tidal signal. Descriptions of each constituent are

in Table 4-2. On the boundary condition the values of the forcing frequency, nodal factor and equilibrium argument are the same for every node for a given period of time (i.e., a given storm). The amplitude and phase are location dependent and vary along the open boundary. To adjust the tide to specific time periods for the various storms, simulated nodal factors and equilibrium arguments specific to the periods of interest were calculated and applied in the model.

Table 4-2. Tidal constituents used to develop tidal boundary condition for BH-FRM.

Abbreviation	Period	Description
M2	12.42	Principal Lunar Semidiurnal
S2	12.00	Principal Solar Semidiurnal
K2	11.97	Lunisolar Semidiurnal
N2	12.66	Larger Lunar Elliptic Semidiurnal
K1	23.93	Lunar Diurnal
O1	25.82	Lunar Diurnal
P1	24.07	Solar Diurnal
Q1	26.87	Larger Lunar Elliptic Diurnal

4.5.2.2 Freshwater Input

A key aspect of potential flooding in the City of Boston and surrounding communities includes the influence of the rivers running through the City and discharging into Boston Harbor. As such, the Charles, Mystic, and Neponset Rivers, as well as their tributaries, were included in the ADCIRC mesh to evaluate the combined impact of watershed discharge and storm surge based flooding. River flow was specified at the upstream boundaries of each river to represent the discharge expected for different return period rainfall storm events, as well as projected changes in precipitation due to climate change¹⁰. Table 4-3 presents

the total rainfall amount (in inches) associated with present day (2013) and projected return period rainfall event precipitation amounts. These data were provided by Kleinfelder, Inc. (2014) and were determined as part of the City of Cambridge's climate change vulnerability project.

Table 4-3. Present day (2013) and projected future return period rainfall event total precipitation amounts (inches).

Rainfall Event	Rainfall total (inches)		
	2013	2030	2070
10 Year-24hr	4.9	5.6	6.4
10 Year-48hr	5.5	6.4	7.2
25 Year-24hr	6.2	7.3	8.2
25 Year-48hr	7.0	8.6	9.8
100 Year-24hr	8.9	10.2	11.7
100 Year-48hr	10.0	13.2	15.7

These rainfall events (for present day and climate change conditions) were translated into river discharge hydrographs using watershed and river modeling performed for other studies (MWH Global, 2014; VHB, 2014). Storm hydrographs for the Charles and Mystic River were input into the model and provided through other study efforts (MWH Global, 2014; VHB, 2014). Storm hydrographs consisted not only of present day conditions (2013), but also future climate change conditions. The Charles River discharge data were provided by MWH Global (2014) and included all contributors combined (Cambridge, MWRA overflows south and north of the Charles, Watertown and Newton) to arrive at the peak flows and discharge hydrographs. Table 4-4 shows the present day and projected future peak flow values for the Charles River. Similarly, the Mystic River discharge hydrographs were provided by VHB, Inc. (2014) utilizing their Mystic River HEC-RAS model. These discharge

¹⁰ Discharges associated with climate change conditions were only specified at the Charles and

Mystic Rivers, the Neponset River only used present day discharge values.

hydrographs focused only on the current (2001-2050) and future (2051-2100) epochs for climate changes.

Prior to simulation of all the various storm events (tropical and extra-tropical Monte Carlo simulations), the combined impact of river discharge and storm surge on the flooding potential was investigated to determine the sensitivity of the model to variations in river discharge (as presented in Tables 4-4 and 4-5). While independently, river flow can have a significant impact on upstream flooding in the system (e.g., due to poor drainage capacity and high river discharge), when combined with storm surge flooding the model is relatively insensitive to the river discharge volume, especially considering the dam operations on the Charles and Mystic Rivers (section 4.5.3). Unless the dams are flanked or overtopped, the existing pump systems (if functional) are able to adequately handle expected increases in river discharge due to climate change conditions. In order to test the combined effects of increased discharge and storm surge, a coastal storm was simulated that overtopped the dams with no river discharge, and with the maximum river discharge. In both cases, the spatial extents and depths of the flooding was essentially the same and flooding was dominated by the storm surge component. Though the variation of river inflow was determined not to be a significant factor in the overall flooding during storm surge events, the inclusion of a 100-yr, 24-hr event was included in all simulations, and the peak of the discharge hydrograph was temporally

Unless the dams are flanked or overtopped, the existing pump systems (if functional) are able to adequately handle the all potential discharges, including climate change conditions.

aligned with the peak of the storm surge event, thereby assuming a conservative case and ensuring that as many physical processes as possible are included in the flooding potential.

Table 4-4. Present day (2013) and projected future return period peak discharge flows (cubic feet per second) for the Charles River.

Rainfall Event	Charles River Peak Flow (cfs)		
	2013	2030	2070
10 Year-24hr	1726	1848	1974
10 Year-48hr	1786	1926	2064
25 Year-24hr	1945	2120	2284
25 Year-48hr	2027	2292	2487
100 Year-24hr	2395	2615	2869
100 Year-48hr	2523	3027	3443

Table 4-5. Present day (2013) and projected future return period peak discharge flows (cubic feet per second) for the Mystic River.

Rainfall Event	Mystic River Peak Flow (cfs)	
	Current Epoch (2001-2050)	Future Epoch (2051-2100)
10 Year-24hr	1370	1673
10 Year-48hr	1525	1884
25 Year-24hr	2032	2165
25 Year-48hr	2190	N/A
100 Year-24hr	2200	2300
100 Year-48hr	N/A	N/A

4.5.2.3 Bottom Friction

The bottom friction throughout the model domain is assigned to individual nodes based on the Manning's n frictional approach. Manning's roughness values for the nodes were assigned based on the USGS land cover data set. All model nodes are assigned a Manning's n value so that ADCIRC can appropriately adjust flow for local friction conditions. In the model these values were derived from the National Land Cover Database (NLCD) 2006 dataset. The NLCD is in the form of a raster grid with varying values denoting land cover characteristics. Each land cover characteristic also has an associated friction, in the form of a Manning's n value. The following table (Table 4-6) shows the land

cover type, and the associated Manning's n value that was assigned in model calibration. All model nodes below mean sea level were assigned the open water value of 0.02.

In addition, influences of urban infrastructure and buildings were included in the model as frictional elements. For example, for areas with dense building and infrastructure, the Manning's n values were increased, and horizontal eddy viscosity values changed, to represent the increased disturbance to the flow caused by the buildings. These values were modified as needed to ensure adequate calibration to observed high water mark data (Section 4.6).

Table 4-6. Manning's n values applied in BH-FRM based on land cover types.

Land Usage	Manning's n
Open Water	0.020
Perennial Ice/Snow nld changed	0.010
Developed - Open Space	0.020
Developed - Low Intensity	0.050
Developed - Medium Intensity	0.100
Developed - High Intensity	0.150
Barren Land (Rock/Sand/Clay)	0.090
Unconsolidated Shore	0.040
Deciduous Forest	0.100
Evergreen Forest	0.110
Mixed Forest	0.100
Dwarf Scrub	0.040
Shrub/Scrub	0.050
Grassland/Herbaceous	0.034
Sedge/Herbaceous	0.030
Lichens	0.027
Moss	0.025
Pasture/Hay	0.033
Cultivated Crops	0.037
Woody Wetlands	0.100
Palustrine Forested Wetland	0.100
Palustrine Scrub/Shrub Wetland	0.048
Estuarine Forested Wetland	0.100
Estuarine Scrub/Shrub Wetland	0.048
Emergent Herbaceous Wetlands	0.045
Palustrine Emergent Wetland (Persistent)	0.045
Estuarine Emergent Wetland	0.045
Palustrine Aquatic Bed	0.015
Estuarine Aquatic Bed	0.015

4.5.2.4 Horizontal Eddy Viscosity

The horizontal eddy viscosity parameter was another value that was adjusted during model calibration to ensure the model results adequately represented observed conditions (water surface elevation time series and high water marks). Nodes that were inter-tidal and sub-tidal were assigned a viscosity of $5 \text{ m}^2/\text{s}$, while land-based nodes were assigned a viscosity of $40 \text{ m}^2/\text{s}$. This value of horizontal eddy viscosity falls within the typical range of values, between 10 to $50 \text{ m}^2/\text{s}$, used in previous storm surge studies with ADCIRC. Many ADCIRC modeling efforts have set the value as high as $50 \text{ m}^2/\text{s}$, including Bunya et al. (2009) and URS (2006). Due to the dense urban environment and presence of significant anthropogenic features, the land-based viscosity values were determined to be near the upper end of the viscosity range. These values were optimized during the calibration process to ensure model results closely replicated measured data.

4.5.2.5 Primitive Weighting Coefficient

The generation of the primitive weighting coefficients follows the standard methodology and is based on both depth and nodal spacing (ADCIRC, 2013). Specifically, if the average distance between a node and its adjacently connected neighbor nodes is less than 500 meters, then coefficient is set to 0.030. If the average distance between a node and its adjacently connected neighbor nodes is greater than 500 meters and depth less than 10 meters, then the coefficient set to 0.02. If the distance between a node and its adjacently connected neighbor nodes is greater than 500 meters and depths are greater than 10 meters the value of coefficient is set to 0.005. This is assignment simply weights the relative contribution of the primitive and wave portions of the Generalized Wave-Continuity Equation.

4.5.2.6 Directional Wind Reduction

The surface directional wind reduction factors makes adjustments to the winds through evaluation of the land use type data in 12 directional bands around each node. This parameterization allows for variations in how the wind is assessed in the model over various water and land areas. For example, wind over open water behaves completely differently than wind over various land types, especially in urban environments. As such, this parameter allows for different surface roughness values for areas over open water as compared to various over land areas. The directional wind reduction consists of a set of 12 values assigned to each node, with each value corresponding to a 30 degree wedge emanating from a given node. Each wedge represents a potential direction from which winds can come towards the node. For each of the 12 wedges, a wind reduction factor is assigned to the node, based on the land cover type upwind of the node. Additional details can be found in Westerink et al. (2008).

4.5.3 Dam Operations and Modeling

The New Charles River Dam (NCRD) and the Amelia Earhart Dam (AED) have a strong influence on flood control within the system. Modeling present and future scenarios for flooding requires incorporating these structures and operational characteristics into the ADCIRC application. This section provides a brief overview of the two dams, as well as the formulation within ADCIRC.

The NCRD (Figure 4-10) is located on the Charles River, and was constructed in 1978 to replace the original dam from 1908. The NCRD is a complex sluice, lock, and pump system, and is used to manage freshwater draining from the Charles River Basin, sea water from Boston Harbor, and vessel

navigation. Typically, the lower basin (LB) drains into Boston Harbor by gravity over the NCRD sluice. The operational goal is to maintain the basin (upstream side of NCRD) between elevations of 106.5 and 108.5 feet (Metropolitan District Commission [MDC] Boston City Base datum), so the pumps are generally activated to maintain these levels. There are a total of six pumps. Practically, three pumps are activated when the operator (manned station) perceives the water level will exceed 108, and all six can be activated as needed per the operational guidance. Each pump has a capacity of 1,400 cfs. When a storm is in the forecast, pumps also are activated to proactively reduce the water level to accommodate storm waters. The Boston Harbor side downstream from NCRD typically fluctuates between 100 and 111 feet with the tides and storm surge, and the dam would overtop at 118 feet; however, it has been reported that the highest tide on record is less than 116 feet.



Figure 4-10. New Charles River Dam (NCRD).

The AED (Figure 4-11) is located on the Mystic River, and was constructed between 1963 and 1968 with pumps installed in 1978. There is a dam and lock system, but no sluice. There are three pumps with a bay for a 4th pump, and the basin range is maintained between 104.5 and 106.5. Like the NCRD, pumps are “exercised” monthly

for approximately 2 hours. Each pump has a capacity of 1,400 cfs.



Figure 4-11. Amelia Earhart Dam (AED).

While the actual operation of the dams involve a certain human element (e.g., exactly when to turn the pumps on and off, how many pumps to turn on and at what capacity) and their respective operational protocol is more complicated than can actually be input into a model, both dam systems have been incorporated into the ADCIRC formulation. This consisted of developing a new dam-pump boundary condition within the ADCIRC computation code. When enabled, the model activated pumping upstream of the dam when a certain water level is reached (prescribed by the user). The model effectively moves a volume of water (based on the specified

Modeling present and future scenarios for flooding requires incorporating these structures and operational characteristics into the ADCIRC application. Dam systems have been incorporated into the BH-FRM formulation.

capacity) from prescribed locations (nodes) upstream from the dam to a prescribed location downstream from the dam. Pumps will stay active until the water level reduces to a level also prescribed by the user. A flow rate is also specified by the user as a parameter to simulate the volume of water pumped. The rate is per unit width of the dam; thus, the total flow rate pumped depends up on the width of the dam and the flow rate (e.g., pumping with a flow rate of 100 cfs along a 25 feet long boundary requires specifying a discharge per unit width of 4 cfs/ft at each node on the boundary node string defining the 25 ft long dam). Table 4-7 below summarizes the operational parameters input to the model for the NCRD and AED. For NCRD, six pumps are activated in the ADCIRC model with a total flow rate of 8,400 cfs when the model elevation reaches 108.5 feet MDC, and the pumps remain active until the elevation is reduced to 106.5 feet MDC. Likewise for AED, three pumps are activated in the ADCIRC model with a total flow rate of 4,200 cfs when the model elevation reaches 106.5 feet MDC, and the pumps remain active until the elevation is reduced to 104.5 feet MDC.

Table 4-7. Pump summary for BH-FRM dams (all pumps have maximum capacity of 1400 cfs).

Dam	Pumps	Total Flow Rate (cfs)	Model Segment Width (m)	Flow Rate per Length ($m^3/m*s$)	Pump on Elevation (MDC ft)	Pump on Elevation (NAVD-m)	Pump off Elevation (MDC ft)	Pump off Elevation (NAVD-m)
AED	3	4200	43	2.77	106.5	0.16	104.5	-0.45
NCRD	6	8400	68	3.49	108.5	0.77	106.5	0.16

It was assumed that when a storm surge event is occurring, the dams close all sluices and gates such that water cannot get into the basin from the ocean side unless the dam is overtopped or flanked. Similarly during these storm conditions, it is assumed that the only way for freshwater discharge to be passed downstream is via the pump systems. In this scenario, this numerical approach functions well and is able to determine the influence of both increased discharges propagating down the river systems as well as any excess storm surge water that may overtop or flank the dams. The model always will attempt to keep the upstream basins between the required water levels, dynamically incorporating all inputs into the basin. For example, if the discharge down the Charles River increases, pumps are activated in the model to keep the basin below 108.5 feet MDC. If the dam is overtopped or flanked, then excess water arriving in the basin will attempt to be handled by the pumps as well. Since the rivers and their discharge hydrographs (section 4.5.2.2) for both present day and climate change conditions are dynamically included in the model, this model pump operation is able to determine if the pumps can adequately handle the increased discharge, and potential combination of discharge and overtopping, if it occurs. The model always assumes that all the pumps will be operational and would be able to operate at full capacity, if needed. Simulations could be conducted that evaluate the impacts if one or more of the pump systems failed during a heavy

discharge event, significant surge event, or the combination of both. For the current pilot study, those scenarios were not considered.

Since the rivers and their discharge hydrographs for both present day and climate change conditions are dynamically included in the model, this model pump operation is able to determine if the pumps can adequately handle the increased discharge, and potential combination of discharge and overtopping, if it occurs.

A summary of the assumptions in the model for the NCRD include:

- The model keeps the upstream basin between 108.5 feet MDC and 106.5 feet MDC, just like the actual operations. When the water in the basin reaches the 108.5 level, the pumps turn on in the model and pump water downstream of the dam, when it is lowered to 106.5, the pumps turn off. It is a simple binary on/off operation in the model, where in actuality there may be more of a management/human element.
- In all storm cases, a Charles River 100-yr, 24 hour discharge hydrograph (for the appropriate year scenario 2030, 2070, 2100) is applied such that the peak discharge approximately aligns with the peak of the storm surge.

- The model assumes all pumps are operational and have full capacity, if needed. Cases where the pumps fail or are inoperable are not included.
- Each pump (6 total) has a maximum capacity of 1400 cfs.

A summary of the assumptions in the model for the AED include:

- The model keeps the upstream basin between 106.5 ft MDC and 104.5 ft MDC, just like the actual operations. When the water in the basin reaches the 106.5 level, the pumps turn on in the model and pump water downstream of the dam, when it is lowered to 104.5, the pumps turn off.
- In all storm cases, a Mystic River 100-yr, 24 hour discharge hydrograph (for the appropriate year scenario 2030, 2070, 2100) is applied such that the peak discharge approximately aligns with the peak of the storm surge.
- We assume all pumps are operational and have full capacity if needed. Cases where the pumps fail or are inoperable are not included.
- All pumps (3 total) have a maximum capacity of 1400 cfs.

4.6 Model Calibration and Validation

While the models used in this pilot project (ADCIRC, SWAN) are rooted in sound science and utilize standard governing equations of water motion, the propagation of water through a unique geographic setting results in site-specific variations that may require adjustment of model parameters to more accurately represent the real world system. For example, in an urban landscape, an area consisting of numerous buildings will influence flow differently than a marsh, which will influence flow differently than a parking area, which will influence flow

differently than a sub-tidal estuary. For these types of cases, it is reasonable to adjust parameters, such as frictional factors within accepted bounds to better represent the water propagation. As such, the BH-FRM model was calibrated using both normal tidal conditions and representative storm events for the northeast. The calibrated model was then validated to another storm event to ensure accuracy (section 4.6.2). Finally, the calibrated model was utilized to simulate a wide range of storm events (both hurricanes and Nor'easters) and sea level rise conditions (section 4.7) using a Monte Carlo statistical approach.

4.6.1 Storm Selection

In order to select appropriate historical storm events for model calibration and validation, a number of key factors were considered, including:

- The historic storm must be considered a significant storm for the Boston area (a historic storm of record) that was of large enough magnitude to produce substantial upland flooding.
- The historic storm must have adequate meteorological conditions to be able to generate pressure and wind fields for ADCIRC input. This required the use of global reanalysis data, which was generally available for historic storm events post-1957.
- The historic storm must have sufficient observations and/or measurements of flooding within the northeast and Boston area. This could consist of high water marks data, tide station observations, wave observations, and other data measures.

Historic storm events were analyzed with these three conditions in mind. To determine potential candidate storms, as

well as identify storms for the Monte Carlo simulations, residual surge data (non-tidal) were collected from the National Oceanic and Atmospheric Administration (NOAA) station in Boston, MA (station ID: 8443970) (NOAA, 2014a). The NOAA tide gage station is located in the Fort Point Channel and the period of record for the station begins on May 3, 1921 and extends to the present day. Hourly observed water levels (identified as “verified water level” by NOAA), as well as the predicted tidal based water levels, for the station between May 3, 1921 and July 31, 2014 were obtained. This 92 year period of record is more than 99% complete, but does include limited periods when no water level data were recorded. These data were used to identify a total of 333 historic surge events that impacted the Boston area (see section 4.7).

The BH-FRM model was calibrated using both normal tidal conditions and representative storm events for the northeast. The calibrated model was then validated to another storm event to ensure accuracy.

From these events, the highest two residual surge events identified were the Blizzard of 1978 and the Perfect Storm of 1991. The “Blizzard of 1978”, which was generated by a stationary off-shore Nor’easter on Feb 6-7, 1978, generated record-setting flood levels from Provincetown, MA to eastern Maine. This storm has the highest recorded total water surface elevation (tides plus surge) at the Boston tide gauge of 9.52 feet NAVD88 and met all the requirements for a model calibration storm event. The storm surge peaked at 3.64 feet above predicted tide levels at the Boston tide gage. The “Blizzard of 1978” had significant impact on the coastline since it stalled in a critical

location and arrived during a spring tidal cycle with strong onshore winds.

Due to the magnitude of this Nor’easter event, a comprehensive record of high water marks was documented throughout the northeast by USGS (Gadoury, 1979). This collection of high water marks constitutes the largest collection of observations for any storm in the northeast. Due to the onshore (northeast) winds, the measured flood levels were produced by a combination of tide, surge, and wave action, depending on the site location. Each site observation was detected by direct evidence, namely a line of debris/trash/salt/oil/snow with varying degrees of confidence. These degrees are classified as “excellent” where a clear constant line was observed, “good” where a clear line was visible with some vertical variation (average elevation reported), and “fair” or “poor” where a line was visible with significant variation in elevations (average elevation reported). Each line was marked by USGS personnel (corroborated by witnesses when possible) within the first week post-storm with few exceptions, and flood elevation recorded from spirit-leveling from points of known elevation, accurate to within a hundredth of a foot. Along with the flood elevation, the site was referenced by latitude/longitude and by location relative to the nearest town with a clear description of the site. Most of the flood mark sites were in exposed areas with greater chances of wave action (not recorded in tidal gauges); however each elevation was measured in protected areas, free of spray caused by winds and waves, wherever possible in order to measure the average location rather than extremes caused by single waves or by wind. The data set also specifies whether the flood elevations are expected to result from surge or wave action/bores. This distinction is important since the validity of high water marks used for model calibration could more easily be determined. While the

BH-FRM model simulates the combined surge and wave impact, it does not model wave run-up or overtopping. The Blizzard of 1978 storm represented an ideal historic event for calibration of the BH-FRM model due to its historic significance (highest observed total water level), its spatial influence (most of the northeast), and the ample observed data.

The so-called “Perfect” Storm of October, 1991 (and of movie fame) was a Nor’easter that absorbed Hurricane Grace producing the largest observed storm surge at the Boston tide gage (4.1 feet). Damage from the Perfect Storm totaled over \$200 million, 13 people were killed, and in Massachusetts, where damage was heaviest, over 100 homes were destroyed or severely damaged. The total water surface elevation observed at the Boston tide gage was 8.66 feet, the second highest observed total water level. Although the Perfect Storm had the highest surge, it did not occur during high tide. Due to its significance, availability of observed data, and unique nature of this event, this storm was selected for model validation.

4.6.2 Model Calibration

Model calibration is the process in which model parameters are systematically adjusted through a range of acceptable values and results are examined using standard measures. Through a number of iterative simulations the configuration of model parameters (e.g., roughness lengths, culvert friction factors, diffusivity parameters, etc.) that provided the best agreement between modeled variables and observed measurements is determined. The BH-FRM model was calibrated to normal tidal conditions to ensure the model could adequately predict water surface elevations for average weather conditions, as well as to the Blizzard of 1978 to determine the performance for storm conditions.

For the observed high water marks, the key target for calibration was the maximum water surface elevation observed during the storm event. Therefore, the peak of the modeled storm surge event is compared to the observed high water mark. For observed time series of water levels, the model performance is evaluated by comparing time series output from the model to observed time series for water surface elevation at specific locations throughout the modeling domain. The results are presented visually as time series plots, and absolute error of the model is quantified by calculating the bias and Root Mean Square Error (RMSE). The overall error for a given observation time series is quantified in two ways: where P_{mod} and P_{obs} are the modeled and observed values respectively and n is the number of discrete measurements in the time series. The bias provides a measure of how close on average the modeled results are to the observed data.

$$\text{Bias} = \frac{\sum_1^n (p_{\text{mod}} - P_{\text{obs}})}{n} \quad (4.7)$$

$$\text{RMSE} = \sqrt{\frac{\sum_1^n (p_{\text{mod}} - P_{\text{obs}})^2}{n}} \quad (4.8)$$

A positive value indicates that the model is over-predicting the observation while a negative value indicates that the model is under-predicting the observations; a bias of zero indicates that on average over the time series the model reproduces the observations. The RMSE is an average of the magnitude of the error of each measurement in the time series. RMSE is always positive with smaller values indicating better model performance. Both the bias and RMSE are measures of absolute error having the same units of the measured quantity from which they are computed.

4.6.2.1 Tidal Calibration

To ensure the BH-FRM model is capable of predicting water levels and coastal hydrodynamics during typical weather conditions, the model was utilized to predict average tidal conditions over the entire model domain, with focus on the study region. The model was forced with tidal constituents at the open ocean boundary in order to simulate water levels, and then compared with known tidal conditions at several NOAA stations within the model domain, and in the vicinity of Boston Harbor. Figure 4-12 shows the locations for the tidal comparisons, shown as yellow dots, while Table 4-8 summarizes the error measures for all observation locations.

Overall the agreement is reasonable. The magnitude of the bias is equal or less than 0.02 feet at all locations meaning that the calibration simulation reproduced average water levels within a quarter of an inch at all locations. RMSE is less than 0.05 feet for all locations indicating that on average the modeled water level is within a half an inch of the observed level at any given time.

4.6.2.2 Storm Calibration (Blizzard of 1978)

As noted earlier, in addition to the normal tidal conditions, BH-FRM was also calibrated to a storm event (the Blizzard of 1978). The Blizzard of 1978 was simulated in BH-FRM using the methods described in Section 4.7. Since the goal of the BH-FRM model was to identify the maximum flooding occurring with an individual storm

event, the key target for calibration was the maximum water surface elevation observed during the storm event. As such, the model was calibrated such that the peak of the total water surface elevation was adequately captured, including the spatial variation of the peak throughout the Boston region. Peak water surface elevation results from the model were compared to both observed high water marks (Gadoury, 1979) and tide station measurements (Figure 4-12) during the Blizzard.

Similar to the average tidal calibration (section 4.6.2.1), the times series of modeled water surface elevation during the Blizzard of 1978 was compared to the observed water surface elevation time series to generate bias and RMSE errors. Table 4-9 presents the results of the comparison. The bias in Boston is less than a quarter of an inch, while the RMSE error is 3 inches, which considering a total surge elevation of approximately 10 feet, is a reasonable error magnitude (2.5% error).

While the comparison of the water surface elevation time series measurements and model results at the various tide stations provides reasonable agreement and verifies the model is adequately functioning in the sub-tidal areas, a comparison to recorded high water marks in upland areas was also completed to assess the model performance for overland flooding. As described in Section 4.6.1, high water marks recorded for the Blizzard of 1978 were used for model comparison.

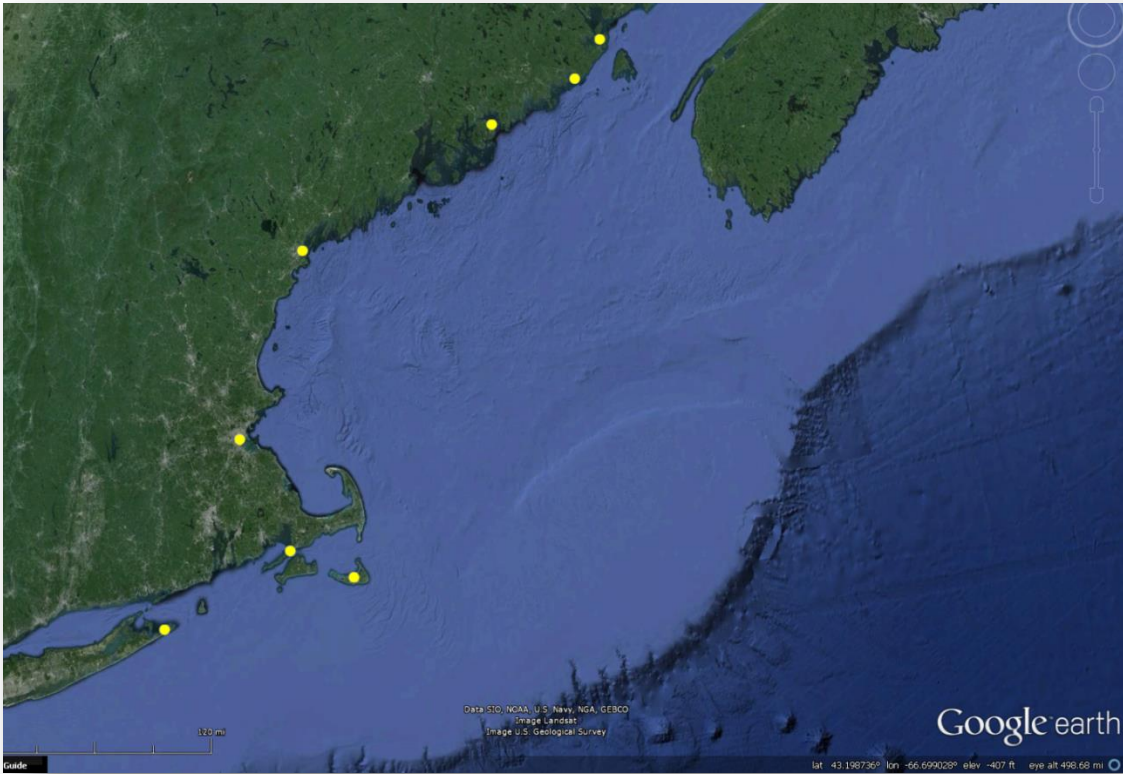


Figure 4-12. Location of tide stations in the vicinity of Boston Harbor. These stations were used for calibration of the BH-FRM model.

Table 4-8. Calibration water surface elevation error measures for average tidal conditions. Relative error based on the average tidal range at each station.

NOAA station	RMSE (ft)	Bias (ft)	Relative Error (%)
4810140, Eastport, Maine	0.05	-0.02	0.3
8411250, Cutler Naval Base, Maine	0.05	-0.02	0.4
8413320, Bar Harbor, Maine	0.04	-0.02	0.4
8418150, Portland, Maine	0.04	-0.02	0.4
8443970, Boston, Massachusetts	0.05	-0.02	0.5
8449130, Nantucket Island, Massachusetts	0.03	-0.01	1.0
8447930, Woods Hole, Massachusetts	0.03	-0.01	1.7
8510560, Montauk, New York	0.03	-0.02	1.4

Table 4-9. Calibration water surface elevation error measures for the Blizzard of 1978.

NOAA station	RMSE (ft)	Bias (ft)
4810140, Eastport, Maine	0.33	-0.09
8411250, Cutler Naval Base, Maine	N/A	N/A
8413320, Bar Harbor, Maine	0.21	-0.04
8418150, Portland, Maine	0.23	-0.03
8443970, Boston, Massachusetts	0.23	-0.02
8449130, Nantucket Island, Massachusetts	0.11	-0.04
8447930, Woods Hole, Massachusetts	0.16	-0.05
8510560, Montauk, New York	0.19	-0.02

There are detailed descriptions of each observed high water mark in Gadoury (1979) and these descriptions were used to select the most appropriate water levels for model comparison. For example, high water marks that were classified as “poor” (high uncertainty) or “fair” were discarded due to their uncertainty, and those that included the influence of wave overtopping and run-up (processes that are not modeled in BH-FRM¹¹) were not used for model calibration. Figure 4-13 shows an example of the first step in the high water mark calibration process, consisting of visual comparison of model results and high water mark observations. The pink dots on the map show some of the high water mark locations that were selected for model calibration due to their classification, location, and water mark type (e.g., surge only, etc.). The zoom out panel to the right shows the water surface elevation model results (blue line in meters NAVD88) extracted from the model at the location of the observed high water

mark. The results show the water surface elevation leading up to and during the Blizzard of 1978. The broken red line shows the elevation of the associated high water mark at that location. During the peak of the modeled storm (blue arrow), the water surface elevation matches the observed high water mark, indicating the model adequately represented the dynamics of the storm in this area.

Figure 4-14 shows another visual comparison at a location in Winthrop, Massachusetts within Boston Harbor. This location is normally dry upland area during normal tidal conditions. However, as shown in the model time series, as the surge rises, this area becomes inundated during high tides and goes dry during low tides. The model water surface elevation peaks slightly above the observed high water mark at this location (blue arrow) at just under 3 meters NAVD88 (9.8 feet NAVD88). Figure 4-15 shows a third example of the model comparison to observed high water marks, in this case for a location south of the City of Boston in Cohasset, Massachusetts. At this location, the observed high water mark was approximately 9.4 feet NAVD88 and the model does a reasonable job of replicating this peak. The model generally did a reasonable job of predicting peak water surface elevations throughout the regional area.

¹¹ Wave run-up and overtopping can be important in local areas directly adjacent to the coastline, especially those with large wave exposure (open facing Atlantic Ocean). However, Boston Harbor is relatively sheltered from wave energy and experiences lower wave heights, run-up, and overtopping. Additionally, the CA/T system is not located on the coastline and flooding will be dominated by increased water surface elevations due to winds, surge, and SLR.

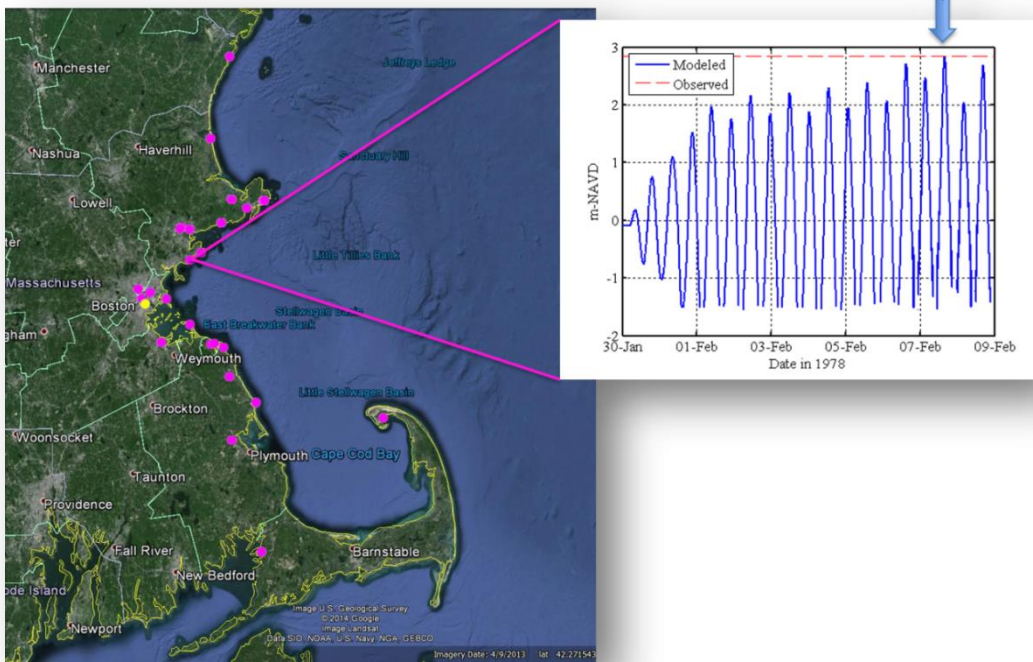


Figure 4-13. Model calibration results for the Blizzard of 1978. Comparison of modeled time series of water surface elevation with observed high water mark in Swampscott, Massachusetts.

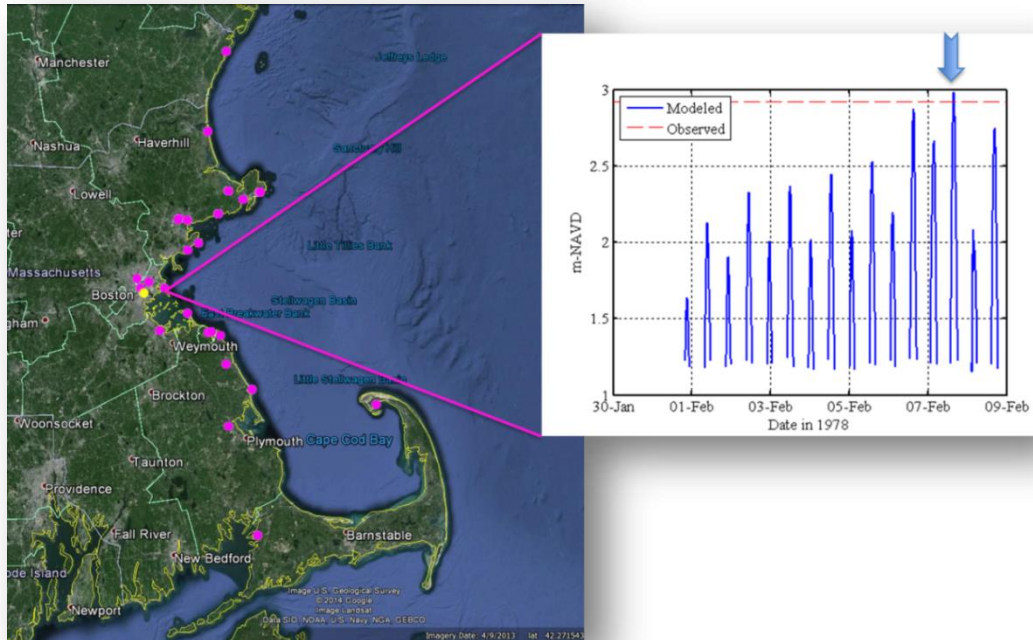


Figure 4-14. Model calibration results for the Blizzard of 1978. Comparison of modeled time series of water surface elevation with observed high water mark in Winthrop, Massachusetts.

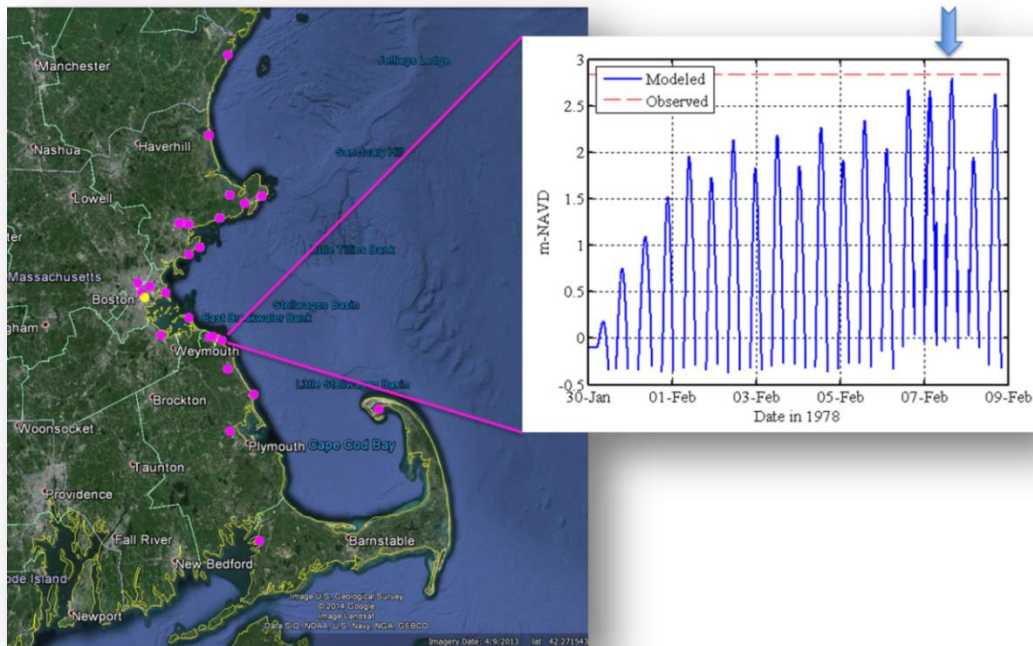


Figure 4-15. Model calibration results for the Blizzard of 1978. Comparison of modeled time series of water surface elevation with observed high water mark in Cohasset, Massachusetts.

Following the visual comparison, which was conducted using high water marks from New Hampshire to Cape Cod, the BH-FRM model results were also quantified through a statistical comparison to selected high water marks (good or excellent quality surge only observations) in the Boston Harbor region only, since this was the focus area of the modeling effort. Figure 4-16 presents a scatter plot of the modeled water surface elevation (wse) on the horizontal axis and the observed water surface elevation (wse) on the vertical axis. If the model matched the observed results exactly, the markers would lie directly on the red line. The bias and RMSE errors for the high water mark data are -0.45 feet and 0.8 feet, respectively. Greater error is expected when comparing model results to observed high water marks due to the uncertainty associated with the high water marks, which are subject to human interpretation and judgment errors (Gadoury, 1979); however this is a reasonable error, representing an 8% relative

error. This is quite reasonable considering the uncertainty associated with the observed high water mark data.

4.6.3 Model Validation

In addition to calibrating a model, it is common practice to validate a calibrated model to confirm the model's applicability to a reasonable range of conditions prior to use as a predictive tool. Validation involves applying the calibrated model to set of observed data that are independent from the calibration data set by modifying the boundary conditions without changing the model configuration or parameterization. Error statistics for model validation should meet the same criteria as those applied to model calibration. The Perfect Storm was used to validate the BH-FRM model. While no high water mark data existed for the Perfect Storm, tide gage stations in the northeast did record water surface elevations throughout the storm.

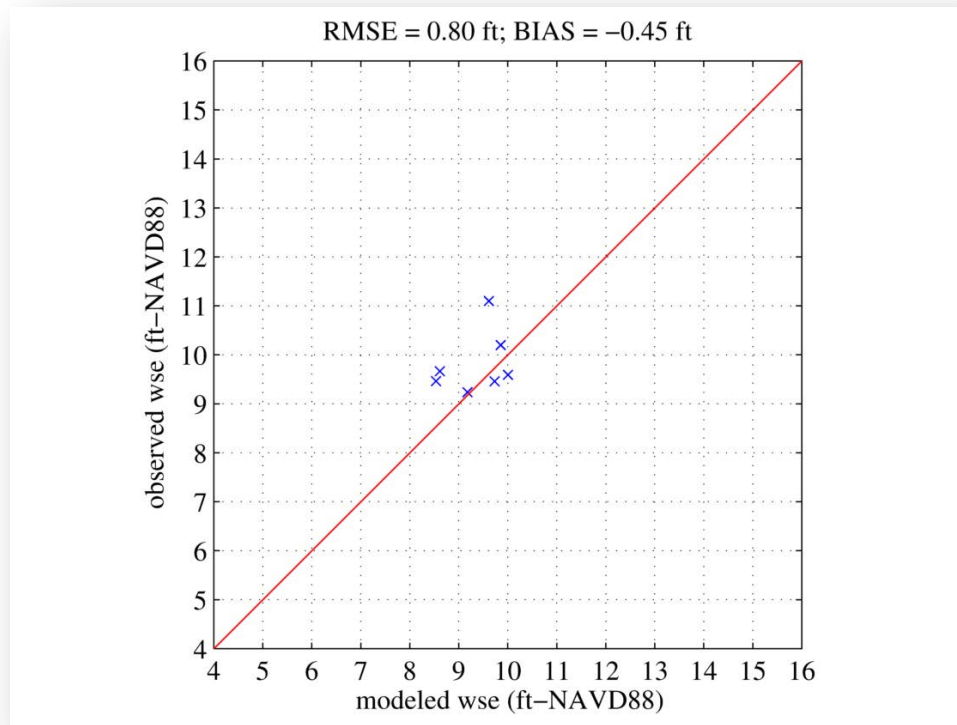


Figure 4-16. Model calibration results for the Blizzard of 1978. Comparison of observed high water marks to peak model results at the same locations within Boston Harbor.

Figure 4-17 shows an example of the model comparison to the observed time series in Narragansett Bay, Rhode Island. The model does a reasonable job of replicating the passage of the storm at this location. Table 4-10 summarizes the error measures for all observation locations. The bias is small at all tide stations (less than $\frac{1}{4}$ of an inch), while the largest RMSE is approximately $\frac{3}{4}$ of an inch. These results used the same model parameters (e.g., bottom friction, diffusivity, etc.) as used to simulate the Blizzard of 1978. The model validation also represents a different type of storm. While the calibration event (Blizzard of 1978) was a purely extra-tropical event, the validation event (Perfect Storm of 1991) was a hybrid of a tropical and extra-tropical event. In both cases, the BH-FRM model was able to accurately simulate the historic storm conditions.

4.7 Sea Level Rise and Storm Climatology

This section describes the development and implementation of the sea level rise scenarios and the storm climatology (pressure and wind fields) data sets. Sea level rise scenarios were selected for four distinct time periods (2013, 2030, 2070, and 2100) and projected rates were chosen to bracket the potential future sea level rise outcomes for the Boston Harbor area. Both tropical and extra-tropical storm conditions were evaluated in the model, and are an important consideration for the northeast. Tropical storms were developed using a large statistically robust set of synthetic hurricanes spanning 20th and 21st century

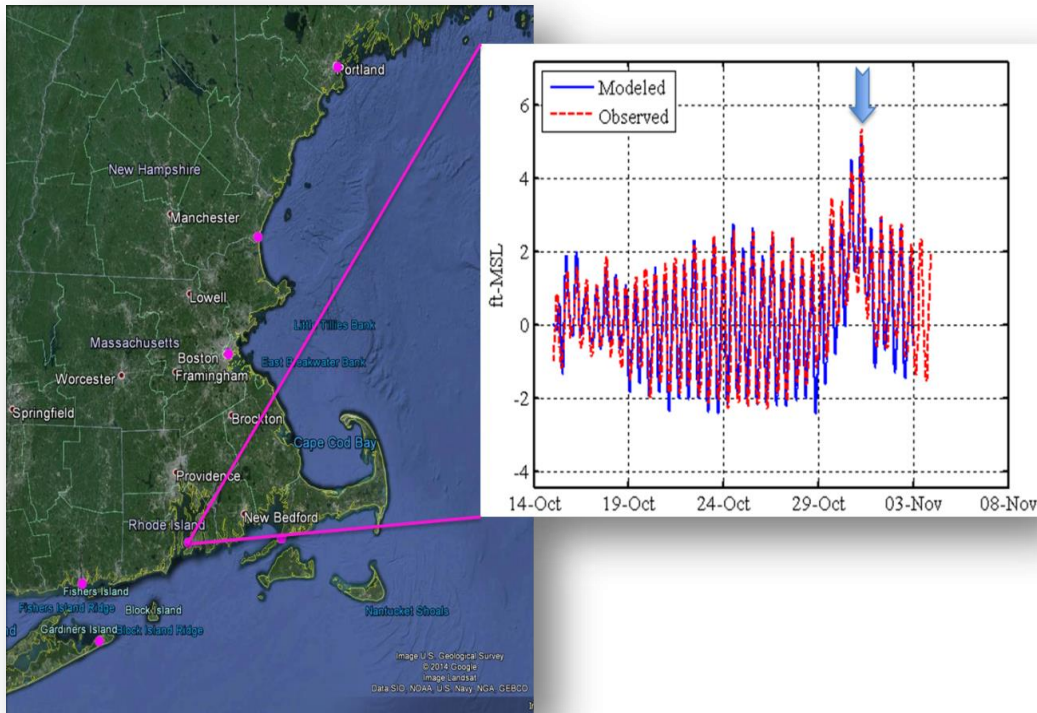


Figure 4-17. Model validation results for the Perfect Storm of 1991. Comparison of modeled time series of water surface elevation with observed high water mark in Narragansett Bay, Rhode Island.

Table 4-10. Validation water surface elevation error measures for the Perfect Storm of 1991.

NOAA station	RMSE (ft)	Bias (ft)
4810140, Eastport, Maine	0.06	-0.02
8411250, Cutler Naval Base, Maine	0.05	-0.02
8413320, Bar Harbor, Maine	0.04	-0.01
8418150, Portland, Maine	0.05	-0.01
8443970, Boston, Massachusetts	0.07	0.00
8449130, Nantucket Island, Massachusetts	0.04	0.00
8447930, Woods Hole, Massachusetts	0.03	-0.01
8510560, Montauk, New York	0.04	-0.01

climates. Extra-tropical storms were developed from historical observed storms over from 1900 to present. A Monte Carlo statistical approach was utilized to simulate the storm events in the model to determine the probability of flooding throughout the Boston Harbor region.

This section also describes the potential impact of climate change on storm intensity and frequency, which is integrated into the model effort such that storm intensities increase in future conditions scenarios. Finally, this section also explains the implementation of tide and storm phasing within the model. In the northeast, where

tidal ranges are significantly larger than the storm surge itself, the timing of the peak of the storm relative to the phase of the tide has a major influence on the level of flooding, waves, and potential impact to the CA/T system. A storm that aligns with high tide carries significantly more risk than that same storm aligning with a low tide.

4.7.1 Sea level rise scenarios

Sea level rise (SLR) is one of the most certain (Meehl et al., 2007) and potentially destructive impacts of climate change. Rates of sea level rise along the Northeastern U.S. since the late 19th century are unprecedented at least since 100 AD (Kemp et al., 2011). The local relative sea level rise is a function of global and regional changes. As discussed in more detail subsequently, global increases by 2100 may range from 0.2 m (0.7 ft) to 2.0 m (6.6 ft). Regional variations in sea level rise arise because of such factors as vertical land movement (uplift or subsidence), changing gravitational attraction in some sections of the oceans due to ice masses, and changes in regional ocean circulation (Nicholls et al, 2014).

One of the challenges presented by the wide range of SLR projections is the inability to assign likelihood to any particular scenario. According to Parris et al. (2012), probabilistic projections are simply not available at scales that are relevant for vulnerability assessment and adaptation planning. Furthermore, they state that, “coastal management decisions based solely on a most probable or likely outcome can lead to vulnerable assets resulting from inaction or maladaptation. Given the range of uncertainty in future global SLR, using multiple scenarios encourages experts and decision makers to consider multiple future conditions and to develop multiple response options.” For this reason, we have chosen to adopt the SLR scenarios recommended by

Parris et al (2012) for the U. S. National Climate Assessment as illustrated in Figure 4-18 (modified from Figure ES1 in *Global Sea Level Rise Scenarios for the United States National Climate Assessment*, NOAA Technical Report OAR CPO-1, December 12, 2012). We used this scenario despite the maximum of 1.2 m recently presented in the IPCC Fifth Assessment Report (AR5) WG1 material.

As previously noted, the CA/T must be considered to have a very low tolerance for risk of failure and hence, should require the highest level of preparedness. Critical infrastructure that is integral to Central Artery operations (e.g. vent buildings, switches, low elevation pump stations, tunnel entrances) also has low risk tolerance and may require the highest level of protection. Therefore, the use of the highest scenario (H) from Parris et al (2012, shown in Figure 4-18), which combines thermal expansion estimates from the IPCC AR4 global SLR projections and the maximum possible glacier and ice sheet loss by the end of the century and “should be considered in situations where there is little tolerance for risk” was selected for utilization in this study. Use of the Highest scenario is also recommended because they represent the earliest times adaptation actions will need to be implemented. We considered the outcomes of lower, plausible SLR estimates as well. We have selected points along the Highest curve that also correspond with the same SLR heights at a later time following lower curves. For example, in Figure 4-18, Point 2 at approximately 35 cm (1 foot) represents the highest SLR height for 2030, but this height also represents SLR by 2070 (Point 2a) following the intermediate low curve. Point 3 (highest SLR height for 2070) also represents SLR by 2100 (Point 3a) following the intermediate high curve. Hence, the four selected SLR heights (and the corresponding modeling simulations)

actually represent eight potential SLR scenarios that bracket, to the best of our current knowledge, the potential future SLR outcomes for the CA/T systems.

This is consistent with US Army Corps of Engineers Circular No 1165-2-212, 10 1 12, Sea-Level Change Considerations for Civil Works Programs (most recent, October 01, 2011) where on page B-11 it states that a reasonable credible upper bound for 21st century global mean sea level rise is 2 meters (6.6 ft), the approximate value from Parris et al (2013) for 2100.

The time periods for MassDOT CA/T vulnerability analysis are 2030, 2070 and 2100. The dynamic model simulated storm climatologies representative of pre-2050 and post-2050 ocean and climate conditions. We recommended using the SLR estimates associated with these time periods as described below because they minimized the number of time consuming dynamic model runs while at the same time allowed us to assess the plausible high and low range of global SLR to 2100. These SLR estimates (corresponding to points in Figure 4-18) used in this project are:

- 1) Existing conditions for the current time period (considered to be 2013).
- 2) The value for the Highest (H) scenario at 2030 (**19 cm [approximately 0.6 ft] of SLR since 2013**), which is also close to the Intermediate High (IH) value at that same time period, pre 2050 climatology, and approximately the Intermediate Low value for 2100.
- 3) The value for the H scenario at 2070 (**98 cm [approximately 3.2 ft] of SLR since 2013**), which is also approximately the IH scenario value for 2100, post 2050 climatology.
- 4) The value for IH at 2100 (**98 cm [approximately 3.2 ft] since 2013**), which represents a reasonably

plausible projection. The selection of 2100 IH allowed us to use the same model runs as for 2070 H and was chosen for the sake of time and computational efficiency.

The final values were adjusted for local subsidence following Kirshen et al. (2008). Local subsidence is approximately 1.1 mm/year or approximately 0.4 feet per 100 years. The impacts of changes in gravitation forces are not significant near Boston (Kopp, 2014) and were not considered in our analysis. The impacts of possible ocean circulation changes were not considered due to their high uncertainty and relatively small impact here.

4.7.2 Tropical Storm Selection

To define the tropical storm (hurricane) climatology, a large, statistically robust set of synthetic storms generated using the statistical-deterministic approach of Emanuel et al. (2006) were utilized. This approach uses a combination of statistical and physics based modeling to produce parameterized storms with behavior that mimics the natural variation commonly observed in nature, including storm genesis location, storm movement, evolution of storm size and intensity. When compared to storm sets produced using traditional Joint Probability Methods (JPM) or Joint Probability with Optimal Sampling Methods (JPM-OS), storm sets produced with the statistical-deterministic approach are more realistic because they do not make assumptions about the path of the storm, the landfall location, variations in intensity in size, etc. Furthermore, statistical-deterministic storm sets have the advantage that their statistical properties (e.g. the probability distribution of central pressure at landfall) are not dependent on curve fitting of historic data to assumed probability distributions as they are in the JPM

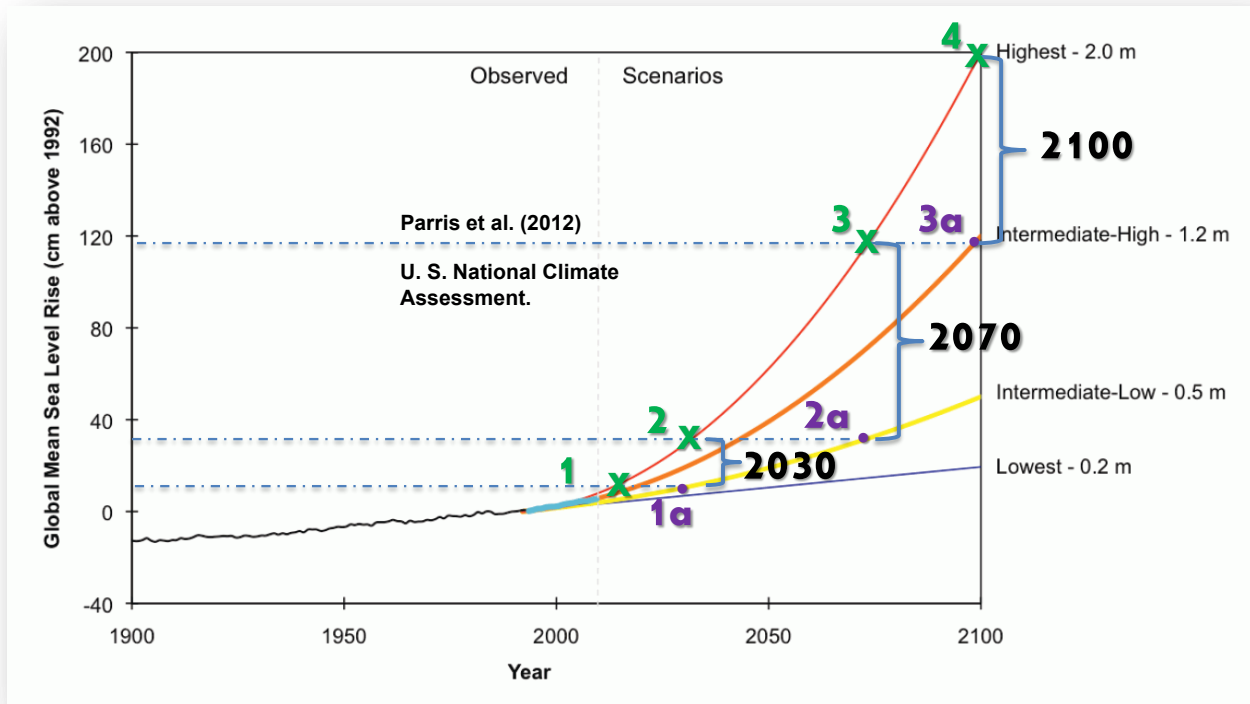


Figure 4-18. Selection of sea level rise rates that span multiple time frame (modified from Figure ES1 in Global Sea Level Rise Scenarios for the United States National Climate Assessment, NOAA Technical Report OAR CPO-1, December 12, 2012).

methods; although they can be validated by comparison to historic data and will be statistically similar to JPM produced sets.

Tropical storm data were supplied by WindRiskTech Inc. and included a total storm set of 40,000 total synthetic tropical storms. These storms were created using four different climatological models and were generated by a storm seeding process following Emanuel et al., (2006). The global climatological models used in the seeding process were NOAA's geophysical fluid dynamics laboratory's model, the UK Met Office's Hadley Centre Global Environmental Model, Japan's Model for Interdisciplinary Research on Climate and Max Planck Institute's ECHAM model.

Storms were specifically selected from the seeding based on a screening process that

evaluated storm tracks capable of entering the northeast area, thereby potentially impacting the Boston Harbor region. The storms were developed for two storm climates (see section 4.7.4), a 20th century and a 21st century, each century containing 20,000 storms. Based on the above climatological models, each storm was provided with a probability of occurrence and each storm set includes an average annual probability of occurrence, which translates to the average number of storms occurring in a given year. These data were utilized to determine the probability associated with each storm in the data set. Figure 4-19 presents an example of the tropical storm track lines associated with one of the global climate model storm sets.

All storms in the data set were categorized by intensity based on hurricane surge index

(HSI) at landfall. The HSI, which is based on the integrated kinetic energy of the storm, has been proposed as an alternative or supplement to the Saffir-Simpson scale with a physical basis that makes it specifically applicable to storm surge (Jordan and Clayson, 2008). HSI is defined by the formula:

$$HSI = \frac{R}{R_0} \left(\frac{V_{max}}{V_{max0}} \right)^2$$

Where R is the radius to maximum winds, R_0 is equal to 60 miles, V_{max} is maximum wind velocity and V_{max0} is 74 mph. The larger the HSI, the more intense the storm, and these data are utilized to create a cumulative distribution function (CDF) curve of the probability of exceedance versus HSI.

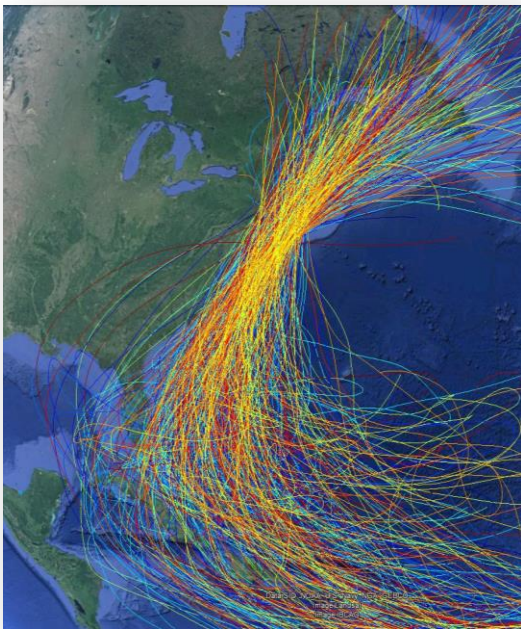


Figure 4-19. Example of the tropical storm track lines associated with one of the global climate model storm sets from WindRiskTech, Inc.

To expedite the analysis, and to reduce High Performance Computing requirements, a storm screening process was implemented.

This process reduced the number of ADCIRC/SWAN simulations required such that 40,000 cases were not required for simulation. Since a relatively large number of storms in the set are relatively weak, small, or do not track close enough to Boston, they do not result in significant flooding in the Boston Harbor area. These storms were easily identified in the HSI distribution and trackline evaluation. From these results a smaller sub set of storms was selected, which adequately approximated the larger set, in a similar methodology FEMA has developed for verifying storm sets when using the Bayesian Quadrature JPM-OS approach (FEMA 2012). Storms were chosen in such a manner to give a good representation of the overall data set's probability of exceedance versus HSI curve and were still statistically robust enough to represent a Monte Carlo approach.

4.7.3 Extra-tropical Storm Selection

While hurricanes are intense, fast moving storms that have a significant impact on coastal communities, they are not as common in the northeast as extra-tropical storm events (at least in the contemporary and historical time frames). Therefore, in addition to the tropical storms, it was critical to develop a set of extra-tropical storms for simulation in BH-FRM.

4.7.3.1 Storm Identification

As a first step, historical extra-tropical cyclone events and storm surge for Boston were evaluated. Historical water level records and historical meteorological records were compared in order to pair individual storm surge levels with individual storm events. The resulting dataset allowed determination of the probability of a given storm surge event and assisted in the selection of a representative set of events to model in BH-FRM.

Historical water level data from the National Oceanic and Atmospheric Agency (NOAA) at the tide gage station in Boston, MA (station ID: 8443970) (NOAA, 2014a) were collected as hourly observations between May 3, 1921 and July 31, 2014. This 92 year period of record is more than 99% complete. Water levels for the station have been rising continuously for each epoch since the beginning of data collection in 1921. Therefore, the water levels were adjusted based on the observed annual sea-level rise for the station (NOAA, 2014b) to adjust historic water levels to present day levels for storm events.

Meteorological data (air pressure) were obtained from the European Center for Medium Range Weather Forecasts Global Reanalysis models (ECMWF, 2014). The ECMWF is an independent intergovernmental organization that provides numerical weather predictions. In addition to forecasts of future weather patterns, the ECMWF provides hind-casts of historical weather patterns. These weather models provide global coverage of best estimate atmospheric conditions for a given period of time. The weather model data were compared to the water level data to identify specific events in the historical record.

In order to pair storm surge events with individual storms, the methodology described in the Federal Emergency Management (FEMA) Region III Storm Surge Study Coastal Storm Surge Analysis: Storm Forcing Report 3: Intermediate Submission No. 1.3 (Vickery et al., 2013) was used. The steps described in this report are:

1. Calculate residual (Observed minus Predicted) water level.
2. Calculate 99th percentile residual water level.

3. Identify all high tide peak water levels that also include a residual greater than or equal to the 99th percentile residual water level.

4. Group high tide peak water levels that occur within 3 days of each other as a single surge event.

The resulting dataset of timestamps, water levels, and residuals constitutes the set of storm surge events. A total of 333 storm surge events were identified, of which 214 were identified as extra-tropical cyclones. Extra-tropical cyclones were identified as storm events that included a low pressure system (at least 5 millibars between lowest pressure and last closed isobar) within approximately 300 miles of Boston at the time of the storm and were not defined as a tropical system. Typically, non-tropical cyclones originate north of the Tropic of Cancer (latitude: 23.43478° N). Figure 4-20 shows a cumulative distribution function (CDF) of the 214 identified extra-tropical storms.

A statistically robust set of both tropical and extra-tropical storm events was simulated in the BH-FRM to evaluate a full range of potential storm conditions that can occur in the northeast.

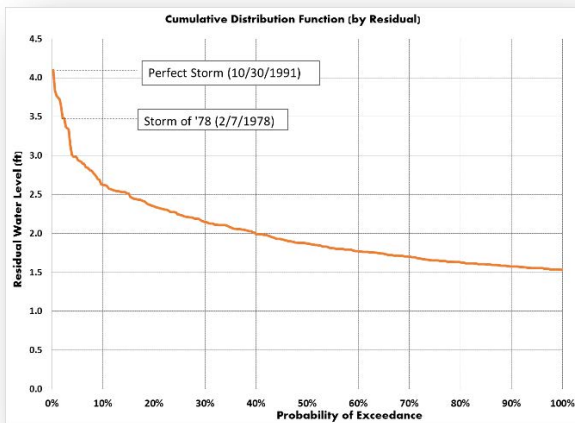


Figure 4-20. Cumulative distribution function of historical extra-tropical storms affecting Boston Harbor area.

In order to ensure a more complete representation of extra-tropical storms in the data set, which were assigned a probability based on an empirical probability of exceedance, the Generalized Extreme Value (GEV) method was used to augment the historical record with lower probability extra-tropical events based on the annual maxima of the observed residual storm surge data.

4.7.3.2 Wind Field Generation

In order to model the storm surge in Boston generated by extra-tropical cyclones it is necessary to incorporate the storm event into the BH-FRM model. There are many physical characteristics of an extra-tropical cyclone, but the wind pattern is the primary characteristic that drives storm surge. A secondary, but much less significant, characteristic that may influence storm surge is the low pressure center of an extra-tropical cyclone. Both wind and air pressure for extra-tropical events were incorporated into the BH-FRM model.

The BH-FRM model domain is too large for a single meteorological station to provide an accurate description of winds and air

pressure across the entire model domain. Therefore, the meteorological data from the ECMWF Global Reanalysis models (ECMWF, 2014) was used.

The ECMWF models provide global coverage of meteorological conditions at a resolution ranging between 0.75 degrees and 1.125 degrees (approximately 60 miles). After an initial investigation of the wind patterns provided by the ECMWF models, the ECMWF models did not provide appropriate resolution to represent storm events in the BH-FRM model. Therefore, in order to achieve appropriate resolution for the wind field, the ECMWF meteorological data was used as input to the “Synthetic Nor’easter Model” as described in Stone and Webster (1978). The Synthetic Nor’easter Model is the application of the “Adjusted Equilibrium Wind” model for hurricanes developed by Myers and Malkin (1961). Stone and Webster concluded that the mathematical formulation of the wind field in hurricanes (tropical cyclones) described by Myers and Malkin is appropriate for simulating Nor’easters (extra-tropical cyclones).

The synthetic Nor’easter model calculates the predicted wind speed and direction at any point within a cyclone based on six parameters:

- The air pressure at a point,
- The distance from the low pressure center of the cyclone,
- The location of a point relative to the low pressure center of the cyclone,
- The radial gradient of pressure at the point,
- The rotational gradient of pressure at the point; and
- The track speed of the extra-tropical cyclone.

The first step in applying the synthetic Nor'easter model was interpolation of the air pressure field from the coarse grid ECMWF grid to a finer grid (0.25 degrees). A two-dimensional spatial cubic interpolation was completed for each time step of the ECMWF dataset. Then the storm track was identified by finding the low pressure storm center that existed within approximately 300 miles of Boston, Massachusetts at the time of the associated storm surge event. The storm track was determined by following this low pressure center backwards and forwards in time. The storm was followed by searching for the minimum pressure at each subsequent and/or previous time step based on the following criteria.

- The storm center cannot move at a speed greater than 60 miles per hour (assumed maximum cyclone storm track speed), and
- The storm intensity (difference between low pressure center and the last closed isobar) is greater than 5 millibars.

When either of these criteria are not met, it is assumed that the storm no longer exists. By applying these criteria backwards and forwards in time, a storm track was able to develop in space and time.

The ECMWF data are available every 6 hours. In order to develop an appropriate resolution in time, the location of the storm (and the associated air pressure was interpolated to an hourly scale based on the storm track and radial pressure gradients away from the storm center.

The net result is the development of the air pressure over the entire BH-FRM model domain at a resolution of 0.25 degrees in space and 1 hour in time. The synthetic Nor'easter model was then applied to each location and time of the high resolution dataset in order to predict wind speed and

wind direction for the storm event. In applying the synthetic Nor'easter model for this study, it was spatially extended further than originally described in Stone & Webster (1978). Stone & Webster applied the synthetic Nor'easter model to all points within the last closed isobar of the extra-tropical cyclone. In this study, it was concluded that limiting the application of the synthetic Nor'easter model to the last closed isobar did not appropriately incorporate high winds in the days and hours in advance of the storm surge event. Therefore, observed wind conditions in Boston, Massachusetts for the time period leading up to the storm surge event were compared to predicted wind conditions and found that extending the use of the synthetic Nor'easter model to the limits of the air pressure data, resulted in a much better match between observed and predicted wind conditions. This process was completed for every storm event in the historic data set and used as input into the BH-FRM model. The generated winds from the synthetic nor'easter model were calibrated and compared to observed wind data at various stations along the northeast coast for some of the simulated events, showing reasonable comparison.

4.7.4 Climate Change impacts on Storm Frequency and Intensity

While rising sea levels will increase water depths along the coastline, which will in turn result in the greater potential for wave and surge propagation further inland, there may also be increased intensity and frequency of large coastal storm events that are induced by the changing climate. Essentially, the heating of the ocean may also be increasing the probability and intensity of storm events.

4.7.4.1 Tropical Cyclone (Hurricane) Intensity

The formation of tropical cyclones is not fully understood; however, typically there

are a number of factors that are required to make tropical cyclone formation possible including:

- Water temperatures of at least 26.5 C (80°F) down to a depth of at least 50 meters (150 feet).
- An atmosphere which cools fast enough with height such that it is potentially unstable to moist convection.
- High humidity, especially in the lower-to-mid troposphere.
- Low values (less than about 37 kilometers/hour or 23 miles per hour) of vertical wind shear, the change in wind speed with height, between the surface and the upper troposphere. When wind shear is high, the convection in a cyclone or disturbance will be disrupted, blowing the system apart.
- Generally, a minimum distance of at least 480 kilometers (300 miles) from the equator.
- A pre-existing system of disturbed weather.

If some or all of these factors are being modified by changes in the climate, then it may be feasible that hurricane intensity and/or frequency are also changing. Figure 4-21 shows the annual number of tropical cyclones in the North Atlantic, beginning in 1870. The trend shows an increase in key measures of Atlantic hurricane activity over recent decades. These changes are believed to reflect, in large part, contemporaneous increases in tropical Atlantic warmth (e.g., Emanuel 2005). Figure 4-22 shows a comparison of the annual tropical storm count in comparison to the average ocean surface temperature between August and October. There appears to be a relationship between the frequency of tropical cyclones and the surface ocean temperature; however, it is still debated if this relationship indicates

that tropical storm frequency is increasing for the northeast. However, the intensity of tropical cyclones has clearly been on the rise in concert with the ocean temperature. The Power Dissipation Index (PDI) is a way to calculate the intensity of a Hurricane. The PDI is a measure of the total amount of wind energy produced by hurricanes over their lifetimes, and sums the cubed maximum wind velocities at each instant over the life of the storm. Figure 4-23 shows the post-1970 PDI, compared to ocean temperature in the Atlantic. The intensity of the hurricanes in the Atlantic is shown to be increasing.

In the Atlantic, the frequency, intensity and duration of hurricane events are all increasing in concert with tropical ocean temperature (Emanuel, 2005).

While global frequency of events has remained relatively constant, the intensity of tropical cyclones is increasing and the duration of tropical cyclones is increasing. There also may be an increase in the frequency of tropical cyclones in the Atlantic (making up 11% of the total global hurricanes), indicating a potential shift in hurricane activity. This activity is increasing in concert with ocean temperature. In the Atlantic, therefore, the intensity and duration of events are clearly increasing in concert with tropical ocean temperature (Emanuel, 2005), and perhaps the frequency is as well. This is also reflected in numerous Global Climate Models that are used to represent the current (20th century) and projected (21st century) climate produced for this study. Figure 4-24 shows the comparison of the 20th (red line) and 21st (blue line) century hurricane distributions using Emanuel's hurricane data sets. The vertical axis presents the annual exceedance probability, while the horizontal axis presents the Hurricane Surge Index

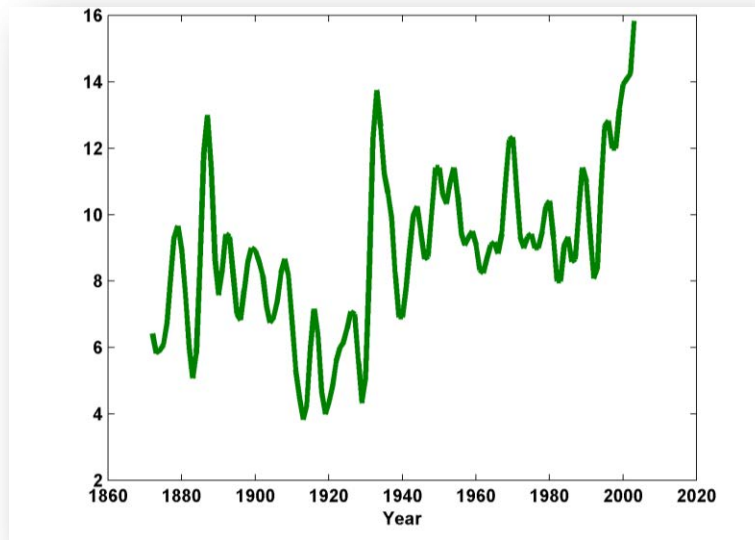


Figure 4-21. Annual number of tropical cyclones (vertical axis) including hurricanes and tropical storms in the North Atlantic, beginning in 1870 (acknowledgement to Dr. Kerry A. Emanuel, Massachusetts Institute of Technology).

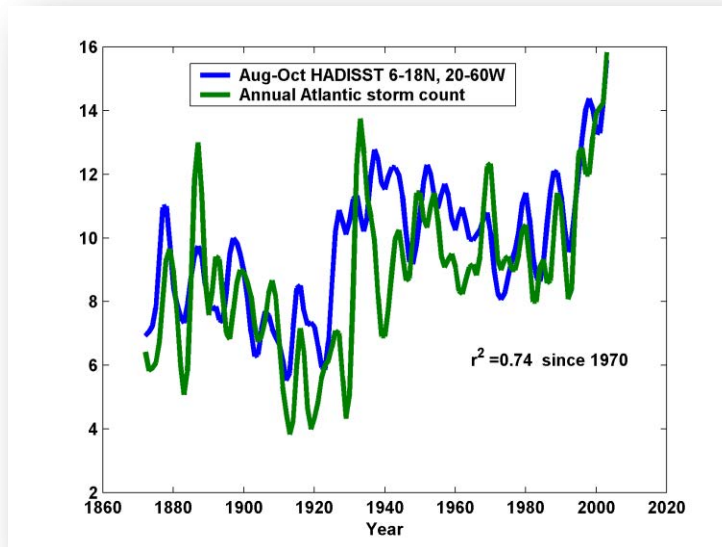


Figure 4-22. Annual number of tropical cyclones (green) compared to average ocean surface temperature (blue) during August to October (acknowledgement to Dr. Kerry A. Emanuel, Massachusetts Institute of Technology).

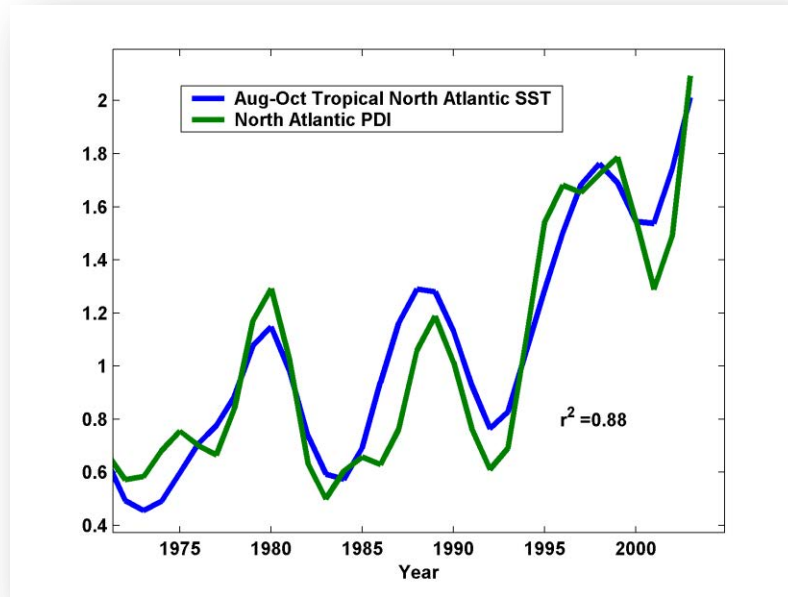


Figure 4-23. Post-1970 PDI (green), compared to ocean surface temperature in the Atlantic (blue) (acknowledgement to Dr. Kerry A. Emanuel, Massachusetts Institute of Technology).

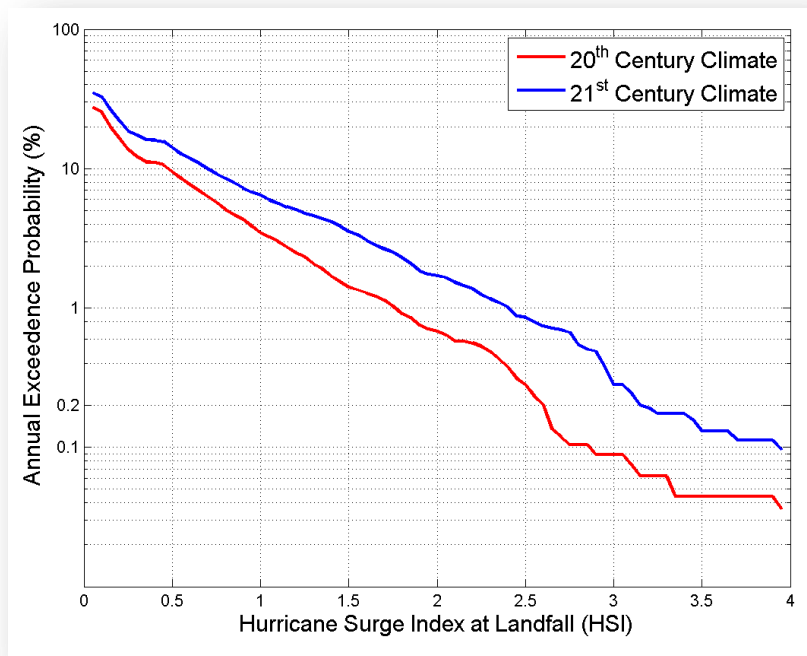


Figure 4-24. Hurricane Surge Index (HSI) at landfall compared to annual exceedance probability. The red line represents the distribution of the 20th century storms used in this study, while the blue line represents the distribution of the 21st century storms used in this study.

(HSI) at landfall. The figure shows the increase in the probability of higher energy storms in the 21st century, indicating an expected increase in frequency of tropical events.

4.7.4.2 Extra-Tropical Cyclone (Nor'easter) Intensity

Extra-tropical cyclones derive their energy from unstable pressure systems in the atmosphere. These conditions arise from temperature differences between warm and cold air masses in the atmosphere (NOAA, 2014c). The most intense extra-tropical storms occur in the winter because the temperature contrast between warm and cold air masses is at their greatest in the cold months. Generally speaking, a warmer global climate would serve to reduce the temperature difference between warm and cold air masses in the winter and potentially reduce the number of extra-tropical cyclones. Bengtsson et al. (2006) concluded that climate change will not lead to an increase in intensity of extra-tropical storms based on a comprehensive modeling study of likely future climates. They also concluded that the storm tracks of extra-tropical cyclones are likely to move poleward. This means that under climate change conditions, extra-tropical cyclones are more likely to form further north than they do under current conditions. The findings of Bengtsson et al. (2006) are consistent with other studies as well. For example, Catto et al. (2011) determined North Atlantic storm tracks are influenced by the slowdown of the Meridional overturning circulation (MOC), the enhanced surface polar warming, and the enhanced upper tropical-troposphere warming, giving a northeastward shift to the extra-tropical storm tracks, while intensities decreased.

Additionally, historical water level data were collected from the National Oceanic and Atmospheric Agency (NOAA) for the

tide gage station in Boston, MA (station ID: 8443970) (NOAA, 2014a). In order to evaluate the relationship between storm surge and extra-tropical cyclones for Boston, historical water level records and historical meteorological records were compared in order to align individual storm surge events with extra-tropical storms. The events were used to develop a cumulative distribution function (CDF) of storm surge events for Boston, Massachusetts based on the residual water levels (excluding tides) for all total events, as well as for those events that occurred after September 1, 1957. The two temporal time periods were evaluated to see if there was any noticeable change in frequency (number) or intensity (surge level) of events. Figure 4-25 presents the CDFs, with the black line representing the CDF for all storm surge events, and the orange broken line representing the CDF for storm surge events occurring after September 1, 1957. There is little variation in the storm surge residual indicating no observable difference in increased storm surge (intensity) from extra-tropical storms. As such, based on both literature and examination of the historical extra-tropical cyclones impacting the Commonwealth of Massachusetts, the storm intensity in the 21st century is not likely to be statistically different than storm intensity for the 20th century.

4.7.5 Influence of tidal cycle on flood elevation

In the northeast, where tidal ranges are significantly larger than the storm surge itself, the timing of the peak of the storm relative to the phase of the tide has a major influence on the level of flooding, waves, and potential impact to the CA/T system. A storm that aligns with high tide carries significantly more risk than that same storm aligning with a low tide. This section evaluates how storm timing (in relationship

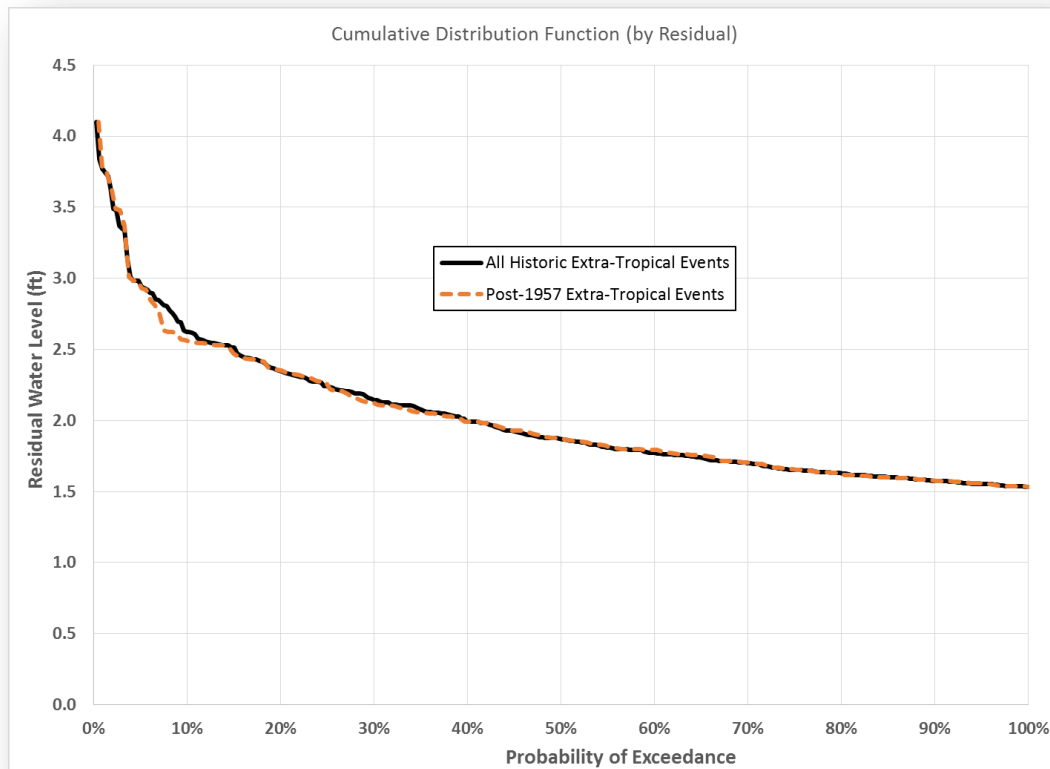


Figure 4-25. Extra-tropical storm surge CDF based on residual high water levels at Boston.

to the tidal cycle) affects the maximum predicted water level in Boston Harbor. Both tropical and extra-tropical storms are evaluated. Typically, tropical storms, while containing significant power, are relatively short-duration, fast moving systems. Extra-tropical storms, while many times being lower in strength, can be longer duration events, usually lasting through at least a tidal cycle. While there is much consensus that storm timing relative to the tide affects the maximum water level of the event, little quantitative analyses exist demonstrating any relationship between peak meteorological storm conditions and tidal phase.

Therefore, the timing of a storm, relative to a tidal cycle, is an important consideration in the BH-FRM modeling approach. While tides are dynamically rising and falling

within the model, the alignment of the storm with various stages of the tide needs to be considered. If all storms are simulated such that the peak of the storm surge occurs near

Generally speaking, a warmer global climate would serve to reduce the temperature difference between warm and cold air masses in the winter and potentially reduce the number of extra-tropical cyclones. Bengtsson et al. (2006) concluded that climate change will not lead to an increase in intensity of extra-tropical storms based on a comprehensive modeling study of likely future climates.

high tide, then the flooding probabilities will be overestimated since this would assume every storm occurs at high tide. If all storms are simulated such that the peak of the storm surge occurs near low tide, then the flooding probabilities will be underestimated since this would assume every storm occurs at low tide. Since a Monte Carlo approach is being used, the tides could be included as another random factor; however, in order to comprehensively capture risk and probabilities, the storms need to be simulated with varying alignments of the tidal cycle (with associated probabilities) to ensure that the full range of potential flooding scenarios can be captured.

Given the shallow water depths at the coast, the hydrodynamics are nonlinear. For any shallow water wave, there are nonlinear terms in the governing equations (mass and momentum balances) that can produce interactions between different processes. In the case of tides alone, these nonlinearities are observed in the generation of overtides near the coasts (Parker, B.B., 1991). In the case of extreme meteorological events producing a storm surge, the same nonlinearities can produce an interaction between the tides and the surge itself. This has been observed and theorized for decades (Prandle, 1978; Pugh, 1996; Horsburgh, 2007), though only with the recent improvement in numerical modeling can these theories be tested, as is done using BH-FRM herein. These studies show that the highest observed surge is when the peak

The timing of a storm, relative to a tidal cycle, is an important consideration in the BH-FRM modeling

surge occurs on the rising tide, just prior (~3 hours) to high tide. Further detail on tide-surge interaction in bays and tidal rivers shows that the interaction is stronger at low tide rather than at high tide (Antony, 2013).

4.7.5.1 Extra-Tropical Storms Evaluation

In order to evaluate the relationship between extra-tropical storms and the phase of the tide, a few of the more significant extra-tropical storm events from those developed in section 4.7.2 were selected for this evaluation. This consisted of the Halloween storm of 1991, otherwise known as the “Perfect Storm”, the Blizzard of 1978, as well as a couple other significant Nor’easters. These storms were then simulated thirteen times in BH-FRM with the start of the simulation corresponding to a different phase in the twelve hour tidal cycle each run. This provided results for each storm that encompassed an entire tidal cycle, including one high tide and one low tide to capture any nonlinear response over the entire tidal cycle to the storm meteorological conditions. Recording stations were created at buoy locations throughout the domain in order to compare recorded data to model predictions.

The time series of seven of the tide varying model runs for the 1991 Perfect Storm scenario are shown in Figure 4-26. Two days of the simulation are shown, which includes the time period of the maximum wind velocity. Results indicate that the maximum water surface elevation occurs when the high tide occurs approximately 3-4 hours prior to the maximum wind velocity, not when high tide occurs in concert with the maximum wind velocity. This is consistent with theories presented in existing literature (Prandle, 1978; Pugh, 1996; Horsburgh, 2007). Due to the length of the storm event, which lasts nearly two complete tidal cycles, the peak water surface elevation in Boston Harbor does not vary significantly, regardless of the phasing with the tide. For example, the maximum water surface elevation at a 0 hour tide delay is only slightly higher than the maximum water surface elevation associated with a 6 hour tide delay.

Given the water surface elevation range of nearly 14 feet, the fact that the standard deviation of the maximum water surface elevation is only 0.25 feet suggests there is only a small dependence on tidal phase relative to the peak of a typical longer-duration Nor'easter (extra-tropical) storm event. Similar results were obtained for all the Nor'easter events that were simulated. As such, extra-tropical events were simulated with dynamic tides, where high tide occurred 3 hours prior to the maximum winds associated with the extra-tropical event. This alignment results in a slightly conservative (highest level of flooding) approach to the extra-tropical and tidal phasing coupling; however, as shown in Figure 4-26, the maximum water surface elevation attained for these events varies little with tidal phasing.

4.7.5.2 Tropical Storms Evaluation

A similar analysis was conducted for tropical events, where a number of representative hurricanes were selected and then simulated with phasing relationships throughout the tidal cycle. This again provided results for each storm that encompassed an entire tidal cycle, including one high tide and one low tide to capture any nonlinear response over the entire tidal cycle to the storm meteorological conditions. Figure 4-27 shows the time series of water surface elevation for seven of the tide varying model runs over a 2 day timeframe. The higher intensity of the

tropical storm, as well as the shorter duration is evident when compared to Figure 4-26. As for the extra-tropical case, the maximum predicted water surface elevation occurs with the high tide is prior (approximately 3 hours) to the peak of the storm (i.e., when the surge and tide are both rising). The timing of the highest observed water level confirms that even for a hurricane, the maximum predicted water levels may not coincide with peak meteorological conditions.

In contrast to the extra-tropical storms, the tropical storms show a much stronger dependence and relationship to the phasing of the tide. For example, the peak water surface elevation associated with the 2 hour delay is over 2.5 feet higher than the peak water surface elevation associated with 6 hour delay. When considering the maximum predicted water level in Boston Harbor over this series of simulations, as shown in Figure 4-28, there is a large (2.5 foot) range in expected maxima, depending on the timing of the storm. Consistent with what is suggested in the literature, this trend follows a sinusoidal pattern, as shown by the red curve in Figure 4-28. Given that the standard deviation for the maximum predicted water level is approximately 1 foot, it therefore becomes critical to account for storm timing in relationship to the tide for tropical storm events.

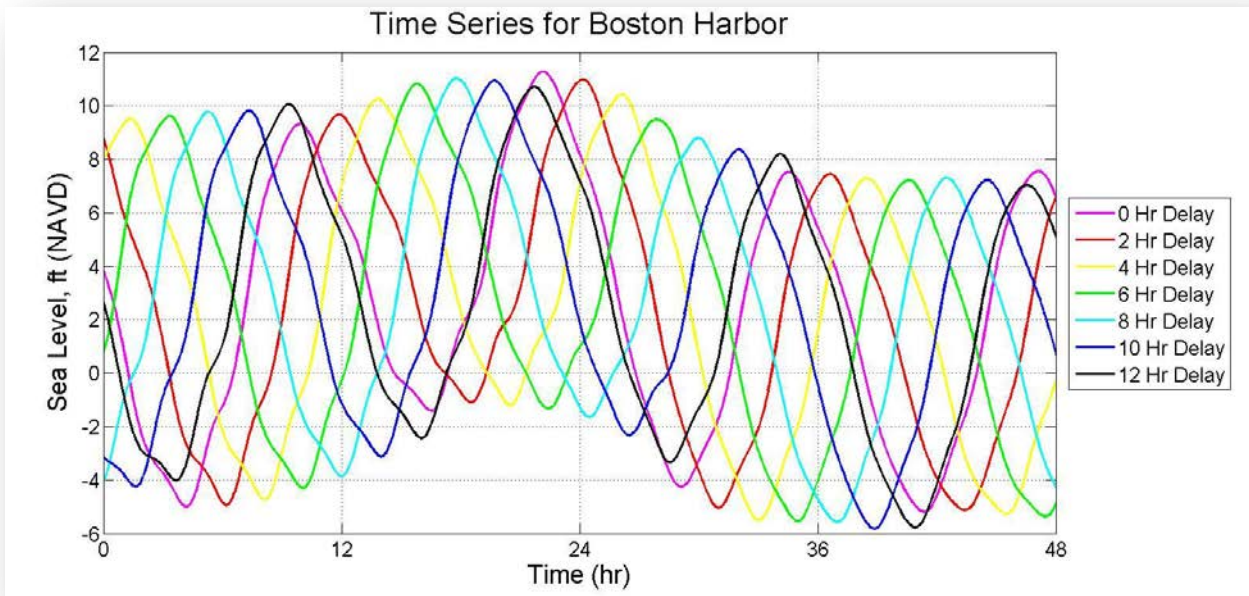


Figure 4-26. Time series of model sea level (feet, NAVD88) versus hours over the two day maximum sustained winds. Each model run uses the same meteorological forcing, but gives the tides an added phase (in hours), as indicated in the legend. Notice the location of maximum high water changes with increasing delay, but since the storm duration is so long, this is not a temporal linear process.

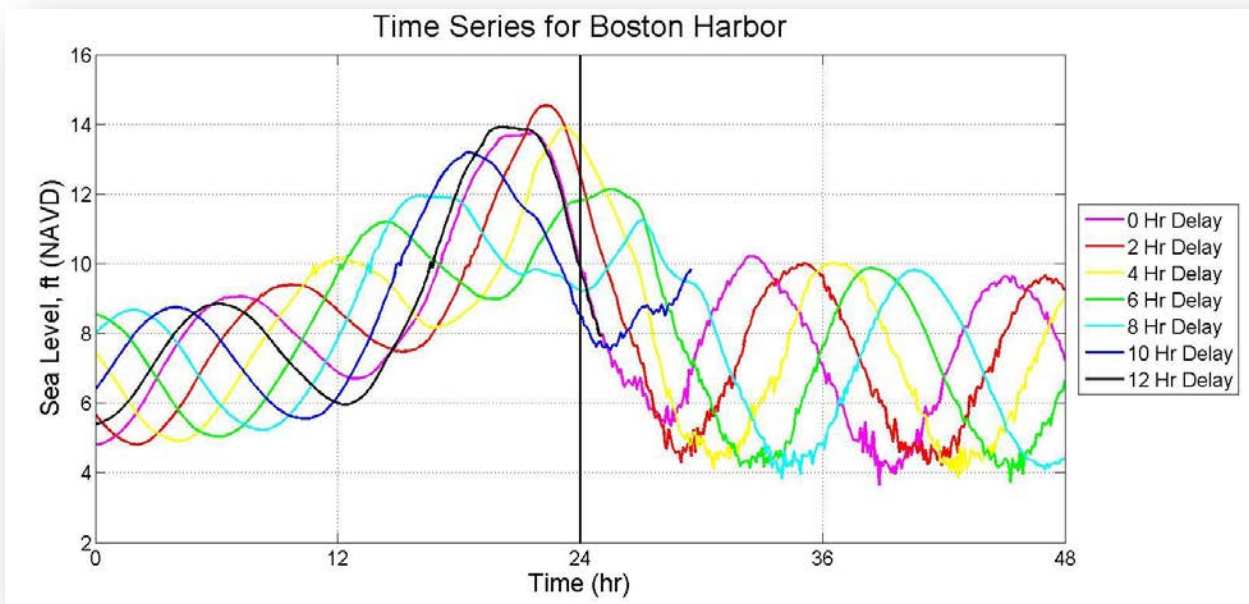


Figure 4-27. Time series of model sea level (feet, NAVD88) versus hours for a representative hurricane event. Each model run uses the same meteorological forcing, but gives the tides an added phase (in hours), as indicated in the legend.

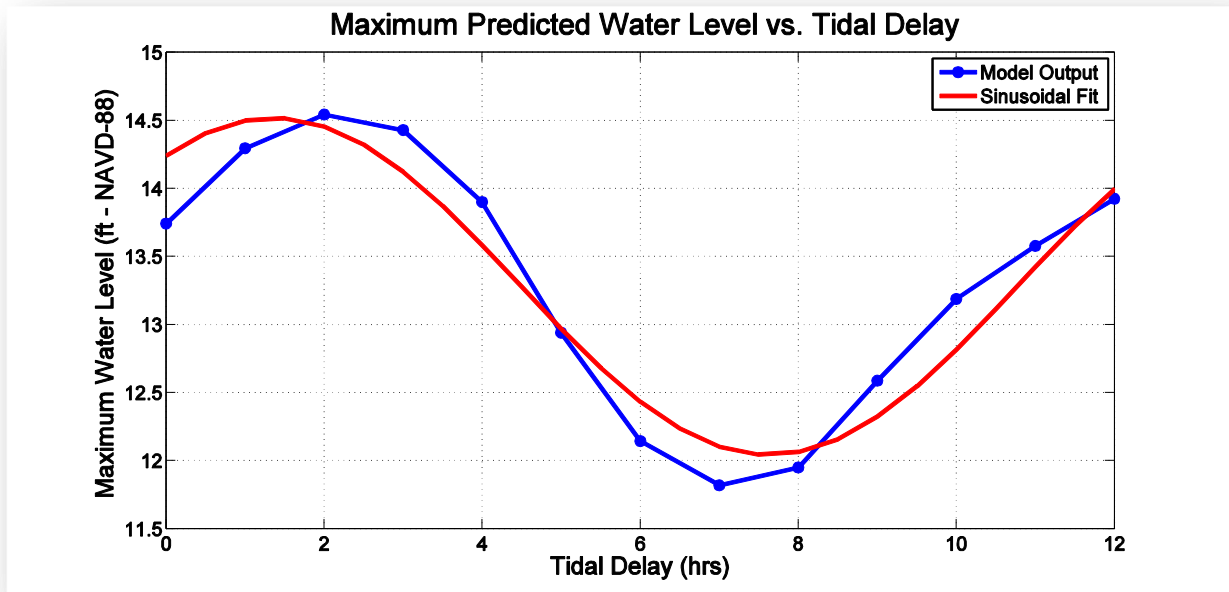


Figure 4-28. Maximum predicted water level as a function of tidal delay in the tropical storm model simulations (blue line) in Boston Harbor. There is a strong sinusoidal fit (red line) to the results that was utilized to produce an equation utilized as a transfer function.

Figure 4-29 shows the similar trend as Figure 4-28; however, the maximum water surface elevations are normalized by the expected high tide levels. This provides an excess in water level during the peak of the storm compared to conditions without a storm. As expected, all runs with the storm forcing show a maximum predicted water level higher than the normal high tide. The normalization gives the added benefit of considering the storm impact relative to high tide during non-storm conditions. In this particular case, the average maximum predicted water level is about 56% above the normal high tide water levels, while worst case scenario (with a 1/12 probability) is over 70% above the normal high tide. These results were used to produce a transfer function for the tropical storm simulations by determining the variation in the observed

water surface elevation results as a function of tidal alignment (red line in Figure 4-29), as given by Equation 4.9.

$$\eta = 1.56 - 0.146 * \sin\left(T \frac{2\pi}{12.54} + 0.89\right) \quad (4.9)$$

where η is the water surface elevation and T is the relative tidal delay compared to the tide level when the model simulation was conducted. As such, for tropical storm simulations, the BH-FRM model was simulated once for each tropical storm in the data set, but results were produced for all the various tidal alignments based on the relationship determined herein. Therefore, for each hurricane (tropical storm) simulation, a total of 12 model results were produced, one for each phase of the tide, and each with a 1/12 probability of occurrence included into the overall storm occurrence probability.

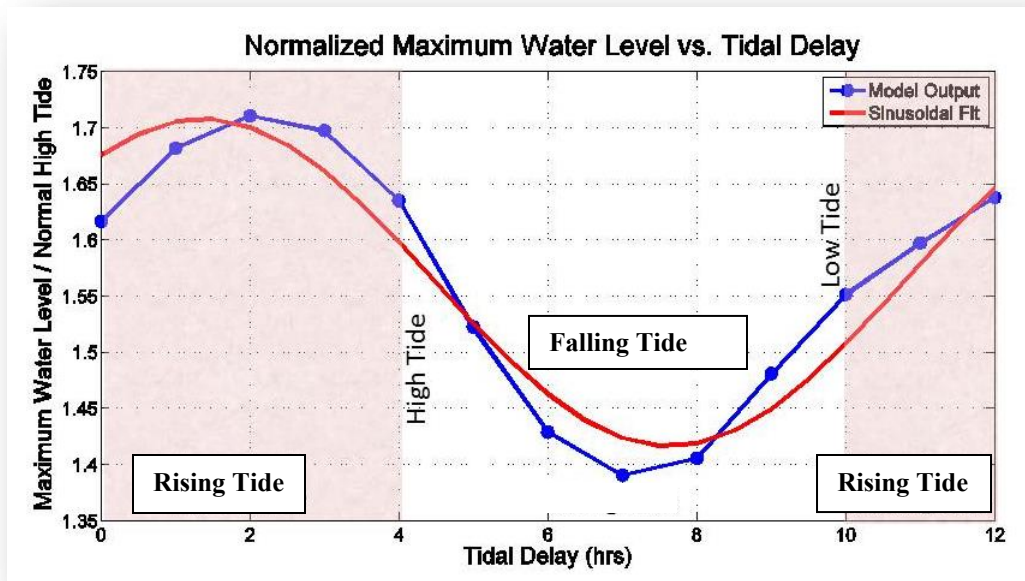


Figure 4-29. Maximum predicted water level (normalized by the spring high tide level) in the tropical storm model simulations (blue line) in Boston Harbor. Values above 1 indicate an increased expected maximum water level relative to the expected high tidal value. Red shaded regions are the runs where the maximum meteorological forcing occurs during the rising tide.

4.8 Developing the Composite Probability Distribution of Storm-Related Flooding

Flood frequency analysis usually seeks to estimate the cumulative distribution function (cdf) of annual maximum flood height or discharges. We assume that the composite or total cdf of flood height or discharges arises from a number of different component cdf's each corresponding to different flood generating processes. In our case, we assume that flooding only results from two different flood generating processes: floods due to hurricanes and floods due to Nor'easters. Our aim is then to determine the cdf of the annual maximum flood depth (h_m) from the combination of these processes

$$h_m = \max[h_H, h_N] \quad (4.10)$$

where h_H and h_N are the annual maximum flood heights corresponding to hurricanes and Nor'easters. The cdf of h_m , denoted

$F_m(h_m)$ is found by integrating the joint probability density function (pdf) of h_H and h_N over the region where the maximum of both h_H and h_N is less than h_m (as shown in equation 4.11)

$$F_m(h_m) = P[\max[h_H, h_N] < h_m] \\ = \int_{-\infty}^{h_m} \int_{-\infty}^{h_m} f_{H,N}(h_H, h_N) dh_H dh_N \quad (4.11)$$

Here upper case is used to denote the theoretical random variable and lower case is used to denote realizations of the associated random variable. We can assume that the flood generating processes are independent because of the Monte Carlo simulation approach, in which case one obtains

$$F_m(h_m) = F_H(h_m)F_N(h_m) \quad (4.12)$$

Vogel and Stedinger (1984) and Stedinger et al. (1993) recommended the use of (4.12) for determination of the composite

distribution of flood risk. Their expressions are written in terms of exceedance probabilities rather than nonexceedance probabilities as was done above. Defining the exceedance probabilities

$$P_m(h_m) = 1 - F_m(h_m), \quad P_H(h_H) = 1 - F_H(h_H)$$

and $P_N(h_N) = 1 - F_N(h_N)$ their approach is

$$P_m(h_m) = P_H(h_m) + P_N(h_m) - P_H(h_m) \cdot P_N(h_m) \quad (4.13)$$

Equation (4.13) is the approach introduced by the U.S. Army Corps of Engineers (1958) which was recommended by the U.S. Water Resource Council (1982), and the U.S. Bureau of Reclamation (Cudworth, 1989) as well as others.

Before we could implement 4.13 to estimate the probability of flooding, we first had to convert the time series output by the model, which was in the form of a partial duration series (PDS, meaning all flood heights above zero) into an annual maximum series (AMS). First the model generated PDS was ranked from highest to lowest and each flood height assigned an exceedance probability, Q , using the unbiased Weibull plotting position formula (Stedinger et al, 1993)

$$Q = M / (N + 1) \quad (4.14)$$

where M is the rank (in descending order, with 1 corresponding to the highest flood height) and N is the time series length. Q (exceedance probability associated with PDS) was converted to P (exceedance probability associated with AMS) following equation 18.6.3a in Stedinger et al (1993)

$$P = 1 - \exp(-\lambda \cdot Q) \quad (4.15)$$

where λ is the average annual frequency of Nor'easters or hurricanes. The AMS probabilities could then be combined using 4.13 by evaluating the AMS for hurricanes and for Nor'easters at the same flood height, h_m . Normally, this would be done by fitting as quantile function to each AMS and then using the quantile estimate of probability at specified h_m , but given that there were hundreds of thousands of model nodes for which this would have to be done, this approach was considered untenable. Instead we used linear interpolation of the empirical AMS to estimate $P_m(h_m)$. Figure 4-30 compares the empirical AMS for hurricanes and Nor'easters and shows the combined probability series. As expected, the probability of flooding due to a Nor'easter dominates because of their higher frequency and their storm tracks.

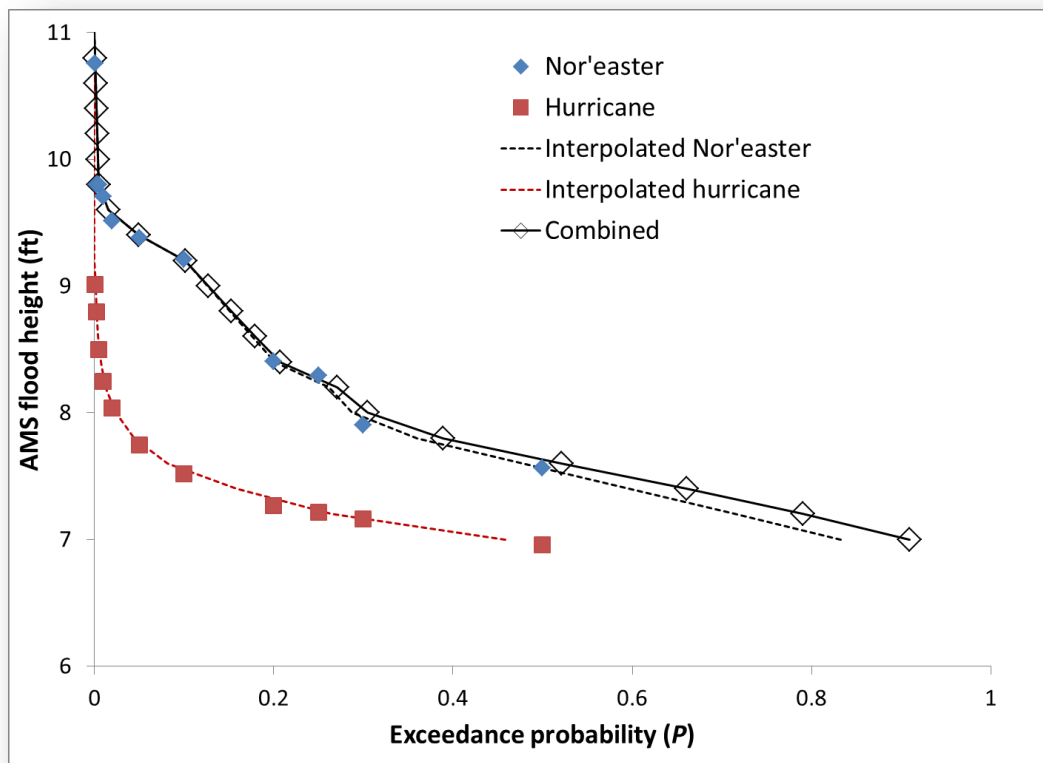


Figure 4-30. Example AMS flood probabilities for a Nor'easter (blue diamonds) and hurricane (red square) and the combined flood probability distribution (open diamonds).

4.9 BH-FRM Results

This section provides a brief summary of the primary BH-FRM output, a summary of some of the other additional results that can be gained from the model, and an example of the potential utilization of the model results at a local scale.

Model simulations were conducted for all the extra-tropical and tropical storms within the sets, developed as described in Section 4.7. Figure 4-31 presents a snapshot in time of a typical hurricane (tropical) storm simulation for an event that impacted the Boston area. The figure shows the wind velocities associated with the hurricane event (black arrows), and the changes in the water surface elevation (color contours in meters NAVD88 datum) as the storm

approaches the Massachusetts coastline. Reds and yellows indicate an increased water surface elevation (storm surge). This figure represents a single time step within the BH-FRM model.

After simulation of the scenarios, BH-FRM model results were analyzed to provide various types of output and flooding risk information. This involved a number of post-processing steps including:

1. Extraction of the maximum water surface elevation and flooding depth at each node in the model domain for every simulated storm event. This elevation is the maximum flooding depth at each location (if flooded) and may occur at varying times in the storm simulation for various areas in the domain.

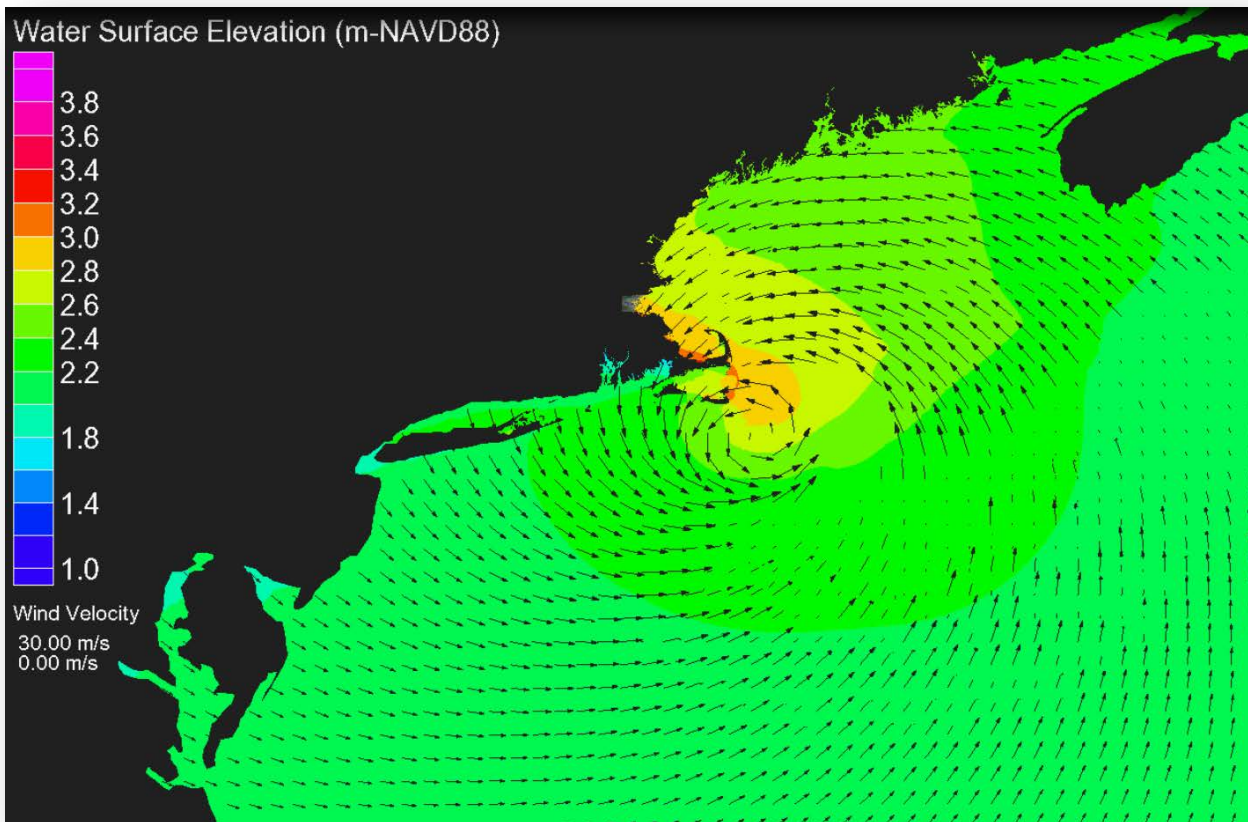


Figure 4-31. Snapshot of a typical hurricane (tropical) storm simulation within BH-FRM for a storm event that impacted the Boston area.

2. Development of an exceedance probability at each node in the model domain based on the maximum water surface elevation distribution and storm probability level (as described in Section 4.8).
3. Adjustment of the exceedance probability to an annual maximum exceedance probability, and combination of the extra-tropical and tropical storm probabilities to a composite storm exceedance probability (as described in Section 4.8)

These results are then used to generate maps of potential flooding and associated water depths throughout the area of interest. The BH-FRM also provides a number of other

useful flooding parameters and valuable information including, but not limited to:

- Dynamic (time-varying) identification of flooding pathways and flooding points of entry through the City of Boston. This includes variations due to storm types (Nor'easters and hurricane) and individual storm characteristics.
- Residence times of associated flooding (e.g., how long an area remains flooded before the storm surge retreats).
- Animations of flooding caused by individual hurricane and Nor'easter events, including the temporal flooding processes.
- Wave heights, energy and impacts throughout the modeling domain.

- Effects of increased river discharge and bank flooding.
- Variation in flooding extents, probabilities, and depths associated with present day flooding potential (2013), as well as future sea level rise conditions and storm climatology (2030, 2070, and 2100). Maps of these parameters can be compared to determine when assets become vulnerable and by when adaptation actions may need to be taken.
- Wind distribution and conditions.

4.9.1 Probability of Flooding

Before presenting the results of the vulnerability assessment for individual CA/T structures (Chapter 5), it is good to have an overview of model predicted flood exceedance probabilities across the CA/T domain. As already noted, flood exceedance probability is defined as the probability of flood water (at a depth greater than or equal to 2 inches or 5 cm) encroaching on the land surface at a particular location in any given year. Figures 4-32, 4-33a, and 4-33b show flood exceedance probabilities across the CA/T domain for current climatic conditions (represented by the 2013 scenario) and near-term future conditions late 21st century (represented by the 2030 and 2070/2100 scenario), respectively. Exceedance probabilities shown on these maps range from 0.1% (0.001, otherwise known as the 1000-year flood level) to 100%, which generally corresponds to intertidal locations such as Fort Point Channel or Boston Harbor. These maps can be used to identify locations, structures, assets, etc. that lie within different risk levels within the area. For example, a building that lies within the 2% flooding exceedance probability zone would have a 2% chance of flooding in any year (under the assumed climatology). In other words, in each year there is a 2% percent chance that this location will get

wet. Stakeholders can then determine if that level of risk is acceptable, or if some action may be required to improve resiliency, engineer an adaptation, consider relocation, or implement an operational plan.

Under current (2013) conditions, Figure 4-32 shows flooding present in downtown Boston (from the North End through the Financial District, intersecting the Rose Kennedy Greenway, entrances to I93 and other CA/T structures), South Boston (from the east side of Fort Point Channel through the Innovation District to the Massport terminals), East Boston (near the entrance to the Sumner and Callahan tunnel through the East Boston Greenway along Rt. 1A) and along waterfront areas of East Boston, Charlestown and Dorchester. However, the exceedance probabilities of this flooding is generally quite low, ranging from 0.1% to 0.5%, with the predominant exceedance probability being in the range of 0.5% (0.005, also known as the 200-year flood). Hence, the vulnerability concerns under current climate conditions are mostly focused on Boat Sections with Portals as described in more detail in Chapter 5. Under near-term future (2030) conditions, Figure 4-33a shows an increase in both the spatial expanse of flooding and exceedance probability levels. For example, the area of flooding in the vicinity landward of the New England Aquarium and Long Wharf area has expanded and the probability of flooding has increased. The predominant exceedance probability in all these areas by 2030 is 2% (0.02, also known as the 50-year flood). In 2030, both dams (the AED and NCRD) provide flood protection from coastal surge events. Neither dam is overtopped or flanked for any reasonable risk level (e.g., there may always be a storm that is rare enough that has the ability to overtop the dams; however, the probability is extremely low up to 2030). There is some flooding that occurs upstream of the dams; however

this is caused by precipitation effects due to poor drainage and higher river discharge, not coastal storm surge. The model includes increased freshwater discharge expected due to the changing climate as explained in Section 4.5.2.2.

By late in the 21st Century (2070 or 2100, depending on the actual rate of SLR), the picture changes quite dramatically. Flood exceedance probabilities in Boston exceed 10 percent in many locations, particularly along the Rose Kennedy Greenway, near the North End and in the South End. Flood probabilities in the financial district and along the waterfront exceed 50%. Flooding in South Boston and East Boston is also more extensive with flood probabilities exceeding 50%. Flooding also occurs on Logan International Airport property with a probability as high as 1%. The CRD and AE dams are flanked or overtopped, resulting in more extensive inland flooding in the Back Bay, Cambridge, Somerville and Charlestown, with probabilities of 1% or higher.

By comparing the 2013 flood probability map (Figure 4-32) with the 2030 flood probability map (Figure 4-33a and b), individual structures, assets, and areas can be assessed to determine how flooding is changing as a function of time and the overall influence of climate change projections can also be evaluated. These maps can also be used to assess flood entry points and pathways and thereby identify potential regional adaptations. In many cases, large upland areas are flooded by a relatively small and distinct entry point (e.g., a low elevation area along the coastline). For example, the coastline along the Mystic River near the Schrafft's building in East Somerville represents a relatively small point of entry to flooding that inundates a large landward area. In cases like this, a more cost effective solution (rather than

evaluating local adaptation options at each building in the area) would be a target coastal protection project at the flood entry point (e.g., increase seawall elevation, a natural berm, etc.). As such, a single project at this location may result in protection of a whole neighborhood or beyond.

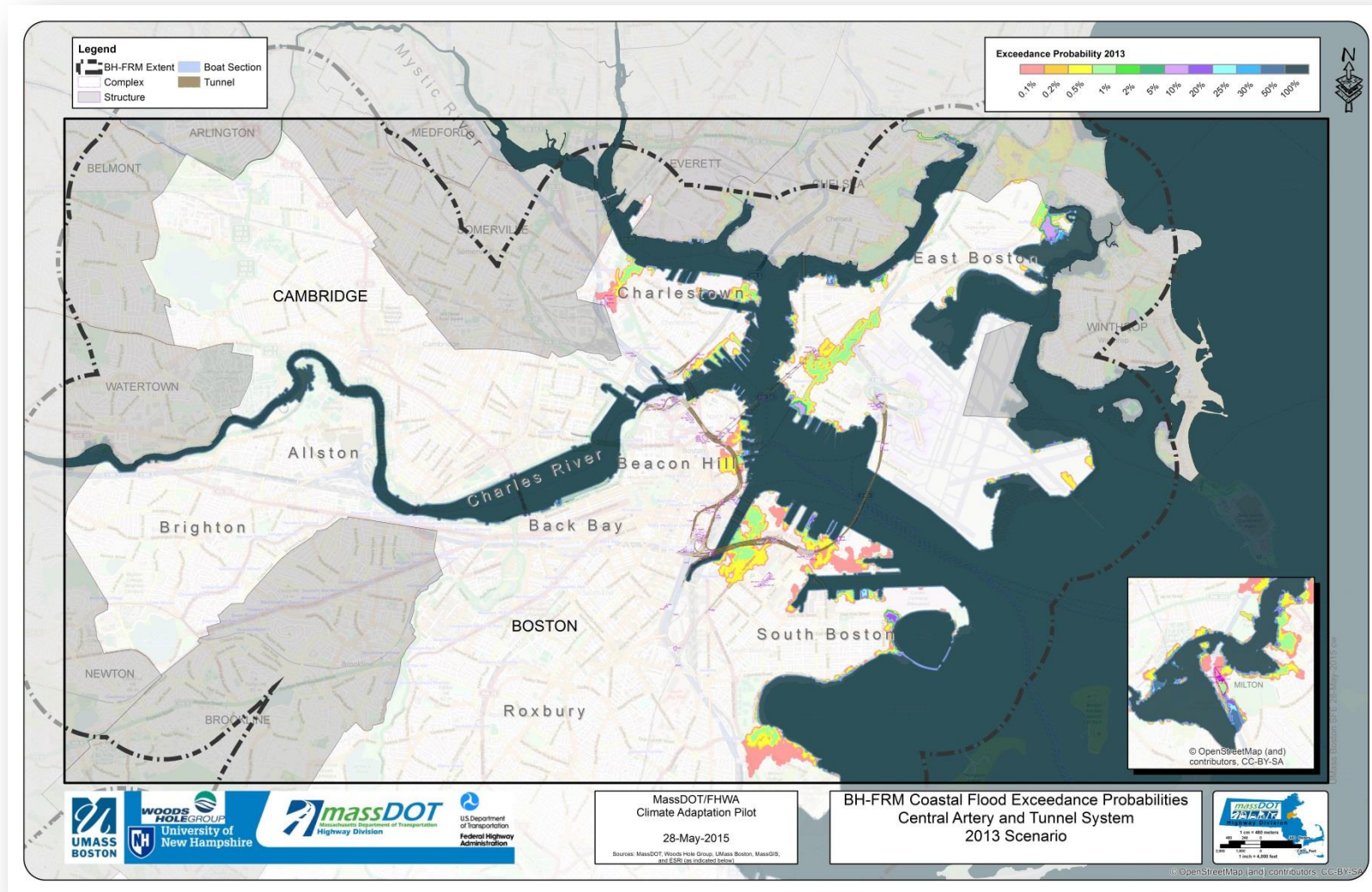


Figure 4-32. BH-FRM results showing probability of flooding in 2013.

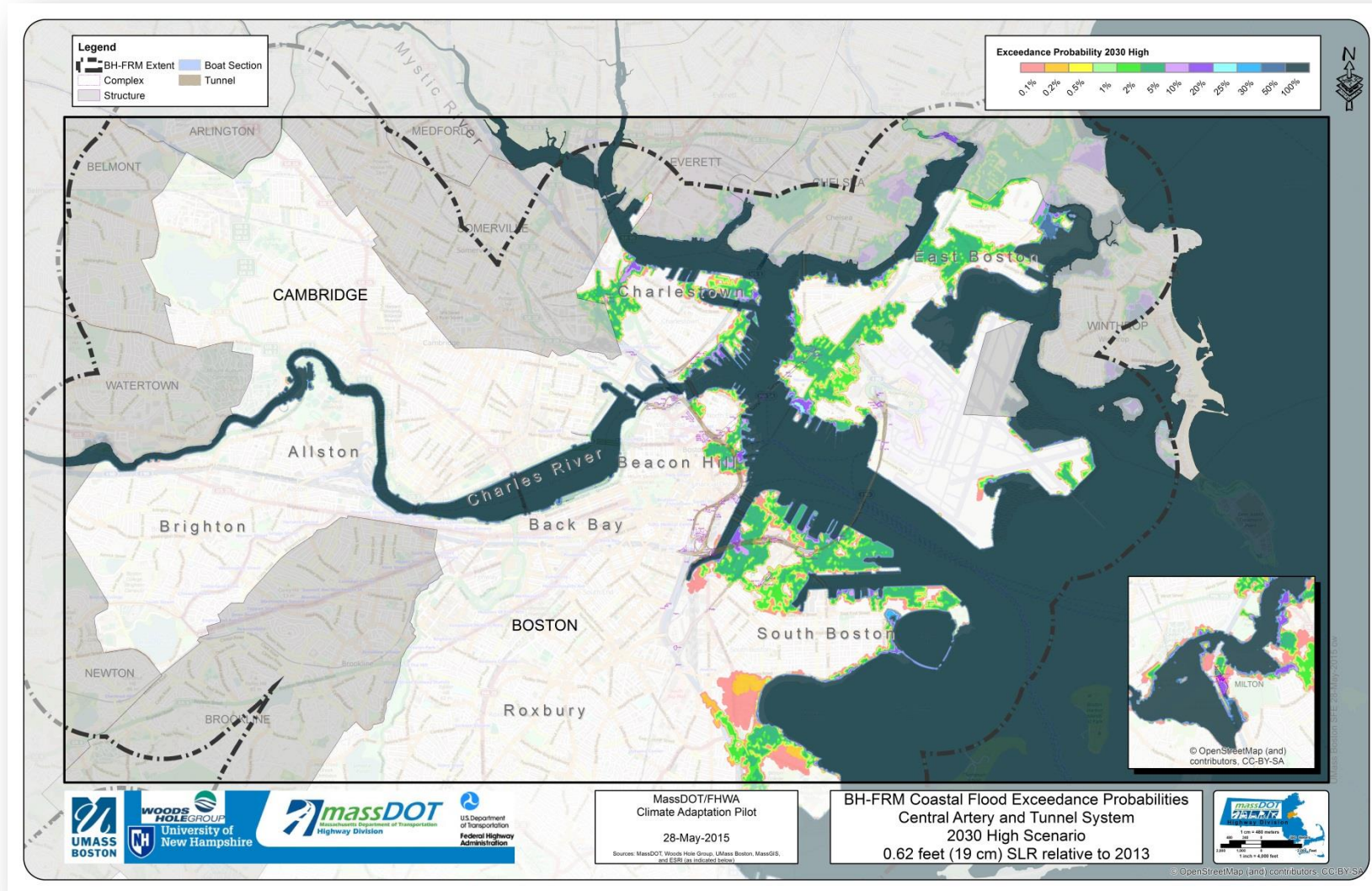


Figure 4-33a. BH-FRM results showing probability of flooding in 2030. An additional 0.74 in (1.9 cm) due to subsidence was added to the 0.62 feet SLR.

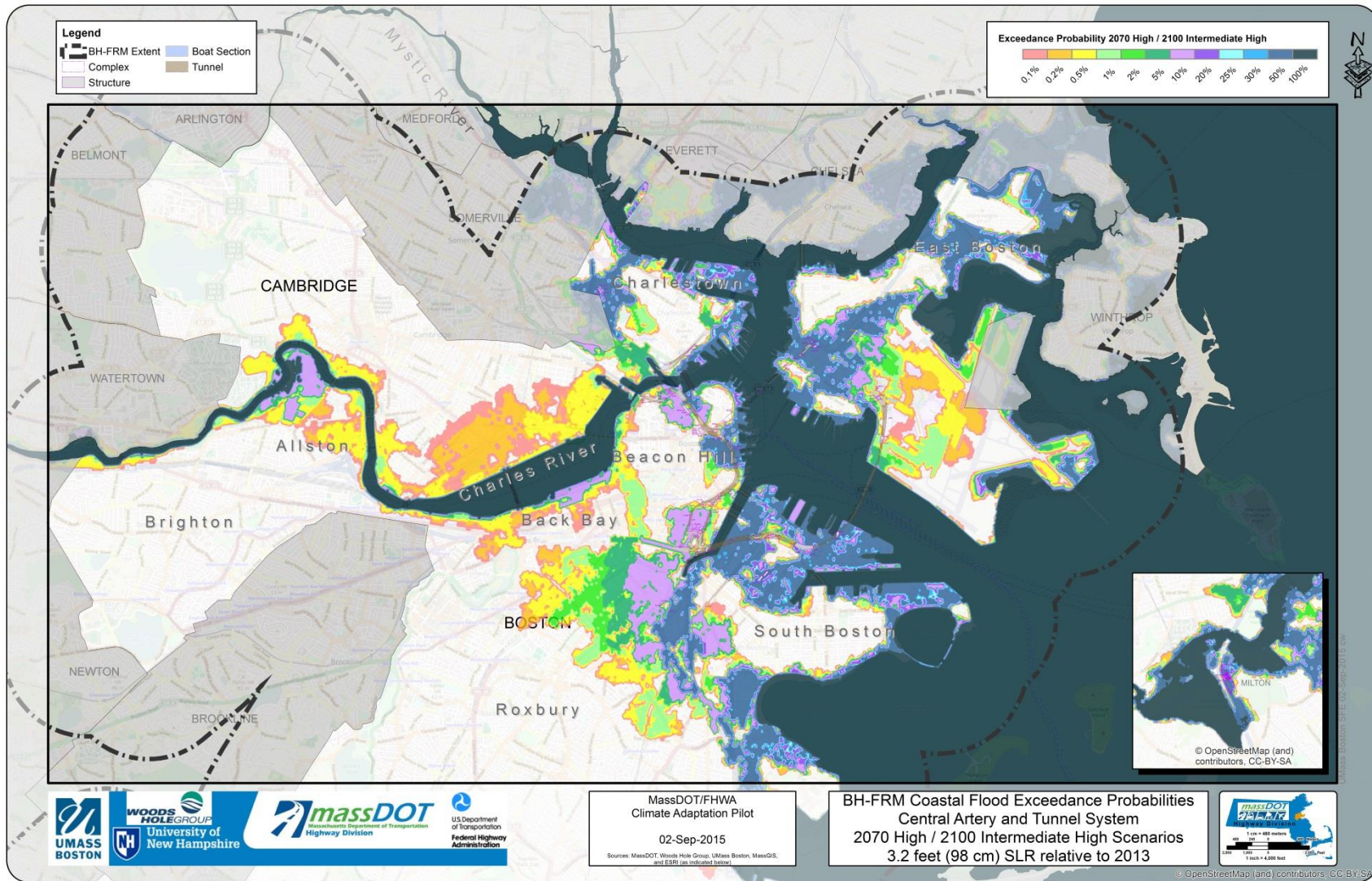


Figure 4-33b. BH-FRM results showing probability of flooding in 2070. An additional 2.5 in (6.3 cm) due to subsidence was added to the 3.2 feet SLR..

4.9.2 Depth of Flooding

The probability of flooding maps presented in the previous section provide stakeholders the ability to determine if areas, buildings, etc. are expected to be flooded and at what probability flooding is expected to be initiated. This is important for weighing the tolerance for risk and evaluating when adaptation options may need to be considered. Perhaps equally as important is the magnitude, or depth, of flooding expected. BH-FRM model results also provide this information at every node in the model domain. These results can be used to produce a depth of flooding map for any given flooding probability level. For example, the flooding depths (at 0.5 ft increments) associated with the 1% probability level (100-year return period water level) in 2013, 2030 and 2070/2100 are presented in Figures 4-34, 4-35a and 4-35b, respectively. Therefore, the depth of flooding can also be evaluated when assessing the risk to a system. Using the coastline along the Mystic River near the Schrafft's building in Charlestown as an example, the water depths in 2013 for the 1% flooding probability range between 0.5 to 1.0 feet; however, in 2070/2100 the area indicates water depths between 4 to 10 feet and covers a much larger area. By late in the 21st century, flooding around the Schrafft's building increases, which allows encroachment of flood waters further into Somerville and the surrounding area. The progression of flooding over these time frames targets the coastline near the Schrafft's building for potential regional adaptation actions.

As mentioned, the model results at each node include a probability exceedance curve that provides the water depth and water surface elevation as a function of the probability of exceedance. For example, Figure 4-36 presents the 2030 output of the exceedance probability curve from a BH-

FRM model node at 93 Granite Ave. site in Milton, MA (one of the current buildings). This location is currently home to the MassDOT Fuel Depot Complex as discussed in more detail in Section 4.9.4. At this particular location, there is a 10% flooding probability (or 10% chance of getting wet). As the percent exceedance decreases (less probable flooding scenarios), the water surface elevation and depth increases. At a 1% flooding probability (100-year water level), the water depth is 2.1 feet, but for a 0.2% flooding probability (500-year water level), the water depth increases to 3.1 feet. These depth data, for various flooding probabilities, can be used to help planning and assist in engineering design of adaptations.

For example, if a certain building is risk adverse and only willing to accept a 0.5% risk or less, then (1) the time this occurs could be identified in the flooding probability maps, and (2) the associated depth corresponding to that risk level could be evaluated for engineering planning and design. The depth could then be used to design elevated structural components or ensure that critical systems are elevated above the expected water surface elevation levels. Appendix VI includes zoomable pdf versions of estimated flood probabilities and flood depths across the CA/T domain for 2013, 2030, and 2070/2100.

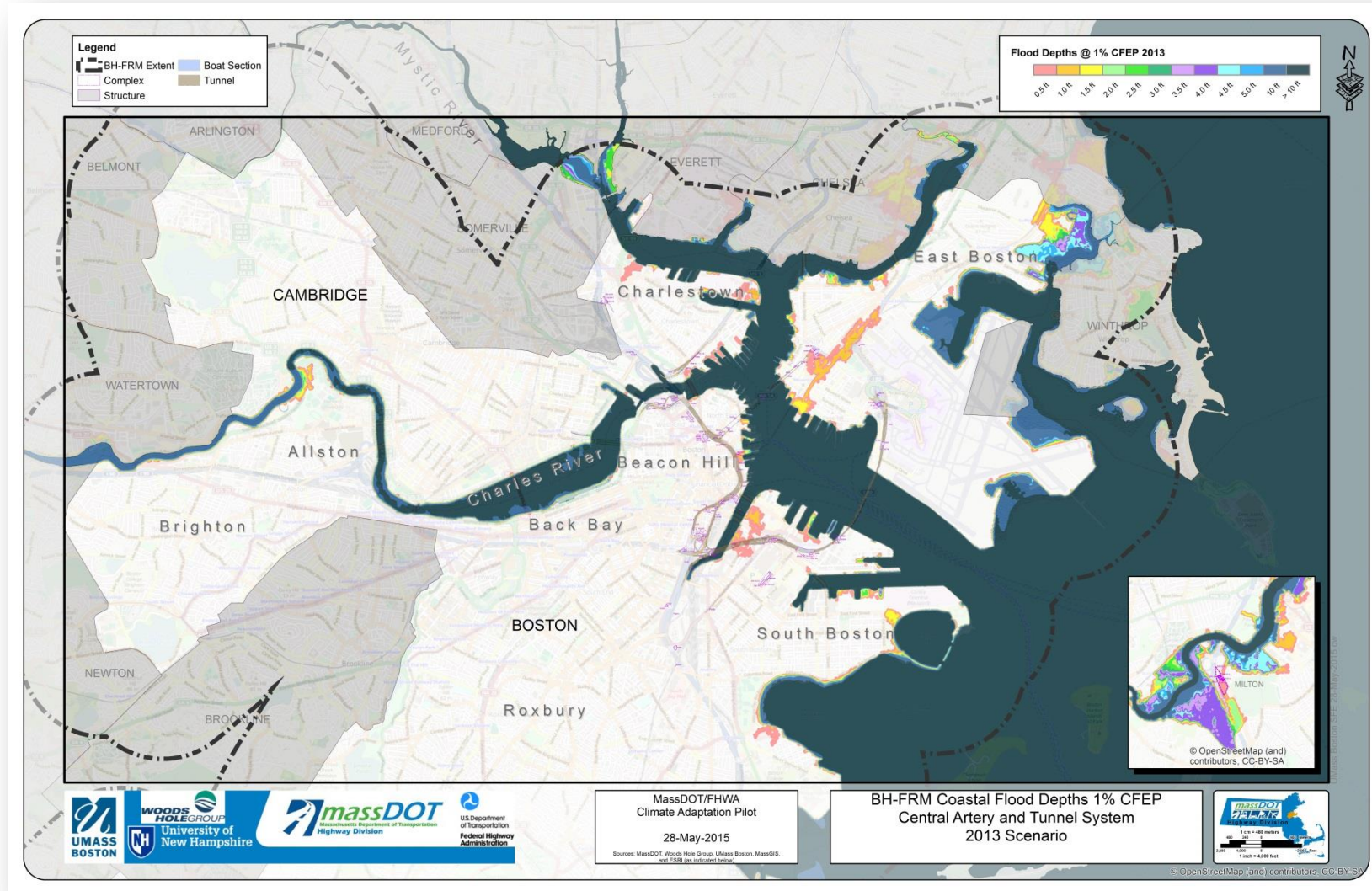


Figure 4-34. BH-FRM results showing flooding depth for a 1% probability of flooding in 2013.

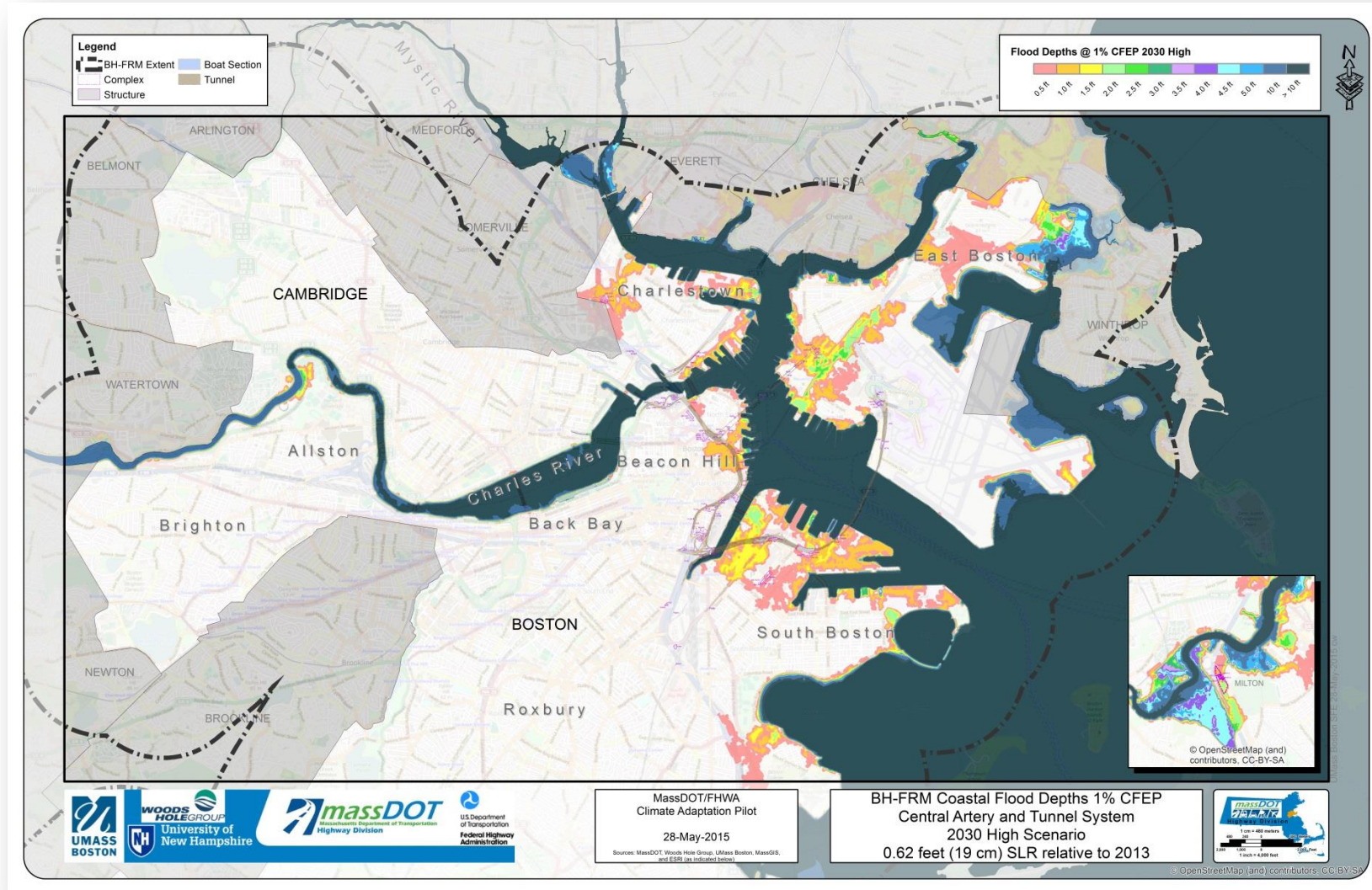


Figure 4-35a. BH-FRM results showing flooding depth for a 1% probability of flooding in 2030. An additional 0.74 in (1.9 cm) due to land subsidence was added to the 0.62 feet SLR.

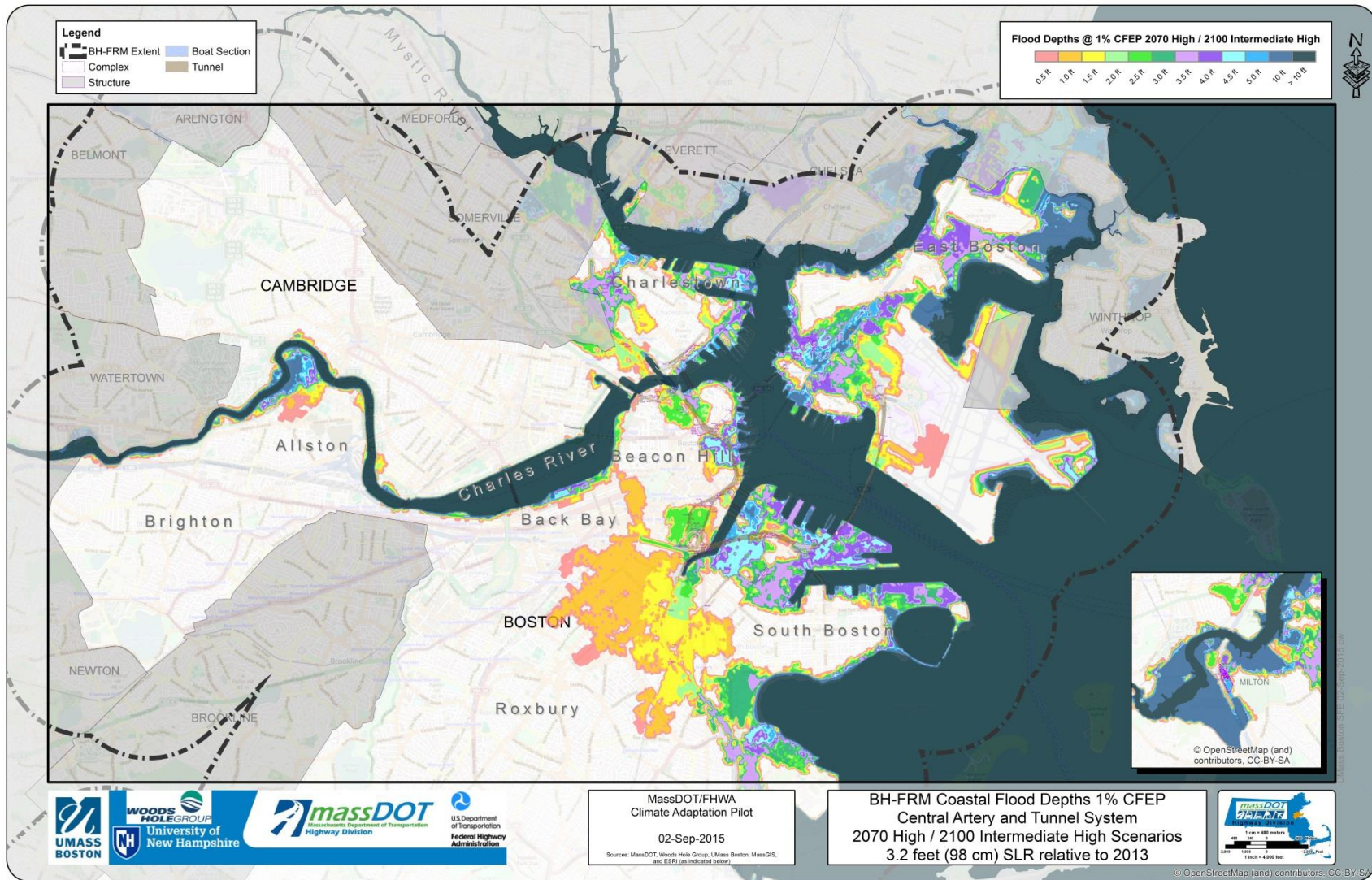


Figure 4-35b. BH-FRM results showing flooding depth for a 1% probability of flooding in 2070. An additional 2.5 in (6.3 cm) due to land subsidence was added to the 3.2 feet SLR.

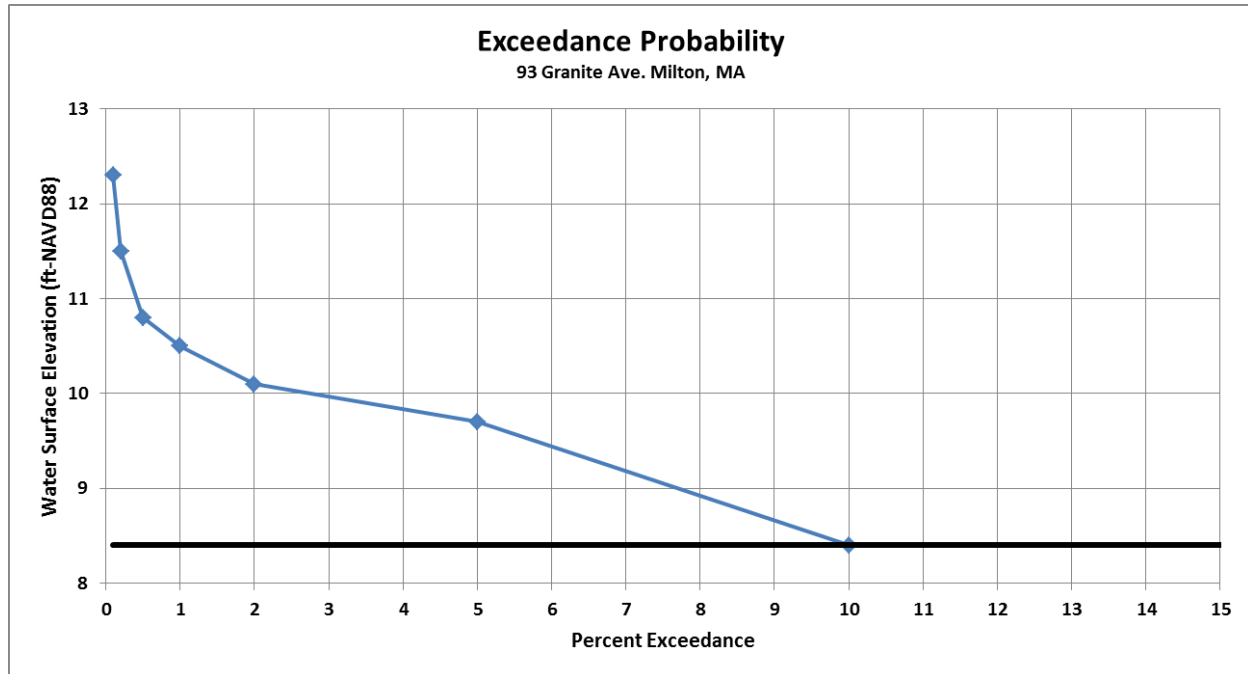


Figure 4-36. Example exceedance probability curve for 93 Granite Ave. in Milton, Massachusetts (MassDOT Fuel Depot Complex).

4.9.3 Additional Results

The primary output for assessing vulnerabilities and adaptation options related to the CA/T are the flooding probabilities and depth levels as presented in the previous sections. While not within the scope of this pilot project, the BH-FRM model also provides a number of other useful flooding parameters and valuable information that could be used in the future to assess other aspects of climate change and storm risk. These products could be useful in future assessments and subsequent MassDOT evaluation efforts. For example, Figure 4-37 provides a wave energy distribution map for the Boston Harbor area for a representative extra-tropical (Nor'easter event). The color contours show the distribution of wave heights in the vicinity of Boston Harbor, while the arrows indicate wave direction. For this particular Nor'easter storm, wave heights of greater than 7 feet offshore (likely expected to exceed 20 feet) are attenuated to 1 to 3 feet in the Inner Harbor. In general, the sheltering provided by the offshore

islands, Cape Cod, and the complex shoreline of Boston Harbor result in significant attenuation of the waves. As such, for areas far upstream in the Harbor, minimal wave action is expected for most storms. Areas to the south generally receive more wave energy due to the more open exposure and the stronger northeast winds associated with most extra-tropical and tropical storm events. These winds also can generate local wind-generated waves on confined and sheltered water bodies, which is also included in the BH-FRM model.

Additional useful results include, but are not limited to:

- Dynamic (time-varying) identification of flooding pathways and flooding points of entry through the City of Boston. This includes variations due to storm types (Nor'easters and hurricane) and individual storm characteristics.
- Residence times of associated flooding (e.g., how long an area remains flooded before the storm surge retreats).

- Animations of flooding caused by individual hurricane and Nor'easter events, including the temporal flooding processes.
- Effects of increased river discharge and bank flooding.
- Variation in flooding extents, probabilities, and depths associated with present day flooding potential (2013), as well as future sea level rise conditions and storm climatology (2030, 2070, and 2100). Maps of these parameters can be compared to determine when assets become vulnerable and by when adaptation actions may need to be taken.
- Wind distribution and conditions.

4.9.4 BH-FRM Results at a Local Scale

This section presents some of the BH-FRM results at a more local scale and provides an example of how these results could potentially be utilized to evaluate a site of interest. Specifically, this section evaluates the 93 Granite Ave. site in Milton, Massachusetts. This location is currently home to the MassDOT Fuel Depot Complex and is also being considered for the potential future residence of the primary MassDOT maintenance facility. As such, this location represents a critical site for MassDOT from both a current operational perspective, but also from an engineering design and future use standpoint. The figures presented in this section evaluate the site in the present day (2013) and the near-term future (2030). Figure 4-38 present the 2013 flooding probability for this area. The dashed black line shows the parcel of interest, while the solid black lines show the existing structures. The maps shows flooding probabilities of 1% (100-year return period water level) in the southern portion of the parcel, 0.5% probabilities at the southern buildings, and approximately 0.1% flooding probabilities for the northern section of the

parcel. The low lying wetland area to the south of the parcel, shows an even higher probability of getting wet. Overall, this region has some risk for flooding (1% chance) in present day conditions.

Figure 4-39 presents the associated present day flooding depths corresponding to the 1% flooding probability level (areas of 1% probability or greater). Depths of flooding are generally small for present day, with depth of water in the parcel of approximately 6 inches and restricted to the southern parking area and the two southern buildings. Accessibility to the site (via Granite Ave.) remains viable for the 1% return period water level in present day conditions.

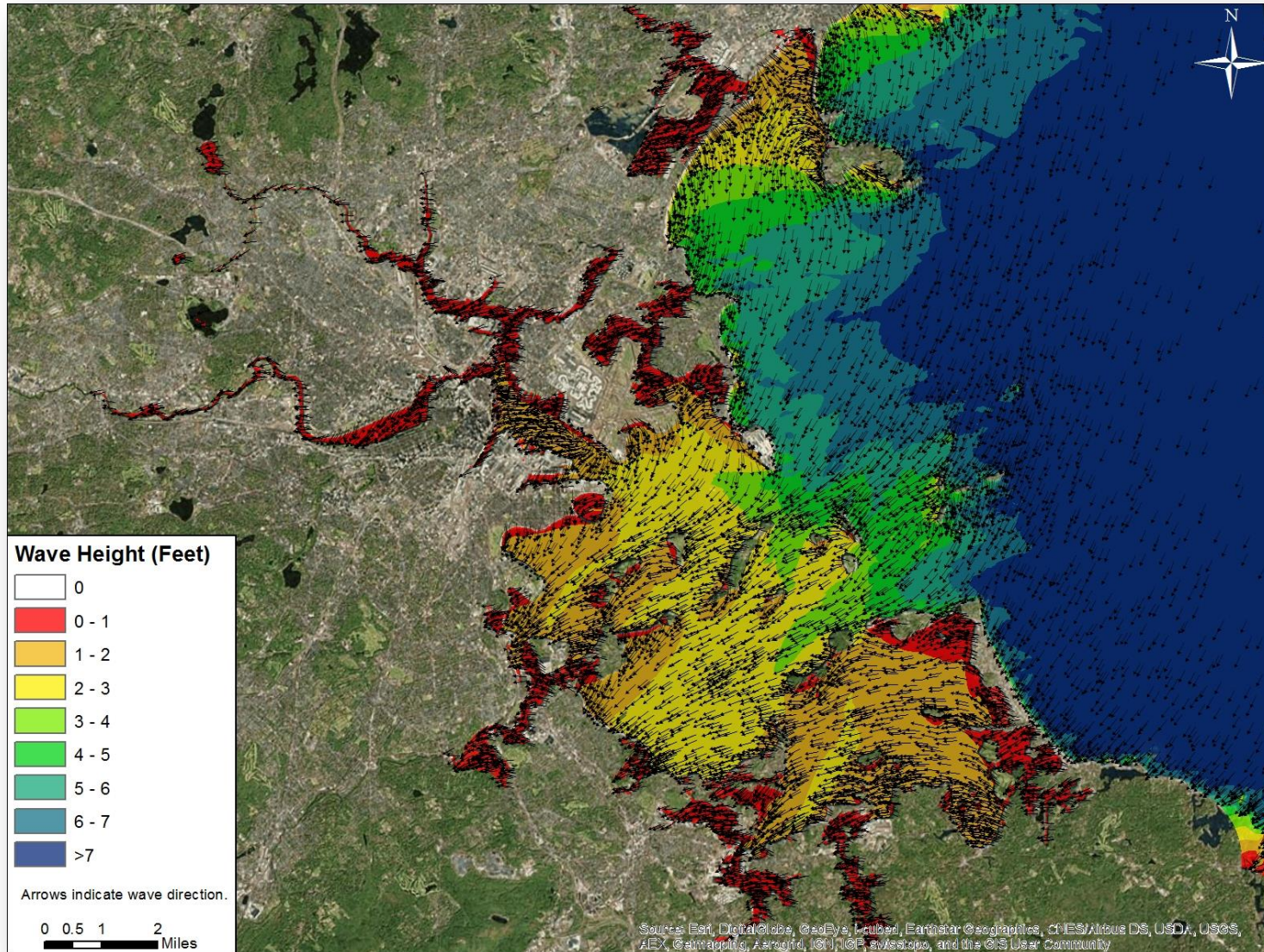


Figure 4-37. BH-FRM wave results for a typical extra-tropical (Nor'easter) event.

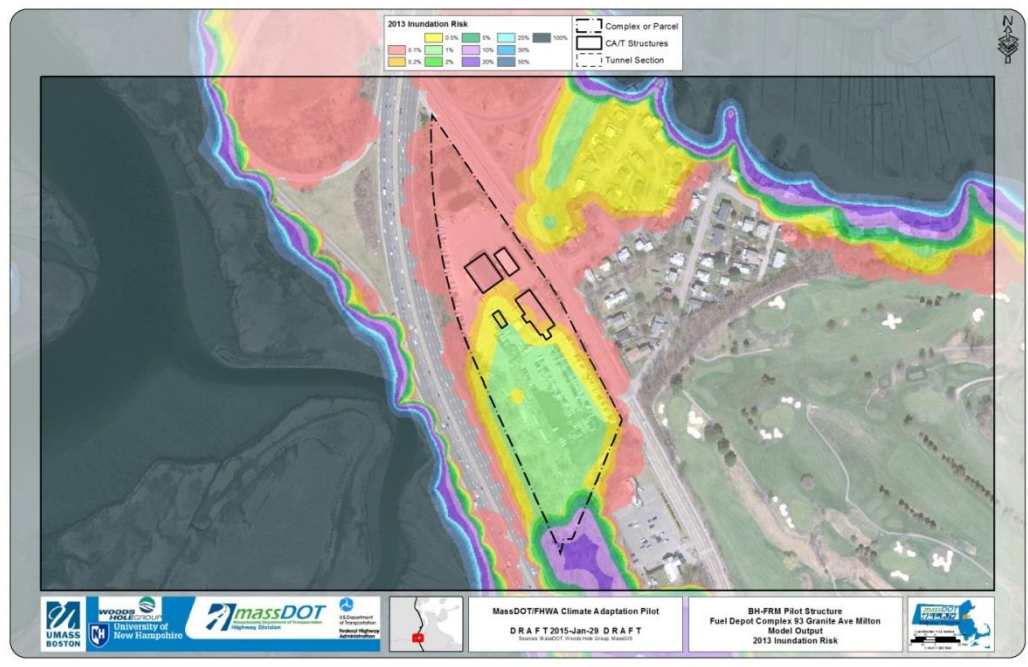


Figure 4-38. BH-FRM results showing probability of flooding in 2013 for the 93 Granite Ave. location.

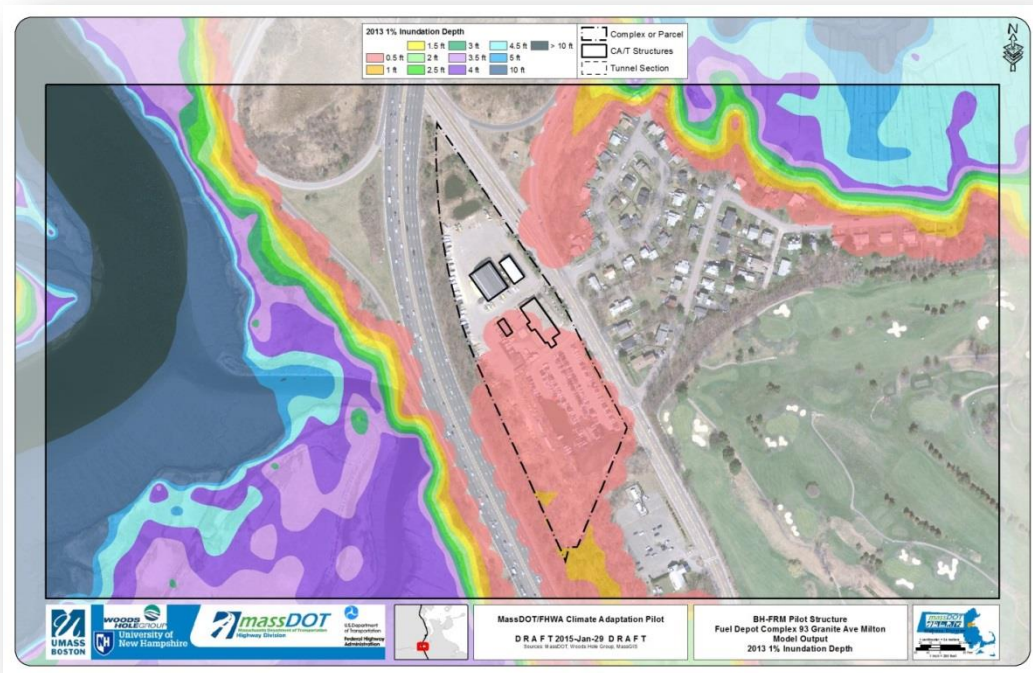


Figure 4-39. BH-FRM results showing flooding depth for a 1% flooding probability in 2013 at the 93 Granite Ave. location.

Figure 4-40 again shows the flooding depths corresponding to the 1% flooding probability level; as well as the residence time of the flooding and flood pathways to the site. The residence time gives an indication of how long the flooding is expected to last for the 1% probability. This type of information can only be obtained from a dynamic temporal model such as BH-FRM. For present day (2013), the residence time of the flooding is 7.33 hours. In other words, the flooding remains at the site for 7.33 hours before it recedes (and peaks at 0.5 feet). The figure also shows the two local flood pathways that influence the area. The flood pathway to the north originates in a small marsh creek that allows water to propagate landward and flood into the local neighborhood and road system. The flood pathway to the south is the low lying wetland area that connects further to the south to the Neponset River. Potential adaptations could consider local measures (e.g., raising the elevations of the buildings on the parcel, flood proofing structures, local on-site berms or walls) or more regional approaches (e.g., berms, tide gates, flood walls, etc.) at the source of the flooding for the area that would not only serve to protect the 93 Granite Ave. site, but also other assets (e.g., roads, homes, etc.).

Looking forward in time to 2030, Figure 4-41 presents the flooding probabilities at 93 Granite Ave. site. The probabilities of flooding and risk have increased significantly at this location compared to 2013. The southern portion of the parcel now has a flooding probability of 20%, while all the buildings are in the 2-5% probability zones. There is also significant risk of flooding for Granite Ave. itself. Figure 4-42 shows the depth for the 1% flooding probability, which have now increased to an average of 1.5 feet for a good portion of the parcel, while also showing inhibited accessibility to the site via Granite Ave. The entire parcel has depths of at least 0.5 feet, and reaches depths of 2 feet. Figure 4-43 shows a residence time that is now 10 hours indicating access to the site would be unavailable for that length of time. The pathways of flooding remain the same and I-93 is at a high enough elevation to remain unaffected in this area, as well as provide a barrier to flooding. This increased risk of flooding at this location gives an indication that, at minimum, careful engineering approaches and planning should be taken if the primary maintenance facility is to be relocated to this site.

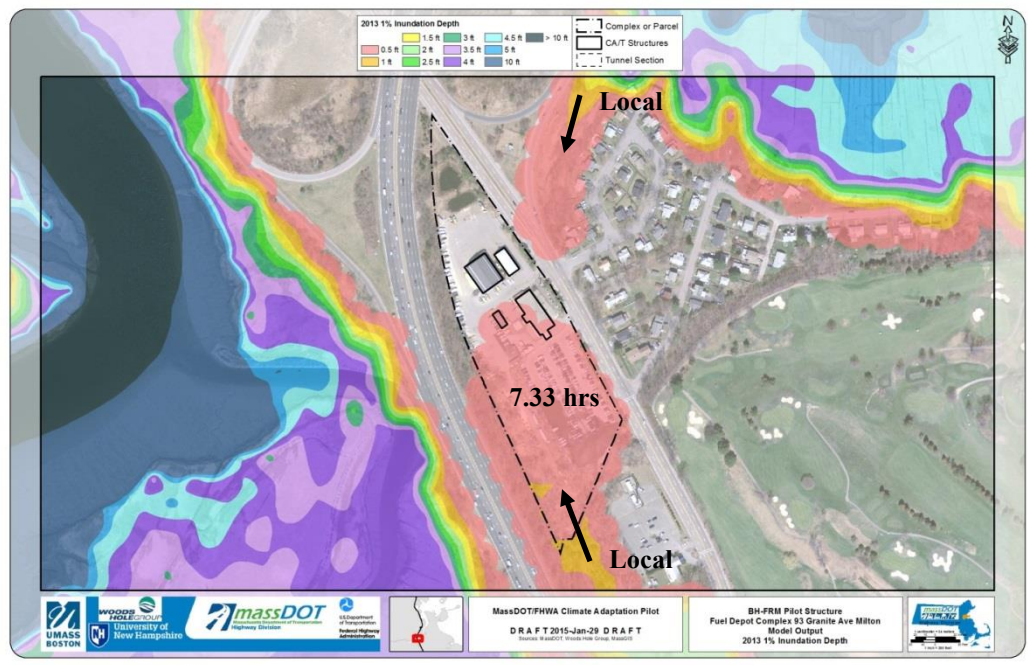


Figure 4-40. BH-FRM results showing flooding depth for a 1% flooding probability in 2013 at the 93 Granite Ave. location, as well as residence time and local flood pathways.

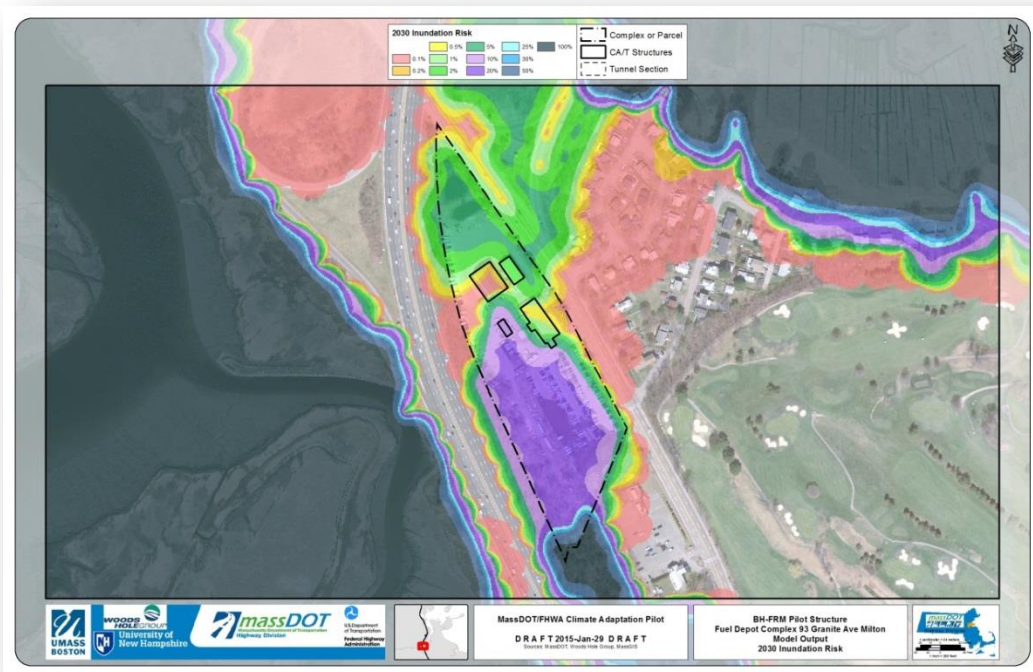


Figure 4-41. BH-FRM results showing probability of flooding in 2030 for the 93 Granite Ave. location. An additional 0.74 in (1.9 cm) due to land subsidence was added to the 0.62 feet SLR.

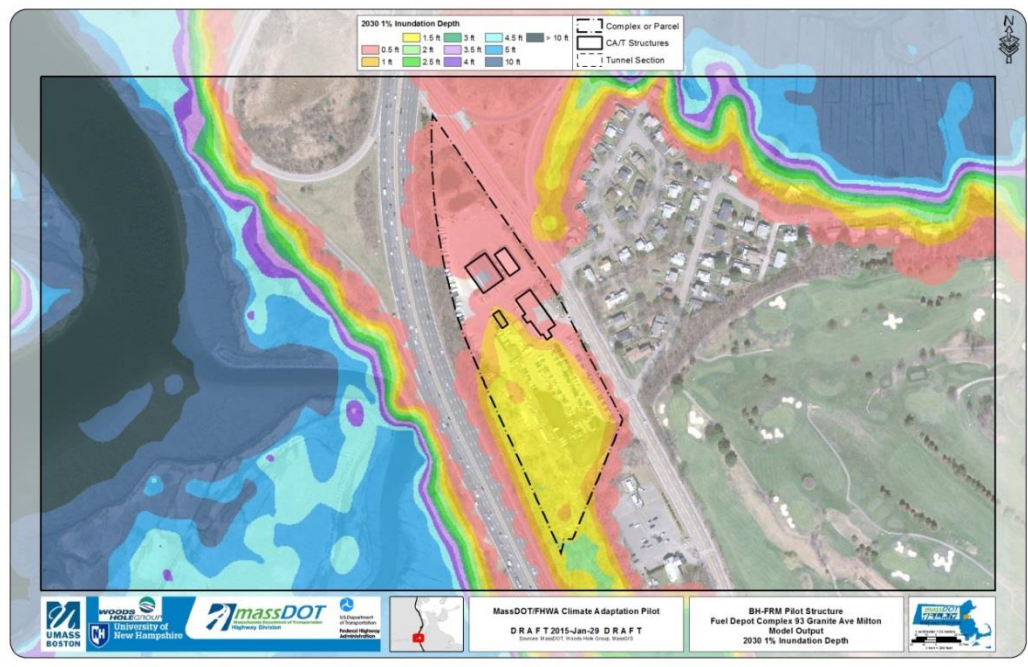


Figure 4-42. BH-FRM results showing flooding depth for a 1% flooding probability in 2030 at the 93 Granite Ave. location. An additional 0.74 in (1.9 cm) due to land subsidence was added to the 0.62 feet SLR.

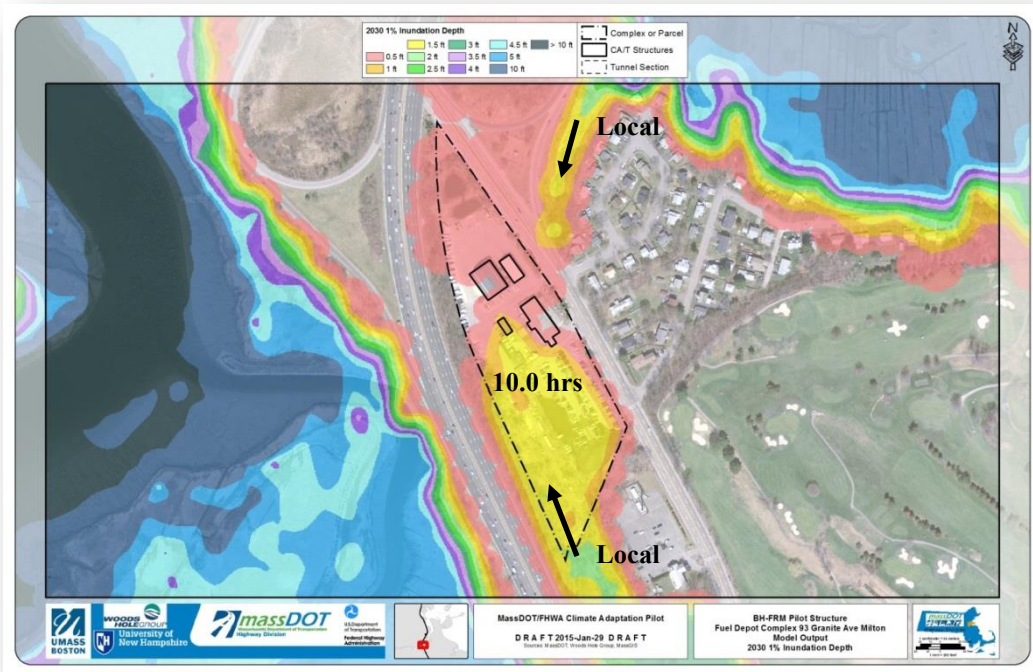


Figure 4-43. BH-FRM results showing flooding depth for a 1% flooding probability in 2030 at the 93 Granite Ave. location, as well as residence time and local flood pathways. An additional 0.74 in (1.9 cm) due to land subsidence was added to the 0.62 feet SLR.

VULNERABILITY ASSESSMENT

5.1 Development of the Vulnerability Assessment Process

The Vulnerability Assessment was originally designed to follow the formal process of exposure, sensitivity, and adaptive capacity (as described in Sec 1.4), but after the October 2014 IK meetings (described below) the vulnerability assessment procedure was modified. It has since been based upon the amount of flooding experienced at a non-Boat Section Structure or at the at-grade area around a Boat Section with Portal when the thresholds of the design standards that governed the original design of the CA/T are exceeded. Essentially what this means from a vulnerability assessment perspective is that, on a scale from zero to one, the sensitivity of CA/T Structures is one. For the CA/T system to perform, it is critical that all components of the system operate properly. In addition, this means that the adaptive capacity of all components of the CA/T is essentially zero because if one component is impacted by flooding and fails, the performance of the entire system is impacted.

IK Meeting: Sensitivity of Structures and Tunnels to Flooding, October 9, 2014: This meeting started out with the project team reviewing each structure listed in Table 5-1 (locations shown in Figure 5-1) with the IK Team for its sensitivity to flooding and any capacity for adjustment in the operation of the CA/T if it failed (“adaptive capacity”). After reviewing several Structures, it readily became apparent that the flooding sensitivity was high for almost all Structures and there was little redundancy in the system. Thus the project team with MassDOT agreed all Structures had equal priority.

IK meeting: critical thresholds/boat sections, October 15, 2014: Our original scope of work included the determination of critical threshold flood elevations for all Structures and Boat Sections with Portals (that is, tunnel entrances and exits) within the MassDOT CA/T system domain. The result would be an estimate of when flooding would occur based upon the ADCIRC model output and associated sea-level rise scenarios. Critical threshold elevations for a non-Boat Section structure would include sill elevations for doors, window, vents, etc. – any potential opening which could allow water to enter the Structure. For Boat Sections, critical thresholds would include the elevations of the tops of walls that surround them as well as the roadway elevation leading to or from a tunnel. This changed, however, during the IK meeting on October 15, 2014. Here the MassDOT IK Team stated that “any water at grade is a problem” because of possible leaky foundations, doorways, etc. at grade. Therefore, we discontinued surveying structure features for critical elevations but recommend that all Structures be inspected for possible flood pathways at grade into them. It was also decided that since all outfalls and doors in the system (eg. those in tunnels) could not be located, all outfalls should have tide gates on them and all doors exposed to possible flooding should have water tight doors.

All Structures have an equal priority, since flooding sensitivity is high and there is little redundancy in the system.

Table 5-1. List of facilities and structure for mini-pilot analysis.

Structure Name	Structure Street	Structure Type	Facility ID	Facility Name
District 6 Headquarters	185 Kneeland Street	Administrative	D6HQ	District 6 Headquarters
Air Intake Structure	275 Congress Street	Air Intake Structure	AIS	Air Intake Structure
BIN5VA	Ramp-RTS 93 NB/3NB to North Street	Boat Section	BIN5VA	BIN5VA Ramp CN-SA
Electrical Substation 2	480 Albany Street	Electrical Substation	ERS04	Emergency Response Station 4
Electrical Substation 2	480 Albany Street	Electrical Substation	ESS02	Electrical Substation 2
Emergency Platform 6	Atlantic Avenue	Emergency Platform	EP06	Emergency Platform 6
Emergency Response Station 2	100 Massport Haul Road	Emergency Response Station	ERS02	Emergency Response Station 2
Fan Chamber Essex St. – FC-313 On 93SB	Essex Street	Fan Chamber	FC313	Fan Chamber 313
D6 Granite Ave Fuel Depot	93 Granite Ave.	Fuel Depot	D6FDG	D6 Granite Ave Fuel Depot
Central Maintenance Facility	370 D Street	Maintenance Facility	D6CMF	Central maintenance Facility
MBTA Aquarium Station	Atlantic Avenue	MBTA Station	TE434	Tunnel Egress 434
MBTA Aquarium Station	Atlantic Avenue	MBTA Station	MBTAAQ	MBTA Aquarium Station
Highway Operation Center	50 Massport Haul Road	Operations	D6HOC	Highway Operation Center
Storm Water Pump Station 9	Rear of 185 Kneeland Street	Storm Water Pump Station	SW09	Storm Water Pump Station 9
Stormwater Outfall 96F	Frontage Road	Stormwater Outfall	OF96F	Stormwater Outfall 96F
Toll Facility Bldg 1	4 Harborside Drive	Toll Plaza	ESS01	Electrical Substation 1
Toll Facility Bldg 1	4 Harborside Drive	Toll Plaza	O90P31	I-90 Toll Plaza31
Toll Facility Bldg 1	4 Harborside Drive	Toll Plaza	TFB01	Toll Facility Building 1
Tunnel Egress 425	Atlantic Avenue	Tunnel Egress	TE425	Tunnel Egress 425
Ventilation Bldg 4	136 Blackstone Street	Ventilation Bldg	VB04R	Ventilation Building 4 Retail/Office Space
Ventilation Bldg 4	136 Blackstone Street	Ventilation Bldg	LP08	Low Point Pump Station 8
Ventilation Bldg 4	136 Blackstone Street	Ventilation Bldg	MBTAHA	MBTA Haymarket Station
Ventilation Bldg 4	136 Blackstone Street	Ventilation Bldg	SW15	Storm Water Pump Station 15
Ventilation Bldg 4	136 Blackstone Street	Ventilation Bldg	VB04	Ventilation Building 4
Ventilation Bldg 4	136 Blackstone Street	Ventilation Bldg	VB04G	Ventilation Building 4 Garage



Figure 5-1. Location of mini-pilot Facilities and Structures listed in Table 5-1.

For Boat-Sections, we did not have an adequate assessment of whether or not the surrounding walls can withstand flood waters or whether or not they are water tight. For example, we observed several Boat Sections walls, such as those on Parcel 6 (Rose Kennedy Greenway Parcel 6 includes Ramps SA-CN, SA-CT, SA-CS, ST-CN and ST-SA), which are primarily constructed of “Jersey Barriers,” which cannot be expected to be watertight or withstand floods. At other Boat Sections, electrical equipment was observed located outside the walls; this equipment is therefore vulnerable to flooding at ground-level. We therefore recommended that the ground level elevations surrounding each Boat

Section be used as the critical threshold elevation regardless of the higher elevations of any surrounding walls. While we could have assumed that some of walls would be strong enough to withstand flood flows and are floodproof, we do not want to make that assumption without a detailed engineering inspection of each wall. We recommend that each wall be inspected to determine if it is floodproof and/or if it protects associated electrical equipment.

In preparation for the vulnerability assessment, we reviewed the CA/T design standards (CAT Project Design Criteria, Bechtel/Parsons Brinckerhoff, various dates, Volumes 1 – 3) and found that the design

criterion for the tunnel entrances was the so-called “1000-year” flood elevation or more properly defined, the flood elevation that has a 0.1% probability of being equaled or exceeded in any one year. A minimum wave height of 1.5 feet was to be added to these flood elevations in locations subject to wave action. A review of the Massachusetts State Code in 1990 (<https://archive.org/stream/commonwealthofma1990mass#page/66/module/2up>) indicated that the design elevation for all other CA/T Structures was the “100-year” flood elevation or the flood elevation that has a 1% probability of being equaled or exceeded in any one year. It also required wave heights be added. There is no mention in the document about the need to adjust the elevations over time to account for SLR and climate change. We also found design criteria for stormwater, buoyancy and other impacts, but our vulnerability analysis was limited to surface flooding impacts, and so these other criteria were not applied.

The actual process followed for each climate change scenario was as follows:

1. A GIS spatial location query was performed to initially identify the CA/T non-boat section Structures at risk for any flooding using two datasets: the BH-FRM 1% CFEP interpolated flood depths and the polygon feature class representing the Structures. This process was repeated for Boat Sections with Portals using the 0.1% interpolated flood depths.

2. The results of the spatial query were manually reviewed and adjusted to also include additional potentially impacted CA/T Facilities associated with each Structure identified; for example a Tunnel Egress located within a Boat Section wall.
3. Then for each Structure in Steps 1 and 2, the Project Team manually reviewed 1.0 % nodal maps to determine in more detail the extent of flooding and the estimated flood depths for non-Boat Section Structures. This analysis was repeated using the 0.1% nodal maps for each Boat Section with Portal. The team also used their own knowledge of the site and photographs to interpret the present and potential future flooding.

An example 1% interpolated flood depth map overlain with nodal results for a typical CA/T Structure is shown in Figure 5-2 and illustrates the importance of using the nodal maps to determine site specific flooding probabilities.

Here it can be seen by examining the nodal depths surrounding the example Structure (VB6) that most of VB6 is surrounded by a flood depth of 0.4 feet but perhaps the NW corner is at a greater depth. Project Team knowledge obtained from field data collection and photos indicated that the terrain to the northwest of VB6 is actually quite steep and the 0.4 ft depth shown represents the depth around the entire building.

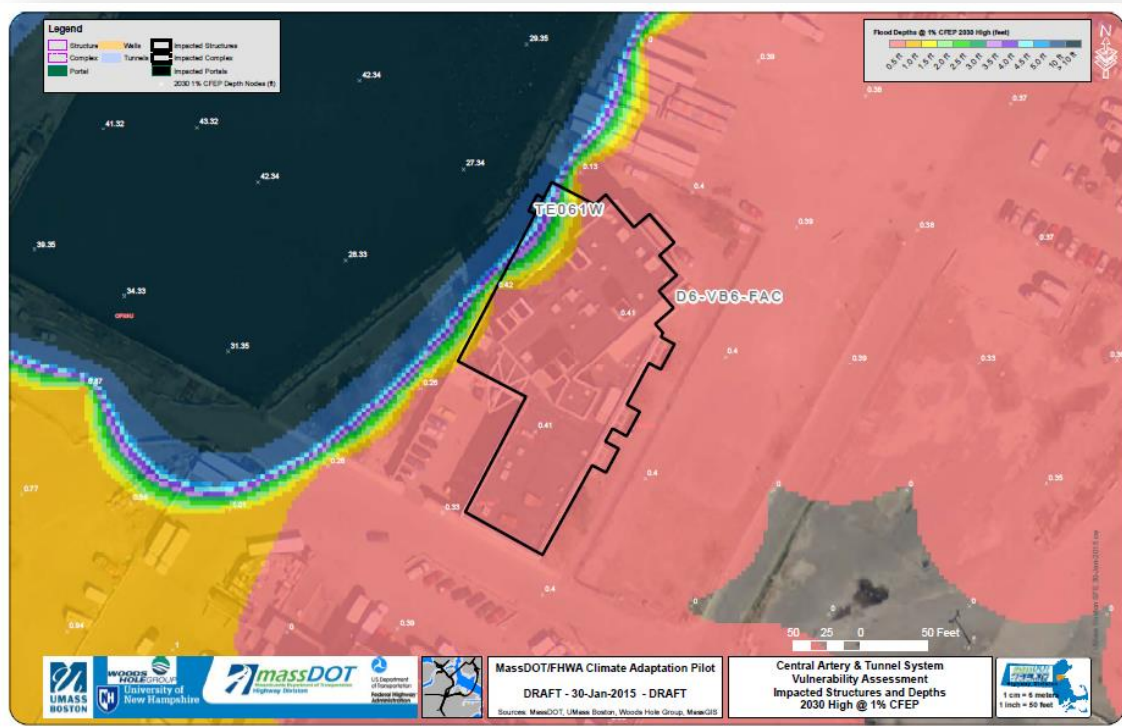


Figure 5-2. Example of 1% interpolated flood-depth map overlain with nodal information (data points) for a typical CA/T Structure – specifically Vent Building 6 (VB6) in South Boston.

5.2 Results of Vulnerability Assessment of Individual Structures

5.2.1 Vulnerability of Non-Boat Section Structures.

The vulnerability results for non-Boat Section Structures is shown in Table 5-2. The column labeled “2013 1% Depth (ft)” represents the vulnerability of CA/T Structures under present climate conditions. Using the 2030 climate change scenario (shown as point #2 in Figure 4-18), the column entitled “2013 to 2030 1% Depth (ft)” represents the flooding scenario combined with sea level rise by 2030. The 2030 maps show a snapshot of flooding, but not the year at which flooding at a particular location begins to be probable. For example, if a particular location shows no vulnerability to flooding from a 1% storm in 2013 but 1.5 ft of flooding from a similar

storm in 2030, then this location will become vulnerable to flooding sometime between 2013 and 2030.

Using the 2070 climate change scenario (shown as point #3 in Figure 4-18), the column entitled “2030 to 2070 or to 2100” indicates vulnerability over the period just past 2030 to 2070 under a higher SLR scenario, or over the period just past 2030 to 2100 under a lower SLR scenario.

As can be seen in Table 5-2, the number of non-Boat Section structures that will experience flooding grows over time, as does the depth of flooding. For example, under current climatic conditions (the “2013 scenario”), only six Structures are vulnerable to flooding from a 1% storm and the flood depths at any of these Structures range from 0.1 to 0.5 ft. However, by 2030, the flood depths at all of these six Structures have increased and nineteen more Structures

have become vulnerable to flooding. By 2070 or 2100 depending upon the SLR, an additional twenty-six Structures have become vulnerable.

5.2.2 Vulnerability of Boat Sections with Portals.

As noted previously, only the vulnerability of Boat Sections with associated tunnel Portals were evaluated. For example, BIN1aN (Route 1A Southbound near MBTA Airport Station) in East Boston does not lead to tunnel Portals and therefore its vulnerability was not assessed. However, we noted that flooding at Boat Sections even without Portals, such as BIN1aN in East Boston, can impact other aspects of the CA/T operations. In this case, excessive flooding of BIN1aN can potentially lead to overloading or flooding of a key stormwater pump station, SW06, which could reportedly impact the operability of other drainage systems upstream of this location.

Table 5-3 shows the flood depths of the at-grade land surrounding Boat Sections with Portals. Many of the Portals are adjacent to each other as illustrated in Figure 5-3. In these cases, if at least one of the Boat Sections was flooded, it was assumed all the other sections were also flooded. Under current climate conditions (2013 0.1% flood depths), twelve Portals are vulnerable to flooding. The same twelve Portals remain vulnerable in 2030. As shown in Table 5-3, however, the flood depths on the surface surrounding the Boat Sections increase by approximately 1 to 2 feet by 2030 when compared to 2013 depths. Over the period 2030 to 2070 or 2100, an additional forty-two Portals become vulnerable.

Table 5-2. The vulnerability results of non-Boat Section Structures for flooding scenarios: “2013” indicates present vulnerability, “2013 to 2030” indicates vulnerability over the period from the just past the present to 2030, “2030 to 2070 or to 2100” indicates vulnerability over the period just past 2030 to 2070 under a higher SLR scenario, or over the period just past 2030 to 2100 under a lower SLR scenario. Underlined Structures are Complexes; Italicized Structures are located within each Complex.

Note: when a range of depths is shown, it means that flood depth varies along the perimeter of the Structure.

Structure_ID	2013 1 % Depth (ft)	2013 to 2030 1 % Depth (ft)	2030 to 2070/2100 1 % Depth (ft)	Structure Location and Notes
<u>D6A-DC01</u>	0	0 to 0.1	2.2 to 3.3	<u>Central Maintenance Facility Complex</u> 400 D Street, South Boston - this Complex also contains <i>D6-CMF-FAC</i> , <i>D6A-D1</i> and <i>MHRML</i>
<i>D6-CMF-FAC</i>	0	0 to 0.1	2.6 to 3.3	<i>Central Maintenance Facility</i>
<i>D6A-D1</i>	0	0.1	2.7 to 2.9	<i>Fuel Depot CMF South Boston</i>
<i>MHRML</i>	0	0.1	2.9 to 3.3	<i>Mass Highway Research & Materials Laboratory</i>
<u>D6A-DC03</u>	0	0 to 0.5	0.5 to 3.2	<u>Depot-Main Complex SMF</u> Rutherford Street, Charlestown -this Complex also contains <i>D6-ES10-FAC</i> , <i>D6-SMF-SAC</i> and <i>DA6-D3</i>
<i>D6-ES10-FAC</i>	0	0 to 0.5	1.9 to 3.2	<i>Emergency Response Station 10</i>
<i>D6-SMF-FAC</i>	0	0 to 0.5	2.2 to 3.2	<i>Satellite Maintenance Facility</i>
<i>D6A-D3</i>	0	0 to 0.2	2.3 to 3.0	<i>SMF Fuel Depot</i>
<i>D6-AIS-FAC</i>	0	0	0.0 to 0.7	Air Intake Structure – Atlantic Avenue, Boston
<u>D6D-DC01</u>	0 to 0.5	0 to 1.7	0.0 to 4.9	<u>Depot-Main Complex</u> 93 Granite Ave, Milton - this Complex also contains <i>Buildings A, B, C, D</i> and <i>D6D-D1</i>
<i>D6D-D1-B</i>	0 to 0.5	0.9 to 1.7	4.0 to 4.9	<i>D6 Granite Ave Building B</i>
<i>D6D-D1-C</i>	0	0 to 0.7	2.7 to 3.8	<i>D6 Granite Ave Building C</i>
<i>D6D-D1-A</i>	0	0 to 0.5	2.2 to 3.2	<i>D6 Granite Ave Building A</i>
<i>D6D-D1-D</i>	0	0	3.2 to 4.6	<i>D6 Granite Ave Building D</i>
<i>D6D-D1</i>	0	0 to 1.4	0 to 3.1	<i>D6 Granite Ave Fuel Depot</i>
<u>HOC-D6</u>	0	0 to 0.7	1.6 to 3.9	<u>Complex HOC</u> 50 Massport Haul Road, South Boston - this Complex also contains <i>D6-HOC-FAC</i> , <i>D6-ES02-FAC</i> and <i>D6-SW04-FAC</i>
<i>D6-HOC-FAC</i>	0	0 to 0.6	1.5 to 1.6	<i>Highway Operation Center</i>
<i>D6-ES02-FAC</i>	0	0 to 0.3	1.2 to 3.0	<i>Emergency Response Station 2</i>
<i>D6-SW04-FAC</i>	0	0 to 0.6	1.6 to 3.4	<i>Storm Water Pump Station 4</i> - This is the vent. Door to pump station located in boat section, upstream of BIN7J8-POR. Needs water tight door. Its vent structure is at surface grade directly above. Vent protected by wall around D6-HOC-FAC Complex.
<i>D6-ESS2-FAC</i>	0	0	0.0 to 1.2	Electrical Substation 2 - Albany Street, Boston
<i>D6-ESS3-FAC</i>	0	0	0.0 to 1.8	Electrical Substation 3 – Austin Street, Boston
<i>D6-FCB-FAC</i>	0	0	2.4	Fan Chamber - Beach Street, Boston
<i>D6-LP11-FAC</i>	0	0	0.0 to 1.0	Low Point Pump Station 11 – This is the street grate on Atlantic Avenue, Boston
<i>D6-SW07-FAC</i>	0	0	2.5	Storm Water Pump Station 7 – Albany Street, Boston
<i>D6-SW09-FAC</i>	0	0	2.4	Storm Water Pump Station 9 – Rear of Rear of 185 Kneeland Street
<i>D6-SW12-FAC</i>	0	0	1.7	Storm Water Pump Station 12 – Frontage Road, Boston
<i>D6-SW16-FAC</i>	0	0	2.0 to 2.9	Storm Water Pump Station 16 – Dock Square, Boston
<i>D6-SW17-FAC</i>	0	0	2.0 to 2.5	Storm Water Pump Station 17 – Leverett Circle, Boston
<i>D6-SW18-FAC</i>	0	0	0.0 to 1.4	Storm Water Pump Station 18 – Austin Street, Boston
<i>D6-TA05-FAC</i>	0	0	0.0 to 1.2	Sumner/Callahan Administration – North Street, Boston
<i>D6-SW25-FAC</i>	0	0	0	Storm Water Pump Station 25 outside (upstream) of BIN7GA-POR (Sumner Tunnel Exit), See note for BIN7GA-POR in Table 5.3. Needs watertight door.
<i>D6-SW27-FAC</i>	0	0	0	Storm Water Pump Station 27 outside (upstream) of BINC01-POR (Callahan Tunnel Entrance), See note for BINC01-POR in Table 5.3. Needs watertight door.
<u>D6-HQC</u>	0	0	0 to 2.5	<u>District 6 Headquarters Complex</u> Kneeland Street, Boston – this Complex also contains <i>D6-185K-FAC</i>
<i>D6-185K-FAC</i>	0	0	0 to 2.4	<i>District 6 Headquarters</i>
<u>TB03-D6</u>	0 to 0.1	0.4 to 1.4	3.7 to 4.5	<u>Sumner Toll Plaza Complex</u> Porter Street, East Boston– this Complex also contains <i>D6-TB03-FAC</i> and <i>ERS07</i>
<i>D6-TB03-FAC</i>	0	0.1 to 0.45	3.5 to 3.9	<i>Toll Facility Building Sumner Tunnel</i>
<i>ERS07</i>	0	0.4 to 1.4	3.7 to 4.5	<i>Emergency Response Station 7</i>
<u>TA03-D6</u>	0 to 0.1	0.1 to 0.8	3.5 to 4.5	<u>Have Street Administrative Complex</u> Have Street, East Boston - this Complex also contains <i>D6-TA03-FAC</i>
<i>D6-TA03-FAC</i>	0	0.4 to 0.8	3.9 to 4.3	<i>Sumner/Callahan Tolls/Administration/Engineering</i>
<i>D6-VB11-FAC</i>	0	0 to 0.25	1.6 to 2.5	Vent Building 11 - Liverpool Street, East Boston
<i>D6-VB12-FAC</i>	0	0	0.0 to 3.1	Vent Building 12 – North Street, Boston
<i>D6-VB13-FAC</i>	0	0.05 to 0.7	3.5 to 4.0	Vent Building 13 - Decatur Street, East Boston
<i>D6-VB1-FAC</i>	0	0	0.0 to 0.7	Vent Building 1 - 55 Dorchester Avenue, Boston
<i>D6-VB3-FAC</i>	0	0	0.6 to 1.8	Vent Building 3– Atlantic Avenue, Boston
<i>D6-VB6-FAC</i>	0	0.4	3.5 to 3.8	Vent Building 6 - 2 Fid Kennedy Drive, South Boston – this Structure also includes TE061E and TE061W
<i>D6-VB7-FAC</i>	0	0	0 to 0.5	Vent Building 7 - Harborside Drive, East Boston – this Structure also includes TE071W
<i>D6-VB8-FAC</i>	0	0	3.0 to 5.3	Vent Building 8 - Accolon Way, Boston
<i>LP-UNK</i>	0	0	2.3	Low point pump station – this is a vent structure located on Kneeland Street near Lincoln Street, Boston
<i>SW06</i>	0	0	~ 1.0	Massport Storm Water Pump Station – Service Road East Boston
<i>TE061W</i>	0	0.4	3.8	Tunnel Egress 61W at VB6
<i>TE061E</i>	0	0	3.8	Tunnel Egress 61E at VB6
<i>TE071W</i>	0	0	0 to 0.5	Tunnel Egress 71W at VB7
<i>MBTAAQ</i>	0.4	0.5 to 1.5	4.0 to 5.0	MBTA Aquarium Station – Atlantic Avenue, Boston – this Structure also includes TE434
<i>TE434</i>	0.4	1.5	5.0	Tunnel Egress 434 at MBTA Aquarium Station
<i>TE161</i>	0	1	3.6 to 4.4	Tunnel Egress 161 - Binford Street, South Boston
<i>TE173</i>	0	0	0	Tunnel Egress 173 inside (downstream) of BIN62B (I-90 EB HOV Lane), so protected if Portal protected. See note for BIN62B-POR in Table 5.3
<i>TE183</i>	0	0	2.7	Tunnel Egress 183 - Frontage Road, Boston
<i>TE185</i>	0	<2.0	<2.0	Tunnel Egress 185 - West Broadway, Boston
<i>TE201</i>	0	0	0.4 to 1.5	Tunnel Egress 201 – Atlantic Avenue, Boston at South Station
<i>TE425</i>	0	0.4	2.2 to 4.0	Tunnel Egress 425 - Atlantic Avenue, Boston near Milk Street
<i>CP534</i>	0	0	0	Tunnel Egress CP534 - Outside (upstream) of BIN7UG-POR (Ted Williams Tunnel Exit). See note for BIN7UG-POR in Table 5.3. Needs watertight door.
<i>VG999</i>			0.4 to 1.5	Vent grate adjacent to TE201 – Atlantic Avenue, Boston at South Station

Notes: ^a Inside (downstream) of Portal BIN62B-POR, so protected if portal protected.

^b Outside (upstream) of Portal BIN7UG-POR, floods if Boat Section floods.

^c See note b. Also in 2030, 1% flood, there is only minor flooding of the Boat Section.

^d Door to pump station located in boat section, south and outside of Portal 7J8-POR. Portal is flooded under 1% flood level in 2030..

Table 5-3. Flood depths of the at-grade land around Boat Sections with Portals: “2013” indicates present vulnerability, “2013 to 2030” indicates vulnerability over the period from the just past the present to 2030, “2030 to 2070 or to 2100” indicates vulnerability over the period just past 2030 to 2070 under a higher SLR scenario, or over the period just past 2030 to 2100 under a lower SLR scenario.

Notes: * = majority of depth exceeds 0.5 ft around perimeter; when a range of depths is shown, it means that flood depth varies along the perimeter of the Boat Section.

Structure_ID	2013 0.1 Depth (ft)	2013 to 2030 0.1 Depth (ft)	2030 to 2070/2100 0.1 Depth (ft)	Ramp Area or Roadway Area and Notes
BIN5UR -POR	0	0	*0 to 3.2	Ramp CS-SA Central Artery Southbound to Surface Artery
BIN5VQ-POR	0	0	*0 to 1.4	Rose Kennedy Greenway Parcel 18: Ramp A-CN Atlantic Avenue to I-93 Northbound
BIN5VA-POR	*0 to 1.0	*0 to 1.7	*0 to 4.4	Rose Kennedy Greenway Parcel 12: Ramp CN-SA Central Artery Northbound to Surface Artery
BIN59Y-POR	0	0	*0 to 2.3	Ramp CN-S Central Artery Northbound to Storrow Drive
BIN5AF-POR	0	0	*0 to 1.6	Storrow Drive Northbound entrance to Leverett Circle Tunnel
BIN5K2-POR	0	0	*0 to 1.5	Storrow Drive Northbound exit from Leverett Circle Tunnel
BIN59K-POR	0	0	*0 to 1.7	Ramp L-CS Leverett Circle to Central Artery Southbound
BIN7BC-POR	0	0	*0 to 2.8	Ramp B Massport Haul Road to I-90 Westbound
BIN7BB-POR	0	0	*2.2 to 2.8	Ramp D Congress Street to I-93 from Ramp Area F
BIN7BL-POR BIN7BM	0	0	*0 to 2.8	Ramp L I-93 North Bound to I-90 Eastbound – includes a short underpass from BIN7BM to BIN7BL
BIN7DE-POR BIN7D5-POR BIN7DX-POR BIN7BN-POR	0	0	*0 to 3.4	I-90 / I-93 Interchange: Ramp D tunnel exit to I-93 Southbound, I-90 West Bound tunnel exit, I-90 East Bound tunnel entrance and Ramp C entrance to I-93 Northbound / Tip O’Neill Tunnel
BIN7GA-POR BIN7FX-POR BIN7FL-POR	0	0	*0 to 1.9	Sumner Tunnel Exit: Ramp ST-CN to Central Artery Northbound, and Ramp ST-S to Storrow Drive Also, door to D6-SW25-FAC is located in the Boat Section outside (upstream) of BIN7GA-POR
BIN7HV-POR	0	0	*0 to 3.3	I-93 Northbound entrance to Ted Williams Tunnel
BIN7EK-POR BIN7E7-POR BIN7F6-POR BIN7FQ-POR BIN7FN-POR	0	0	*0 to 3.0	Rose Kennedy Greenway Parcel 6: Ramp SA-CS Surface Artery to Central Artery South, Ramp SA-CN Surface Artery to Central Artery North, Ramp SA-CT Surface Artery to Callahan Tunnel Ramp ST-SA Sumner Tunnel to Surface Artery Ramp ST-CN Sumner Tunnel to Central Artery North
BIN6HB	0	0	*0 to 3.3	I-93 Southbound exits from Ted Williams Tunnel and I-90 Collector
BIN7J8-POR BIN7J9-POR BIN7JD-POR BIN7JE-POR BIN7JF-POR BIN7RX-POR	*0 to 0.9	*0 to 2.9	*0 .5 to 5.8	I-90 Main Line entrance to and exit from Ted Williams Tunnel, Ramp F I-90 West to Congress Street, and HOVEB Also, door to D6-SW04-FAC is located in the Boat Section outside (upstream) of BIN7J8-POR.
BIN7UG-POR BIN7GC-POR BIN7MD-POR	0 to 0.4	*0 to 1.4	*0 to 4.5	I-93 Northbound and Southbound Tip O’Neill Tunnel Portals at Zakim Bridge, and Ramp SA-CN Surface Artery to Central Artery North Also, Tunnel Egress CP534 is located in the Boat Section outside (upstream) of BIN7UG-POR.
BIN7B9-POR	0	0	*0 to 2.8	Ramp F I-90 West to Congress Street
BIN7T8-POR	0	0	*0 to 1.5	Ramp I I-90 East Ramp Area L To Congress Street
BIN5JR-POR	0	0	*2.4 to 10.3	Ramp L-CS Leverett Circle to Central Artery Southbound
BIN62B-POR	0	0	*2.8 to 4.0	I-90 EB HOV Lane Also, Tunnel Egress TE173 is located inside (downstream) of BIN62B-POR, so protected if Portal protected.
BIN6HD-POR	0	0	*0.4 to 3.2	Ramp RV Surface Road to I93 South Bound
BINA07-POR	0.3	*0.7	*4.0 to 5.3	Sumner Tunnel Entrance East Boston
BIN9BU-POR BIN9BV-POR BIN9BW-POR BIN9CT-POR BIN9CU-POR	0	0	*0 to 2.3	I-90 Main Line entrance to and exit from Ted Williams Tunnel adjacent to Logan Airport: Ramp E-T I-90 West Logan Entrance, and Ramp TA-D I-90 East Logan Exit
BINC00-POR	0 to 0.4	*0.3 to 0.8	*4.4 to 5.3	Callahan Tunnel Exit East Boston
BINC01-POR BIN7EC-POR BIN7ED-POR	0	0	*0 to 3.8	Callahan Tunnel Entrance: Ramp CS-CT from Central Artery South Bound, and Ramp SA-CT from Surface Artery Also, door to D6-SW27-FAC is located in the Boat Section outside (upstream) of BINC01-POR
BINLT1-POR	0	0	*As much as 4 ft	Ramp LT Rutherford Avenue to Tobin Bridge
BINCT1-POR	0	0	*As much as 3 ft	Ramp C-T I-93 Northbound to Tobin Bridge
BINTC1-POR	0	0	*As much as 3.5 ft	Ramp T-C Tobin Bridge to I-93 Southbound
BINSS1-POR	0	0	*0.7 to 1.8	Storrow Drive Southbound exit from Leverett Circle Tunnel
BINSS3-POR	0	0	*1 to 2.1	Storrow Drive Southbound entrance to Leverett Circle Tunnel

Notes: ^d more than 20% of perimeter at a depth >0.9 ft.

^e most of the perimeter is flooded at 1.1 ft.

^f most of the perimeter is flooded at 1.9 ft.

^g more than 80% of the perimeter is not flooded (0.0 ft depth).

ⁱ most of the perimeter is flooded at 1.0 ft

^j more than 30% of the perimeter is flooded at >0.3 ft.

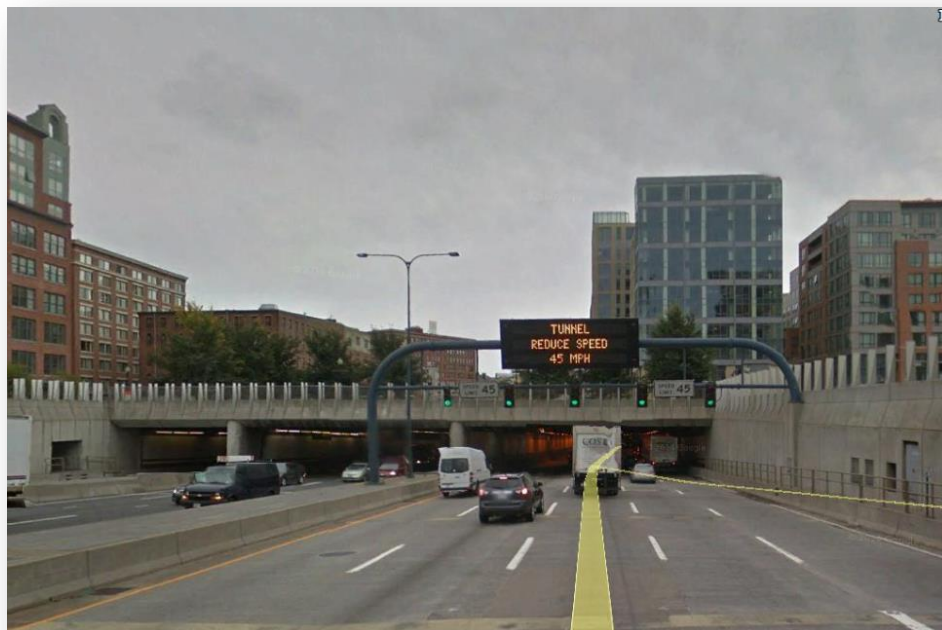


Figure 5-3. Street View of Combined Bins 7UG, 7MD, and 7GC (from Google Earth).

ADAPTATION

Adaptation is generally defined as the process of adjusting to the vulnerability of climate change. It consists of a series of actions taken over time and space (Kirshen et, 2014). Here we evaluate local adaptation options for protecting the individual non-Boat Section Structures and Boat Sections with Portals over time as flooding increases. An alternative plan that focuses less on individual Structures and Portals and more on blocking the regional flood pathways as they grow in height and extent over time is presented.

Focusing first on local actions means that MassDOT is less reliant on other organizations and agencies to manage the CA/T adaptation as it will own the land necessary for any changes and will only have to manage its own efforts. The regional plan has the co-benefits that it will protect more assets in the region than just the CA/T and there is the possibility that the cost can be shared among more agencies and organizations than just MassDOT. Hence, it will be important for MassDOT to consider the local adaptation options outlined here within the context of the regional adaptation options. The actual adaptation plan that is eventually designed and implemented for the CA/T will very likely consist of a combination of both local and regional actions.

6.1 Local Adaptation Plan

This strategy is generally conservative, meaning that the local protection for each structure and tunnel may not be the least expensive approach but it would provide adequate protection. Thus, it provides an estimated upper bound on the cost of local adaptation. The adaptation plan for the non-boat section Structures was based upon the sensitivity requirement that no flooding be

allowed near the foundations of the Structures. If flood depths were less than 2 feet, then relatively inexpensive temporary flood barriers would be used. As stated by FEMA (2013) self-supporting temporary barriers are only designed to protect against river flood depths of 3 feet. Therefore the 2 feet value was selected to be conservative. Once 1 % flood depths exceeded 2 feet around any portion of the structure perimeter, then a wall would be constructed around the flooded perimeter. As the extent of the flooding and the height of the flooding increased over time, the wall height would be increased; hence, any wall constructed as a local adaptation will be designed to be expanded beyond its initial height. As shown in Table 5-2, none of the flood depths around the non-Boat Section Structures in 2013 or in the period from now through 2030 exceeded 2 feet. The only exceptions to the need for protection of non-Boat Section Structures before 2030 is for the watertight doors noted in Table 6-1, which lists the wall lengths and the costs of protecting the non-Boat Section Structures.

Cost estimates for non-Boat Section walls shown in Table 6-1 were based upon two sources. It was recently estimated in 2015 for Massport that a cantilevered concrete floodwall 8 feet above the ground around the perimeter of a building of 830 feet with 3 vehicle access openings and two pedestrian openings with chain link double gates at one vehicle entry point would cost \$4,150,000 including excavation, construction, labor, materials, and design. This is \$5000/linear foot. Aerts et al (2013) presented costs for T Walls of various heights for New York City. Within height ranges of 8 to 20 feet, the cost per foot are approximately linear. Since most of the flood wall heights needed for MassDOT between 2030 and 2070, or 2100 depending

upon the rate of SLR, are in the range of 2 to 4 feet but may need to be increased in height by several feet over their assumed lifetime of 50 years, we assumed a unit cost of \$3500/foot and that the walls had lifetimes of 50 years. Maintenance costs were not included. As noted earlier, some of the non-Boat Section Structures in Table 5.2 require watertight doors. These costs are not included.

As described earlier, the plan for tunnels was to not rely on the walls surrounding the Boat Sections for flood protection because their strength and water tightness are unknown. Therefore, flood water flowing into the Boat Sections with Portals from the sides needs to be kept from entering the tunnels by watertight gates – covering the full height of the Portal. A gate would be installed when the 0.1 % flood depth exceeded 0.5 feet at most of the land surrounding Boat Section walls. At depths less than this, relatively inexpensive methods are assumed to be used such as local blocking of the lower part of the Portals with sand bags, or inflatable dams. The actual decision on when full gates would be needed at the Portals depends upon the rate of the flooding entering the boat section, and the pumping capacity of the tunnel drainage system.

Table 6-2 shows the number of lanes and dimensions for the Portals in Table 5-3 requiring gates either now or in the future. The number of lanes was determined by review of aerial photographs, the width was estimated based on the length of the GIS features, the height was estimated to be 14 feet based upon MassDOT design standards for the CA/T, and a hydrostatic pressure at the bottom of the Portal of 5 additional feet was used. The table also includes estimated materials and installation costs to construct watertight gates. The approximate year of installation was based upon when flooding

exceeded the threshold value of 0.5 feet. Costs estimates for our recommended adaptation options were provided by Presray Corporation, Wassaic, NY in February 2015. These costs were provided on a purely conceptual basis and will likely change as the actual design occurs. These costs are for steel watertight doors that are permanently hung on hinges and are swung into place before floods. Pneumatic seals around all sides of the door provide a full perimeter water seal. Large Portal openings (larger than approximately 60 feet) would be broken up into 2 panels with a removable center mullion that would attach to the header for strength, as well as the base. The installation costs are estimated to be 65% of the material cost. Additional costs for engineering design, extended warranty, yearly maintenance services, field or factory testing, shipping, rigging, as well as handling and other costs are not included here. Costs were determined for the representative Portals and then scaled for others based on dimensions.

6.2 Regional Adaptations

In addition to the local, facility-based adaptations that are intended to improve resiliency of an individual facility, structure, or asset, there are also potential regional adaptations that can be utilized to protect an area from flooding risk. Typically, these regional adaptations focus on renovation at a flood entry points, where a larger upland area is flooded by water arriving from a vulnerable section of the coastline. These regional solutions can be more cost effective than local adaptations by protecting a larger upland area consisting of numerous buildings, facilities, homes, roads, etc. that encompass multiple stakeholders. As such, in many cases the overall cost of the adaptation can then be shared. The challenges with regional adaptations typically involve coordination,

communication, and agreement between various stakeholders, all of whom may have different agendas or needs for protection. However, if these challenges can be overcome, regional adaptations usually provide the most cost-effective resiliency option, while also providing ancillary benefits beyond just protection of an individual structure. For example, while a local adaptation may reduce flooding of a structure itself, a regional solution may also maintain access to the structure by protection of the surrounding area and transportation services.

In order to assess potential viable regional adaptations, the flood risk maps (as presented in Chapter 4) were evaluated for each climate change scenario to identify key flood entry points and flood pathways along Boston Harbor. Figure 6-1 illustrates the flood entry point locations that are viable sites for regional adaptations under the 2013 scenario, shown as black circles and arrows indicating the pathway of flooding. While there are other flood entry points and flood pathways that may be viable sites for regional adaptations, only flood pathways that impact MassDOT facilities are evaluated herein. For example, there is a flood entry point that exists in the vicinity of Long Wharf and the Boston Aquarium region that could be a potential viable site for a regional solution; however, since minimal MassDOT facilities are impacted by the flood pathway, it was not identified for a potential regional adaptation as part of this pilot project. Under current (2013) conditions, there were three flood entry points where a potential regional solution was deemed feasible. These included:

- 1) The Sullivan Square area, where a regional flood entry point was identified at the Schrafft's building and parking area. This location, downstream of the Amelia Earhart

Dam on the Mystic River, is prone to potential flooding under current day storm surge conditions through a fairly well confined flood entry point, as shown in Figure 6-1. Sea water that enters through the parking lot propagates upland and is able to inundate a significant spatial area, impacting multiple structures, roadways, and parcels. In the 2030 and 2070 projections (Figures 6-2 and 6-3), the extent of upland flooding increases; however, the flood entry point remains relatively confined to the same location and impacts a large upland area, making this an ideal site for a regional adaptation. Eventually this flood entry point flanks the Charles River Dam from the north.

- 2) The East Boston Greenway located adjacent to Logan International Airport. At this location, flooding initially occurs along a 1,500-2,000 linear foot stretch of the Boston Harbor shoreline, but is subsequently confined to a fairly narrow (approximately 50 foot) flood pathway extending to the northeast and spreading to a larger regional area, including portions of Logan International Airport. While other potential flood pathways develop and add to the flooding of the East Boston area by 2030 and 2070, the East Boston Greenway remains confined to a fairly focused pathway and a regional solution implemented at this location would protect against a wide range of storm events, including the more probable moderate events in future years. There are numerous MassDOT facilities impacted by this flood pathway.

- 3) The third potential flood entry point is the Granite Ave. area located in Milton, MA adjacent to the Neponset River. This area was described in detail in Chapter 4. The flooding enters the MassDOT facility from two clear flood pathways and could be controlled by regional adaptations at the source of the flooding rather than flood proofing the facility itself.

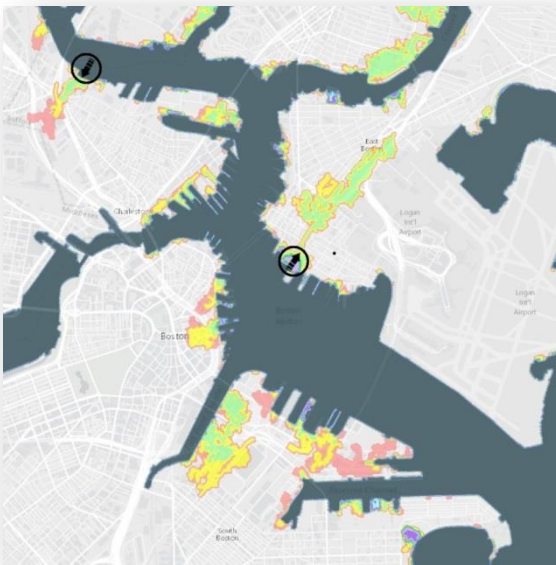


Figure 6-1. Flood entry point locations that are viable sites for regional adaptations under the 2013 scenario (Milton site not shown).

Figure 6-2 illustrates the additional flood entry point locations that are viable sites for regional adaptations under the 2030 scenario, shown as red circles and arrows indicating the pathway of flooding. The previously identified regional adaptation sites are also shown again as the black circles and arrows. By 2030, there is an additional flood entry point that influences the East Boston and Logan International Airport locations. Specifically, a secondary flood pathway exists initiating at the Border Street, Liberty Plaza area (red circle and arrow in Figure 6-2). This flood entry point spans approximately 1,500 to 2,000 feet

along the shoreline and serves as a secondary contributor to the flooding in East Boston. While not as spatially confined as the East Boston Greenway flood pathway, this flood entry point could also be reasonably controlled through implementation of a regional adaptation.

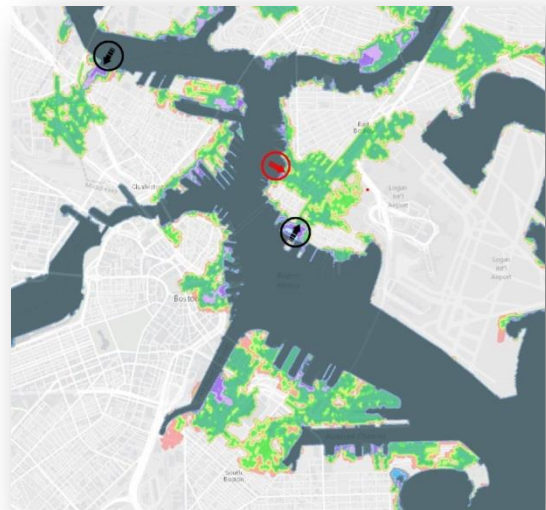


Figure 6-2. Flood entry point locations that are viable sites for regional adaptations under the 2030 scenario.

Figure 6-3 illustrates the additional flood entry point locations that are viable sites for regional adaptations under the 2070 scenario, shown as yellow circles and arrows indicating the pathway of flooding. The previously identified regional adaptation sites are also shown again as the red and black circles and arrows. By 2070, there are a number of additional flood entry points where a potential regional solution was deemed feasible. These included:

- 1) The Charles River Dam (CRD) and adjacent flanked areas. The CRD becomes more probable for overtopping and flanking in 2070/2100 scenarios. This flood entry point impacts the upstream areas of the Charles River, including Cambridge and other areas inundated

- once the Charles River becomes flooded.
- 2) The railroad crossing on the western side of Fort Point Channel. This flood pathway becomes prevalent in the 2070/2100 time frames and represents a narrow entry point that produces flooding over a large urban area, including flooding of major roadways and significant MassDOT facilities.
 - 3) Two additional areas at the Wood Island area and the Jeffries Point area lead to flooding in the East Boston area initially started at the East Boston Greenway. Addressing these combined sites (Jeffries Point, East Boston Greenway, Wood Island, and Border Street) through regional adaptations provides protection for East Boston and Logan International Airport.

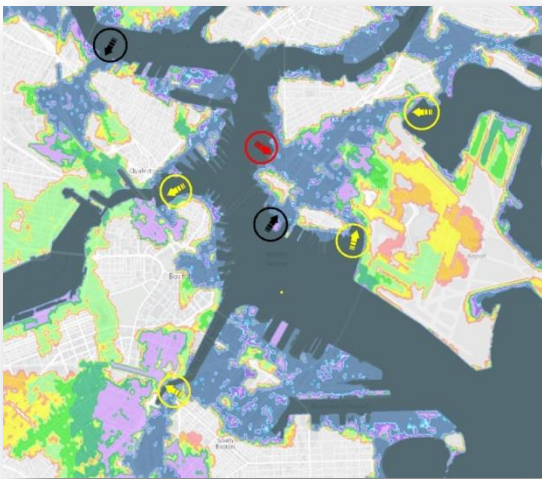


Figure 6-3. Flood entry point locations that are viable sites for regional adaptations under the 2070 scenario.

A summary of the locations identified for regional adaptations are shown in Table 6-3. The table presents an overview of each regional adaptation site, identifies the MassDOT facilities that would be protected by the potential regional adaptation,

summarizes the upland flooding risk, and provides a recommended conceptual engineering adaptation and associated cost (capital and annual maintenance estimates). Recommendations are also presented as a function of time, and recommendations on phased adaptations are included. Proposed recommendations and actions need to be implemented and in place by the date shown. For example, the adaptations shown in 2030 need to be in place by 2030.

Table 6-1. Dimensions, and estimated material and installation costs, for Complexes and Structures listed in Table 5 -2 requiring walls or other specific solutions: except where noted, installation of all walls or other solutions recommended in the period either just after 2030 to 2070 under a higher SLR scenario, or just after 2030 to 2100 under a lower SLR scenario






Note: n/a = not applicable

Structure_ID	Estimated Wall Length (ft)	Estimated Cost (\$Million)	Notes
D6A-DC03	1500	5.3	Wall around Complex also protects D6-ES10-FAC, D6-SMF-FAC, D6A-D3 and yards around them.
D6D-DC01	1400	4.9	Wall around Complex also protects D6D-D1-A, D6D-D1-B, D6D-D1-C, D6D-D1-D and D6D-D1, yards around them, but not entire parking lot.
HOC-D6	1640	5.7	Wall around Complex also protects D6-HOC-FAC, D6-ES02-FAC, D6-SW04-FAC (wall protects surface vent only, also needs watertight door, see note below).
D6-SW04-FAC	n/a	n/a	Needs watertight door , upstream of BIN7J8-POR; installation recommended by 2013
D6-FCB-FAC	49	0.2	
D6-SW07-FAC	279	1.0	
D6-SW09-FAC	197	0.7	
D6-SW16-FAC	39	0.1	
D6-SW25-FAC	n/a	n/a	Needs watertight door , upstream of BIN7GA-POR.
D6-SW17-FAC	66	0.2	
D6-SW27-FAC	n/a	n/a	Needs watertight door , upstream of BIN7C01-POR.
D6A-DC01	2116	7.4	Wall around Complex also protects D6-CMF-FAC, D6A-D1, MHRML and yards around them.
D6-HQC	1739	6.1	Wall around Complex also protects D6-185K-FAC, parking area north of I-90/I-93 interchange Boat Sections and adjacent electric power plant owned by others.
TB03-D6	n/a	n/a	Structures ERS07 and D6-TB03-FAC are protected by walls around buildings only; vehicles in this Complex to be relocated.
D6-TB03-FAC	381	1.3	See note above re: TB03-D6 Complex
ERS07	190	0.7	See note above re: TB03-D6 Complex
TA03-D6	787	2.8	Wall around Complex also protects D6-TA03-FAC and parking lot.
D6-VB11-FAC	328	1.1	
D6-VB12-FAC	328	1.1	
D6-VB13-FAC	328	1.1	
D6-VB6-FAC	951	3.3	Wall around this Structure also protects TE061E and TE061W
D6-VB8-FAC	410	1.4	
LP-UNK	49	0.2	
MBTAAQ	328	1.1	Wall around this Structure also protects TE434
TE161	105	0.4	
TE173	n/a	n/a	Inside (downstream) of BIN62B-POR, so protected if Portal protected
TE183	75	0.3	
TE425	75	0.3	
CP534	n/a	n/a	Needs watertight door , upstream of BIN7UG-POR, installation recommended by 2030 .

Table 6-2. Number of lanes and dimensions, and material and installation costs, for the Portals requiring gates in listed Table 5 -3: “2013” indicates installation recommended now, “<2030” indicates installation recommended during the period from the just past the present to 2030, “<2070 or <2100” indicates installation recommended over the period just past 2030 to 2070 under a higher SLR scenario, or over the period just past 2030 to 2100 under a lower SLR scenario.

Portal Locations	No. of Lanes	Est. Total Width (feet)	Year Installed	Gate Material (\$Million)	Installation (\$Million)	Total Cost (\$Million)
BIN5VA	2	38	2013	1.7	1.1	2.8
BIN7J8/7J9/7JD/7JE/7JF/7RX (also need watertight door for D6-SW04-FAC)	4,2,1, 2,2,1	308	2013	14.9	9.7	24.6
BINA07	2	29	≤2030	1.5	1.0	2.5
BINC00	2	28	≤2030	1.5	1.0	2.5
BIN7UG/BIN7MD/BIN7GC	2,4,5	181	≤2030	8.7	5.7	14.4
BIN5UR	2	35	≤2070 or ≤2100	1.5	1.0	2.5
BIN5VQ	2	37	≤2070 or ≤2100	1.7	1.1	2.8
BIN59Y	2	52	≤2070 or ≤2100	2.6	1.7	4.3
BIN5K2	2	52	≤2070 or ≤2100	2.6	1.7	4.3
BIN59K	2	40	≤2070 or ≤2100	2	1.3	3.3
BIN5AF	2	33	≤2070 or ≤2100	1.5	1.0	2.5
BIN5JR	1	44	≤2070 or ≤2100	2.3	1.5	3.8
BIN62B	2	42	≤2070 or ≤2100	2.2	1.4	3.6
BIN6HD	1	31	≤2070 or ≤2100	1.4	0.9	2.3
BIN7B9	2	50	≤2070 or ≤2100	2.6	1.7	4.3
BIN7T8	1	33	≤2070 or ≤2100	1.5	1.0	2.5
BIN7BC	2	39	≤2070 or ≤2100	2	1.3	3.3
BIN7BB	2	56	≤2070 or ≤2100	2.8	1.8	4.6
BIN7BL(floods via BI7BM)	1	40	≤2070 or ≤2100	2.1	1.4	3.5
BIN7DE/7D5/7DX/7BN	1,2,2,1	198	≤2070 or ≤2100	9.8	6.4	16.2
BIN7HV	3	60	≤2070 or ≤2100	3	2.0	5.0
BIN9P8	4	61	≤2070 or ≤2100	3	2.0	5.0
BINC01	2	38	≤2070 or ≤2100	2	1.3	3.3
BIN7EK/7E7/7F6/7FQ/7FN	1,2,1, 2,1	196	≤2070 or ≤2100	9.1	5.9	15.0
BIN7GA/7FX/7FL	2,1,2	124	≤2070 or ≤2100	6.3	4.1	10.4
BINC01/7EC/7ED	2,2,1	106	≤2070 or ≤2100	5	3.3	8.3
BIN9BU/9BV/9BW/9CT/9CU	2,2,2, 1,2	248	≤2070 or ≤2100	12.4	8.1	20.5
BINLT1	1	47	≤2070 or ≤2100	2.3	1.5	3.8
BINCT1	2	49	≤2070 or ≤2100	2.6	1.7	4.3
BINTC1	2	46	≤2070 or ≤2100	2.6	1.7	4.3
BINSS1	2	36	≤2070 or ≤2100	1.5	1.0	2.5
BINSS3	2	37	≤2070 or ≤2100	1.5	1.0	2.5

Table 6-3. A summary of the locations identified for regional adaptations.

Regional Adaptation Planning	Regional Flood Entry Points														
	Sullivan Square			East Boston Greenway / Border Street / Wood Island / Jefferies Point			Granite Avenue			Fort Point Channel			Charles River Dam		
General Description	The regional flood entry point in the vicinity of Sullivan Square is located at the Schrafft's building and parking area, shown below. This location, downstream of the Amelia Earhart Dam on the Mystic River, is prone to potential flooding under current day storm surge conditions through a fairly well confined flood entry point, as shown in the 2013 Flood Probability results. Sea water that enters through the parking lot propagates upland and is able to inundate a significant spatial area, impacting multiple structures, roadways, and parcels. In the 2030 and 2070 (eventually flanking the Charles River Dam) projections, the extent of upland flooding increases; however, the flood entry point remains relatively confined to the same location, making this an ideal site for a regional adaptation.			This regional flood entry point is located at the East Boston Greenway adjacent to Logan International Airport. At this location, flooding initially occurs along a 1,500-2,000 linear foot stretch of the Boston Harbor shoreline, but is subsequently confined to a fairly narrow (approximately 50 foot) flood pathway (the Greenway) extending to the northeast and spreading to a larger regional area, including portions of Logan International Airport. While other potential flood pathways develop to add to the flooding of the East Boston area by 2030 and 2070, the East Boston Greenway remains confined to a fairly focused pathway and a regional solution implemented at this location would cover a wide range of storm events, including covering the more probable moderate events in future years. In 2030, flooding expands via a secondary flood pathway exists initiating at the Border Street, Liberty Plaza area that spans approximately 1,500 to 2,000 feet. In 2070, flood entry points at the Wood Island area and the Jefferies Point area that contribute to the overall flooding risk initially started at the East Boston Greenway.			The location consists of two distinct flood entry points that flood a large MassDOT parcel, but also flood local neighborhoods and roadways. The flood pathways occur on both sides of the MassDOT parcel. At this location, there is a viable threat of flooding even under current day conditions, and that threat is expanded in frequency, magnitude, and extent of flooding in the future.			This location is at the far upstream end of the Fort Point Channel. There is a railroad crossing on the western side of Fort Point Channel that resides at a lower elevation than the surrounding wall bordering the channel. This flood pathway becomes prevalent in the 2070 and 2100 time frames and represents a narrow flood entry point that produces flooding over a large urban area, including major roadways and significant MassDOT facilities.			The Charles River Dam and adjacent local flanked areas represent another regional flood pathway that impacts significant MassDOT facilities. This flood pathway occurs with dam overtopping and flanking in 2070 and 2100 scenarios. This flood entry point impacts the upstream areas of the Charles River, including Cambridge.		
Site Overview at Flood Entry Point and Flood Pathway (Black Arrows)															
MassDOT Facilities Protected by Potential Regional Adaptation	Complex D6A-DC03 and all associated Structures, D6-ESS3-FAC, D6-SW18-FAC, BINt1-POR, BINt11-POR, BIN-t1-POR			BIN9BW-POR, BIN9BV-POR, BINmL2-POR, BIN9CU-POR, BIN9CT-POR, BINA07-POR, BINCO0-POR, D6-TA03-FAC, D6-TB03-FAC, ERS07, D6-VB13-FAC, D6-VB11-FAC, TA03-D6, SW06			D6D-DC01, D6D-D1, D6D-D1-B, D6D-D1-A, D6D-D1-C, and D6D-D1-D			D6-FCB-FAC, D6-HQC, D6-185K-FAC, D6-SW07-FAC, D6-SW09-FAC, TE173, TE183, TE310, TE201, V999, BIN62B-POR, BIN7BN-POR, BIN7D5-POR, BIN7DE-POR, BIN7DFPOR, BIN7DX-POR, BIN7HV-POR, BINco1-POR, BIN6HD-POR & BIN9P8-POR			D6-SW17-FAC, D6-LP09-FAC, D6-SW02-FAC, D6-VB8-FAC, TE601, TE605, TE606, TE609, TE611 & TE617, BIN7UG-POR, BIN7MG-POR, BIN7GC-POR, BIN5JR-POR, BIN59Y-POR, BIN59KPOR, BIN5K2-POR, BINss3-POR, Blss1 & B15AF-POR, TE526, BIN7E7-POR, BIN7EK-POR, BIN7F6-POR, BIN7FQ-POR, BIN7FN-POR		
Adaptation Concepts	Upland Flooding Potential	Recommended Engineering Adaptations	Estimated Adaptation Cost*	Upland Flooding Potential	Recommended Engineering Adaptations	Estimated Adaptation Cost*	Upland Flooding Potential	Recommended Engineering Adaptations	Estimated Adaptation Cost*	Upland Flooding Potential	Recommended Engineering Adaptations	Estimated Adaptation Cost*	Upland Flooding Potential	Recommended Engineering Adaptations	Estimated Adaptation Cost*
2013	Flood probabilities reach 1-2% for potential flood entry into this region. Depths of 1-1.5 feet maximum in flooded areas.	Modular Seawall installation fronting the Schrafft's parking area. The solution could also be integrated with closable doors and/or elevated walkways to provide access to the shoreline. Boat ramp would be closed.	Capital Cost: \$3.0-3.5 million (1,000 foot length) Annual Maintenance Costs: \$15,000	Flood probabilities reach 10% along the shoreline, with 1% risk of flooding advancing down the Greenway. Depths of 1.5 feet maximum in flooded areas down the Greenway.	Redevelopment of shoreline at the Greenway, including mix of gray and green resiliency design of shoreline fronting the Greenway, and elevated entry way to the greenway from the coastline.	Broad range of costs depending on conceptual solution developed. Detailed cost to be developed in next phases of design.	Flood probabilities reach 10% at the southern parking lot, with 2% risk at the existing building structures. Depths of a maximum of 0.5 - 1 feet	Increased elevation through use of natural berms at both flood pathway locations.	Capital Cost: \$1.0-1.5 million Annual Maintenance Costs: \$30,000	No Flooding Expected	No Action Required	N/A	No Flooding Expected	No Action Required	N/A
2030 (High Sea Level Rise Projection)	Flood probabilities reach 20-25% for potential flood entry into this region. Depths of 2.5-3 feet maximum in flooded areas.	No modification required to 2013 solution	N/A	Flood probabilities reach 25% along the shoreline, with 2-5% risk of flooding advancing down the Greenway. A secondary flood entry point develops near Border Street. Depths of 2.5-3 feet maximum in flooded areas down the Greenway.	In addition to above: - Improved revetment and enhanced bioengineered berm along the shoreline in vicinity of Liberty Plaza and Border St. A mix of gray and green resiliency design.	Broad range of costs depending on conceptual solution developed. Detailed cost to be developed in next phases of design.	Flood probabilities reach 50% at the southern parking lot, with 10-20% risk at the existing building structures. Depths of a maximum of 1.5-2.0 feet.	No modification required to 2013 solution	N/A	No Flooding Expected	No Action Required	N/A	No Flooding Expected	No Action Required	N/A
2070 (High Sea Level Rise Projection)	Flood probabilities reach 50% (2-year return period water level) for potential flood entry into this region. Depths of 5-10 feet maximum in flooded areas.	Phased increases in elevation and length of seawall	Capital Cost: \$10.0-12.0 million (3,500 ft additional length) Annual Maintenance Costs: \$25,000	Flood probabilities reach 50% throughout the area, with depths reaching maximums of 10 feet. Two additional flood pathways develop at Wood Island and Jefferies Point.	In addition to above: - Marsh restoration and natural shoreline enhancement at Wood Island entry way. - Enhancement of Massport Harbor Walk along the Jefferies point region with seawall	Broad range of costs depending on conceptual solution developed. Detailed cost to be developed in next phases of design.	Flood probabilities reach 50% throughout the area, with depths reaching maximums of 5 feet.	Compliment natural berms with targeted walls in locations to reduce flood risk.	Capital Cost: \$5.0-7.0 million Annual Maintenance Costs: \$15,000	Flood probabilities reach 10% for potential flood entry into this region. Depths of 3-4 feet maximum in flooded areas.	Increased elevation to existing Fort Point Channel wall and design of a removable flood barrier at RR crossing	Capital Cost: \$5-6 million Annual Maintenance Costs: N/A	Flood probabilities reach 10% for potential flood entry into this region. Depths of 3 flanking the dam on the south side.	Potential adaptations involve raising the dam, and designing systems to reduce potential flanking of the dam on the south side. Solutions related to the Sullivan Square flood pathway must also be included.	These costs would need to be developed based on site specific engineering development.

* = Initial Capital Costs and Operational and Maintenance costs provided are rough estimates based on costs from similar types of projects. More detailed and accurate costs would be required for actual engineering and construction. Estimated costs are based on 2015 dollar value.

- Depends on length of seawall installed.

CONCLUSIONS AND LESSONS LEARNED

7.1 Conclusions

We have successfully carried out a pilot project involving:

- Inventorying of a large amount of CA/T related data – often relying upon Institutional Knowledge and field work to understand complexities not evident in available data sources;
- Assessing MassDOT’s preferences for flood management;
- Applying a state-of-the-art hydrodynamic model which includes the impacts of extratropical as well as tropical storms, freshwater inflows and flood-control dam operations, and uses a Monte Carlo simulation approach to determine flood depths and their probabilities under current and future sea level rise scenarios;
- Processing a very large set of flood model output results to produce both visual and tabular summary information essential for analyzing and interpreting the results so that decision-makers can understand the vulnerability of the CA/T system; and
- Developing a conservative adaptation strategy that allows for staging adaptation actions over time in a flexible manner to account for sea level rise and future storm uncertainties.

Although even in 2030 no non-boat section CA/T structure exceeds its critical depth threshold of 2 feet and may be able to be protected with temporary barriers, a critical elevation of 0.5 feet at boat sections with portals is already exceeded presently.

The end result of this process was that none of the flood depths around the non-Boat-Section CA/T Structures under present conditions (circa 2013), or in the period from just-past-the-present to 2030, exceed the critical depth threshold of 2 feet at the flood exceedance probability of 1% even as the flood depths increase over time due to SLR (with the exception of the few watertight doors noted in Table 6.1.). Therefore, given the uncertainties and limitation of our analysis, it is likely that relatively self-supporting temporary barriers will be sufficient to manage flooding up to at least 2030 at non-Boat-Section CA/T Structures. By 2070 or 2100 depending on SLR however, approximately 30 non-boat section structures will need protection with flood walls under a local adaptation strategy. In addition, under a local adaptation strategy, seven portals require gates now and the number grows to a total of over 50 by 2070 or 2100 depending upon SLR.

Regional adaptation solutions were also explored. Whereas local adaptation options focus on protecting individual structures, regional adaptation focuses on flood pathways, where a larger upland area is flooded by water arriving from a vulnerable section of the coastline. Regional solutions can be more cost effective than local adaptation solutions but often require coordination between and investment by multiple stakeholders. Three flood pathways that could be addressed by regional solutions were identified under current (2013) climate conditions: near the Schrafft’s building in Charlestown, the East Boston Greenway and the MassDOT property on Granite Ave., in Milton. An additional flood pathway (near Liberty Plaza in East Boston) was identified under near term future conditions (by 2030). In

addition to those already mentioned, a number of additional flood pathways were identified under late 21st century conditions (2070 or 2100), including Wood Island and Jefferies Point in East Boston, the western side of Fort Point Channel and adjacent to the Charles River dam. Conceptual engineering strategies and cost estimates were presented.

This pilot project has illustrated that it is valuable and feasible to combine a state-of-the-art hydrodynamic flood model with agency-driven knowledge and priorities to assess vulnerabilities and develop adaptation strategies. From an infrastructure maintenance and planning perspective, this vulnerability assessment offers both good news and bad. The good news is that the extent of flooding under current climatic conditions is fairly limited with low exceedance probabilities. This allows MassDOT to focus their efforts on reducing the vulnerability of individual Structures and on local adaptation strategies. The bad news is that 1) vulnerable Structures under current conditions include some Tunnel Portals and 2) the vulnerability and number of Portals affected triples by 2030. By late 21st century (2070 or 2100, depending on actual rate of SLR), there is considerable flooding at non-boat sections and the number of vulnerable Portals more than doubles again.

7.2 Additional Notable Project Findings

- The interconnected and complex nature of urban environments spans multiple stakeholders. For example, although we were focused on the CA/T system, its vulnerabilities in some cases were tied to other systems (e.g., the MBTA subway at Aquarium Station, the operation of the Charles River Dam). Therefore, interaction with multiple stakeholders was required at various steps in the assessment.

- Initially, we expected results of the study to be useful sometime in the future (i.e., actions that would need to be taken to provide improved flood mitigation and resiliency in the future for existing MassDOT Structures and Assets). However, results of the modeling and vulnerability assessment yielded almost immediate project and engineering design implications (e.g., development of the maintenance facility at the Granite Ave. Site as noted in Sec 4.10) that may not have been realized without the high-resolution modeling and analysis.
- The lack of redundancy in the CA/T system, and the critical nature of each system component, make the system extremely vulnerable.
- In complex systems like the CA/T, the number and spatial extent of vulnerable Structures increase over time as SLR increases and the intensity of some storms increase, suggesting that local adaptation options may be most applicable in the near-term and regionally based adaptations (safeguarding multiple Structures for multiple stakeholders) will become more cost-effective and necessary solutions in the long-term.
- Because Tunnel Egresses and Stormwater Outfalls are vulnerable to coastal flooding, it is recommended that they are added to Maximo as Facilities. Additionally, based on observations during field visits performed during this study, it is also recommended that all Tunnel Egresses are inspected regularly and maintained to allow for safe egress during emergencies.

7.3 Lessons Learned

This pilot project has illustrated the application of a complex modeling and analysis process for planning coastal flood

adaptations of a tunnel system in a congested metropolitan area and has resulted in two alternative adaptation strategies. This pilot project has also provided valuable lessons in carrying out a project as challenging as this. The lessons learned from the implementation of this pilot project can be categorized as: Project Scoping; Data Inventory; Hydrodynamic Modeling; Vulnerability Assessment and Adaptation Planning; and Interactions with MassDOT, regional stakeholders, and the Technical Advisory Committee.

7.3.1 Scoping

This was an exceedingly complex project because of the data requirements and availability, and the novelty of some the flood modeling applications. The Project Team's scoping underestimated these complexities with the result that the project did not achieve its full potential within the required timeframe. The scoping could have been improved by greater involvement in the scoping process by MassDOT engineering, operations, maintenance, and information technology staff as well as the modeling team. The CA/T system encompasses so many requirements to function, no one department can fully represent them.

The existing data for the system were extensive, but were not in compatible formats. The format of its data and the contents should have been reviewed beforehand to more fully inform the scoping process.

Reflecting upon the challenges, we would have requested a greater amount of time to carry out such a highly technical project that has proven to be both valuable and transferrable to other geographic areas.

7.3.2 Data Inventory

In the original scope, we envisioned that there would be approximately 40 Structures

to evaluate. By the end this pilot project, we had inventoried information on many hundreds of Structures and Facilities and ultimately limited our assessment to the more than 200 Structures prioritized by MassDOT personnel. To date, there remains some missing and incomplete information on Structures such as Tunnel Egresses and Stormwater Outfalls. The delays this incomplete information caused could have been avoided by a data review and tour of the CA/T before the project scoping.

In the early phases of the project, when we were collecting field data on Structures, we assumed that we would need site-specific information on the sensitivity of each Structure to flooding. This resulted in us spending some unnecessary time visiting many Structures and collecting information such as elevations of doors, windows and other openings, that later turned out to be unnecessary. Had the sensitivity of Structures to flooding been discussed beforehand (ie, any level of flooding is harmful), this could have been avoided.

The use of GIS was essential to the success of this project. There were, however, many challenges that needed to be overcome before proceeding, which substantially delayed the project. Again, if these had been known during the scoping phases, some problems could have been avoided. These challenges included:

- MassDOT GIS datalayers were promised and delivered but were not compatible with vulnerability assessment requirements;
- Existing GIS data focused on roadways and state-wide planning, both of which were outside of the scope of this pilot project;
- The data that were made available for Facility and Assets were not

compatible with the scale of our pilot project;

- Conversion of MassDOT data from CAD format to GIS format was an arduous and time consuming process;
- Development of the GIS geodatabase was an enormous effort because of the complexity and interconnectedness of the CA/T system; and
- Experienced GIS staff are critical to efficient development of a spatial database representing a system of this complexity.

Some activities which we had not originally envisioned as necessary turned out to be critical to project success. Examples include:

- Interaction with Institutional Knowledge staff not only resulted in vastly improved data discovery but also resulted in their interest and support of the project.
- Persistence in tracking down disparate data sources resulted in the discovery of several CA/T standard databases unknown to us prior to project scoping. Knowledge of these databases resulted in our eventual use of unique identifiers consistent with MassDOT databases to support the interaction of our CA/T geodatabase with a MassDOT database (Maximo).
- Field observations and ground-truthing played a larger role than we envisioned – even after it was no longer necessary to assess the sensitivity of each Structure. We ended up visiting and photographing the majority of known Structures. This information turned out to be essential in assessing vulnerability and adaptation because local conditions are important and cannot always be captured in digital

data. The field work validated the database in some cases and also resulted in finding and/or identifying new Structures not part of other MassDOT databases.

7.3.3 Hydrodynamic Modeling

Even though the physically-based modeling effort is data, time and resource intensive, there are enough tangible differences between high-resolution model output and other first-order vulnerability assessments (e.g., bathtub modeling) that it is worthwhile. In heavily populated areas with critical transportation infrastructure such as the CA/T, high-resolution hydrodynamic modeling is warranted due to the importance of transportation and human impacts, as well as the spatial complexity of terrain and bathymetry. In less populated areas, it could be coupled with less intensive modeling efforts (i.e., using the high-resolution model results on the coastline and using bathtub or similar modeling over the upland) to obtain adequate results for planning purposes.

Significant, and much greater than anticipated, computational power was needed for the Monte Carlo simulation approach. We underestimated this requirement and were fortunate to be able to eventually use a set of parallel processing computers through the UMass system. By doing so, we effectively halved the amount of time needed to complete the modeling.

7.3.4 Vulnerability Assessment and Adaptation Planning

Accomplishing this required the outputs from many previous steps. By doing a smaller “mini” pilot project within this project, we were able to test out procedures and revise preceding steps as necessary before proceeding to assessing the entire domain. The “mini-pilot” approach also allowed us to interact with MassDOT

personnel to ensure the applicability of our results.

7.3.5 Interaction with MassDOT, regional stakeholders, and Technical Advisory Committee.

The MassDOT and Technical Teams members met weekly by teleconference and met regularly in person as well. This resulted in a good understanding of project requirements, challenges, and outputs on both sides and led to the resolution of problems earlier than would have occurred without the good communication and trust that was present. The project team worked well together as each developed respect for the others complementary strengths.

The project team had the right skills and resources to do this project. However, while deadlines are necessary, some more flexibility in FHWA deadlines would have been useful to adjust for unknown complexities. At times, the project team was entering uncharted territory and therefore needed to have time and flexibility to accommodate discovery and unanticipated complications. This is often the case with research funded by other federal agencies; perhaps FHWA should

consider an approach that allows for a “no cost extension” (common with NASA, NOAA and NSF funded research), which gives extra time to complete projects but does not require additional funding. Having said that, though, we do appreciate FHWA partially funding this project. The FHWA webinars and project updates were also found to be useful.

Having an outside Technical Advisory Committee worked well because they provided a positive environment where we could seek input on difficult scientific issues.

7.4 Continuing Work

The results of this vulnerability assessment will support an evaluation and updating of the emergency response procedures for the CA/T.

And finally, to accommodate both changes in the coastline and improvements in our understanding of climate change and its impacts, we recommend that the hydrodynamic model be updated and re-run and that the vulnerability assessment and adaptation strategies be revisited every seven to ten years.

REFERENCES

- ADCIRC. 2013. <http://adcirc.org/>
- Aerts, J., W. Botzen, H. de Moel, M. Bowman. 2013. Cost Estimates for Flood Resilience and Protection Strategies in New York City, *Annals of NY Academy of Science* 1294, 2013.
- Bengtsson, Lennart and Kevin I. Hodges. 2006. Storm Tracks and Climate Change. *Journal of Climate* Volume 19. American Meteorological Society. August, 2006. P. 3518-3543
- Blumberg, Alan F. and George L. Mellor. 1987. A Description of a Three-Dimensional Coastal Ocean Circulation Model.
- Bunya, S., J.C. Dietrich, J.J. Westerink, B.A. Ebersole, J.M. Smith, J.H. Atkinson, R. Jensen, D.T. Resio, R.A. Luettich, C. Dawson, V.J. Cardone, A.T. Cox, M.D. Powell, H.J. Westerink, and H.J. Roberts. 2009. A High-Resolution Coupled Riverine Flow, Tide, Wind, Wind Wave and Storm Surge Model for Southern Louisiana and Mississippi: Part I – Model Development and Validation.
- Catto, Jennifer L., Len C. Shaffrey, and Kevin I. Hodges. 2011. Northern Hemisphere Extratropical Cyclones in a Warming Climate in the HiGEM High-Resolution Climate Model. *Journal of Climate* Volume 24. American Meteorological Society. 15 October, 2011. P5336 – 5352.
- Chen, Changsheng, Robert C. Beardsley, Geoffrey Cowles, Jianhua Qi, Zhiqiang Lai, Guoping Gao, David Stuebe, Qichun Xu, Pengfei Xue, Jianzhong Ge, Rubao Ji, Song Hu, Rucheng Tian, Haosheng Huang, Lunyu Wu and Huichan Lin. 2011. An Unstructured Grid, Finite-Volume Coastal Ocean Model. FVCOM User Manual.
- Cudworth, A.G. Jr. 1989. Flood Hydrology Manual. A Water Resources Technical Publication, U.S. Department of Interior, Bureau of Reclamation, Denver, Colorado, 243 pp.
- ECMWF. 2014. ECMWF Downloadable Dataset. Accessed on August 5, 2014. Available from: <http://apps.ecmwf.int/datasets/>.
- Ehret, Todd. 2014. Personal communication with Eric Holmes of Woods Hole Group on Wednesday July 9, 2014. Archived in Email.
- Emanuel, Kerry. 2005. [Increasing destructiveness of tropical cyclones over the past 30 years.](#) *Nature*, 436, 686-688. [Online supplement to this paper.](#)
- Emanuel, K., S. A. Ravela, E. A. Vivant and C.A. Risi. 2006. A Statistical-Deterministic Approach to Hurricane Risk Assessment. *Bull. Amer. Meteor. Soc.*, 87, 299-314.
- FEMA. 2012. Joint Probability –Optimal Sampling Method for Tropical Storm Surge Frequency Analysis. FEMA Operating Guidance No. 8-12
- FEMA. 2013. Floodproofing Non-Residential Buildings, FEMA P-936, July 2013
- FHWA. 2012. Climate Change & Extreme Weather Vulnerability Assessment Framework, U.S. Department of Transportation, Federal Highway Administration (FHWA) Publication No: FHWA-HEP-13-005, available on-line at

- http://www.fhwa.dot.gov/environment/climate_change/adaptation/publications_and_tools/vulnerability_assessment_framework/fhwahep13005.pdf, accessed on Jan 15, 2015.
- Gadoury, R.A. 1979. Coastal Flood of February 7, 1978, in Maine, Massachusetts, and New Hampshire. U.S. Geological Survey Water – Resources Investigations 79-61.
- Horsburgh, K. J., and C. Wilson. 2007. Tide-surge interaction and its role in the distribution of surge residuals in the North Sea, *J. Geophys. Res.*, 112, C08003, doi:10.1029/2006JC004033
- Horton, B. P., S. Rahmstorf, S. E. Engelhardt, and A. C. Kemp. 2014. Expert assessment of sea-level rise by AD 2100 and AD 2300, *Quaternary Science Reviews*, 84 (15): 1-6.
- IPCC. 2007. *Climate Change 2007: The Physical Science Basis. Contribution of Working Group I to the Fourth Assessment Report of the Intergovernmental Panel on Climate Change* [Solomon, S., D. Qin, M. Manning, Z. Chen, M. Marquis, K.B. Averyt, M. Tignor and H.L. Miller (eds.)]. Cambridge University Press, Cambridge, United Kingdom and New York, NY, USA.
- Kemp, A. C., B. P. Horton, J. P. Donnelly, M. E. Mann, M. Vermeer and S. Rahmstorf. 2011. Climate related sea-level variations over the past two millennia, *PNAS*, 108 (27): 11017–11022.
- Kinnmark, IP.E. 1984. *The Shallow Water Wave Equations: Formulation, Analysis and Application*, Ph.D. Dissertation, Department of Civil Engineering, Princeton University, NJ.
- Kirshen, P., C. Watson, E. Douglas, A. Gontz, J. Lee, and Y. Tian. 2008. Coastal Flooding in the Northeastern USA under High and Low GHG Emission Scenarios, *Mitigation and Adaptation Strategies for Global Change*, 13:437–451.
- Kirshen, P., L. Caputo, R. Vogel, P. Mathisen, A. Rosner, and R. Renaud. 2014. Adapting Urban Infrastructure to Climate Change: A Drainage Case Study, *Journal of Water Resources Planning and Management*, online publication date 21 July 2014.
- Kopp, R. 2014. Uncertainties and Risks of Regional Sea-Level Change: Past, Present, and Future, presentation to Environmental Research Group, UNH, March 2014.
- Le Mehaute, B. 1976. *An Introduction to Hydrodynamics and Water Waves* (Springer-Verlag, New York, NY).
- Luetlich, R.A., Jr. J.J. Westerink, and N.W. Scheffner. 1992. ADCIRC: An Advanced Three-Dimensional Circulation Model for Shelves, Coasts, and Estuaries. Technical Report DRP-92-6, U.S. Army Engineer Research and Development Center, Vicksburg, MS.
- Luetlich, Rick and Joannes Westerink. 2012. A Parallel Advanced CIRCulation Model for Oceanic, COASTAL, and Estuarine Waters.
- MassDOT. 2013. Scope of Work for the Implementation of an Asset and Maintenance Management System Contract # 66846
- Meehl G.A., T.F. Stocker, W.D. Collins, P. Friedlingstein, et al. 2007. Global climate projections. In: Solomon S, Qin D, Manning M, Chen Z and others (eds) *Climate change*

- 2007: the physical science basis. Contribution of Working Group I to the Fourth Assessment Report of the Intergovernmental Panel on Climate Change. Cambridge University Press, Cambridge, p 749–844.
- MWH Global. 2014. Charles River Discharge Data.
- Myers, Vance A. and William Malkin. 1961. National Hurricane Research Project Report No. 49: Some Properties of Hurricane Wind Fields as Deduced from Trajectories. U.S. Department of Commerce, U.S. Weather Bureau, Hydrometeorological Section, Hydrologic Services Division. Washington, D.C.
- Nicholls, R., S. Hanson, J. Lowe, R. Warrick, X. Lu, and A. Long. 2014. Sea-Level Scenarios for Evaluating Coastal Impacts, WIREs Clim Change, 5, doi:10.1002/wcc.253.
- NOAA. 2014a. NOAA Tides & Currents 8443970 Boston, MA. Accessed on August 5, 2014. Available from: <http://tidesandcurrents.noaa.gov/stationhome.html?id=8443970>
- NOAA. 2014b. Mean Sea Level Trend 8443970 Boston, Massachusetts. Accessed on August, 13, 2014. Available from: http://tidesandcurrents.noaa.gov/sltrends/sltrends_station.shtml?stnid=8443970
- NOAA. 2014c. National Weather Service: National Hurricane Center – Glossary of NHC Terms. Accessed September 12, 2014. Available from: <http://www.nhc.noaa.gov/aboutgloss.shtml#EXTRA>.
- Parker, B. B.(ed). 1991. Tidal Hydrodynamics, 883 pp., John Wiley & Sons, Inc., New York.
- Parris, A., P. Bromirski, V. Burkett, D. Cayan, M. Culver, J. Hall, R. Horton, K. Knuuti, R. Moss, J. Obeysekera, A. Sallenger, and J. Weiss. 2012. Global Sea Level Rise Scenarios for the US National Climate Assessment. NOAA Tech Memo OAR CPO-1. 37 pp.available online December 2012: http://cpo.noaa.gov/sites/cpo/Reports/2012/NOAA_SLR_r3.pdf.
- Prandle, D., and J. Wolf. 1978. The interaction of surge and tide in the North Sea and River Thames, Geophys. J. R. Astron. Soc., 55, 203 – 216.
- Pugh, D. T. 1996. Tides, Surges and Mean Sea-Level, 472 pp., John Wiley, Hoboken, N. J.
- Rudeva, I.A. 2004. On the Relationship of the Number of Extratropical Cyclones to Their Sizes. Atmospheric and Oceanic Physics, 2008. Vol. 44, No. 3. P 273-278.
- Sparks, Jerry W. 2011. Evaluation of Analytical Techniques for Production of a Sea Level Rise Advisory Mapping Layer for the NFIP.
- Stedinger, J.R., R.M. Vogel and E. Foufoula-Georgiou. 1993. Frequency Analysis of Extreme Events, Chapter 18, *Handbook of Hydrology*, M^cGraw-Hill Book Company, David R. Maidment, Editor-in-Chief, 1993.
- Stone & Webster. 1978. Development and Verification of a Synthetic Nor'easter Model for Coastal Flood Analysis. Prepared for Federal Insurance Administration Department of Housing and Urban Development. Stone & Webster Engineering Corporation. Boston, Massachusetts.
- URS. 2006a. HMTAP Task Order 18, Mississippi Coastal Analysis Project, Geospatial Technology Task Report (Task 3).

- U.S. Army Corps of Engineers. 2011. Sea-Level Change Considerations for Civil Works Programs; Department of the Army EC 1165-2-212, CECW-CE Washington, DC 20314-1000, Circular No. 1165-2-212 1 October 2011, EXPIRES 30 September 2013.
- U.S. Army Corps of Engineers. 2015. North Atlantic Coast Comprehensive Study, Main Report, Final Report, January 2015, available on line at:
http://www.nad.usace.army.mil/Portals/40/docs/NACCS/NACCS_main_report.pdf, accessed on January 30, 2015.
- U.S. Army Engineer District, Sacramento, California, Civil Works Investigations Project CW-151, Flood Volume Studies-West Coast. Research Note No. 1, "Frequency of New England Floods," July 1958.
- U.S. Water Resources Council. 1982. Guidelines for determining flood flow frequency, Bull. 17B, Interagency Committee on Water Data, U.S. Geological Survey, Reston, VA 1982.
- VHB. 2014. Mystic River Discharge Data
- Vickery, Peter, Dhiraj Wadhwa, Andrew Cox, Vince Cardone, Jeffrey Hanson, and Brian Blanton. 2013. FEMA Region III Storm Surge Study Coastal Storm Surge Analysis: Storm Forcing Report 3: Intermediate Submission No. 1.3. United States Army Corps of Engineers: Engineer Research and Development Center (ERDC). Accessed from:
<http://acwc.sdp.sirsi.net/client/search/asset/1028322>
- Vogel, R.M. and J.R. Stedinger. 1984. Floodplain Delineation in Ice Jam Prone Regions, *Journal of Water Resources Planning and Management*, 110(2), 206-219.
- Westerink, J.J., K.D. Stolzenbach, and J.J. Connor. 1989. General Spectral Computations of the Nonlinear Shallow Water Tidal Interactions Within the Bight of Abaco, *J. Phys. Oceanog.* 19, 1350-1373.
- Westerink, J.J., R.A. Luetlich, J.C. Feyen, J.H. Atkinson, C. Dawson, H.J. Roberts, M.D. Powell, J.P. Dunion, E.J. Kubatko, and H. Pourtaheri. 2008. A Basin to Channel Scale Unstructured Grid Hurricane Storm Surge Model Applied to Southern Louisiana Monthly Weather Review, 136, 3, 833-864.
- Winkelman, J. Personal communication 1/30/15
- Woods Hole Group, Inc. 2012. Hydrodynamic and Water Quality Modeling at Fort Point Channel, Boston, MA
- Yang, Zizang, Edward P. Myers, Inseong Jeong, and Stephen A. White. 2013. VDatum for the Gulf of Maine: Tidal Datums and the Topography of the Sea Surface.



Appendices

MassDOT-FHWA Pilot Project Report: *Climate Change and Extreme Weather Vulnerability Assessments and Adaptation Options for the Central Artery*

Project Team:

Kirk Bosma, P.E., Woods Hole Group, Inc.

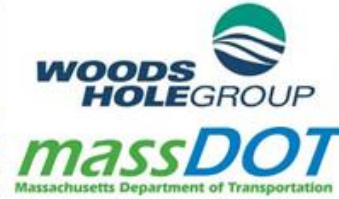
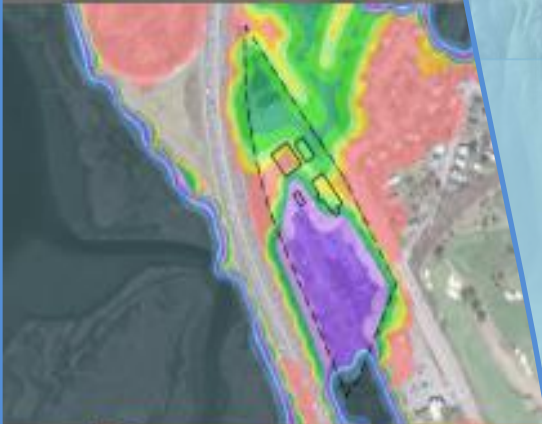
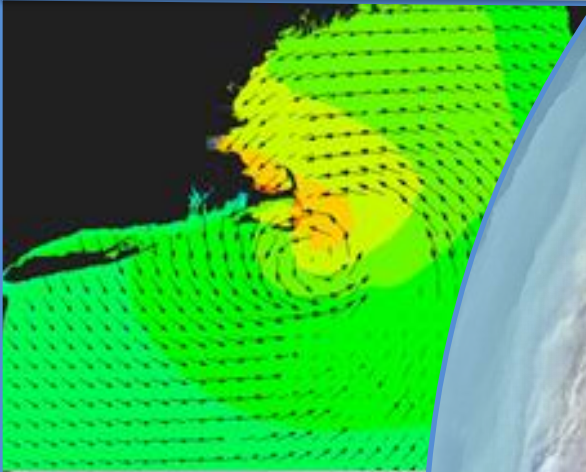
Ellen Douglas, P.E., Ph.D., UMass Boston

Paul Kirshen, Ph.D., University of New Hampshire

Katherin McArthur, MassDOT

Steven Miller, MassDOT

Chris Watson, M.Sc., UMass Boston



Appendix I
Summary of Primary Data Sources provided by MassDOT

GIS Geodatabase

- BostonData.mdb

PDF or Scanned Paper Documents

- CAT_FACIL.PDF
- MassDOT MHS Emergency Response Plan 3.19.13.PDF
- CAT Ramps (Scanned Paper Copy)
- CAT Structure and BIN Drawings.PDF

CAD Data

- CAT_FACIL_BIND.dwg
- SKS1001.dwg
- SKS1005.dwg
- SKS1006.dwg
- SKS1007.dwg
- SKS1020.dwg
- SKS1021.dwg
- SKS1021.wld
- SKS1042.dwg

MMIS

- Vent Building Equipment List (Spreadsheet)
- Pump Station Equipment List (Spreadsheet)
- Other Structure Equipment List (Spreadsheet)

Maximo

- D6 facilities maintenance top level heirarchy in maximo (Spreadsheet)

Miscellaneous

- Various Record Drawings (TIFF images)
- MassDOT Outfalls List (Scanned Paper Copy)
- MassDOT Pump Rooms List (Scanned Paper Copy)
- Low Points and Storm Waters (Spreadsheet)
- CAT Emergency Response Facilities email + selected pages 10.2.09.PDF

Feature classes in the geodatabase provided by MassDOT:

- Bridge arcs
- Bridge off roads
- Bridge pts
- Building footprints
- CA/T facilities
- Communication line
- DCR depots
- Drainage outfall points
- Facilities

Appendix II
Technical memos



School for the Environment
100 Morrissey Blvd
Boston, Massachusetts 02125

Date: June 14, 2013

To: Steven Miller, Supervisor, Environmental Management Systems and Sustainability, Massachusetts Department of Transportation, Highway Division

From: Ellen Douglas, Associate Professor, UMass Boston (UMB)

RE: Change in proposed Phase 2 elevation 14 feet to 18 feet NAVD

Under Phase 2, the proposal states that the technical team will identify and photograph the vulnerable features and assets within the target areas that are located below the elevation of 14 feet NAVD, which represents the estimated elevation of mean higher high water (MHHW) plus sea level rise (SLR), storm surge and wave action circa 2030. We are amending Phase 2 to identify and photograph vulnerable features located below the elevation of 18 feet NAVD which represents MHHW (5 feet) + the estimated 100-year storm surge (5 feet) + SLR by 2100 (6 feet) + wave action (2 feet). The purpose of this amendment is to 1) identify and inventory assets that are potentially vulnerable to coastal flooding impacts through 2100 and 2) to develop adaptation strategies that can accommodate climate change impacts beyond 2030.

Date: April 25, 2014

To: Steven Miller, Supervisor, Environmental Management Systems and Sustainability, Massachusetts Department of Transportation, Highway Division

From: Ellen Douglas, Associate Professor, UMass Boston (UMB), Paul Kirshen, Research Professor, University of New Hampshire, Kirk Bosma, Woods Hole Group, Inc. and Chris Watson, UMB

RE: Sea Level Rise scenarios for vulnerability analysis

This memo is an expansion of the draft submitted on November 13, 2013 to include our responses to the comments of the project Technical Advisory Committee (TAC). The detailed responses are in Appendix A. The responses are integrated into the material below.

Sea level rise (SLR) is one of the most certain (Meehl et al., 2007) and potentially destructive impacts of climate change. Rates of sea level rise along the northeastern U.S. since the late 19th century are unprecedented at least since 100 AD (Kemp et al., 2011). The local relative sea level rise is a function of global and regional changes. As discussed in more detail subsequently, global increases by 2100 may range from 0.2 m (0.7 ft) to 2.0 m (6.6 ft). Regional variations in sea level rise arise because of such factors as vertical land movement (uplift or subsidence), changing gravitational attraction in some sections of the oceans due to ice masses, and changes in regional ocean circulation (Nicholls et al, 2014).

One of the challenges presented by the wide range of SLR projections is the inability to assign a likelihood to any particular scenario. According to Parris et al. (2012), probabilistic projections are simply not available at scales that are relevant for vulnerability assessment and adaptation planning. Furthermore, they state that, "coastal management decisions based solely on a most probable or likely outcome can lead to vulnerable assets resulting from inaction or maladaptation. Given the range of uncertainty in future global SLR, using multiple scenarios encourages experts and decision makers to consider multiple future conditions and to develop multiple response options." For this reason, we have chosen to adopt the SLR scenarios recommended by Parris et al (2012) for the U. S. National Climate Assessment as illustrated in Figure 1 (from Figure ES1 in *Global Sea Level Rise Scenarios for the United States National Climate Assessment*, NOAA Technical Report OAR CPO-1, December 12, 2012). We plan on using this scenario despite the maximum of 1.2 m recently presented in the IPCC Fifth Assessment Report (AR5) WG1 material (shown in Figure 2).

The (CA/T) system is a critical link in the regional transportation network and a vitally important asset to not only the City of Boston, but to the surrounding communities for which Boston is an economic focus. In the event of a disaster, the CA/T is an irreplaceable critical link for evacuation, and for emergency response and recovery services. It also serves as an essential

link to Logan International airport which is the major airport in the region. For all these reasons the CA/T must be considered to have a very low tolerance for risk of failure and hence, should require the highest level of preparedness. Critical infrastructure that is integral to Central Artery operations (e.g. vent buildings, switches, low elevation pump stations, tunnel entrances) also has low risk tolerance and may require the highest level of protection. Therefore, the use of the highest scenario (H) from Parris et al (2013), which combines thermal expansion estimates from the IPCC AR4 global SLR projections and the maximum possible glacier and ice sheet loss by the end of the century and “should be considered in situations where there is little tolerance for risk” was selected for utilization in this study. Use of the highest scenario is also recommended because they represent the earliest times adaptation actions will need to be implemented. We will consider the outcomes of lower, plausible SLR estimates as well.

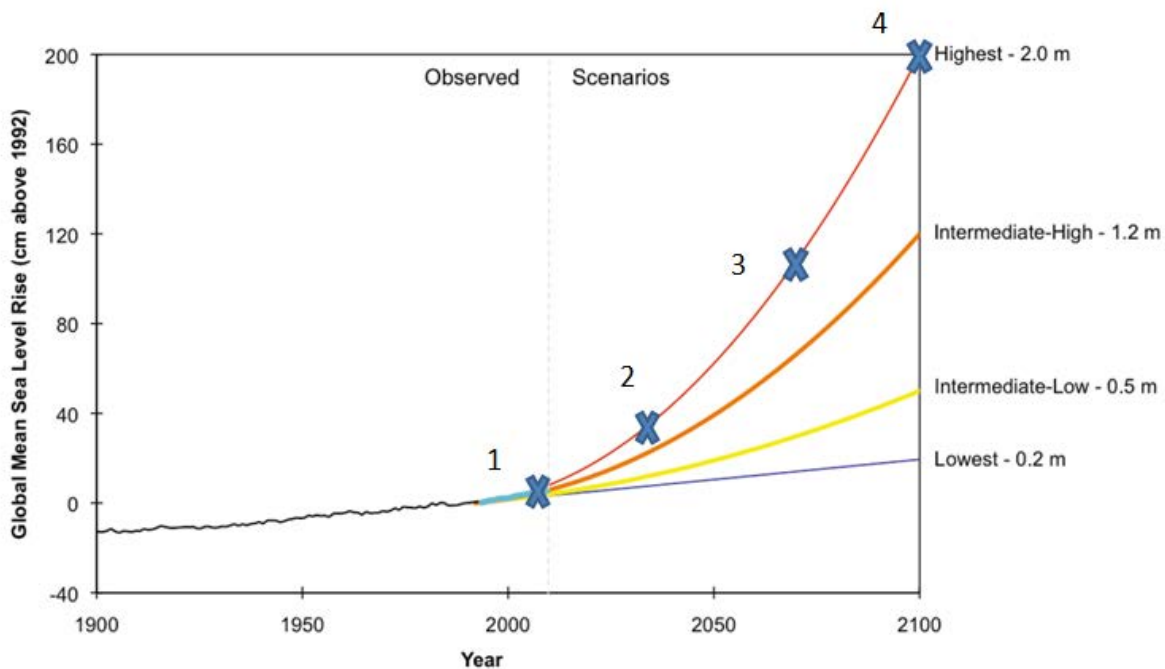


Figure 1: Projections of future sea level rise recommended in Parris et al (2012). Numbered markers illustrate SLR estimates to be used in the MassDOT CA/T vulnerability analysis.

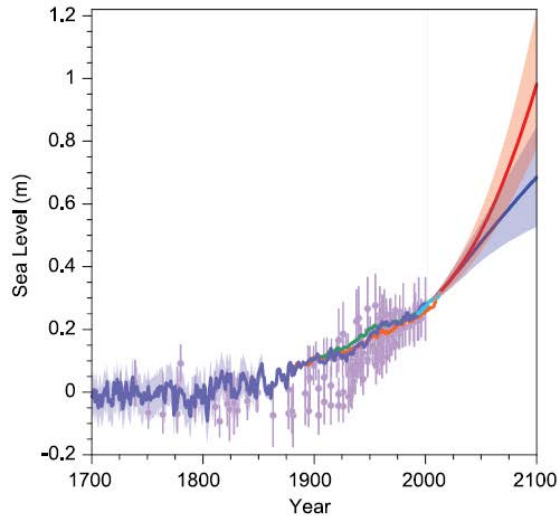


Figure 13.27: Compilation of paleo sea level data, tide gauge data, altimeter data (from Figure 13.3), and central estimates and likely ranges for projections of global-mean sea level rise for RCP2.6 (blue) and RCP8.5 (red) scenarios (Section 13.5.1), all relative to pre-industrial values.

Figure 2: Sea level rise projections in IPCC AR5 WG1 Chapter 13.

There is still considerable scientific support for a maximum value close to 2 m (6.6 ft). The recent survey of exceptional SLR experts by Horton et al (2013) related to possible changes in SLR under a high CMIP5 scenario (RCP 8.5, resulting in a temperature increase of 4.5 C above preindustrial by 2100) is shown in Figure 3. There are many ways to interpret these results, but the authors note that “Thirteen experts (out of ~ 90) estimated a 17 % probability of exceeding 2m of SLR by 2100 under the upper temperature scenario” (RCP 8.5, page 5). Phys.org interpreted the figure as, “The experts were also asked for a “high-end” estimate below which they expect sea-level to stay with 95 percent certainty until the year 2100. This high-end value is relevant for coastal planning. For unmitigated emissions, half of the experts (51%) gave 1.5 meters (4.9 ft) or more and a quarter (27%) 2 meters (6.6 ft) or more. The high-end value in the year 2300 was given as 4.0 meters (13.1 ft) or higher by the majority of experts (58%).” (<http://phys.org/news/2013-11-expert-sea-level-meter-century.html>). Furthermore, US Army Corps of Engineers Circular No 1165-2-212, 10 1 12, Sea-Level Change Considerations for Civil Works Programs (most recent, October 01, 2011) on page B-11 states that a reasonable credible upper bound for 21st century global mean sea level rise is 2 meters (6.6 ft). In his analysis of expert opinion versus IPCC AR5 SLR estimates, Dr. Horton concludes that “AR5 ice sheet projections are incompatible with the views held by about half of ice sheet experts.” (<http://www.glaciology.net/Home/Miscellaneous-Debris/Conservative> and [Overconfident](http://www.glaciology.net/Home/Miscellaneous-Debris/Overconfident)). **Given that there still exists a reasonable expectation that 2 m of SLR is possible by 2100, and given the great local and regional importance of the CA/T system, we have chosen the highest scenario projections (Parris et al., 2012) for use in our assessment.**

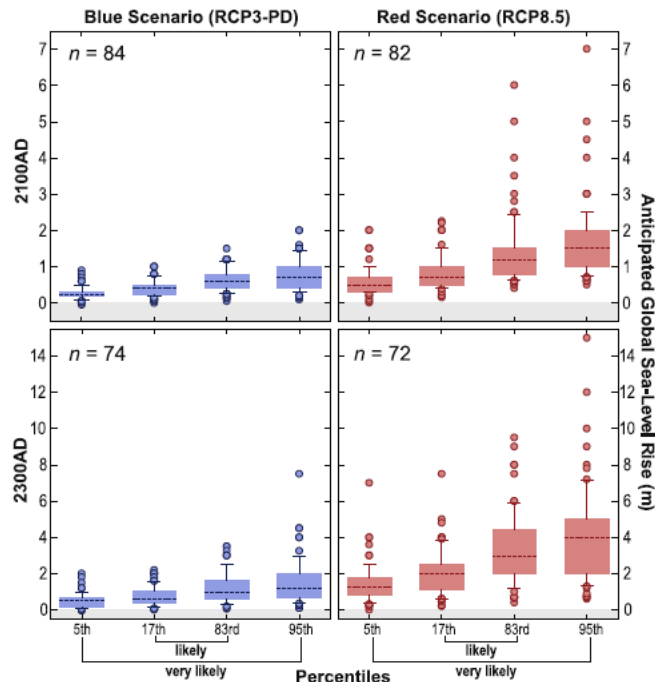


Fig. 2. Box plots of survey results from all experts who provided at least partial responses to questions. The number of respondents for each of the four questions is shown in the top left corner; it is lower than the total of 90 participants since not all answered each question. Participants were asked to estimate likely (17th–83rd percentiles) and very likely (5th–95th percentiles) sea-level rise under two temperature scenarios and at two time points (AD 2100 and AD 2300), resulting in four sets of responses. Shaded boxes represent the range between the first and third quartiles of responses. Dashed horizontal line within the box is the median response. Whiskers (solid lines) represent two standard deviations of the responses. Filled circles show individual responses that are beyond two standard deviations of the median.

Figure 3. Results of expert survey of sea level rise expectations, from Horton et al (2013).

The time periods for MassDOT CA/T vulnerability analysis are 2030, 2070 and 2100. The dynamic model will simulate storm climatologies representative of pre-2050 and post-2050 ocean and climate conditions. We recommend using the SLR estimates associated with these time periods as described below because they will minimize the number of time consuming dynamic model runs while at the same time allow us to assess the plausible high and low range of global SLR to 2100. These SLR estimates are:

1. Existing conditions for the current time period (considered to be 2013).
2. The value for the Highest (H) scenario at 2030 (**19 cm of SLR since 2013**), which is also close to the Intermediate High (IH) value at that same time period, pre 2050 climatology, and approximately the Intermediate Low value for 2100.
3. The value for the H scenario at 2070 (**98 cm of SLR since 2013**), which is also approximately the IH scenario value for 2100, post 2050 climatology.

4. The value for H at 2100 (**190 cm since 2013**), which represents the highest reasonably plausible projection.

The final values will be adjusted for local subsidence and the historical sea level rise trend following Kirshen et al. (2008). The impacts of changes in gravitation forces are not significant near Boston (Kopp, 2014) and will not be considered in our analysis. The impacts of possible circulation changes will not be considered due to their high uncertainty and relatively little impact here.

These scenarios will also be run with freshwater inputs from Cambridge, Boston, upstream and initial elevations in the Charles and Neponset Basins, and Charles River Dam pumping operations. Woods Hole Group will conduct some model sensitivity analysis to the SLR scenarios and the flow estimates to be provided by Boston Water and Sewer Commission and Cambridge consultants before doing the final Monte Carlo runs.

References

- Horton, B. P., S. Rahmstorf, S. E. Engelhardt, and A. C. Kemp, 2014. Expert assessment of sea-level rise by AD 2100 and AD 2300, *Quaternary Science Reviews*, 84 (15): 1-6.
- Kemp, A. C., B. P. Horton, J. P. Donnelly, M. E. Mann, M. Vermeer and S. Rahmstorf, 2011. Climate related sea-level variations over the past two millennia, *PNAS*, 108 (27): 11017–11022.
- Kirshen, P., C. Watson, E. Douglas, A. Gontz, J. Lee, and Y. Tian. Coastal Flooding in the Northeastern USA under High and Low GHG Emission Scenarios, *Mitigation and Adaptation Strategies for Global Change*, 13:437–451, 2008.
- Kopp, R., *Uncertainties and Risks of Regional Sea-Level Change: Past, Present, and Future*, presentation to Environmental Research Group, UNH, March 2014.
- Meehl GA, Stocker TF, Collins WD, Friedlingstein P and others (2007) Global climate projections. In: Solomon S, Qin D, Manning M, Chen Z and others (eds) *Climate change 2007: the physical science basis. Contribution of Working Group I to the Fourth Assessment Report of the Intergovernmental Panel on Climate Change*. Cambridge University Press, Cambridge, p 749–844.
- Nicholls, R., Hanson, S., Lowe, J., Warrick, R., Lu, X., and Long, A., *Sea-Level Scenarios for Evaluating Coastal Impacts*, *WIREs Clim Change*, 5, doi:10.1002/wcc.253, 2014.



School for the Environment
100 Morrissey Blvd
Boston, Massachusetts 02125

Parris, A., P. Bromirski, V. Burkett, D. Cayan, M. Culver, J. Hall, R. Horton, K. Knuuti, R. Moss, J. Obeysekera, A. Sallenger, and J. Weiss. 2012. Global Sea Level Rise Scenarios for the US National Climate Assessment. NOAA Tech Memo OAR CPO-1. 37 pp. available online December 2012: http://cpo.noaa.gov/sites/cpo/Reports/2012/NOAA_SLR_r3.pdf.

U.S. Army Corps of Engineers (2011) Sea-Level Change Considerations for Civil Works Programs; Department of the Army EC 1165-2-212, CECW-CE Washington, DC 20314-1000, Circular No. 1165-2-212 1 October 2011, EXPIRES 30 September 2013.

Date: November 14, 2014

To: Steven Miller, Supervisor, Environmental Management Systems and Sustainability, Massachusetts Department of Transportation, Highway Division

From: Ellen Douglas, Paul Kirshen, Kirk Bosma, Chris Watson

RE: Critical threshold elevations for structures within CA/T system

Our original scope of work included the determination of critical threshold flood elevations for all structures and boat-sections (that is, tunnel entrances and exits) within the MassDOT CA/T system domain. The result would be an estimate of when flooding would occur based upon the ADCIRC model output and associated sea-level rise scenarios. Critical threshold elevations for a structure would include sill elevations for doors, window, vents, etc. – any potential opening which could allow water to enter the structure. For boat-sections, critical thresholds would include the elevations of the tops of walls that surround them as well as the roadway elevation leading to or from a tunnel. **We now recommend that the ground level elevation of each structure be used as the critical threshold elevation regardless of the elevations of any doors, vents or other features which might be higher.** Dan Mullaly stated on a meeting on 10/15/2014 that “any water at grade is a problem” because of possible leaky foundations, doorways, etc. at grade. Therefore, we will not continue to survey structures for critical elevations but in the final report recommend that all structures be inspected for possible flood pathways at grade into them.

For boat sections, we do not have an adequate assessment of whether or not the surrounding walls can withstand flood waters or whether or not they are water tight. For example, UMass Boston observed several boat sections walls, such as those on Parcel 6^a, which are primarily constructed of Jersey Barriers, which cannot be expected to be watertight or withstand floods. **We therefore recommend that the ground level elevations surrounding each boat-section structure be used as the critical threshold elevation regardless of the higher elevations of any surrounding walls (this assumes that the walls surrounding the boat sections will not be water tight if flooding reaches the elevation of the base of the wall).** While we could have assumed that some of walls would be strong enough to withstand flood flows and are floodproof, we do not want to make that assumption without a detailed engineering inspection of each wall. A recommendation will be made to inspect each wall. However, if MassDOT personnel so choose, we can also assume that the walls surrounding certain boat sections will remain intact if flooding reaches the base elevation. **Therefore, before we can assess the vulnerability of the boat sections, we need guidance as to which assumption**



School for the Environment
100 Morrissey Blvd
Boston, Massachusetts 02125

(walls are watertight or not) we should make for the final report. This assumption can be changed at a later date, and the vulnerability re-assessed, if necessary.

Please let us know if you agree with our recommendations.

^aRose Kennedy Greenway Parcel 6 includes Ramps SA-CN, SA-CT, SA-CS, ST-CN and ST-SA

Date: April 1, 2015

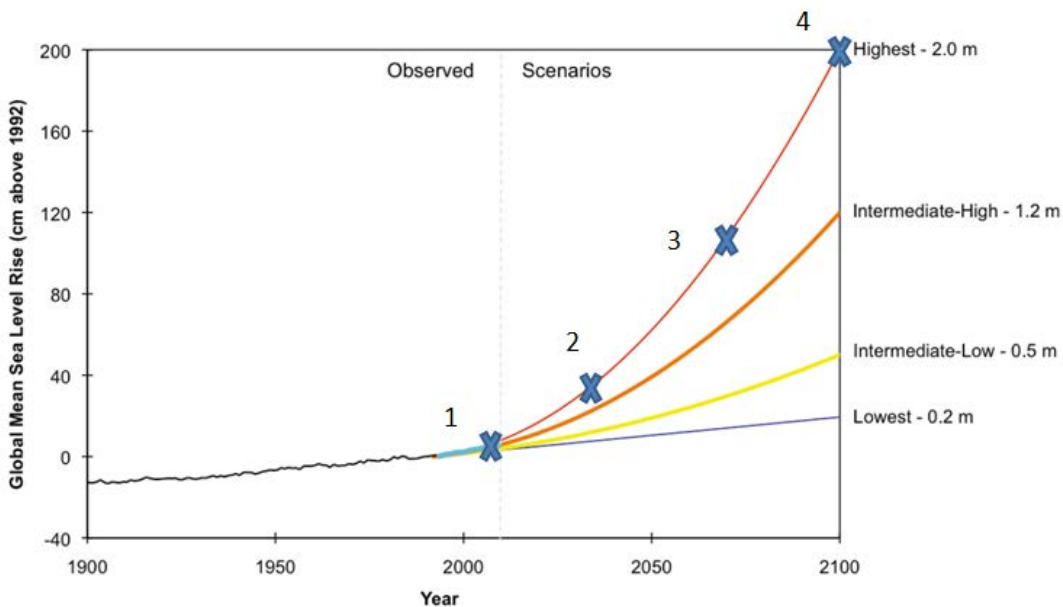
To: Steven Miller, Supervisor, Environmental Management Systems and Sustainability, Massachusetts Department of Transportation, Highway Division

From: Ellen Douglas, Associate Professor, UMass Boston (UMB)

RE: Revision of vulnerability assessment and adaptation strategy analysis for 2100

This memo documents the decision of the project technical team to revise the vulnerability assessment and identification of adaptation options for the 2100 sea level rise (SLR) and coastal storm scenario. Because of the exponentially increased simulation time required for model runs under the original 2100 highest sea level rise (SLR) scenario (shown as point 4 in Figure 1 from the memo dated April 25, 2014), we will be using the 2070 model runs (point 3 in Figure below, model runs already completed) to represent the potential impacts of SLR and coastal storms in 2100. This revised analysis is consistent with the intermediate high SLR estimate by 2100, shown as point 3 in figure below (from memo dated April 25, 2014). The climatology used in the 2070 simulations is the same as for the original 2100 scenario runs. The Highest 2100 scenario (shown as point 4 in Figure 1) will be included as part of the coastal vulnerability project (ISA #85470) now under way.

Model runs for 2070 are complete and data layers are currently being processed. We anticipate the 2070 and new 2100 analyses for the final FHWA report will be complete by April 30, 2015.



(source: Figure 1 in SLR memo dated April 25, 2014).

Appendix III
Fact Sheets

MassDOT-FHWA Pilot Project: *Climate Change and Extreme Weather Vulnerability Assessments and Adaptation Options of the Central Artery*

Project Team:

Steven Miller and Katherin McArthur, MassDOT
Ellen Douglas and Chris Watson, University of Massachusetts Boston
Paul Kirshen, University of New Hampshire
Kirk Bosma, Woods Hole Group, Inc.

Motivation:

Many MassDOT assets, including the Central Artery tunnels, are currently vulnerable to flooding from an extreme coastal storm. This vulnerability will increase in the future due to projected sea level rise due to climate change. The Central Artery is a critical link in regional transportation and a vitally important asset in the Boston metropolitan area. As one of the single most valuable components of Massachusetts infrastructure, its maintenance, protection and enhancement are a priority for the Commonwealth.

Objectives:

- 1) Assess vulnerability of Central Artery to sea level rise and extreme storm events.
- 2) Investigate options to reduce identified vulnerabilities.
- 3) Establish an emergency response plan for tunnel protection and/or shut down in the event of a major storm.

Project Plan:

To achieve the objectives of this project, we will implement the project in the phases outlined below, some of which will occur simultaneously (i.e., Phases 1-4) and others which will be based upon previous phases (i.e., Phases 5-7). Progress will be guided by input from a scientific advisory committee made up of various subject experts.

■ PHASE 1: Initial Determination of Geographical Scope

- Create a GIS-based map of MassDOT assets potentially impacted by flooding.
- Delineate boundaries of critically vulnerable areas such as the Greenway, Tip O'Neil, Ted Williams, Callahan and Sumner tunnel entrances, the MBTA Aquarium station entrance and Red, Blue and Silverline way near South Station.

■ PHASE 2: Detailed Inventory of Assets within the Project Area

- Using the map from Phase I, compile a database of properties and features within critically vulnerable areas such as vents, storm drains, electrical infrastructure that could be impacted by an extreme storm event.

■ PHASE 3: Surveys of Critical Areas of Central Artery

- Elevation surveys of identified critical flow paths and critically vulnerable areas will be completed to support the simulation of coastal flooding events in the hydrodynamic modeling analysis (See Phase 4).

■ PHASE 4: Hydrodynamic Analysis

- Develop a hydrodynamic model of Boston Harbor using the advanced ocean circulation model (ADCIRC) together with simulating waves nearshore (SWAN)

to evaluate current storm surge impacts and impacts of sea level rise and storm surge projected for 2030, 2070 and 2100.

- Use model output to refine Phase 1 map to identify extent and depth of flooding and wave impacts in critically vulnerable areas.

■ PHASE 5: Vulnerability Assessment

- Compile exposure within the critically vulnerable areas based on Phase 1 through 4 results.
- Identify sensitivity and adaptive capacity of MassDOT facilities within the critically vulnerable areas by assessing current flood management protocols, alternative evacuation routes, etc.
- Quantify expected damage function for Central Artery in 2030, 2070, and 2100, and estimate value of wages lost in the event Central Artery is shut down.

■ PHASE 6: Adaptation Strategy

- Develop a regional adaptation strategy that includes specific actions for protection against and management of flooding and storm surge impacts for year 2030. Strategy will be based on trigger points (flooding elevations) identified and actions will be based on impacts identified in previous phases, under consultation with MassDOT personnel.

■ PHASE 7: Present Results and Prepare Final Report to MassDOT Senior Management

- Present final results to MassDOT and FHWA and interested stakeholders.
- Prepare final report.
- Make results available to stakeholder community.



MassDOT-FHWA Climate Resilience Pilot Project

Modeling Overview and Frequently Asked Questions

Overview

The Massachusetts Department of Transportation (MassDOT) and the Federal Highway Administration (FHWA) have commissioned a pilot project to assess and improve the resiliency of the Central Artery and Tunnel System (CA/T) by analyzing its vulnerability to sea level rise and extreme weather events, investigating options for adaptation to the identified vulnerabilities, and establishing an emergency response plan for tunnel protection. A major component of the pilot project is a detailed modeling effort that simulates extreme weather events under both present and future climate conditions. The project is being managed by the MassDOT Highway Division Environmental Services Section and being executed by UMass-Boston, Woods Hole Group, Inc. and University of New Hampshire. The MassDOT Boston Harbor Flood Risk Model (BH-FRM) model is being developed and used to determine inundation risk and flooding pathways; and to simulate the dynamic nature of flooding in the City of Boston that serve as flood pathways affecting the CA/T. BH-FRM is an advanced model that simulates the effects of tides, storm surge, wind, waves, wave setup, river discharge, sea level rise, and future climate change scenarios.

FAQ

Are the results of the BH-FRM applicable to the entire City of Boston and City of Cambridge?

Yes, flood risks results will be available throughout the City of Boston and Cambridge. All parts of the City of Boston and Cambridge that are at an elevation low enough for storm surge-induced flooding to occur are included.

Why does the BH-FRM model include detailed results in the City of Cambridge?

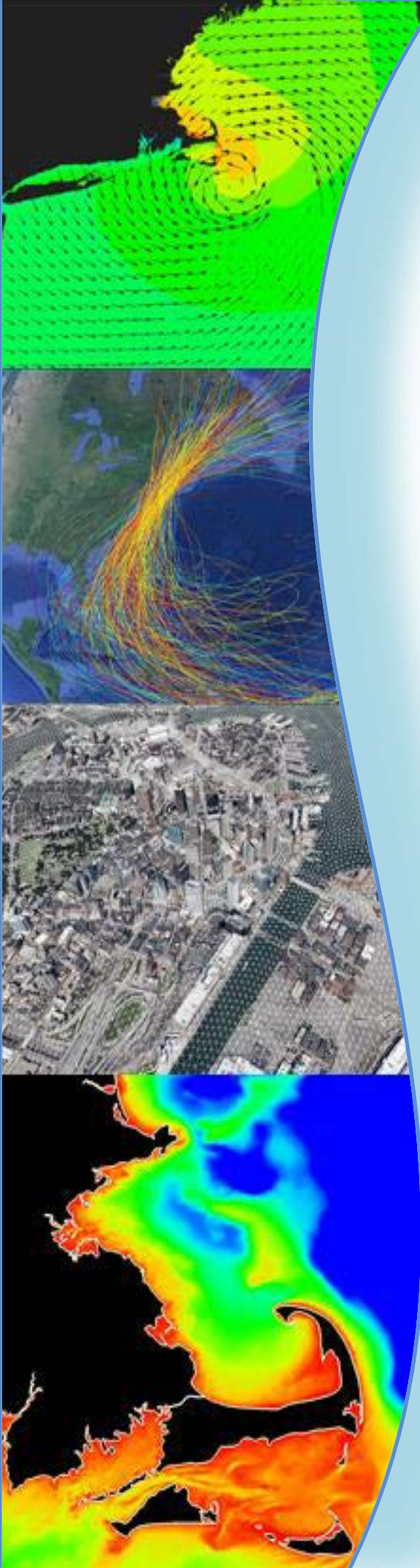
The City of Cambridge provided additional funding to extend the focus area of the BH-FRM model.

Are the BH-FRM results applicable to a specific building or structure located in Boston or Cambridge?

Yes.

Are the results of the BH-FRM applicable to the areas outside the Boston and Cambridge?

BH-FRM provides information for adjacent areas in Massachusetts, as well as Rhode Island, New Hampshire, Maine, and Connecticut, but will not be able to identify risk associated with specific assets for locations outside of the focus area (Boston & Cambridge). However, the model can be extended to do so in the future.



MassDOT Climate Change Adaptation Pilot Project

Modeling Overview and Frequently Asked Questions

What is the resolution of the BH-FRM model grid?

BH-FRM uses an unstructured grid that allows for the grid resolution to vary across the model domain. In the BH-FRM focus area (Boston, Cambridge and Boston Harbor), the model resolution ranges from five to thirty meters for both inland areas and coastal waters. In areas beyond the focus area (Atlantic Ocean), the resolution increases to 100 to 500 meters. Most of the coastal areas in New England have a resolution between 50 to 100 meters.

What is the complete extent of the BH-FRM model domain?

The BH-FRM domain extends from the Gulf Coast to Newfoundland (see attached map).

What is the specific extent of the BH-FRM and the detailed focus area?

See the attached map.

What types of storms does BH-FRM simulate?

BH-FRM simulates storm surge induced flooding that could occur from both tropical (hurricanes) or extra-tropical (nor'easter) storm events. The model also includes climate-change induced increases in river discharge from precipitation and storm water run-off. A statistically robust approach is used to capture variations in storms.

Does the BH-FRM include freshwater flooding?

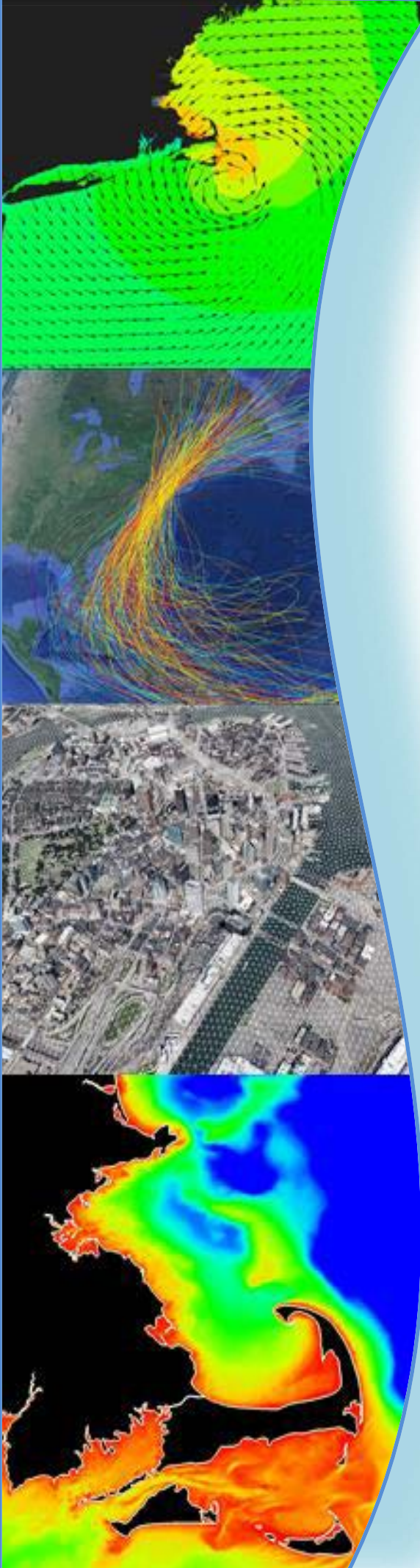
To some extent the Charles and Mystic Rivers are incorporated into the BH-FRM because the freshwater outflows of the rivers interact with storm-surge induced flooding. However, freshwater storm flooding events that have no ocean-based component are not included in the risk analysis (for example, while the flow contribution of precipitation in the upper reaches of the Mystic to flooding in the coastal area are included, the local freshwater flooding in the upper Mystic is not).

Are the Charles River Dam and Amelia Earhart Dam included in the model?

Yes.

What makes BH-FRM more accurate than other inundation models and flood maps that have been created for the region?

The BH-FRM is a more accurate representation of flooding risk because it is (1) a dynamic model that includes the critical processes associated with storm induced flooding (winds, waves, wave-setup, storm surge, river discharge, etc.), (2) calibrated to historical storm events with observed high water data, (3) high enough resolution to capture flood pathways in the complex urban topography of Boston and Cambridge, and (4) able to capture the net effect of varying storm types, magnitudes, and parameters.



MassDOT Climate Change Adaptation Pilot Project

Modeling Overview and Frequently Asked Questions

How do BH-FRM results relate to other existing Sea Level Rise inundation maps (e.g., The Boston Harbor Association flood maps)?

BH-FRM is a dynamic model that includes relevant flooding processes and their interaction. The model includes the dynamic effects of tides, storm surge, land effects, winds, waves, wave setup, etc. Results also include changes in climate to assess variations in storm intensity, etc. These processes can result in significant differences in the magnitude and extent of flooding throughout a region. For example, flooding caused by tropical storm events (such as Hurricane Sandy) are typically not well represented by non-dynamic models based on the expected water surface elevation overlain on land elevation. Flood mapping approaches, such as the TBHA bathtub flood maps, do not include the influence of the storm track, winds, and waves.

How do BH-FRM results relate/compare to the recently released FEMA Preliminary Flood Insurance Rate Maps (FIRMs)?

BH-FRM results are focused on present and future flooding projections, while FEMA results estimate present flood risk based on historical events. The methods used to produce the FIRMs are also substantially different. BH-FRM is also being used to assess present day conditions, simulate historic storm events, and can potentially provide improved input to the FEMA models and mapping.

Will the BH-FRM model show flooding propagating down streets and through buildings?

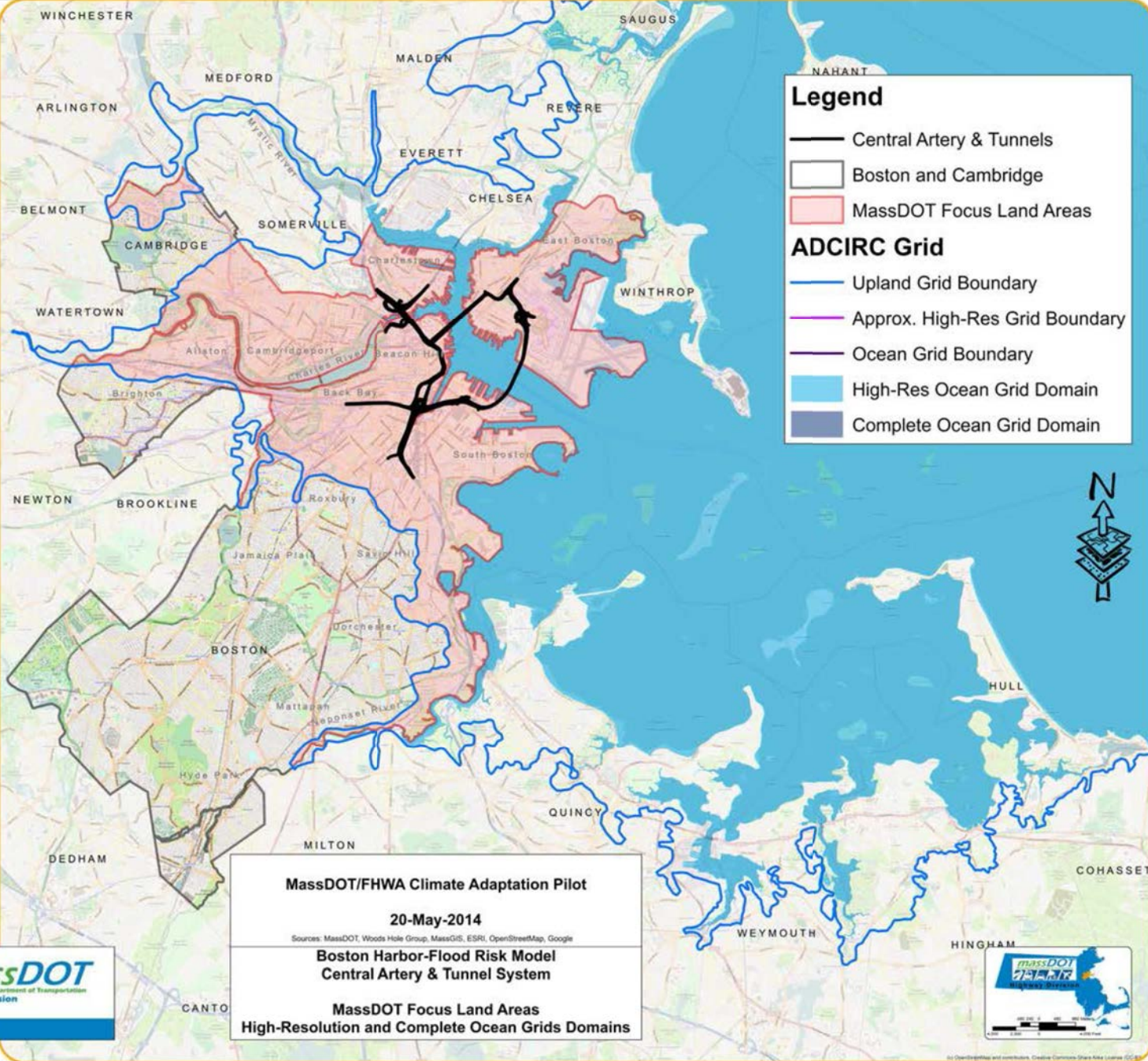
Flood risk and water depths will be available for individual buildings and streets with this model. However, the model does not currently intend to show flooding into buildings or the detailed flow down every street. An extension to the model is being considered to provide visualizations of flood propagation down streets and flood pathways, but it will not model flooding into structures.

Will the BH-FRM results of flooding risk be publically available?

Yes. Full model results for the focus area (Boston and Cambridge) will be publicly available.

What is needed to extend the BH-FRM focus area to my town/area?

To extend the BH-FRM into any specific area requires additional grid development and may also require additional climate input conditions determined by your project requirements.



Legend

- Central Artery & Tunnels
- Boston and Cambridge
- MassDOT Focus Land Areas

ADCIRC Grid

- Upland Grid Boundary
- Approx. High-Res Grid Boundary
- Ocean Grid Boundary
- High-Res Ocean Grid Domain
- Complete Ocean Grid Domain

MassDOT/FHWA Climate Adaptation Pilot
20-May-2014
Sources: MassDOT, Woods Hole Group, MassGIS, ESRI, OpenStreetMap, Google
Boston Harbor-Flood Risk Model
Central Artery & Tunnel System
MassDOT Focus Land Areas
High-Resolution and Complete Ocean Grids Domains



© OpenStreetMap and contributors, Creative Commons Attribution License, CC-BY

Appendix IV
Additional stakeholder coordination meetings and dates

- Federal Highway Administration Hydraulic Engineering Circular-25 Highways in the Coastal Environmental Peer Exchange, NY NY: 5/16-17/13
- 2013 American Association of State Highway Transportation Officials (AASHTO) Extreme Weather Events Symposium, Washington DC: 5/20-23/13
- Environmental Business Council: 6/18/13
- 1st Technical Advisory Committee Meeting 7/9/13
- Massachusetts Bay Transportation Authority Briefing (MBTA): 8/13/13
- 1st Stakeholder Meeting: 8/15/13
- Harvard Climate Change Summit: 8/19/13
- Internal Underwriters Meeting: 10/23/13
- Global Warming Solutions Act, Adaptation Subcommittee, Massachusetts Environmental Policy Act (MEPA) Working Group Meeting: 10/28/13
- Stakeholder Meeting at Boston Water and Sewer Commission (BWSC): 11/12/13
- MBTA Coordination Meeting: 11/21/14
- Boston High Water Seminar: 11/22/14
- Massachusetts Emergency Management Agency Coordination Meeting: 12/3/13
- Netherlands Embassy, Washington DC: 1/15-16/14
- MEPA Policy/SLR meeting: 1/27/14
- MassDOT Innovation Conference: 4/9/14
- University of Massachusetts-Boston Center for Rebuilding Sustainable Communities After Disasters: 5/8/14
- Antioch University, NH: 5/20/14
- MEPA Policy/SLR Meeting: 5/29/14
- Massachusetts Maritime Academy: 6/14/14
- Massachusetts Institute of Technology Sea Grant Program: 6/17/14
- AASHTO Subcommittee on the Environment Annual Meeting: 6/24-27/14
- Massachusetts Department of Public Health-Preparing for Climate Effects at the Municipal Level: A Public Health Symposium: 7/15/14
- Stakeholder Coordination Meeting at BWSC: 8/5/14
- National Hydraulic Engineers Meeting, Iowa City: 8/18-22/14
- Rose Kennedy Greenway Ramp Covering Coordination Meeting: 9/30/14
- Massachusetts Dept. of Conservation and Recreation Coordination Meeting: 10/2/14
- MEPA Policy/SLR Meeting: 11/14/14
- Stakeholder Meeting at BWSC: 11/24/14
- Meet with Harvard to discuss City Of Boston's future regional mayoral meeting on climate change: 12/16/14
- Meeting with Boston Transportation Department: 12/22/14
- 2nd TAC meeting: 12/30/14
- MassBays Management Committee Meeting: 2/4/15

Appendix V
Progression of project inventory and analysis over time

Fourth quarter 2013

- 22-Oct: IK Meeting Two
 - Proposed CATDB Hierarchy to MassDOT
- 28-Oct: Preliminary List of Outfalls
- 05-Nov: Preliminary List of CATDB Structures and Facilities
- 13-Nov: Proposed CATDB Hierarchy to Project Team
- 21-Nov: MBTA Coordination Meeting
- 23-Nov: Phase 1 Complete – CA/T System Defined
- 22-Nov: Field Visits Continue
- 27-Nov: Preliminary Digitization of BINs from PDFs

First quarter 2014

- 21-Jan: Preliminary List of Pump Rooms
- 26-Jan: Preliminary Revisions to Elevation Survey Scope
- 28-Jan: Field Visits Continue
- 14-Feb: Preliminary Locations of Tunnel Egresses Digitized from PDF Maps
- 17-Feb: Record Drawing Review Terminated
 - Review Process Determined to be Inefficient
 - Field Visit Protocols Expanded
- 26-Feb: Preliminary Conversion of BINs to 2D Model of CANA
- 03-Mar: GIS Scope Revaluated
- 07-Mar: MBTA Red and Silver Line Tours
- 21-Mar: Preliminary 2D Model of CANA Complete
 - Preliminary 2D Model of CA/T Continues
- 22-Mar: GIS Scope Revised
- 24-Mar: MBTA Blue Line Aquarium Tour

Second quarter 2014

- 02-Apr: Survey Methodology Redefined
- 06-Apr: Field Visits Continue
- 07-Apr: Field Tour of Pump Stations
- 04-May: CATDB Hierarchy Finalized
- 07-May: Beverly Street Elevation Survey
- 27-May: Refined List of CATDB Structures and Facilities
- 16-Jun: Preliminary Digitization of Outfalls
- 23-Jun: Fort Point Channel Discussions with Boston University
- 24-Jun: Schraffts Elevation Survey

Third quarter 2014

- 14-Jul: Preliminary 2D Model of CA/T Complete
 - Preliminary List of Ramps and Boat Sections
- 18-Jul: MBTA Fort Point Channel and Orange Line Tour
- 20-Aug: Refined List of CATDB Facilities, Structures, and Structural System
- 27-Aug: GIS Scope Expanded
- 03-Sep: Aquarium Area Elevation Survey
- 03-Sep: WHG GIS Kickoff Meeting
- 04-Sep: Rose Kennedy Greenway Development Coordination
- 10-Sep: Preliminary List of CATDB Structure Types
- 12-Sep: Rose Kennedy Greenway GIS Data Acquired from BRA
- 15-Sep: CATDB Structures and Facilities Detailed Review for Pilot VA
- 16-Sep: Field Tour of Pilot VA Structures
 - Field Visits Continue
- 18-Sep: Fort Point Channel Area Elevation Survey Request
 - Preliminary List of CA/T Hazardous Materials Locations
- 23-Sep: Field Tour of Ramps and Tunnel Egresses
- 24-Sep: MassDOT CAD Discussions
 - Drawings in Proprietary GDS Format
 - Export to AutoCAD Format Impractical
 - Alternate AutoCAD Format Data Requested

Fourth quarter 2014

- 01-Oct: BIN Polygon FC Import from CAD Data Complete
- 08-Oct: CATDB Structures and Facilities Detailed Revisions for IK Meeting
- 09-Oct: Pilot VA IK Meeting Part 1
 - Maximo Acquisition
 - Preliminary Emergency Response Site Info
- 14-Oct: Pilot VA Structures Facilities Maximo
- 15-Oct: Pilot VA IK Meeting Part 2
- 13-Nov: Preliminary Digitization of Boat Section Walls
- 26-Nov: GIS Scope Expanded to Complete Ramps Polygon FC
- 11-Dec: Preliminary List of Missing Structures (Data Gaps)
- 12-Dec: Preliminary BH-FRM Raster Data Review
- 15-Dec: Field Visits Continue
- 30-Dec: Preliminary List of Data and Map Deliverables

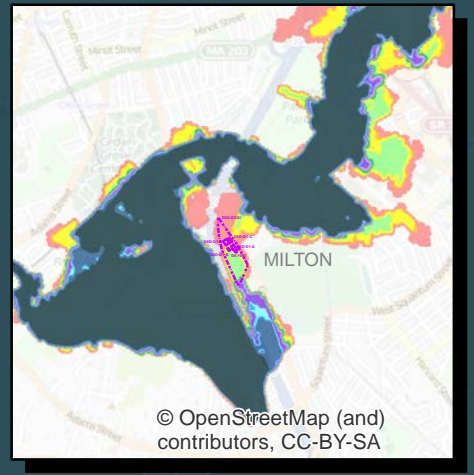
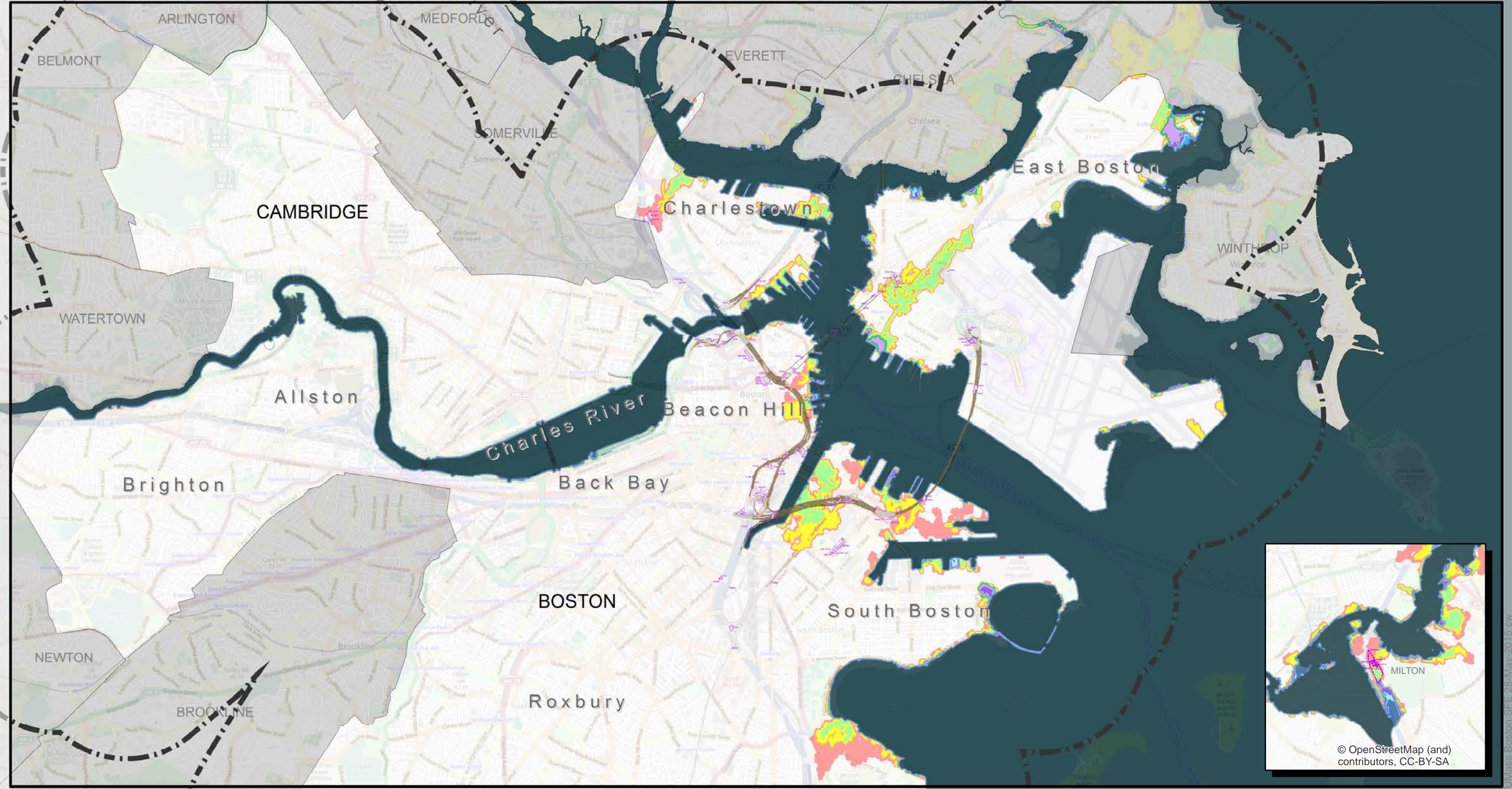
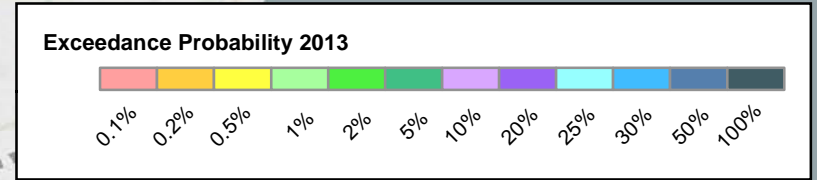
First quarter 2015

- 02-Jan: Preliminary Metadata Compilation
- 04-Jan: Ramps Polygon FC Development Continues
- 05-Jan: Sample Maps Reviewed by Project Team
- 13-Jan: Preliminary VA Results
- 15-Jan: Ramps Polygon FC Completed
- 06-Feb: Final BH-FRM Data Delivered
 - VA for 2013 and 2030 Complete

Appendix VI
Maps of flood exceedance probabilities and flood depths
for the CA/T domain

Legend

- BH-FRM Extent
- Complex
- Structure
- Boat Section
- Tunnel



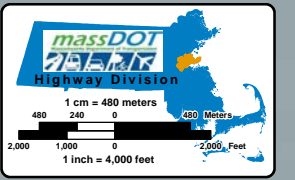
© OpenStreetMap (and contributors, CC-BY-SA)

MassDOT/FHWA
Climate Adaptation Pilot

28-May-2015

Sources: MassDOT, Woods Hole Group, UMass Boston, MassGIS, and ESRI (as indicated below)

**BH-FRM Coastal Flood Exceedance Probabilities
Central Artery and Tunnel System
2013 Scenario**

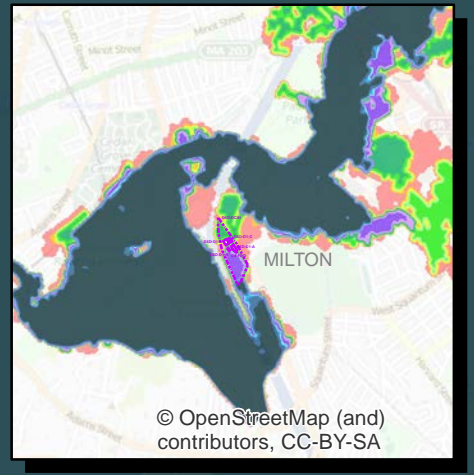
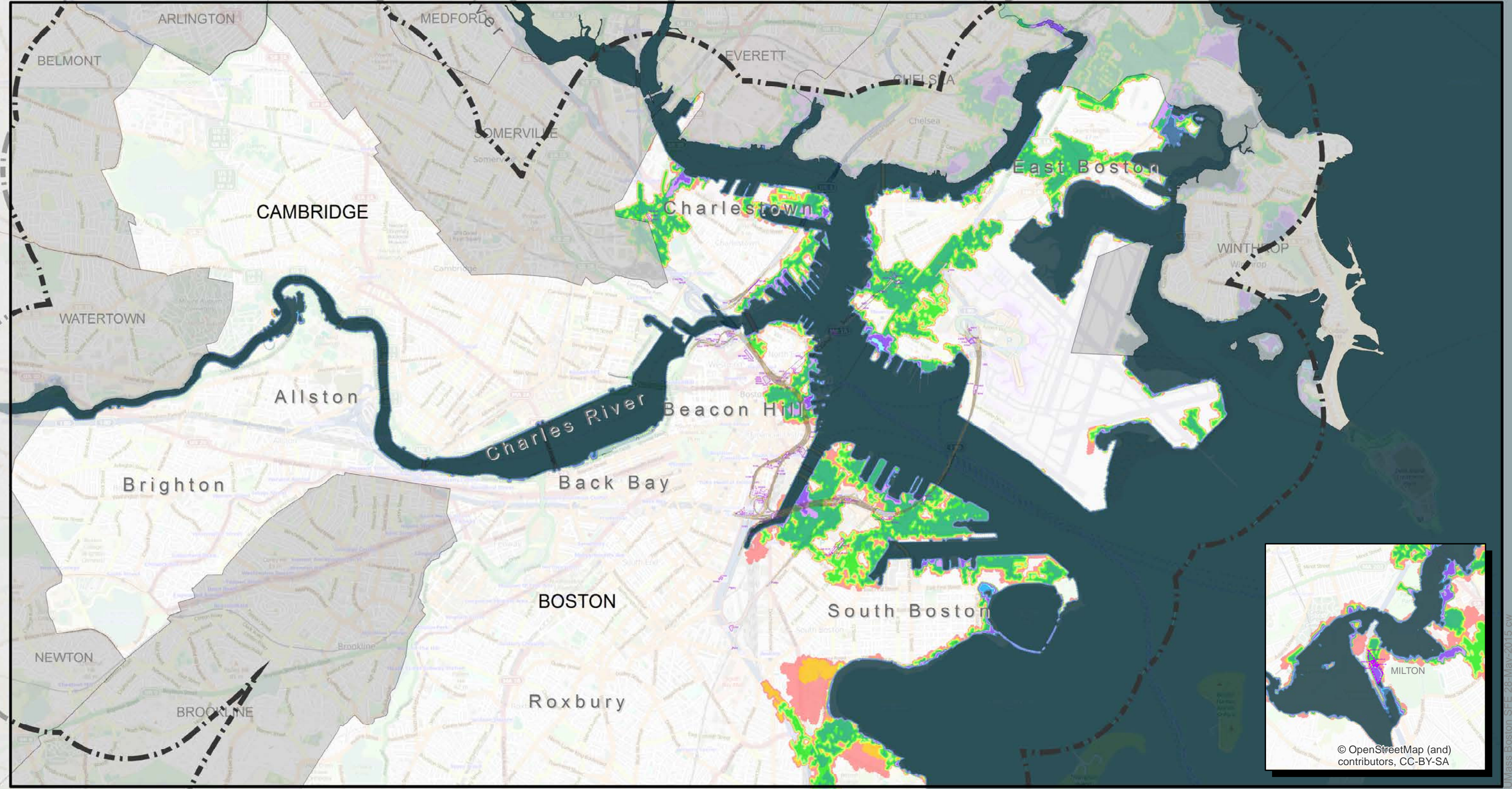
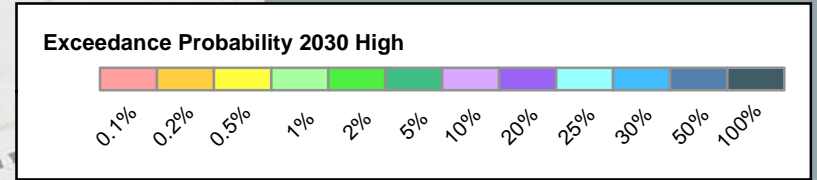


© OpenStreetMap (and contributors, CC-BY-SA)

UMass Boston SFE 28-May-2015.cw

Legend

- BH-FRM Extent
- Complex
- Structure
- Boat Section
- Tunnel

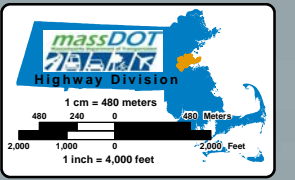


MassDOT/FHWA
Climate Adaptation Pilot

28-May-2015

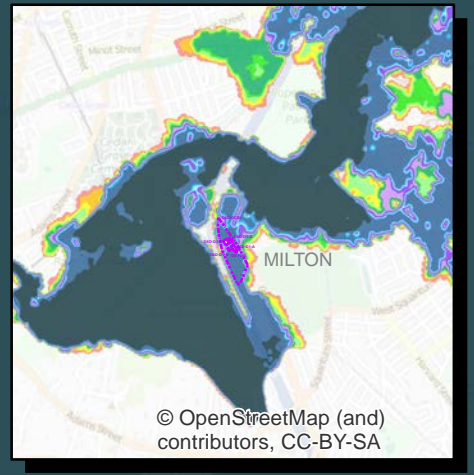
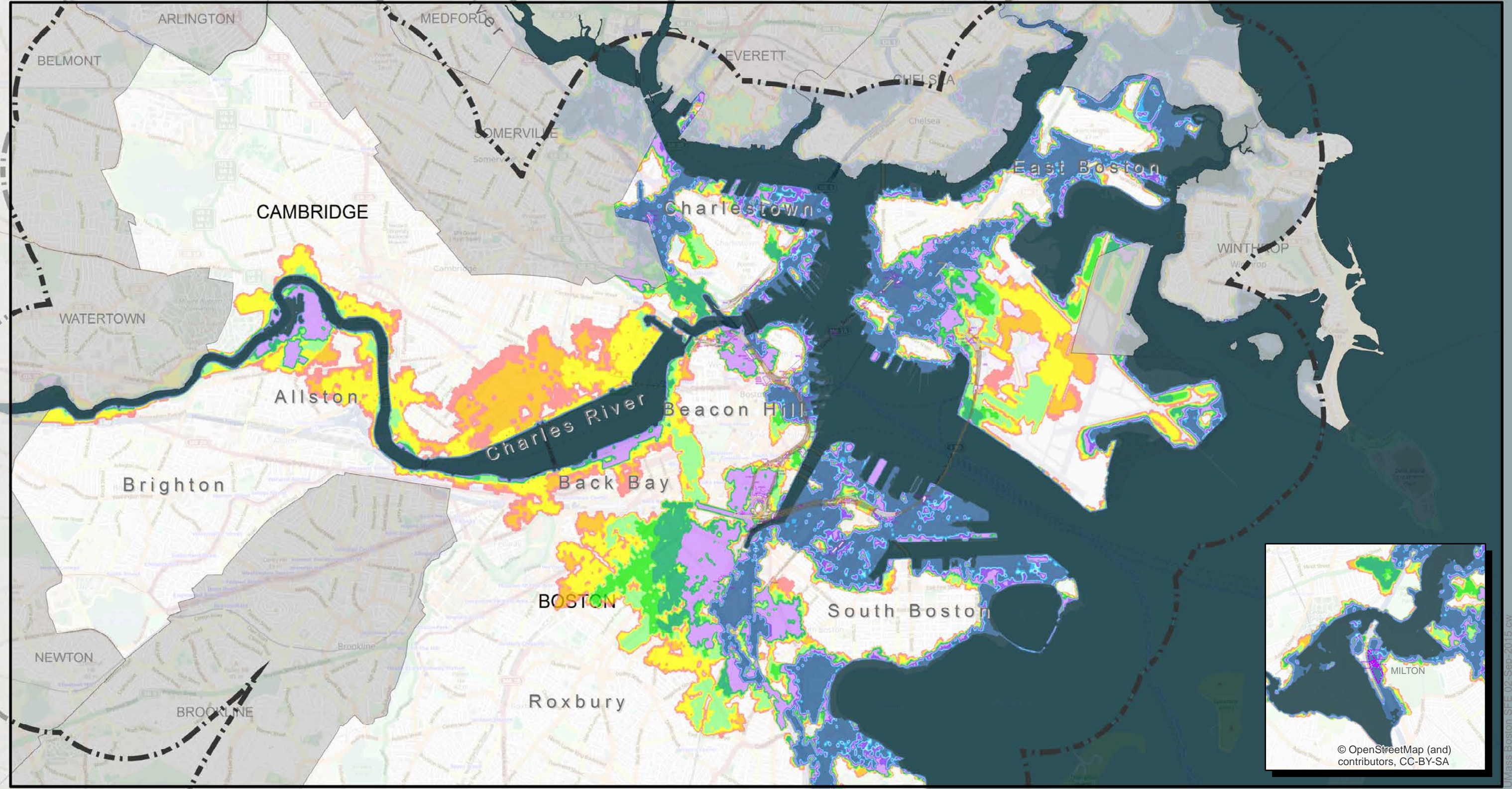
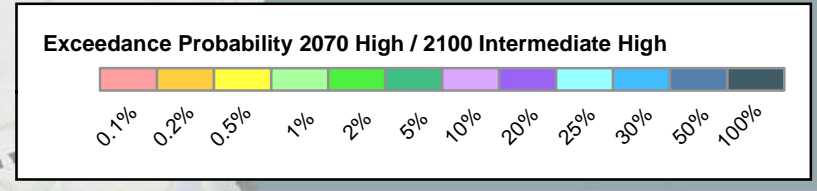
Sources: MassDOT, Woods Hole Group, UMass Boston, MassGIS, and ESRI (as indicated below)

BH-FRM Coastal Flood Exceedance Probabilities
Central Artery and Tunnel System
2030 High Scenario
0.62 feet (19 cm) SLR relative to 2013



Legend

- BH-FRM Extent
- Complex
- Structure
- Boat Section
- Tunnel

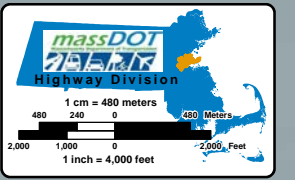


MassDOT/FHWA
Climate Adaptation Pilot

02-Sep-2015

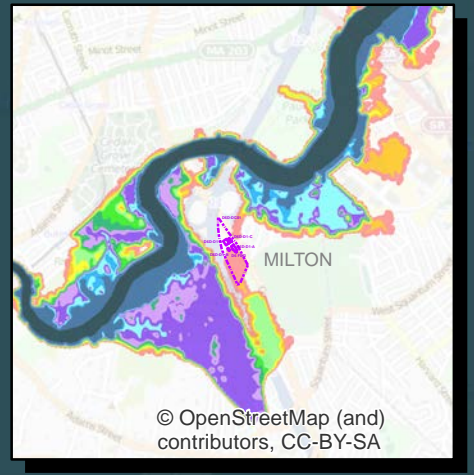
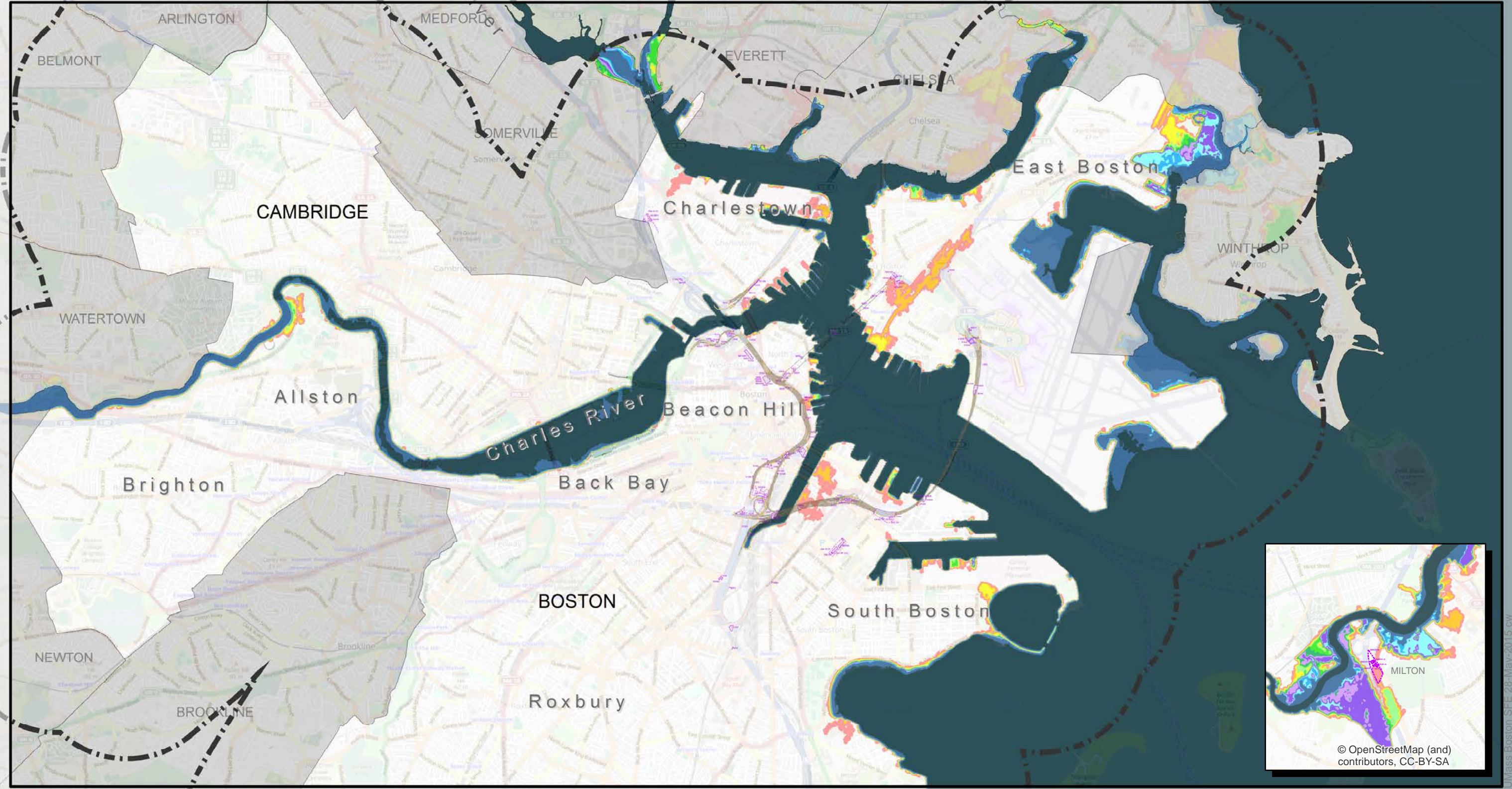
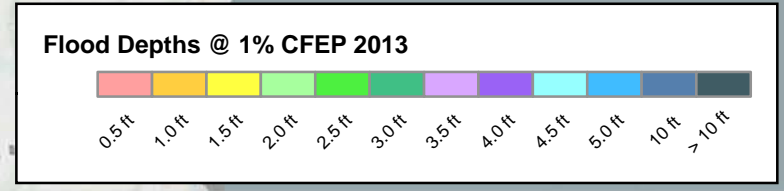
Sources: MassDOT, Woods Hole Group, UMass Boston, MassGIS, and ESRI (as indicated below)

BH-FRM Coastal Flood Exceedance Probabilities
Central Artery and Tunnel System
2070 High / 2100 Intermediate High Scenarios
3.2 feet (98 cm) SLR relative to 2013



Legend

- BH-FRM Extent
- Complex
- Structure
- Boat Section
- Tunnel



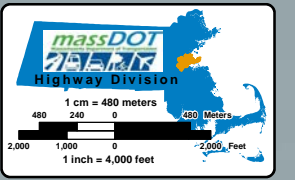
© OpenStreetMap (and contributors, CC-BY-SA)

MassDOT/FHWA
Climate Adaptation Pilot

28-May-2015

Sources: MassDOT, Woods Hole Group, UMass Boston, MassGIS, and ESRI (as indicated below)

BH-FRM Coastal Flood Depths 1% CFEP
Central Artery and Tunnel System
2013 Scenario

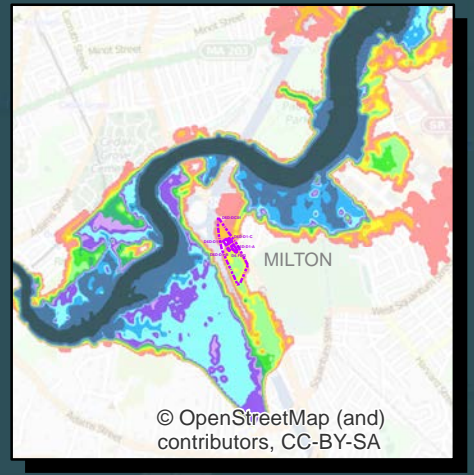
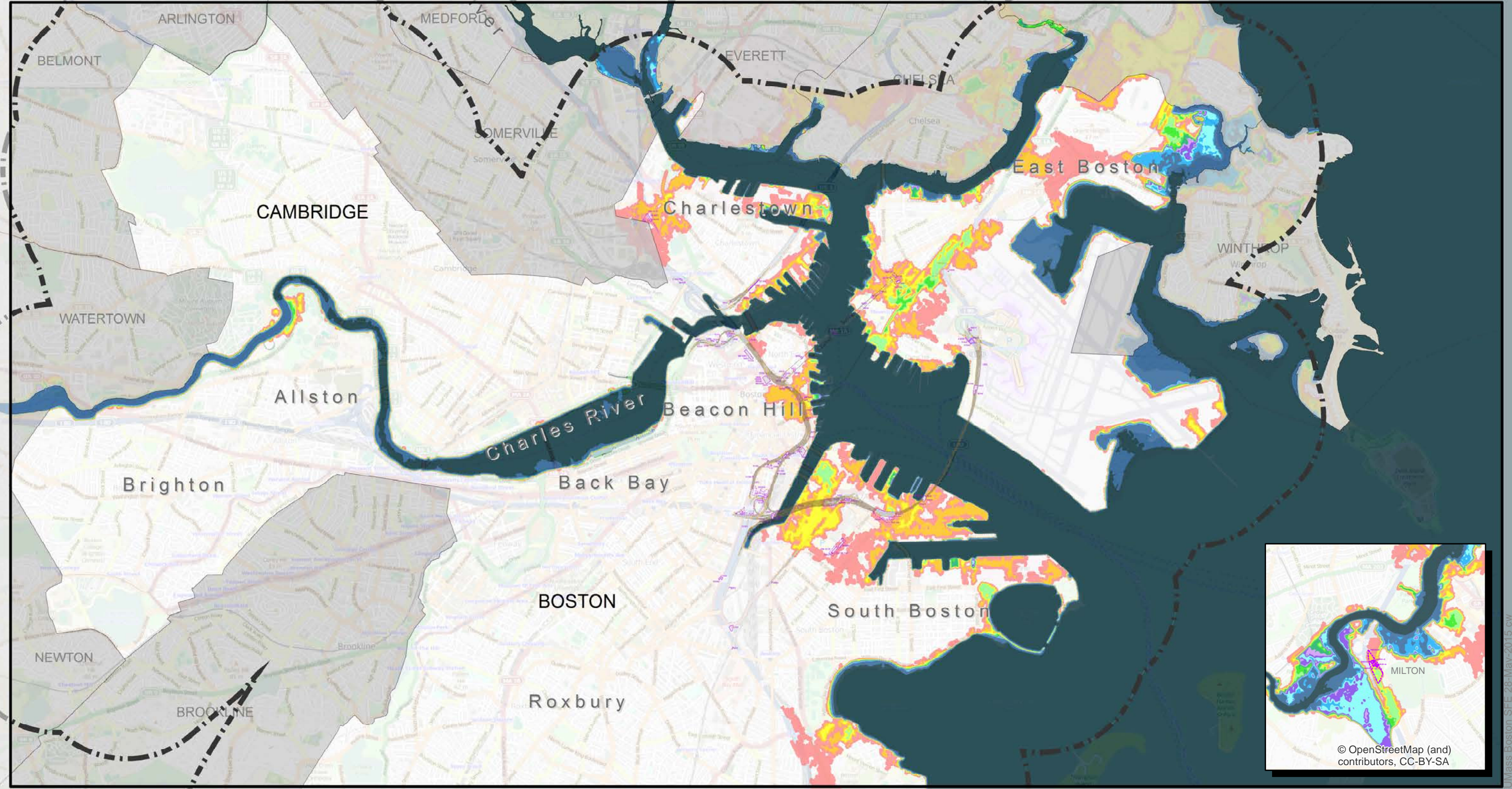
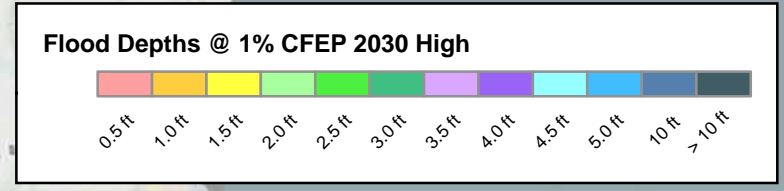


© OpenStreetMap (and contributors, CC-BY-SA)

UMass Boston SFE 28-May-2015 cw

Legend

- BH-FRM Extent
- Complex
- Structure
- Boat Section
- Tunnel

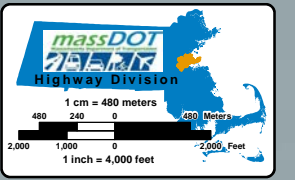


MassDOT/FHWA
Climate Adaptation Pilot

28-May-2015

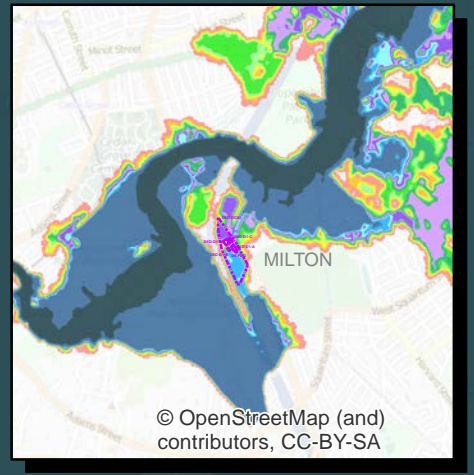
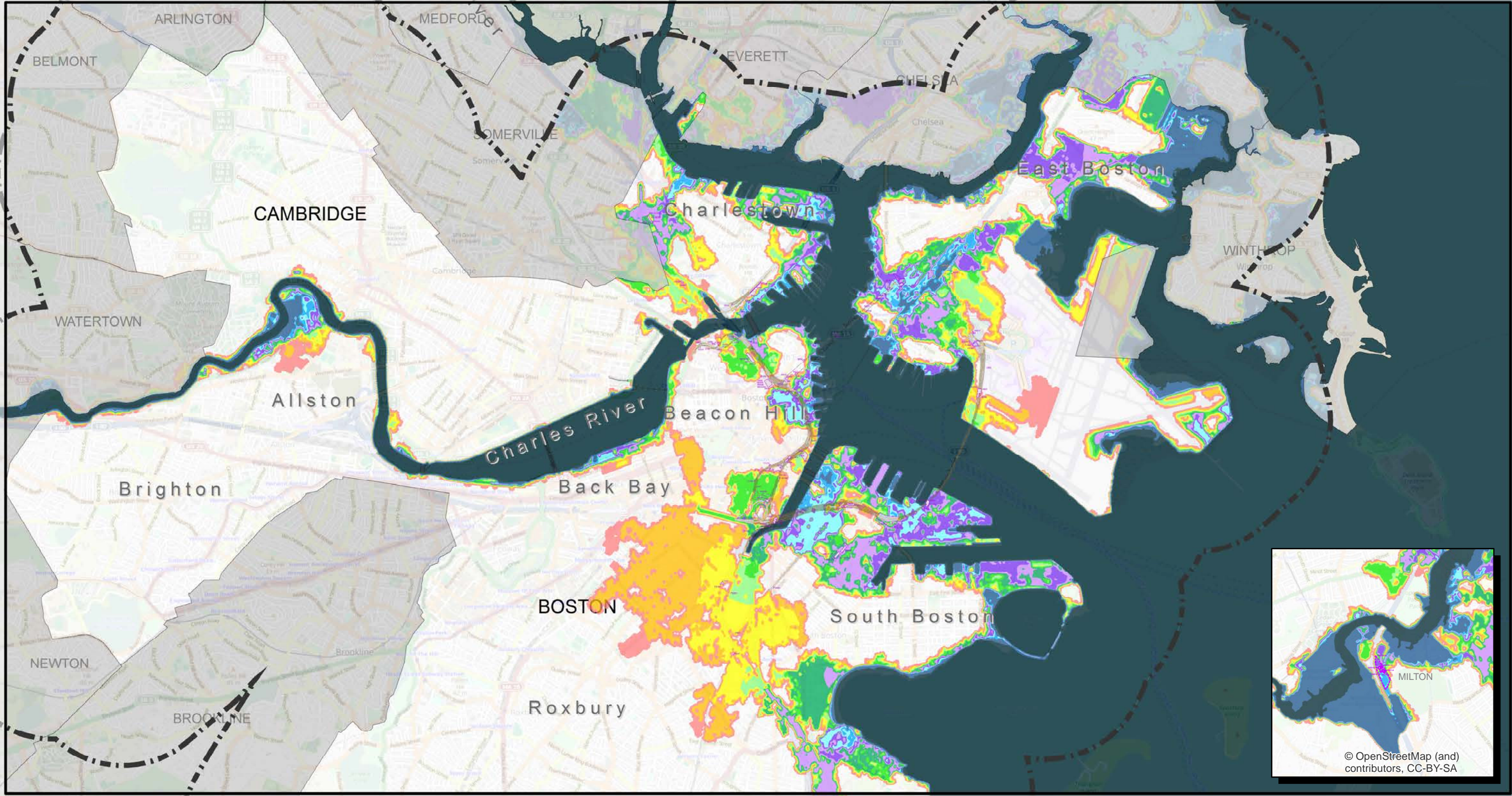
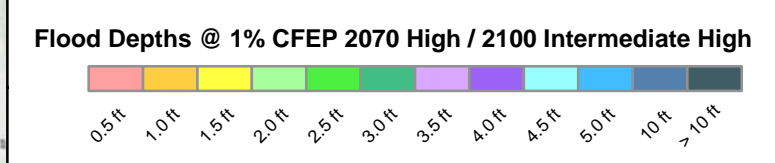
Sources: MassDOT, Woods Hole Group, UMass Boston, MassGIS, and ESRI (as indicated below)

BH-FRM Coastal Flood Depths 1% CFEP
Central Artery and Tunnel System
2030 High Scenario
0.62 feet (19 cm) SLR relative to 2013



Legend

- BH-FRM Extent
- Complex
- Structure
- Boat Section
- Tunnel

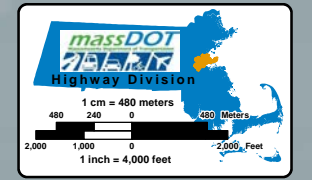


MassDOT/FHWA
Climate Adaptation Pilot

02-Sep-2015

Sources: MassDOT, Woods Hole Group, UMass Boston, MassGIS, and ESRI (as indicated below)

BH-FRM Coastal Flood Depths 1% CFEP
Central Artery and Tunnel System
2070 High / 2100 Intermediate High Scenarios
3.2 feet (98 cm) SLR relative to 2013



UMass Boston SFE 02-Sep-2015 cw